# Geodetic Measurement of Deformation in the Offshore of Southern California

Thesis by

Francis H. Webb

In Partial Fulfillment of the Requirements

for the Degree of

Doctor of Philosophy

California Institute of Technology

Pasadena, California

1991

(Submitted June 4, 1990)

Acknowledgements:

The initial concept of this project was proposed by Duncan C. Agnew and Bradford H. Hager. Financial support was provided through grants from the National Science Foundation, NSF EAR86-18542, and from the National Aeronautics and Space Administration, NASA NAG5-842. The collection of the data was made possible through the help and cooperation of a large number of people and agencies who generously volunteered their time and assistance. The operation of the receivers in the field was handled primarily by volunteers from Scripps Institute of Oceanography, Caltech, University of California, Los Angeles, and Massachusetts Institute of Technology, along with additional support from University of Colorado, UNAVCO, and Jet Propulsion Laboratory. Receivers were provided by UNAVCO, Ohio State University, Defense Mapping Agency, Pacific Missile Test Center. UNAVCO and James Stowell were invaluable in providing support for the field campaigns. At the National Geodetic Survey, Gerry Mader, Bill Strange, and Miranda Chin are thankfully acknowledge for providing software and training for processing the GPS observables. The geodetic strain analysis would have been quite painful and tedious, if it had not been for software developed at the NGS by Nancy Drew and Richard Snay, who have done a great service to the community in developing DYNAP.

Access to geodetic markers was provided in numerous cases through the good will of land owners. The late Carey Stanton is thanked for his assistance in allowing for the occupation of bench marks on his island, Santa Cruz Island. The Pacific Missile Test Center and Rich Dixon are thanked for providing field transportation, personnel, and support for stations on San Nicolas Island and at Point Mugu. Frank Ugollini and the National Park Service are thanked for allowing for, and assisting in, occupations of monuments on Santa Barbara and San Miguel Islands.

I am especially grateful for the support that I have received from Cheryl Contopulous, Mark Fahnestock, Jean Grinnols, Andy Gaynor, Phil Ihinger, Barkley

Kamb, Cathy Smither, and Gerald Wasserburg. It has always been enjoyable working with my peers from the other institutions: Mark Murray and Kurt Feigl at MIT, and Kristine Larson from IGPP. Thanks go to my office mate, Shawn Larsen, for many enlightening conversations on a wide variety of subjects. I am indebted to Bruce Murray for his advice and for his generosity in allowing this research to be performed on his computer.

I also would like to acknowledge the emotional support and encouragement that I have received from my family and friends during these years at Caltech: Terri, Sean, Eugene, Mark, Jon, Paul, and Sacha.

For the record, there are three dates worth mentioning in relation to the completion of this dissertation: March 31, 1990 was the day Caltech withdrew my support despite assurances I had received that I would be supported through June of 1990; June 4, 1990 was the day I defended and the first anniversary of the Tianemen Square massacre; February 28, 1991 was the day Kuwait was liberated by the allied forces and my committee signed off on my revised thesis.

Abstract

Geodetic measurement of deformation in the offshore of southern California.

Geodetic surveys using signals from satellites of the Global Positioning System (GPS) have allowed for the reoccupation of historical triangulation markers for crustal deformation studies and the recovery of a long history of geodetic data that date to the late 1800's. From June 1986 to May 1988, six GPS experiments were conducted in California that incorporated more than 50 first-order triangulation stations on the channel islands of southern California and the mainland into a precise GPS network. Interstation vectors were calculated from the GPS observables using the National Geodetic Survey's (NGS) GPS22 software. The results of these analyses provided baseline component precisions better than several parts in $10^7$. The vectors from all of the GPS surveys were combined and used with historic triangulation observations to estimate shear-strain rates across the Santa Barbara Channel and Oxnard plain, and across the southern California Continental Borderland. Simultaneous reduction was used to evaluate the shear-strain rates from the combination of these data. Shear-strain rates across the Santa Barbara channel are from 0.2 to 0.4 µrad/yr with a direction of maximum contraction of from N23W to N20E, averaged over a hundred years of geodetic data. For networks that cross the Continental Borderland, the data were insufficient to reliably estimate strain rates.

The direction of shortening implied by the geodetic data agrees with that inferred from the trends of late Quaternary and Holocene faults and folds in the Santa Barbara channel. When the shear-strain rates across the channel are modeled as uniaxial convergence, this indicates shortening from 13±5 mm/yr at N23W±5 across the western part of the channel to 18±5 mm/yr at N20E±5 across the eastern part. By adding the western channel velocity to the geodetic velocity of the Vandenberg VLBI site with respect to North America, a velocity path across the Pacific-North American plate boundary can be constructed to the offshore islands of 56±4 mm/yr at N38W±4,

exceeding the NUVEL-1 plate-model velocity for Pacific-North American plate motion in California by 7 mm/yr.

Table of Contents

# Chapter 1

# Introduction

Until recently, our knowledge of plate tectonic motions was based primarily on the analysis of marine magnetic anomalies, the orientations of transform faults in the ocean basins, paleomagnetic pole positions, and earthquake slip vectors. This information has lead to the development of global plate velocity models that have been useful in the quantification of tectonic activity through the predictions from the plate models of the rates of deformation in these areas. The plate motions predicted from these models are averages over several millions of years and have been used to interpret regional geological deformational histories and developments.

While the assumption of rigid plates is generally true for the oceanic plates, apparently continental crust does not behave rigidly. It is the non-rigid behavior of this crust that results in some of the more interesting geology. The detailed understanding of crustal deformation recorded in rocks along plate boundaries is best interpreted with respect to the rates and style of deformation implied by the plate tectonic environment of the region as predicted from plate reconstructions. A more complete understanding of the present day kinematics of the crust along these plate boundaries should create a deeper understanding of the geological development of a region.

The San Andreas fault is generally recognized as the main boundary between the Pacific and North American plates in California. This transcurrent boundary, embedded within the crustal rocks of North America, is the locus of many geological structures that demonstrate substantial non-rigid behavior of the crustal rocks throughout the history of Pacific-North American plate interaction [e.g., Atwater, 1970]. The development of relatively young folds and basins along this boundary is evidence that some of the plate motion is being transferred to the crust and that slip measured along the San Andreas fault alone can not account for all of the relative plate motion. Geologic and geodetic investigations indicate that only about 75% of the relative plate motion can be accounted for as slip along the San Andreas fault [Minster and Jordan, 1984; DeMets et al., 1987]. Deformation both east and west of the San Andreas fault has been proposed to account for the remaining motion, the so-called San Andreas discrepancy. In central California, both extension across a broad region of the North American continent in the Basin and Ranges and faulting along coastal California have been proposed to account for the missing motion [Minster and Jordan, 1984; Minster and Jordan., 1978]. The partitioning of this discrepancy in southern California is more complicated than in central California, because of the presence of more active structures and faults with various trends both west and east of the San Andreas fault. Slip rates have been determined for many of the onshore faults, but they can not account for all of the missing motion. Faults in the offshore have been recognized as active from marine geophysical studies and seismicity [Legg, 1985], but the determination of rates of deformation across them has eluded investigators.

The determination of present day plate motions and the testing of deformation models of the behavior of the plates and the crust have been aided by the development of space based geodetic techniques. Satellite Laser Ranging (SLR) and Very Long Baseline Interferometry (VLBI) have been used since the early to mid 1970's (SLR) and the early 1980's (VLBI) to investigate and monitor strain around the world on baselines from several 100 to many 1000's of km long [NASA, 1988]. Baselines can now be measured to better than the centimeter level allowing for the determination of present day plate motions. Results from these investigations suggest that present day plate velocities between sites in the interior of plates agree well with those predicted from global plate models and that the velocity of sites along plate margins suggests non-rigid plate behavior [Ryan, 1987; Smith et al., 1989b]. These techniques have been very successful in characterizing the deformation, on regional to intercontinental baselines, and have been applied to the onshore region of southern California where they have provided information on the distribution of the plate motion across the onshore part of the Pacific-North American plate boundary [Clark et al., 1987; Sauber, 1989]. However, the cost of deployment makes these techniques impractical for monitoring dense networks covering scales of 1- 100 km.

The development of Global Positioning System (GPS) based geodetic techniques has allowed the investigation of crustal strain in areas that had previously been inaccessible by VLBI and SLR. This is mostly due to the low cost of GPS receivers, their ease of operation, and portability. GPS techniques are being demonstrated to have accuracy and precision that are comparable to that of VLBI and SLR [e.g., Blewitt, 1989], but at a much lower cost. The portability of GPS receivers makes them ideally suited over those other techniques for the densification of geodetic networks in regional areas to further understand the crustal deformation process.

In this study recently developed GPS based geodetic techniques are used in combination with terrestrial geodetic data to characterize the kinematics and strain rates of the deformation in the offshore region of southern California. GPS surveys were performed to first order triangulation monuments along the coast and to the offshore islands of southern California. The data collected during these surveys were analyzed to determine interstation vectors among monuments with historical triangulation observations. The results of the GPS analyses have been used with the historical data to model the strain rates across the offshore region of southern California. The data set is rich enough to delineate the spatial changes in the strain rate field. These changes have implications for the distribution of strain across the Pacific-North American plate boundary in California. Chapter 2 discusses the different types of geodetic data used, the GPS surveys, and the data analyses. Chapter 3 discusses the methods used to model the strain rates from these data and the relative significances of those estimates. Chapter 4 discusses the the strain rate results for the different geodetic networks in the Santa Barbara Channel and Continental borderland with respect to long term geological estimators of strain within those networks. And Chapter 5 discusses the implications of these strain rates for the relative motion between the Pacific and North American plates.

# Chapter 2.

# Geodetic Data

In this chapter, both the triangulation and GPS data sets and the processing that has been applied to each will be described. For the triangulation data, the processing has been minimal relative to that which has been done with the GPS observables. The following analyses have removed most of the blunders and systematic errors present in both sets of data from the final database, so that they do not bias the strain estimates that have been calculated from these data in Chapter 3.

## 2.1 Introduction:

Many types of geodetic observations have been collected in the offshore region of southern California. The data used to estimate crustal strain in Chapter 3 consisted of three types of geodetic data representing several years to many decades of observations. These geodetic observations are of different precisions and have been collected by different agencies, from the first triangulation surveys in the late 1800's to the most recent GPS surveys in 1988. The data include triangulation, trilateration, and interstation vectors determined from the analysis of signals from satellites of the Global Positioning System (GPS). The geodetic observations were made to horizontal control marks of the National Geodetic Survey (NGS) and its predecessor agencies. For the strain analyses it was desirable to reoccupy the original historical geodetic mark with GPS. However, this was not always possible, since some of the original marks had been destroyed and others had poor sky visibility for GPS observations. This resulted in some of the GPS observations being made from eccentric marks that were tied to the historical triangulation stations via a conventional ground survey. (The ties between the triangulation stations and their GPS eccentric marks are found in Appendix A.)

Several organizations have been involved in the collection of the data. The GPS observations were made by a university consortium consisting of Scripps Institute of Oceanography, Massachusetts Institute of Technology, University of California at Los Angeles, and the California Institute of Technology with assistance from Federal and local agencies. The triangulation observations were part of the Project REDEAM data set [Snay et al., 1987] and were provided by the NGS. The trilateration was collected for A. G. Sylvester of the University of California at Santa Barbara (UCSB) by Greenwood and Associates, Santa Barbara, and reduced by Larsen et al. [1988].

## 2.2 Triangulation and trilateration surveys:

### 2.2.1 Introduction:

Triangulation and trilateration collected between 1873 and 1971 are the two types of historic geodetic measurements with which the results of the GPS analyses will be compared. These measurements are very different in their collection and distribution in the study area. Triangulation observations are simple measurements that require little, if any, corrections. The observations are of horizontal angles between stations in the plane of the observing instrument, which is tangent to the geoid. The procedures have remained relatively constant since the first surveys in the late 1800's. The only corrections that need to be applied are for deviations between the geoid normal and the normal to the figure of the earth, the ellipsoid [Bomford, 1980; Vanicek and Krakiwsky, 1986]. Trilateration, introduced in the early 1970's, involves the measurement of the distance between the instrument and the target based on the two way travel time of a light wave that is emitted from the instrument and reflected by the target back to the instrument. Corrections are applied to the measurement to account for variations in the refractive index of the atmosphere along the path of the signal. For long lines, >10's of km, the proper calculation of this correction requires the collection of meteorological data along the path of the signal during the measurement [Bomford, 1980; Vanicek and Krakiwsky, 1986].

Triangulation observations are the oldest, dating back to the late 1800's. Triangulation surveys were performed along the coast primarily to aid navigation through the precise mapping of the coastline [Snay et al., 1987]. Observations from these surveys comprise the majority of the historic geodetic data used in this study. These surveys were performed in the early 1870's, late 1890's, early 1920's, 1940's, 1950's, and 1960's.

The survey of a triangulation network took several years to complete. During the observing campaigns, rigorous field procedures were prescribed in order to ensure that observations of the highest precision were acquired. At most of the triangulation stations, horizontal angle observations are made with a theodolite to other stations in the network. Observations are made in rounds, starting on one station, observing the other stations in the round and closing on the first station. The number of observations depends on the precision of the survey, the survey order, and on the instrument used [Gossett, 1950]. The mean of the observations is reported as the observed direction.

First order surveys are the most precise. Each target station in a first order survey is observed 32-48 times. The standard errors of the mean of each direction are 0.6, 0.7, 1.2, and 2.1 arc seconds for first, second, third, and fourth order surveys, respectively [Gergen, 1975; Snay et al., 1987]. ( 0.6 arc seconds = 15 cm at 50 km). Many stations along the coast of California were observed during these surveys with precisions varying from first order to fourth order. However, during some of the surveys, conditions were such that the observational precision was less than the order of the survey. In these cases the precision of the observation is greater than that of the associated survey order. Some of the first, second and third order directions have standard errors as large as 2.1 arc seconds.

Many stations were surveyed during the last century, but repeat surveys of the coast usually did not repeat the same stations of the original networks. Between surveys, stations were destroyed or rendered unusable by obstructions. Because of this and the low precision of the observations from and to many of the stations, much of the data are of limited utility for evaluating crustal strain.

Since crustal shear strain rates in California are typically ~0.1-0.2 μradians/yr [Savage, 1983] and the precision of a first order triangulation measurement is ~3.0 μradians [Gergen, 1975], only the highest precision triangulation data are capable of providing reliable estimates of crustal strain rates, if collected frequently over several decades. Some of the stations included here fall into this category. Even though they were not occupied with GPS, they have a long history of observation using conventional geodetic techniques and can provide constraints on the other observations within the networks.

In addition to the horizontal direction observations, a limited number of astronomical positions and azimuths were observed for some of the stations during the historical surveys. The astronomical positions have been used to correct the observations for deflections of the vertical, but the astronomical azimuths have not been used. The large standard error in these measurements (> 7 μradians) [Snay et al., 1987] and possible systematic error between the reference frame of these observations and the GPS reference frame (Appendix A) make these azimuths unsuitable for evaluating crustal rotations.

### 2.2.2 Adjustment of the historic geodetic data :

Even when the highest standards are applied during the data collection, blunders and systematic errors can occur. In order to evaluate the data set for blunders, the observations were adjusted on a "survey by survey" basis. In this context, "survey" means a period of time during which the data were collected. The adjustment procedure involves the determination of the horizontal station positions (latitude and longitude) from the observables (i.e., horizontal directions and mark-to-mark distances) using a linearized, weighted least-squares technique. The observation equation is written as

$$\mathbf{F}(\mathbf{x}) = \mathbf{b}^* + \mathbf{V}(\mathbf{x}) \qquad (2\text{-}1)$$

**F** is a model function relating the vector of station positions, **x**, to the vector of true observations, **b***, and **V**(**x**) is a residual function of misfit between the model and the observations.

Because the model, **F** , is non-linear, it is linearized using a first order Taylor expansion about *a priori* station positions, $\mathbf{x}_o$,

$$\mathbf{b} = \mathbf{b}^* - \mathbf{F}(\mathbf{x}_o) = \frac{\partial \mathbf{F}(\mathbf{x}_o)}{\partial \mathbf{x}}(\mathbf{x} - \mathbf{x}_o) - \mathbf{v} \qquad (2\text{-}2)$$

The vector $\mathbf{F}(\mathbf{x}_o)$ is known and subtracted from the observations, **b***, to give the observation residual vector **b**

$$\mathbf{b} = \mathbf{b}^* - \mathbf{F}(\mathbf{x}_o) \qquad (2\text{-}3)$$

Letting the design matrix, **A**, of partial derivatives be

$$\mathbf{A} = \frac{\partial \mathbf{F}(\mathbf{x}_o)}{\partial \mathbf{x}} \qquad (2\text{-}4)$$

the observation equation can be written as

$$\mathbf{A}\mathbf{x}' = \mathbf{b} + \mathbf{v} \tag{2-5}$$

where $\mathbf{x}'$ is a vector of corrections to $\mathbf{x}$. Letting $\mathbf{W}$ be the weight matrix of the inverse of the observational errors, then the least squares estimate is given by

$$\mathbf{x}' = \left(\mathbf{A}^T\mathbf{W}^{-1}\mathbf{A}\right)^{-1} \mathbf{A}^T \mathbf{W}^{-1} \mathbf{b} \tag{2-6}$$

Equations for the partial derivatives relating the observables (horizontal directions and mark-to-mark distances) to the model can be found in Milbert and Kass [1987].

The triangulation surveys contained only precise horizontal direction observations. These surveys thus lack an origin, scale, and orientation, and are insufficient to solve for the station positions. To surmount these deficiencies in the data, a network scale and orientation are introduced during the adjustment of the triangulation surveys, with the adjustment being performed with respect to the station coordinates of a reference station. For trilateration surveys, only a network orientation needs to be constrained.

The triangulation data were provided in computer readable form by the NGS as part of its Project REDEAM data set that was generated for the redefinition of the North American Datum (NAD) in 1983 [Snay et al., 1987]. The REDEAM data set consists of observations from various Federal, state, and local organizations that are archived by the NGS [Snay et al., 1987]. The locations of stations used in this study are shown in Figure 2-1 and tabulated in Table 2-1.

The triangulation data set was divided up into six temporally independent surveys in order to check that all of the observations during a given time period were consistent and that none of the observations were unconstrained by the data within the network. The surveys used are from the 1870's, 1890's, 1920's, 1940's, 1950's, and 1960's.

Observations to or from stations, for which these observations were insufficient to constrain the station positions, were eliminated from the data set, thus removing potentially unchecked sources of systematic error. All of the data are tabulated in Appendix B and the spatial distributions of each survey are show in Figure 2-2.

Histograms of the frequency distribution of the standardized residuals

$$v_i = \frac{x_i - \langle x_i \rangle}{\sigma_i}$$

of the observations for the survey adjustments are shown in Figure 2-3, where $x_i$ is the observed data , $\langle x_i \rangle$ is the estimated observation, and $\sigma_i$ is the standard error of $\langle x_i \rangle$.

These distributions are plotted with normalized Gaussian frequency distributions f(v), [Bevington, 1969],

$$f(v) = \frac{n}{\sqrt{2\pi}} e^{-\frac{1}{2}v}$$

that is implicit in least squares estimation [Press et al., 1987], where v is the standardized residual and n is the number of observations. The Gaussian distributions suggest that the adjusted residuals are close to being normally distributed for all of the surveys except the 1960 survey. Four points from this survey had normalized residuals that were $>10\sigma$. These observations were removed from the data set.

However, for each survey from the 1900's, there are observations with values $>3\sigma$. These data have probabilities of occurring less than 99.7% of the time [Bevington, 1969; Press et al., 1987] and are, thus, most likely data outliers or observational blunders. Because their probability of occurrence, in the assumed Gaussian model, is so small, the inclusion of these observations in the least squares estimation will distort the estimated parameters in an effort to bring these outliers in line with the model [Press et al., 1987].

To counter the effect of these possible blunders on the strain estimation in Chapter 3, a second triangulation data set has been derived. In this set, the surveys were adjusted as before, except that observations with standardized residuals >3$\sigma$ are rejected after each adjustment. This procedure is iterated until all of the adjusted observations were within 3$\sigma$. The data from these surveys are also tabulated in Appendix B and the general spatial distributions are the same as those shown in Figure 2-2, except that the 1870 observations from the southern islands have been removed.

Quantitatively, the relative fit of the data can be compared using the statistic

$$\sigma_o^2 = \frac{\sum_{i=1}^{n}\left(\frac{x_i-\langle x_i\rangle}{\sigma_i}\right)^2}{(n-n_{par})} \qquad (2\text{-}7)$$

called the variance of unit weight, where $x_i$ is the observed data , $\langle x_i\rangle$ is the adjusted observation, $\sigma_i$ is the standard error of $\langle x_i\rangle$, n is the number of observations, and $n_{par}$ is the number of parameters estimated. This is a commonly used statistic in geodesy for evaluating the goodness of fit of the data [Snay, 1986] and is equivalent to a $\chi^2$ over degrees of freedom statistic [Bevington, 1969]. A value of 1 suggests that the residuals are normally distributed and that their standard errors are good estimates of of the true errors. For values other than 1, $\sigma_o$ can be used as a weighting factor for scaling the estimated error [Bevington, 1969]. The variances of unit weight for each survey are tabulated in Table 2-2 and indicate a good fit for each survey, except for the 1950 survey which is notably worse than the other surveys.

## 2.3 GPS

### 2.3.1 Introduction:

As part of a 5 year study to monitor crustal deformation in the central and southern California [Agnew et al., 1988] static GPS relative positioning was used to determine the present positions of many of these historic triangulation markers. The GPS data were collected in six multi-day campaigns conducted between June 1986 and May 1988. The campaigns were designed to characterize the distribution of strain through the recovery of the historical data base and the establishment of a GPS monitoring network. Many historical first order triangulation marks were occupied with GPS receivers, and several new GPS marks were established. Many of these marks have been occupied several times since the first survey in 1986.

Efforts were concentrated on the reoccupation of the same GPS stations in each network during each subsequent occupation. However, expansion of the original networks, limited receiver availability, poor data quality, receiver malfunctions, and other miscellaneous logistical concerns made this unfeasible, resulting in the heterogeneous reoccupation of the GPS networks. Because some of the historical marks were difficult to reach with GPS receivers or unsuited for GPS observations, these marks were tied to the GPS networks through: one-time-only occupations during larger campaigns; short local GPS surveys to the local, primary GPS station; or with conventional geodetic surveys (Appendix A). Over the course of the observational campaigns, approximately 50 first order triangulation marks and/or their reference/eccentric marks have been occupied (Fig. 2-4).

The GPS data consist of approximately 283 station days of data that have been collected over a two year period during six GPS campaigns using Texas Instruments TI4100 GPS receivers provided by UNAVCO, Ohio State University (OSU), Pacific Missile Test Center (PMTC), NGS, and USGS. The data collection involved the cooperation of several different institutions and universities. In addition to these organizations, numerous volunteers participated in operating receivers in the field. The US Forest Service, US Park Service, the FAA, and several land owners generously allowed access to their land.

Before discussing the GPS data and the processing applied to these in this study, GPS, the observables, and the observable models will be reviewed. This review is based primarily on the treatment by King et al. [1985], Wells et al. [1986], and Röcken [1988].

2.3.2 Satellite Geodesy using GPS:

The Global Positioning System (GPS) is a passive navigation system that is being developed and deployed by the United States Department of Defense (DOD) for real time positioning. The system is designed to provide world-wide point-positioning 24 hours a day, through the use of timing and orbital information broadcast by the satellites. The accuracy of the point-positioning depends on the satellite geometry, number of satellites tracked, the accuracy of the satellite ephemerides, and the sophistication of the receiver. Receivers that can receive both carrier signals and decode the timing and ephemeris messages on the carriers can provide real time point-positioning with an accuracy of about 30 m through the acquisition of signals from at least four satellites with which the receiver can calculate its position and time bias from GPS time [Wells et al., 1986]. Sub-meter point-positioning can be obtained with post-processing of the observables [Malys and Jensen, 1989]. Higher accuracy can be attained through *relative* positioning when the signals are received by two or more receivers and the data are post-processed to account for path delays, orbital errors, and the behavior of the satellite and receiver clocks.

The system is divided into three parts, consisting of space, control, and user segments. The space segment is a constellation of satellite transmitters that, when fully operational, will contain 21 satellites, 18 operational and 3 spares, in six 20,000 km orbits inclined at 63° to the earth's equatorial plane. Each satellite is identified by a unique number, called PRN. Three satellites will be evenly spaced in each orbital plane. This orbital configuration will provide the ability for world-wide, around the clock positioning from at least four satellites. Over the period of the observations collected for this thesis, the system has been in a developmental phase. During this phase, only 7 of the prototype Block I satellites were operating properly. The orbital planes of these satellites provided long data arcs over North America with limited sky geometry that was dominated by north-south satellite tracks.

The control segment is responsible for monitoring the accuracy and health of the satellites, updating the broadcast message, and maneuvering the satellites in their orbits when necessary. Five control stations spaced evenly around the world track the satellites and monitor the behavior of their clocks. These data are transmitted to the Master Control Station in Colorado Springs, Colorado, where they are processed and daily satellite ephemerides and satellite clock corrections are calculated. This information is transmitted hourly to the satellites, which in turn transmit them as their broadcast ephemerides. The satellites passively broadcast on two L-band carriers this orbital information and timing codes that can be used by the user segment on the ground, with the appropriate GPS receiver, for navigation, positioning, and surveying.

The two carriers are designated L1 and L2 with frequencies of 1575.42 MHz and 1227.60 MHz, respectively. Two different phase modulations along with the broadcast ephemerides are transmitted on these carriers. These modulations are streams of pseudorandom sequences of $\pm 1$, called P-code and C/A code. P-code is present on both the L1 and L2 carriers and C/A code is only on L1. Each satellite is assigned its own unique C/A and P-codes.

The two observables collected by the TI4100 receiver and used in relative positioning are the carrier phase and pseudorange at both the L1 and L2 frequencies. The pseudorange measurement is derived from the time shift required to correlate the incoming P-code with a replicant generated by the receiver, multiplied by the speed of light. This range does not represent a true range to the satellite, because it is contaminated by propagation path delays and clock biases between the clocks in both the receiver and satellite, and GPS time. The carrier phase is the difference between the incoming, Dopler-shifted satellite signal, with the codes removed, and the phase of the nominally constant frequency oscillator in the receiver. This phase difference is accumulated as the relative positions of the receiver and satellites change.

Precise relative positioning is obtained with GPS through the post-processing of the observables from a network of receivers. During the processing, relative station positions are estimated through the modeling of the observables for the geometric path delay. The models are designed to remove the effects of signal path delays from the ionosphere and troposphere, clock drifts and biases from GPS time, and orbital errors. The most common observable model involves the differencing of phase measurements between satellite and station pairs, called double differencing. Through differencing, the effects of common-mode clock, atmospheric, and orbit errors are reduced [King et al., 1985]. There are other processing schemes, such as the use of undifferenced observable models, which model these "noise" sources rather than reducing them through differencing.

In addition to the observable modeling, post-processing also corrects for data collection defects, known as cycle slips, resulting from the loss of lock by the receiver on the incoming carrier phase. These cycle slips result from the inability of the receiver to accurately predict the phase changes from one measurement to the next, resulting in the resetting of the accumulated phase. Loss of phase lock can occur due to loss of satellite signal from obstructions, erratic receiver or satellite clock behavior, strong ground reflections of the signal (multipath), and the inability of the receiver's ionospheric and tropospheric models to account for unusual ionospheric or tropospheric conditions (e.g., during solar storms and terrestrial storms). The fixing of cycle slips can be a painstaking and tedious task.

2.3.2 Analysis methods:

Most of the GPS observables were analyzed using a double-difference computer algorithm under development at the NGS and provided by Dr. Gerry Mader of the NGS. The NGS GPS processing system will be referred to as GPS22, the observable processing routine; however, other modules are part of this system. A brief description of the processing algorithm is provided below. An undifferenced processing system under development at JPL, called GIPSY, was used to process some of the short GPS ties. A detailed description of the GIPSY algorithm and the observable models can be found in Sovers and Border [1987].

*Phase observable model*

The development of the phase observable model and the partial derivatives required for inverting the GPS observables for station coordinates can be found in King et al. [1985], Wells et al. [1986], and Röcken [1988]. The phase observable model for the phase received at receiver i from satellite j at GPS time $t_{io}$ at receiver i is given by

$$\varphi_{ij}(t_{io}) = \varphi_{Sj}(t_{io}) - \varphi_{Ri}(t_{io}) + n_{ij} + \varphi_{noise} \qquad (2\text{-}8)$$

where $\varphi_{Sj}$ denotes the phase transmitted by satellite j, $\varphi_{Ri}$ is the phase of the oscillator of receiver i , and $n_{ij}$ is the initial integer cycle bias between the satellite and receiver oscillators.

Further simplification is obtained through modeling the transmitted satellite phase as

$$\varphi_{Sj}(t_{io}) = \omega_o(t_{io} - t_o) - \omega_o \tau_{ij} + \varphi_{Sj}(t_o) \tag{2-9}$$

where $\varphi_{Sj}(t_o)$ is the initial phase at an arbitrary initial time $t_o$, $\omega_o$ is the nominal carrier frequency, and $\tau_{ij}$ is the flight time between satellite j and station i. The flight time includes the geometric path delay, the tropospheric delay, and the ionospheric delay and is given by

$$\tau_{ij} = \frac{|\mathbf{r}_i - \mathbf{s}_j|}{c} + \tau_{ij\,trop} + \tau_{ij\,ion} \tag{2-10}$$

where $\mathbf{r}_i$ and $\mathbf{s}_j$ are the earth centered vectors to the receiver and satellite at reception and transmit time, respectively; $\tau_{ij\,trop}$ and $\tau_{ij\,ion}$ are the tropospheric and ionospheric path delays, respectively.

The phase of the receiver's oscillator is modeled as

$$\begin{aligned}\varphi_{Ri}(t_{io}) = {} & \varphi_{Ri}(t_o) - \omega_o(t_{io} - t_o) \\ & + \omega_o\left(q_i + r_i(t_i - t_o) + \frac{1}{2} s_i (t_i - t_o)^2\right)\end{aligned} \tag{2-11}$$

where the first term is the initial phase offset of the receiver oscillator, the second term is the accumulated phase since $t_o$, and the last term describes the behavior of the receiver oscillator with respect to the receiver's time, $t_i$, which is related to the true GPS time, $t_{io}$, by

$$t_i = t_{io} + \Delta t \tag{2-12}$$

where $\Delta t$, the time offset and drift, is modeled as

$$\Delta t = q_i + r_i (t_i - t_o) + \frac{1}{2} s_i (t_i - t_o)^2 \qquad (2\text{-}13)$$

From these equations the phase observable model for the one-way phase from satellite j to receiver i can be written as

$$\begin{aligned}\varphi_{ij}(t_{io}) = -\omega_o \tau_{ij} + n_{ij} \\ + \omega_o \Delta t \\ + \varphi_{Ri}(t_o) + \varphi_{Sj}(t_o) + \varphi_{noise}\end{aligned} \qquad (2\text{-}14)$$

The double differenced observable model can be formed for the phase difference at receivers i and l from satellites j and m by differencing the one-way phase observable model (Eq. 2-14) between satellite and receiver pairs, to get

$$\begin{aligned}\Delta^2 \varphi_{il\,jm}(t_{io}) = -\omega_o(\tau_{lm} - \tau_{lj} + \tau_{ij} - \tau_{im}) \\ + (n_{lm} - n_{lj} + n_{ij} - n_{im}) + \varphi_{noise}\end{aligned} \qquad (2\text{-}15)$$

where the first term contains all the path delays and the second term contains all of the integer biases.

2.3.2.1 GPS22 Analysis

The NGS processing system used consisted primarily of a front end module, MERGE, and an observable modeling and station position estimation module, GPS22. In addition to these routines, the raw TI4100 observables were converted from TI4100 binary to machine readable form with a modified version of the original routine UNPACK written at the USGS. Data editing was done with modified versions of CYFIX and EDATA (NGS routines) and interactive graphics routines written by myself.

The NGS modules written for a Hewlitt-Packard HP9000 were modified to run in a VAX/VMS environment. All the data processing was performed on a MicroVAX II.

The front end modules convert the raw phase and pseudorange observables, orbits, and meteorological data to three databases: DT, OR, and HD. The DT database contains the phase measurements corrected for the TI4100 frequency biases, pseudorange, *a priori* tropospheric corrections, and crude cycle slip fixes for all stations and satellites. The OR database contains the satellite state vectors at each epoch. These vectors are based on a sixth order polynomial interpolation to either a broadcast ephemeris point in the middle of the observing session or to precise, 15 min tabular orbits provided by the Naval Surface Weapons Center (NSWC) through the NGS in the WGS-84 reference frame. The HD database contains *a priori* station coordinates, surface meteorological data, and antennae site vectors (i.e., offsets between the antennae and the ground marks).

These data bases are used by GPS22 to estimate interstation vectors through a double difference technique using one reference station and satellite. Prior to estimating solutions, a single frequency solution is estimated for each frequency. Triple difference residuals are calculated from these solutions for cycle slip fixing. A sixth order polynomial is fit to the triple difference residuals and epochal differences greater than 1 cycle at half cycle increments are resolved. This process is iterated at both frequencies until all of the triple difference cycle slips are fixed. The data are then visually inspected for any remaining cycle slips, which are corrected. Unresolvable cycle slips can not be handled by the software through the estimation of another phase bias parameter, as is done with other GPS processing systems. In these cases, the cycle slip is fixed as best as it can be visually.

Once all of the cycle slips have been removed, the interstation vectors are estimated using the ionosphere free linear combination of the phase observables, L3, (also known as LC)

$$\varphi_{L3} = \varphi_{L1} - \frac{\frac{\omega_2}{\omega_1}\left(\varphi_{L2} - \frac{\omega_2}{\omega_1}\varphi_{L1}\right)}{\left(1 - \left(\frac{\omega_2}{\omega_1}\right)^2\right)} \qquad (2\text{-}15)$$

where $\omega_1$ and $\omega_2$ are the L1 and L2 frequencies respectively [King et al., 1985]. During the estimation, receiver clock drift, $\Delta t$, is modeled by the pseudorange as

$$\Delta t = \frac{\rho_t - \left(\rho_1 + \frac{\omega_2^2}{\left(\omega_2^2 - \omega_1^2\right)}(\rho_1 - \rho_2)\right)}{c} \qquad (2\text{-}16)$$

where $\rho_t$ is the theoretical range, $\rho_1$ and $\rho_2$ are the L1 and L2 pseudoranges, respectively, and c is the speed of light. A constant tropospheric scale height is estimated at each station that is applied to the *a priori* tropospheric correction estimated in the front end processing. When phase and pseudorange data are available from fiducial tracking stations, the Keplerian elements of the satellite orbits are adjusted by holding the coordinates of the tracking stations fixed in the SV3 reference frame of Murray and King [1988]. All solutions are estimated with the initial phase biases, $n_{ij}$, solved for as real numbers, known as bias free estimation. The estimation procedure uses a linearized least squares inversion of the observables through the formation of a design matrix of partial derivatives and the estimation of corrections to the *a priori* estimates. (For a detailed discussion of the least squares inversion of the double differenced phase observable model see King et al. [1985], Wells et al. [1986], and Röcken [1988].)

2.3.2.2 Field Campaigns and procedures:

The location of GPS receivers was controlled by several factors: Access, obstructions, sky visibility, and available historical data. The primary criterion of the historical data recovery part of this cooperative project was the direct occupation of historical triangulation marks with a sufficiently long history of observations. If these marks had been destroyed or were unsuited for GPS observations because of poor sky visibility, obstructions, suspected strong ground-reflections of the signal (multi-path), or lack of easy access to the mark, another near by mark was chosen or established to which a suitable ground survey existed or could be acquired to the triangulation mark. In addition to the historical station recovery, the experiments were conducted to establish a GPS network to monitor crustal strain. For this part of the project, it was not necessarily desirable to establish GPS stations over the historical monuments that are usually found on the tops of mountain peaks, with difficult access. Because of this, the recovery of all of the triangulation stations took six campaigns spread over two years.

The collection of the GPS data for this project involved the mobilization and coordination of a group of field crews and equipment. The networks occupied consisted of from a minimum of 3 to as many as 15 field receivers with a crew of from one to five people for each receiver, depending on site access and safety. Static relative positioning with GPS requires that the receivers acquire data from the same satellites at the same time. In order to assess the precision of the results and to allow for redundancy, observations are usually made over several days for each experiment. Several experiments were usually conducted over a 2 to 3 week period. This required a high degree of coordination among the different investigators, field crews, land owners, and transportation providers to ensure that the receivers were on their stations and tracking the intended satellites on schedule.

Data were collected under a variety of field conditions. Weather varied widely including rain, wind, extreme heat, and freezing temperatures. Antennae were set up on the tops of peaks, along highways, in small clearings and fields, and near chain link fences and radio communication transmitting towers. In designing the experiments, an effort was made to avoid sites that were suspect to have "bad" multipath. It was not always possible to avoid suspected multipath sites. Sites which had been suspected of causing severe multipath problems that might interfere with the data, did not result, for the most part, in significant and/or unusual data loss or data problems.

TI4100 receivers and antennae were used for all of the observations. The operating software for most of the field TI4100's was GESAR versions 1.0 through 1.5 developed at Applied Research Laboratory, Texas. Some receivers used the Texas Instruments navigation software, GEOMARK. The receivers recorded the carrier phase, pseudorange, and the broadcast satellite ephemerides on the two L-band frequencies, L1 and L2, on four dual frequency channels. Phase and pseudorange were usually collected at 30 sec intervals for approximately 8 hours from satellites 3, 6, 8, 9, 11, 12, and 13 (PRN) in 4-satellite observation scenarios. The receivers operated by GEOMARK recorded data at 3 sec intervals. And the data from the June 1986 experiment provided by the NGS were collected at 6 sec intervals. Antennae were set on top of tripods ~1 to 1.5 meters above the mark. Slant heights were measured between the base of the antenna preamplifier and the center of the mark with tape measurers before and after observations. Phase and pseudorange observables were also used, when available, from a continental network of fiducial tracking stations. These data were provided by the NGS from TI4100's of the NGS CIGNET tracking network. These receivers were operated by the NGS's CORE operating system.

### 2.3.3 GPS results:

The data from each experiment have been independently processed by many of the other investigators involved in the experiments [Dong and Bock, 1989; Larsen et al., 1988; Larson, 1990] using several different analysis systems and algorithms. The primary objective of my GPS data analyses was to acquire interstation vectors among these triangulation marks at an accuracy greater than that of the original triangulation surveys for use in conjunction with the historical geodetic data for the evaluation of the distribution of crustal strain rates in the offshore region of southern California. Deformation results based on the repeated GPS occupations have been reported elsewhere [Larson, 1990].

The data from each day of each experiment were analyzed separately. During the analyses, double differences are formed between one reference station and satellite, and the clock at the reference station is used as the reference clock. The estimated interstation vectors in an earth-centered and earth-fixed cartesian system from each day are then adjusted in a weighted least squares vector adjustment to determine the best fit interstation vector for the experiment.

2.3.3.1 Precision

The precision of the interstation vectors can be assessed by calculating the repeatabilities of each interstation vector as determined from several days of GPS solutions, for each experiment. The daily repeatability of a baseline component, S, is defined as:

$$S = \frac{n}{(n-1)} \sqrt{\frac{\sum_{i=1}^{n} \left(\frac{R_i - \langle R \rangle}{\sigma_i}\right)^2}{\sum_{i=1}^{n} \left(\frac{1}{\sigma_i}\right)^2}} \qquad (2\text{-}17)$$

where n is the number of days of observations, $R_i$ and $\sigma_i$ are the estimate and formal error of the estimate on the *i*th day, and $\langle R \rangle$ is the weighted mean [Blewitt, 1989].

The daily repeatabilities are shown for each experiment in Figure 2-5, for the north, east, up, and length components as a function of length. The lines on the plots represent 1 part in $10^6$, $10^7$, and $10^8$ repeatabilities. Each experiment shows low (i.e., good) repeatabilities in the north and length components and relatively worse repeatability in the east and up components. Directions observed during the triangulation surveys were typically < 50 km apart with some as much as ~ 150 km apart. The repeatabilities indicate relative positioning precisions for stations within the historical geodetic network (< 150 km) of about a centimeter in the north and a few centimeters in the east, well below the precision of the triangulation of 15 cm for the typical baseline length and 45 cm for the extreme 150 km baseline.

2.3.3.2 Accuracy:

When combining GPS vectors from different experiments and networks, the primary concern is ensuring that the vectors that were solved for are in a common reference frame. In the most general sense, GPS vectors are in the reference frame of their orbits. During the data processing, the satellite orbits are adjusted into the reference frame of a set of fiducial tracking stations. The accuracy of the coordinates of these tracking stations in an earth-fixed and earth-centered reference frame controls the reference frame of the satellites and thus of the station position solutions. For most of the experiments, tracking station data were available. During the estimation, the tracking station coordinates were constrained to their coordinates in the SV3 reference frame. SV3 has been shown to provide accurate GPS interstation vectors and baseline lengths, when compared with VLBI results for stations in California [Dong and Bock, 1989].

As a test of the accuracy of the results presented here, results from three of the experiments (JAN87, SEP87, and MAY88) have been compared against other techniques at two different length scales. Vectors estimated during the SEP87 experiment between VNDN and CHUR (at Churchill, Manitoba, Canada) have been compared with the SV3 reference frame vector between these two stations. This provides a test of the accuracy of the analysis on an extremely long (> 3200 km) baseline, along which errors should be amplified. A test of the accuracy at short baseline lengths was performed by comparing baseline lengths from two baselines within the network with EDM measurements performed in the 1970's that are present in the REDEAM data set. The baselines are ROAD-JACK, ~1.6 km (MAY88) and SOLI-CHAF ~1.1 km (OCT87). The lines cross regions where significant strain is unlikely to have occurred since the EDM measurements were made.

The VNDN-CHUR comparison is shown in Figure. 2-6. North, east , up, and length scatter relative to the SV3 position (filled circle) are within the *a posteriori* 2-sigma error bars for the GPS estimates and the 2-sigma error of the SV3 relative position. The scatter is on the order of several parts in $10^8$ to a few in $10^7$, in good agreement with the precision of the experiment and with the precision and accuracy of bias free GPS estimates shown by others [Blewitt et al., 1988; Dong and Bock, 1989]. This suggests an accuracy of the measurements equivalent to the precision of the experiment. For the short baselines, the lengths compare well with the EDM lengths (Table 2-3). The GPS estimates are within the precision and accuracy of the EDM measurements of a few millimeters.

2.3.3.3 Differences associated with different orbit sources:

Usable fiducial data from the same tracking stations for each experiment were not always available. Many of these tracking stations were being established and developed during the course of this study. Only a few existed during the earlier experiments and some have experienced unexpected operational problems. This has resulted in a very heterogeneous fiducial network for the study as a whole, from June 1986 to May 1988. A common reference frame for all of the fiducial stations, SV3, has been calculated by Murray and King [1988] and these fiducial station coordinates have been used in the data analysis, when possible.

Orbits have been treated in three different ways during the data analysis. The data from the JUN86, JAN87, and SEP87 experiments were processed by constraining the coordinates of the tracking stations to their SV3 coordinates and adjusting the Keplerian elements of NSWC satellite ephemerides during the solution. During the MAR88 experiment, tracking station data were not available at the time that the data were processed. In order to bring these orbits into the SV3 system, the best fit coordinates of local GPS stations, which had been determined during the JAN87 and SEP87 experiments, were constrained and the orbits adjusted during the processing of the MAR88 data. For the short GPS ties of the MAY88 experiments, broadcast orbits were used. Tracking data from CIGNET tracking stations were obtained, but were unusable, requiring that the solutions be calculated in the reference frame of the broadcast orbits, WGS-84. Errors between broadcast orbits and precise NSWC orbits, both of which are in the WGS-84 reference frame, have been reported to cause no significant differences greater than the several millimeter level for 5 km long baselines [Davis et al., 1989] and at worst 1 part in $10^6$ with typical values of 0.1 to 0.2 parts in $10^6$ for continental scale baselines [Remondi and Hofmann-Wellenhof, 1989]. This would result in negligible errors in the short ties of the MAY88 experiment.

In order to test the effect of adjusting WGS-84 orbits into the SV3 system on the orientation of the network vector solutions, daily solutions were calculated for three days of observations during the SEP87 experiment using both adjusted orbits from fiducial data in the SV3 system and NSWC orbits. Comparison of the orientations of the networks indicate a slight clockwise rotation of the network and slight length scale changes. But these changes are small, on the order of a few parts in $10^7$, and therefore should not significantly effect the local ties that use the non-adjusted orbits (Table 2-4).

In addition to the direct comparison of individual vectors, an effective deformation resulting from the different orbit sources was calculated from the solutions from the three days of observations. This orbit source deformation, **D**, is modeled as

$$\mathbf{u}_{NSWC} = \mathbf{u}_{SV3} + \mathbf{D}(\mathbf{u}_{SV3} - \mathbf{u}_o) \qquad (2\text{-}18)$$

where **u** is the vector of the geodetic positions in longitude, $\lambda$ , latitude, $\varphi$ , and elevation, h,

$$\mathbf{u} = \begin{bmatrix} \lambda \\ \varphi \\ h \end{bmatrix} \tag{2-19}$$

and **D** is the orbit source deformation matrix

$$\mathbf{D} = \begin{bmatrix} d_{\lambda\lambda} & d_{\lambda\varphi} & 0 \\ d_{\varphi\lambda} & d_{\varphi\varphi} & 0 \\ d_{h\lambda} & d_{h\varphi} & 0 \end{bmatrix} \tag{2-20}$$

the components of D are related to the horizontal deformation matrix $\mathbf{L_o}$ via

$$\mathbf{L}_o = \begin{bmatrix} d_{\lambda\lambda} & \frac{r_p}{r_m} d_{\varphi\lambda} \\ \frac{r_m}{r_p} d_{\lambda\varphi} & d_{\varphi\varphi} \end{bmatrix} \tag{2-20}$$

and to the network tilt, $\tau$, via

$$\tau = \begin{bmatrix} \tau_1 \\ \tau_2 \end{bmatrix} = \begin{bmatrix} \frac{-d_{h\lambda}}{r_p} \\ \frac{-d_{h\varphi}}{r_m} \end{bmatrix} \tag{2-21}$$

The terms involving the shape of the earth, $r_p$ and $r_m$, are given by

$$r_p = \frac{a}{w} \cos \varphi \tag{2-22}$$

$$r_m = \frac{a\left(1 - e^2\right)}{w^3} \tag{2-23}$$

$$w = \left(1 - e^2 \sin^2 \varphi\right)^{\frac{1}{2}} \tag{2-24}$$

where *a* and *e* are the WGS-84 ellipsoid radius and eccentricity, and φ is the latitude of a reference position, $\mathbf{u}_o$. These results are summarized in Table 2-5 in terms of the clockwise network rotation, α,

$$\alpha = \frac{d_{\lambda\varphi} - d_{\varphi\lambda}}{2} \tag{2-25}$$

the direction of minimum extension, β ,

$$\beta = \frac{1}{2} \tan^{-1}\left[\frac{d_{\lambda\varphi} + d_{\varphi\lambda}}{d_{\varphi\varphi} - d_{\lambda\lambda}}\right] \tag{2-26}$$

the strain parallel, ε||, and perpendicular, ε ⊥, to β, and the direction, ζ, and magnitude, δ, of maximum network tilt

$$\zeta = \tan^{-1} \frac{d_{h\lambda}^2}{d_{h\varphi}^2} \tag{2-27}$$

$$\delta = \left[d_{h\varphi}^2 + d_{h\lambda}^2\right]^{\frac{1}{2}} \tag{2-28}$$

These results suggest that different orbit sources can have a several part in $10^7$ effect on these GPS solutions. An effect of this magnitude should not significantly affect the short local ties that use these orbits.

2.3.3.4 Interstation GPS vector adjustment:

After all of the experiments were processed, a set of best fit vectors were obtained through a weighted least squares adjustment of all of the interstation vectors from all of the experiments. All of the individual experimental GPS interstation vector solutions are combined into one set of interstation GPS vectors. This was accomplished by using the daily GPS interstation vector solution from each experiment to solve for earth-centered and earth-fixed cartesian coordinates of each station relative to a fixed station using a weighted least squares algorithm.

The interstation vector model for the station positions of station i and j is

$$\mathbf{x}_i - \mathbf{x}_j = \mathbf{x}_{ij} \qquad (2\text{-}29)$$

where $\mathbf{x}_i$ and $\mathbf{x}_j$ are the position vectors of stations i and j, and $\mathbf{x}_{ij}$ is the interstation GPS vector from station j to station i solved for during the processing of the GPS phase observables.

In matrix form, the equations are

$$\mathbf{Ax} = \mathbf{b} \qquad (2\text{-}30)$$

where **A** is the M X N design matrix, **x** is the vector of unknown station positions of length N, and **b** is the vector of interstation GPS vectors of length M. Explicitly, the equation has the form

$$\begin{bmatrix} 1 & 0 & . & . & . & . & . & . & . & . & . & . & . & 0 \\ 0 & 1 & 0 & . & . & . & . & . & . & . & . & . & . & 0 \\ 0 & 0 & 1 & 0 & . & . & . & . & . & . & . & . & . & 0 \\ . & . & . & . & . & . & . & . & . & . & . & . & . & . \\ 1 & 0 & 0 & -1 & 0 & . & . & . & . & . & . & . & . & 0 \\ 0 & 1 & 0 & 0 & -1 & 0 & 0 & . & . & . & . & 0 \\ 0 & 0 & 1 & 0 & 0 & -1 & 0 & . & . & . & . & 0 \\ . & . & . & . & . & . & . & . & . & . & . & . & . & . \\ 0 & . & 0 & 1 & 0 & . & 0 & -1 & 0 & . & . & 0 \\ 0 & . & . & 0 & 1 & 0 & . & 0 & -1 & 0 & 0 & 0 \\ 0 & . & . & . & 0 & 1 & 0 & . & 0 & -1 & 0 & 0 \\ \\ . & . & . & . & . & . & . & . & . & . & . & . & . & . \end{bmatrix} \begin{bmatrix} x_o \\ y_o \\ z_o \\ . \\ x_i \\ y_i \\ z_i \\ . \\ x_j \\ y_j \\ z_j \\ . \\ . \end{bmatrix} = \begin{bmatrix} x_o \\ y_o \\ z_o \\ . \\ x_{oi} \\ y_{oi} \\ z_{oi} \\ . \\ x_{ij} \\ y_{ij} \\ z_{ij} \\ . \\ . \end{bmatrix} \qquad (2\text{-}31)$$

The first three equations are the reference station coordinates( $x_o$, $y_o$, $z_o$) and the other equations relate the interstation vector from station i to the reference station, and from station j to station i to their respective cartesian coordinates.

Weighted least squares is used to estimate the station positions. Each component of the interstation GPS vector is weighted by the inverse of the formal error for that component of the solution. Variance factors calculated for the individual experiment adjustments and the repeatabilities of each experiment suggest that the formal errors of the GPS22 solutions underestimated the interstation vector component errors. (Appendix B contains the final interstation vector database for all of the experiments with the formal errors scaled by the sigma of unit weight for the data set as a whole.) Figure 2-7 shows a histogram of the standardized residuals of the adjustment.

## 2.4 Summary:

The historical triangulation data set contains approximately 900 direction observations collected in the 1870's, 1890's, 1920's, 1940's, 1950's, and 1960's between the mainland of southern California and the offshore islands. A small number of trilateration observations were made in the early 1970's across the Santa Barbara Channel. GPS interstation vectors have been computed from GPS carrier phase and pseudorange observables. These vectors tie the GPS network to the triangulation and trilateration networks at a precision greater than the historical triangulation observations.

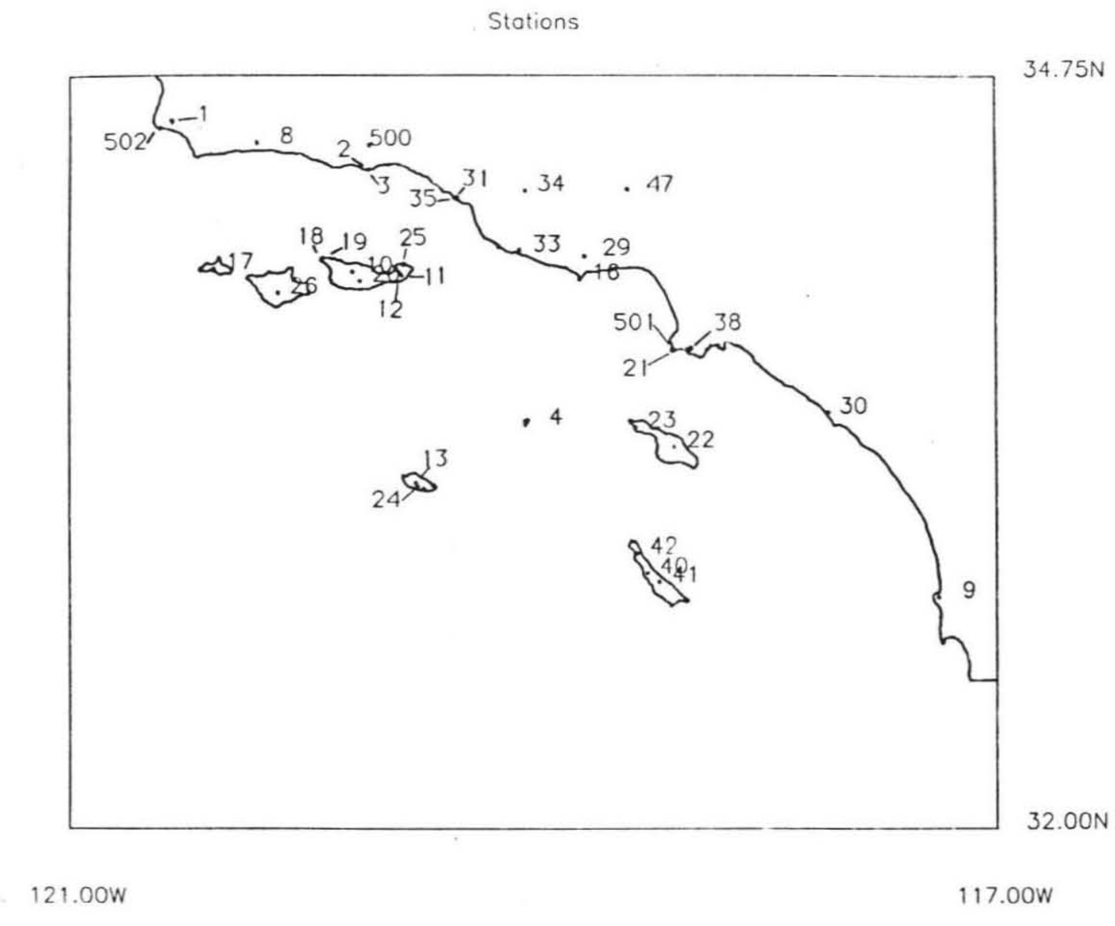


Figure 2-1. Station location map showing the locations of all of the triangulation stations and regional GPS stations used. Numbers refer to stations identified in Table 2-1.

Table 2-1

| Number | ID | Name | Lat | Lon |
|---|---|---|---|---|
| 1 | | ARGUELLO 1875 (destroyed) | 34.583 | 120.561 |
| 2 | | SANTA BARBARA 1857 (destroyed) | 34.405 | 119.715 |
| 3 | sbao | SANTA BARBARA 2 1956 | 34.404 | 119.716 |
| 4 | sbis | SANTA BARBARA ID 2 1940 | 33.472 | 119.041 |
| 8 | gavi | GAVIOTA 1873 | 34.502 | 120.199 |
| 9 | sdad | SOLEDAD 1887 | 32.840 | 117.252 |
| 10 | devl | DEVILS PEAK 2 1951 | 34.029 | 119.784 |
| 11 | high | HIGH 1951 | 34.019 | 119.576 |
| 12 | himt | HIGH MOUNT 1857 | 34.026 | 119.584 |
| 13 | road | ROAD1951 | 33.253 | 119.514 |
| 16 | | POINT DUME 18561947 | 34.002 | 118.807 |
| 17 | nsmi | NEW SAN MIGUEL 1873 (destroyed) | 34.040 | 120.387 |
| 18 | scw2 | SANTA CRUZ WEST 2 1956 | 34.073 | 119.918 |
| 19 | scw1 | SANTA CRUZ WEST 1874 (destroyed) | 34.073 | 119.918 |
| 20 | cent | CENTER 2 1934 | 33.995 | 119.753 |
| 21 | | VICENTE 1951 | 33.741 | 118.411 |
| 22 | | CATALINA PEAK 1876 (destroyed) | 33.387 | 118.401 |
| 23 | west | WEST PEAK 1875 | 33.460 | 118.569 |
| 24 | jack | JACKSON 1951 | 33.240 | 119.505 |
| 25 | scre | SANTA CRUZ EAST 1857 | 34.055 | 119.565 |
| 26 | sole | SOLEDAD 1872 | 33.951 | 120.106 |
| 28 | ctr3 | CASTRO 1898 RM3 | 34.086 | 118.786 |
| 29 | ctro | CASTRO 1898 | 34.086 | 118.786 |
| 30 | nigl | NIGUEL 1884 (destroyed) | 33.512 | 117.734 |
| 31 | chaf | CHAFFEE 2 1923 | 34.301 | 119.331 |
| 33 | lag2 | LAGUNA 2 1951 | 34.109 | 119.065 |
| 34 | scla | SANTA CLARA 1898 | 34.326 | 119.039 |
| 35 | soli | SOLIMAR CADH 1974 | 34.298 | 119.343 |
| 38 | | SAN PEDRO 1853 (destroyed) | 33.746 | 118.336 |
| 40 | bluf | BLUFF 1862 | 32.927 | 118.519 |
| 41 | boul | BOULDER 1862 | 32.896 | 118.468 |
| 42 | harb | HARBOR 1860 | 32.998 | 118.562 |
| 43 | saf3 | SAN FERNANDO 1898 RM3 | 34.330 | 118.601 |
| 46 | l_9a | PICO L-9A LACO 1971 | 34.329 | 118.601 |
| 47 | safo | SAN FERNANDO 1898 (destroyed) | 34.330 | 118.601 |
| 50 | | LAGUNA 1857 (destroyed) | 34.109 | 119.065 |
| 201 | safe | PICO L9-C | 34.330 | 118.601 |
| 202 | smig | NEW SAN MIGUEL RM2 | 34.040 | 120.387 |
| 203 | scrw | SANTA CRUZWEST 1923 RM2 | 34.073 | 119.918 |
| 204 | sba2 | Temp GPS mark (destroyed) | 34.405 | 119.717 |
| 205 | cato | SOSTICE CYN B2 AUX | 34.086 | 118.786 |
| 206 | nigu | NIGUEL 1884 A | 33.515 | 117.730 |
| 207 | twin | TWIN | 33.232 | 119.479 |
| 208 | cotr | COTAR | 34.120 | 119.154 |
| 209 | ctr1 | CASTRO PEAK RM1 | 34.086 | 118.786 |
| 210 | nigb | NIGUEL 1884 B | 33.514 | 117.730 |
| 211 | sbat | Temp.survey station (destroyed) | 34.404 | 119.716 |
| 212 | sba5 | SANTA BARBARA 2 1956 RM5 | 34.404 | 119.716 |
| 500 | lacu | La Cumbre Peak GPS | 34.494 | 119.714 |
| 501 | pver | PVER7268(SV3) | 33.744 | 118.404 |
| 502 | vndn | VNDNRM1(SV3) | 34.556 | 120.616 |
| 503 | brus | BRUSH(NGS), Catalina Island | 33.407 | 118.405 |
| 701 | algo | ALGORMA3(SV3) | 45.763 | 78.073 |
| 702 | aust | AUSTGPS(SV3) | 30.144 | 97.756 |
| 703 | chur | CHURGPS(SV3) | 58.588 | 94.088 |
| 704 | ftdv | FTDRM4(SV3) | 30.468 | 103.947 |
| 705 | ftor | FTOR7266(SV3) | 36.486 | 121.773 |
| 706 | moja | GOLDUTEX(SV3) | 35.150 | 116.888 |
| 707 | moj1 | GOLDNCMN1(SV3) | 35.150 | 116.891 |
| 708 | ovro | OVRO7114(SV3) | 37.047 | 118.294 |
| 709 | plat | PLAT7258(SV3) | 39.993 | 104.726 |
| 710 | rich | RICHGPS(SV3) | 25.464 | 80.384 |
| 711 | vslr | VNDN7880(SV3) | 34.376 | 120.616 |
| 712 | hayo | HAYOCP3(SV3) | 42.431 | 71.488 |
| 713 | wsfd | WESTGPS(SV3) | 42.421 | 71.493 |
| 714 | yknf | YELLGPS(SV3) | 62.319 | 114.469 |

Table 2-1. This table lists the station names, identification numbers, and 4-character ID's corresponding to the locations marked in Figure 2-1. Stations without a 4-character ID are not tied to the GPS network. SV3 indicates that the station was used as a fiducial station during the GPS processing, if the GPS data were available and that the station coordinates were held fixed in the SV3 reference system of Murray and King [1988].

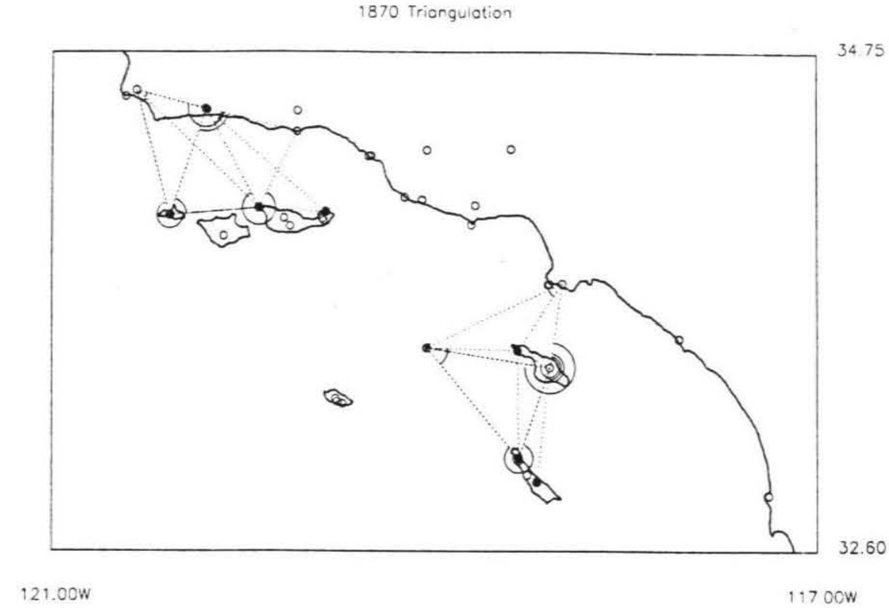


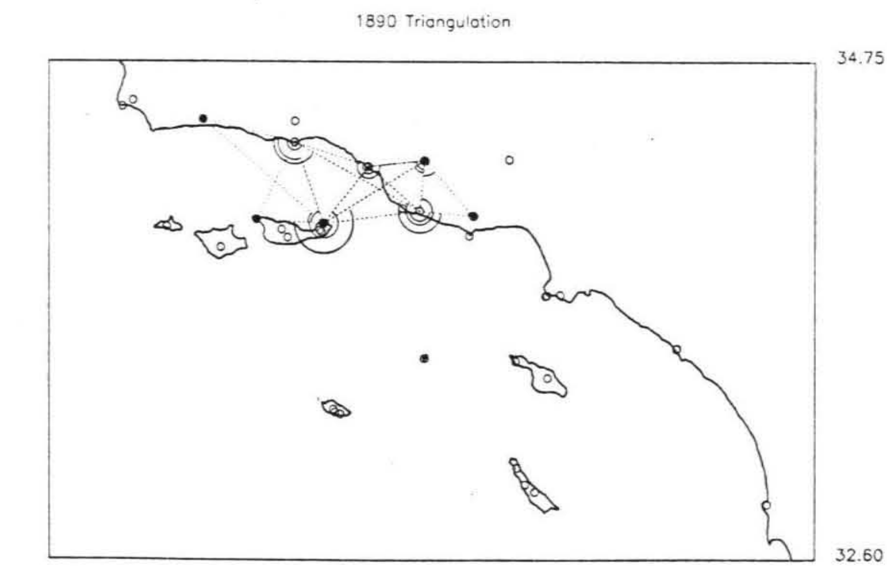


Figure 2-2 The maps show the distribution of the geodetic observations with time. A solid circle indicates that the station is tied to the GPS network. The dotted lines and arcs indicate the observed directions.

*1870's and 1890's triangulation* - The survey networks were first established during the mid- to late- 1800's. During this period, stations were established along the coast of southern California and on the offshore islands. The offshore networks were fairly sparse with observations in the Santa Barbara channel area and among the islands of the Continental Borderland. Almost all of the observations from the Santa Barbara channel have standard errors of 1.2 arc seconds (i.e. mostly third order ). However, some of the observations are less precise with standard errors of 2.1 arc seconds. Almost all of the

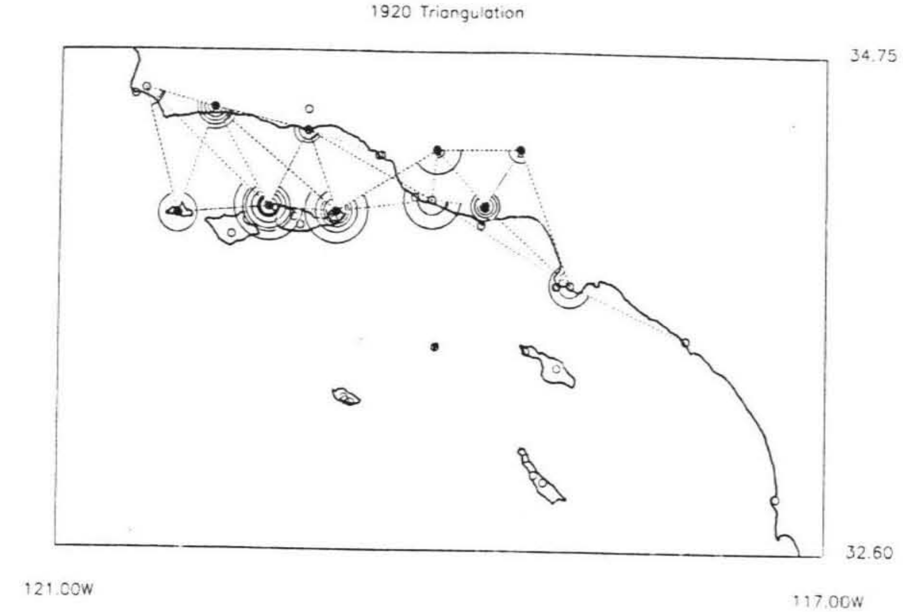


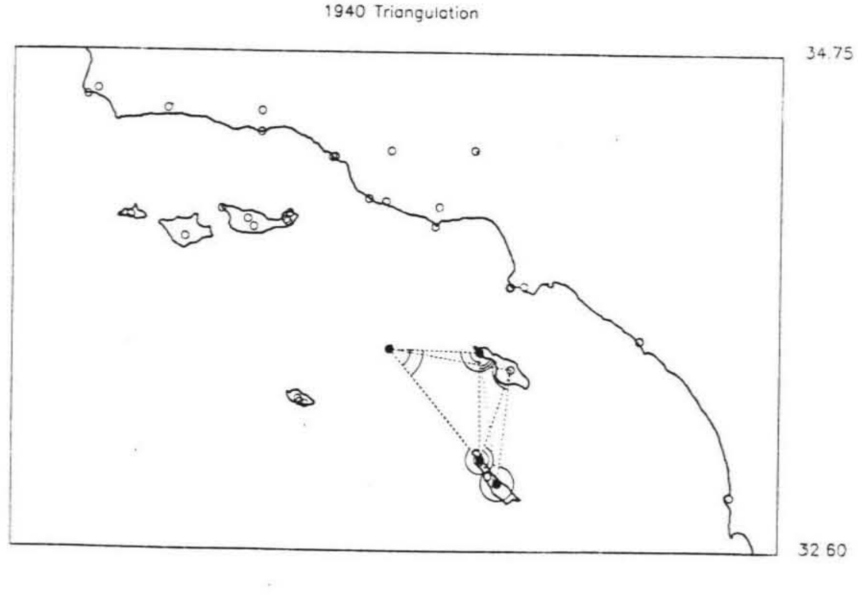


observations from the Continental Borderland have standard errors of 2.1 arc seconds; the other two are third order.

*1920's triangulation* - The surveys of the 1920's observed many of the stations surveyed during the 1800's in the Santa Barbara Channel, but none in the Continental Borderland. The observations are almost entirely first and second order with standard errors of 0.6 and 0.7 arc seconds, respectively.

*1940's triangulation* - The survey of the 1940's was a first order reoccupation of the marks on Santa Catalina and San Clemente islands since the the surveys of the late 1800's. A new mark was established on Santa Barbara Island that was not tied to the older network.

1950 Triangulation

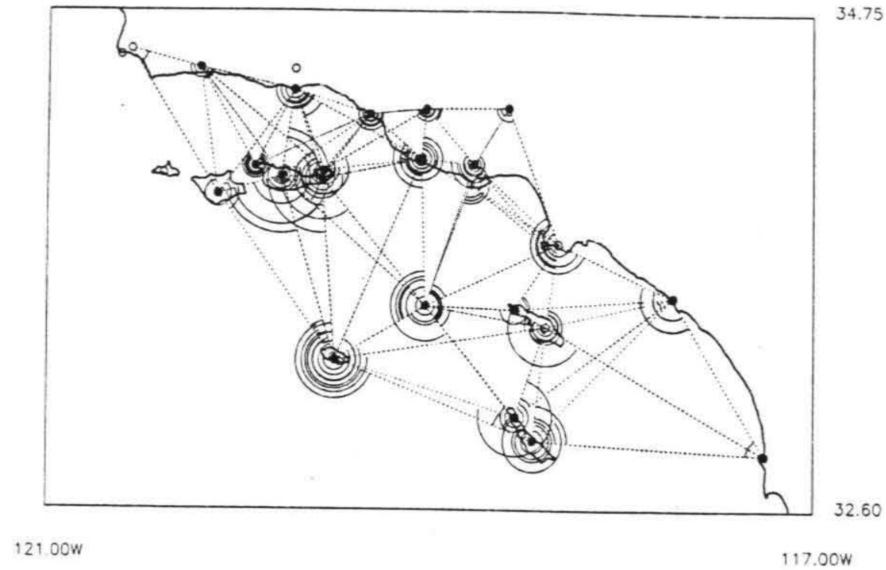


1960 Triangulation

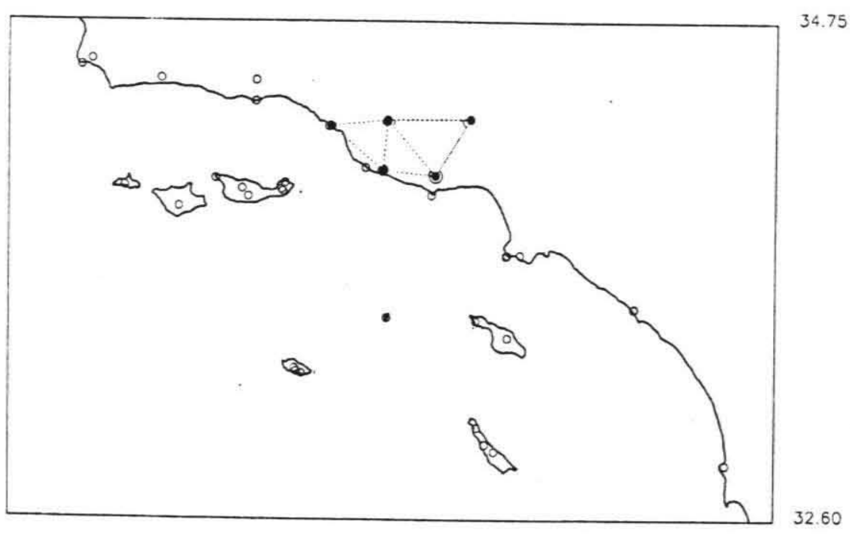


*1950's triangulation* - This is the most complete and extensive first order triangulation survey. The entire offshore area was covered during this survey from Point Arguello to La Jolla and out to San Nicolas Island. Many stations were reoccupied for the first time since they were established in the late 1800's. Some of the marks at these stations had been destroyed or obstructions had been built making the original mark, if it remained, unusable. At these stations new marks were established. The new marks were not necessarily tied to the original marks, resulting in a loss of the original data history.
*1960's triangulation* - The survey of the 1960's was a first order reoccupation of the marks in the Oxnard Plain area

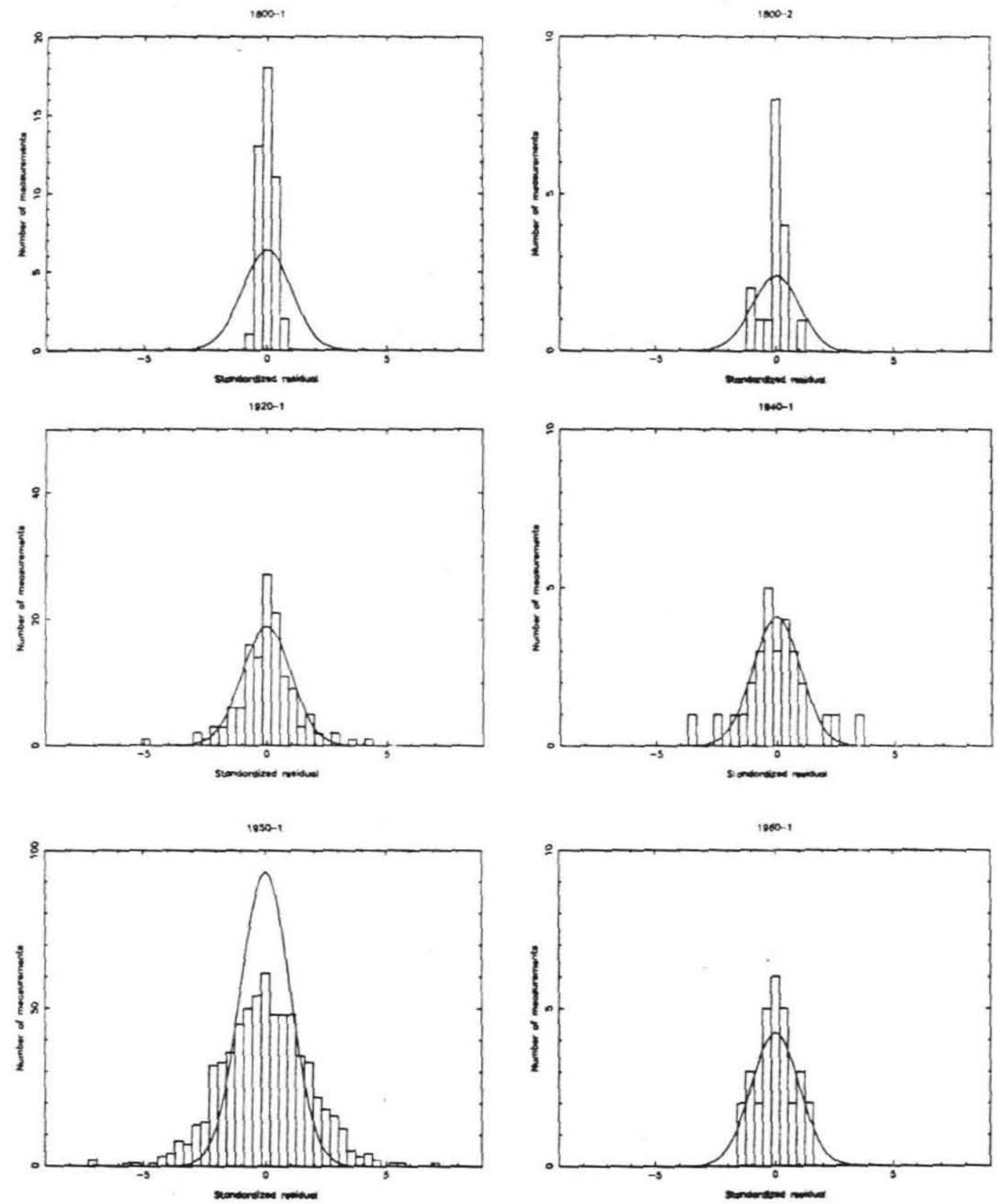


Figure 2-3 The quality of each of the triangulation surveys was evaluated by performing a network adjustment on the data from each survey. Because of the limited temporal overlap and the low precision of the surveys from the 1870's and 1890's, observations from these surveys were adjusted together as two independent networks: 1800-1 and 1800-2, for the Santa Barbara channel and Continental Borderland networks, respectively. The results of the adjustments are shown in Table 4. a) Histograms of the standardized residuals for each of the network adjustments are shown. The x-axes are in units of the standard error, $\sigma$, of the adjusted value. The solid line plotted on the

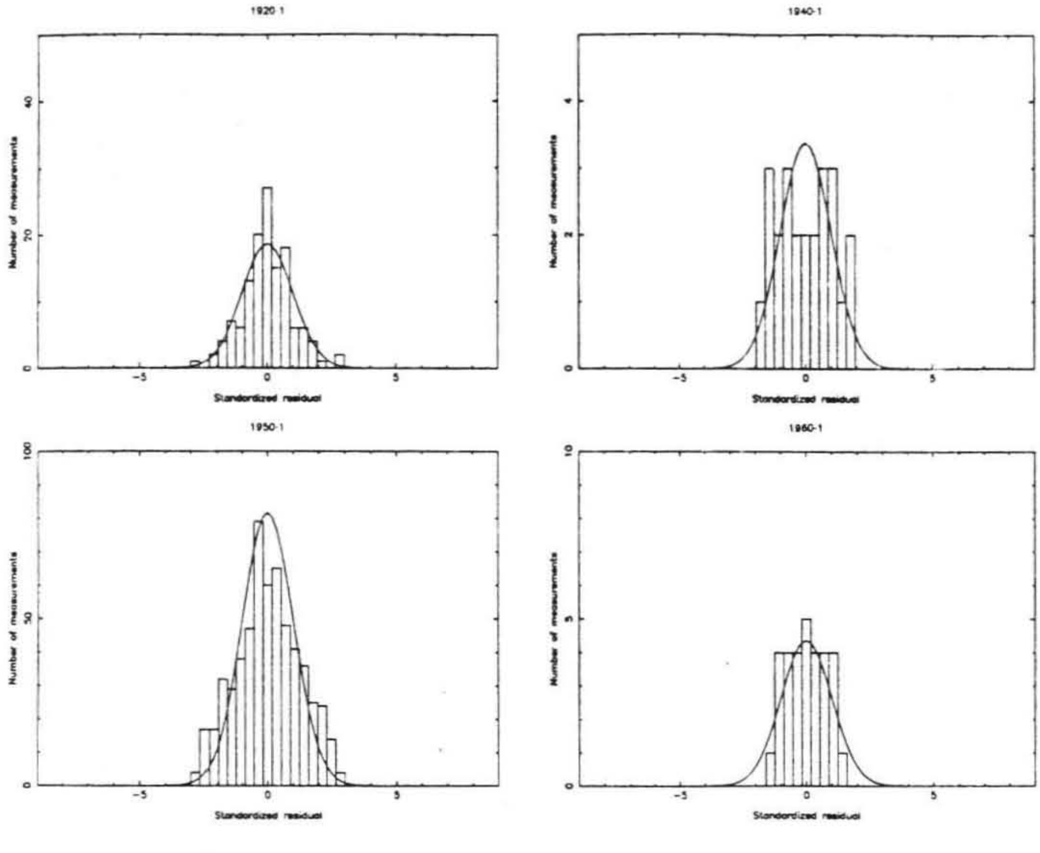


histograms is a Gaussian distribution. Note that almost every survey has highly improbable adjusted values $>3\sigma$. (The triangulation of the 1960's contains 4 adjusted values $>10\sigma$ that are not shown.) These observations are considered to be possible blunders within the data set. b) Histograms for a sub-set of the triangulation observations in which only observations with adjustments $<3\sigma$ were retained.

Table 2-2
Summary of triangulation survey adjustments

| Period | Stations | Directions | DOF | $\chi 2$ | $\sigma_o^2$ |
|---|---|---|---|---|---|
| 1800-1 | 10 | 38 (37) | 13 (12) | 1.0 (0.7) | 0.08 (0.06) |
| 1800-2 | 6 | 14 (14) | 3 (3) | 1.6 (1.6) | 0.54 (0.54) |
| 1920 | 11 | 131 (129) | 72 (70) | 110.9 (66.7) | 1.54 (0.93) |
| 1940 | 5 | 26 (24) | 12 (10) | 23.7 (10.5) | 1.98 (1.05) |
| 1950 | 27 | 659 (580) | 363 (307) | 1096.7 (474.6) | 3.02 (1.55) |
| 1960 | 6 | 31 (29) | 11 (9) | 5.8 (5.5) | 0.52 (0.61) |
| (1960 | 6 | 34 | 11 | 132.2 | 10.15) |

Table 2-2. DOF is the number of degrees of freedom during the adjustments. $\sigma_o^2$ is the reduced $\chi^2$ for the adjustment. 1800-1 is data from the Santa Barbara Channel, 1800-2 is data from the Continental Borderland. The values for 1960 in parentheses are for the survey data set that includes four rejected observations with standardized residuals > $10\sigma$ that are not show in Figure 2-3. The other values in parentheses are for the reduced data set in which data outliers > $3\sigma$ and unconstrained observations have been removed.

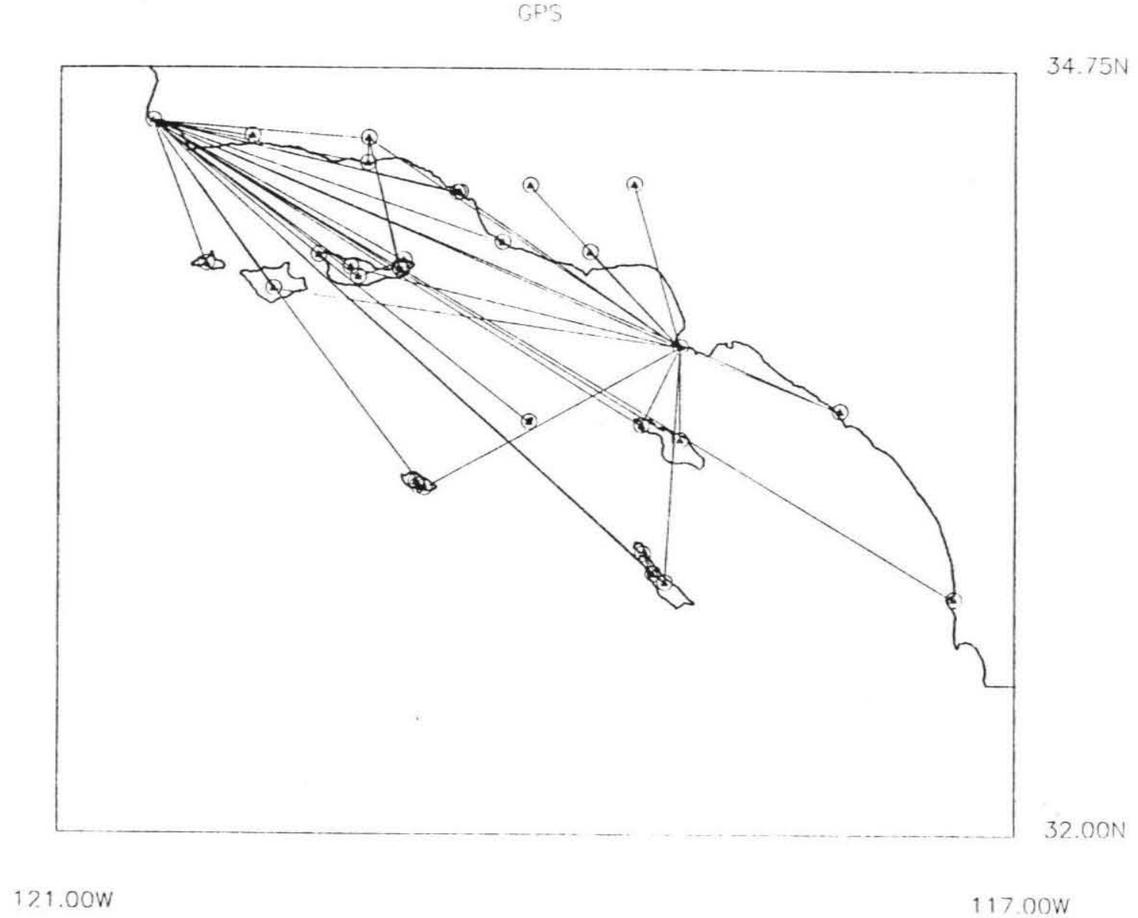


Figure 2-4. The solid lines connecting stations indicate the baselines estimated from the six GPS experiments conducted between 1986 and 1988 summarized in Table 2-6.

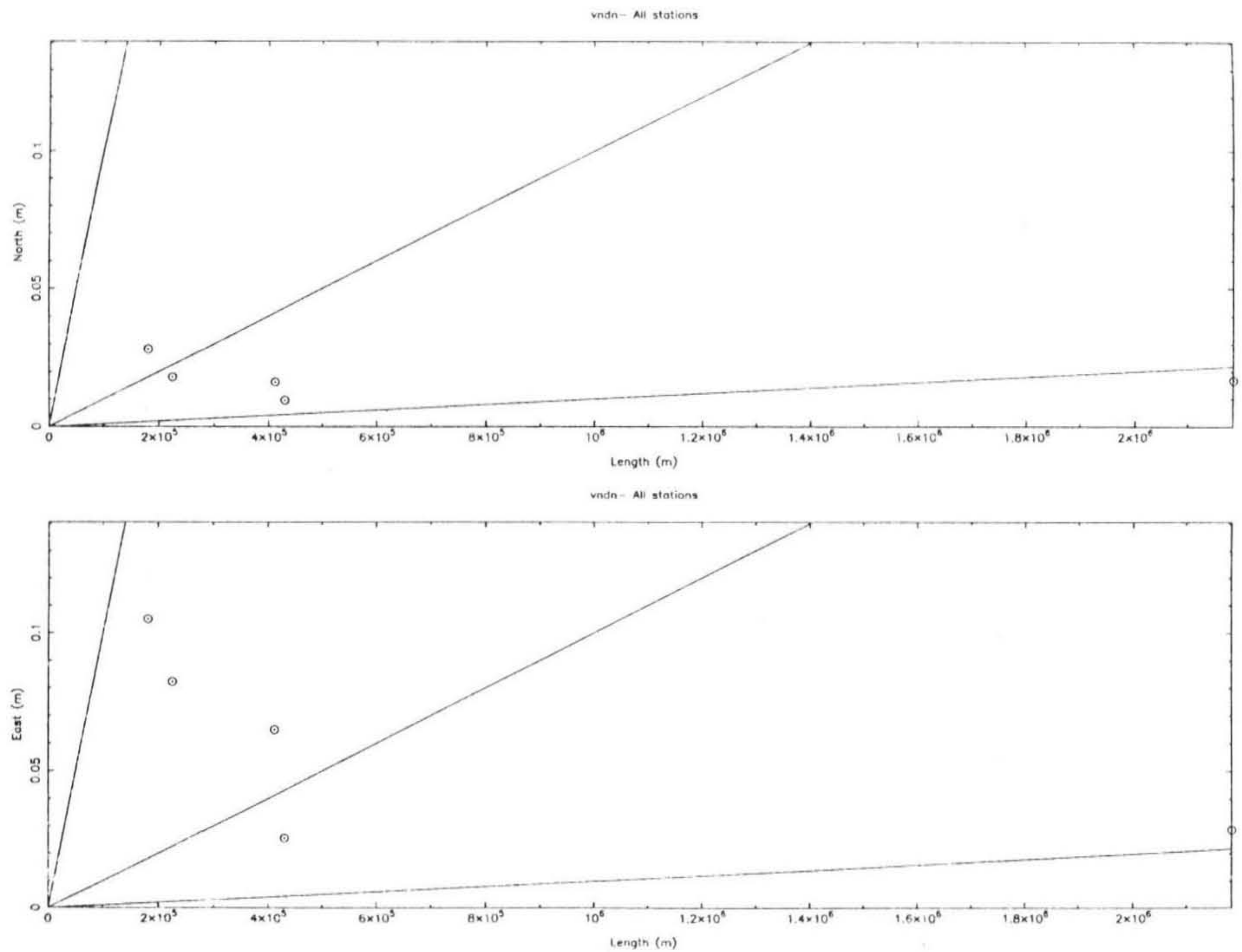


Figure 2-5. North, east, up, and length repeatability plots for the GPS experiments. Lines of constant repeatability are plotted for 1 part in $10^6$, $10^7$, and $10^8$. a) JUN86

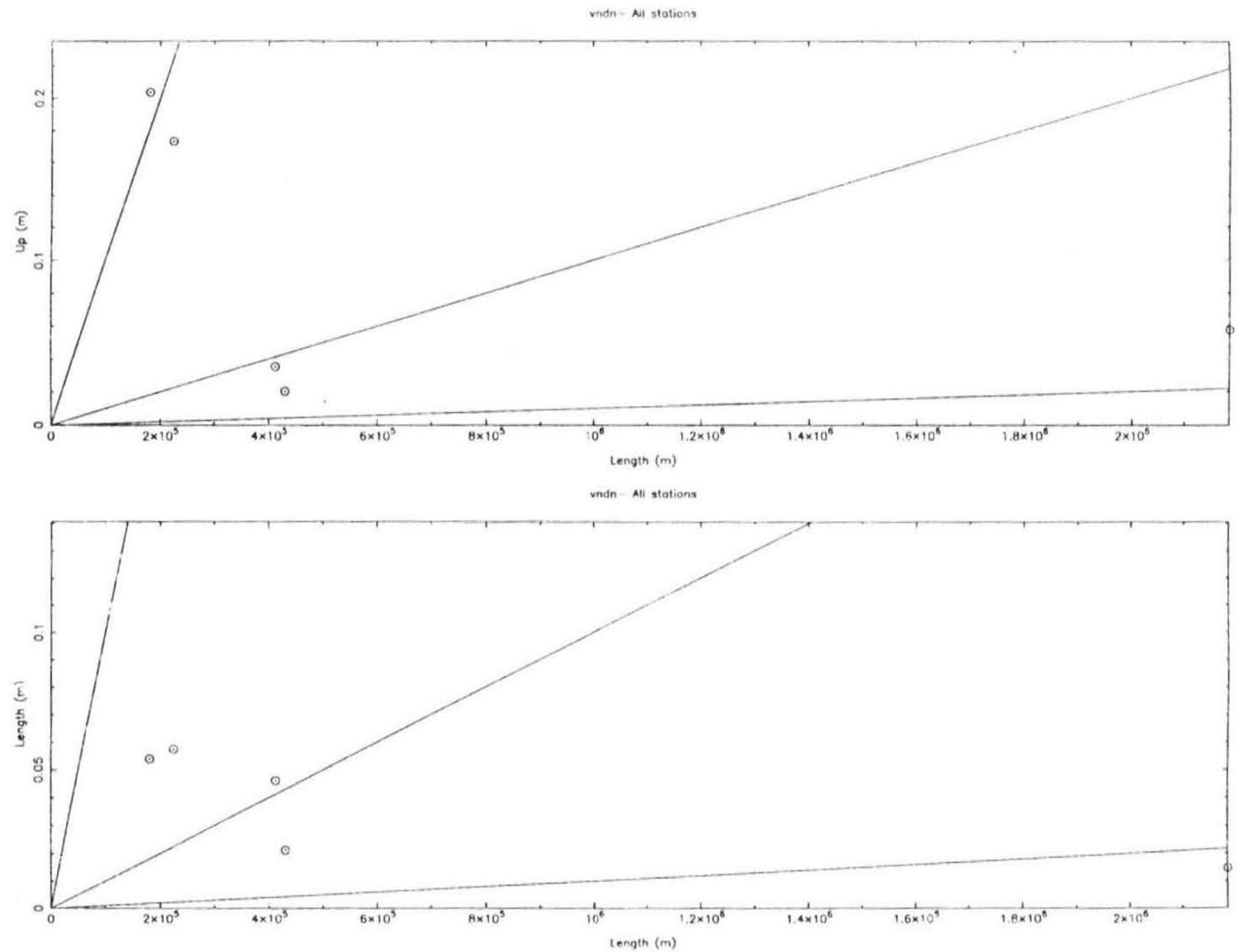
vndn – All stations
Up (m)
Length (m)
vndn – All stations
Length (m)
Length (m)

Fig. 2-5a (cont.)

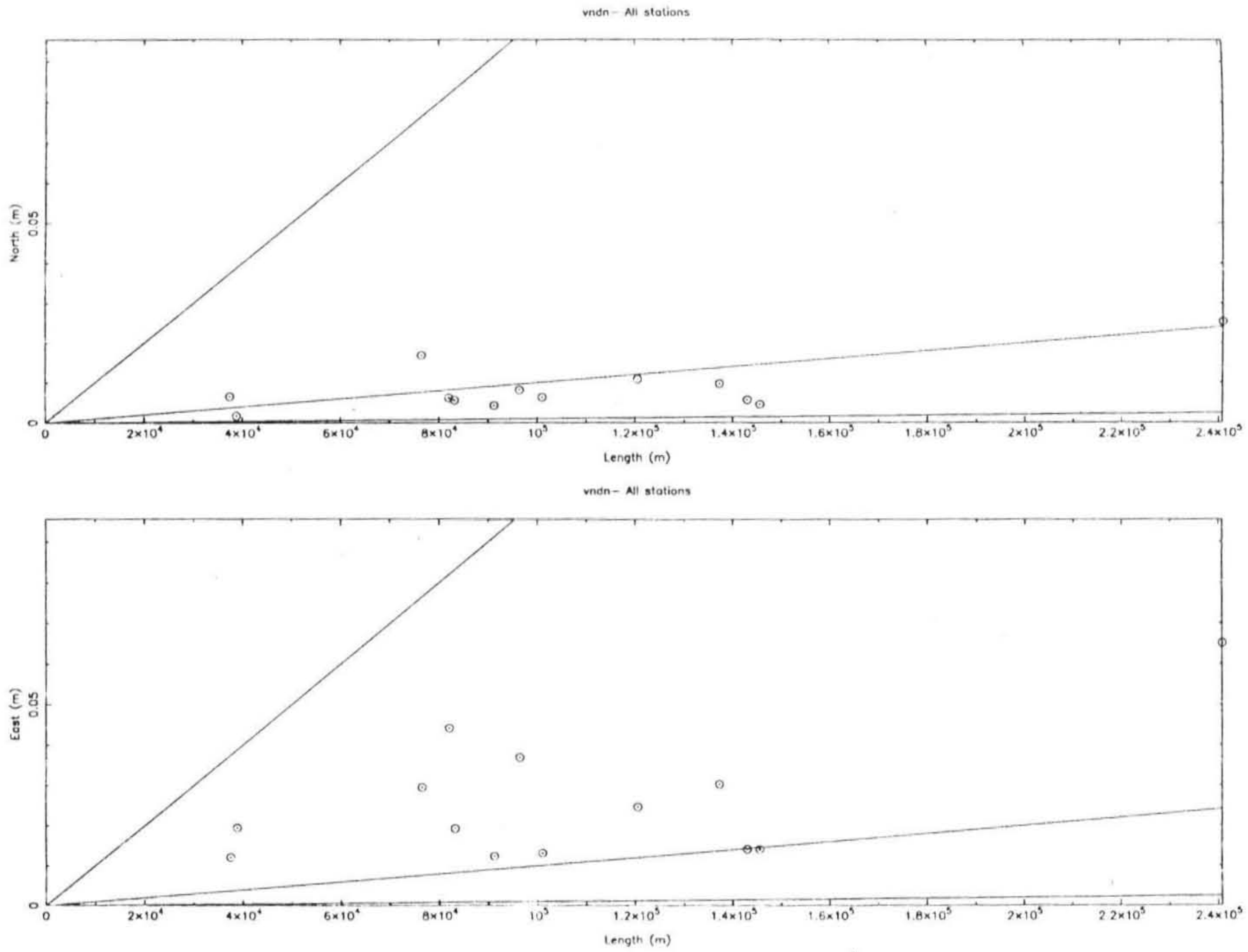


Fig. 2-5b JAN87

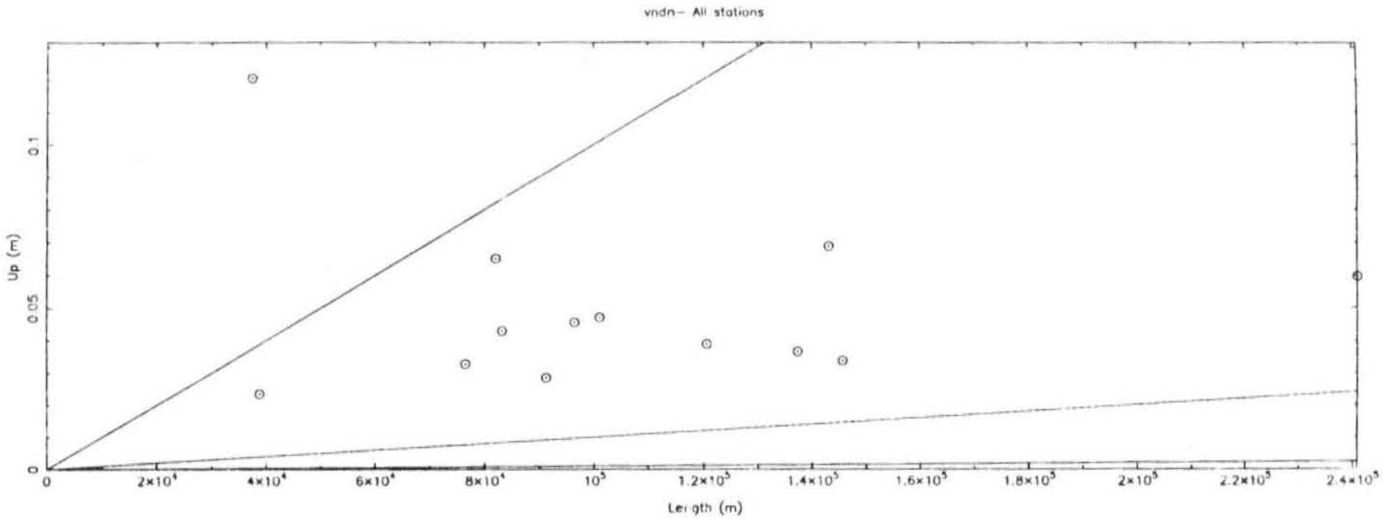
vndn– All stations
Up (m)
0
0.05
0.1
0
2×10⁴
4×10⁴
6×10⁴
8×10⁴
10⁵
1.2×10⁵
1.4×10⁵
1.6×10⁵
1.8×10⁵
2×10⁵
2.2×10⁵
2.4×10⁵
Length (m)

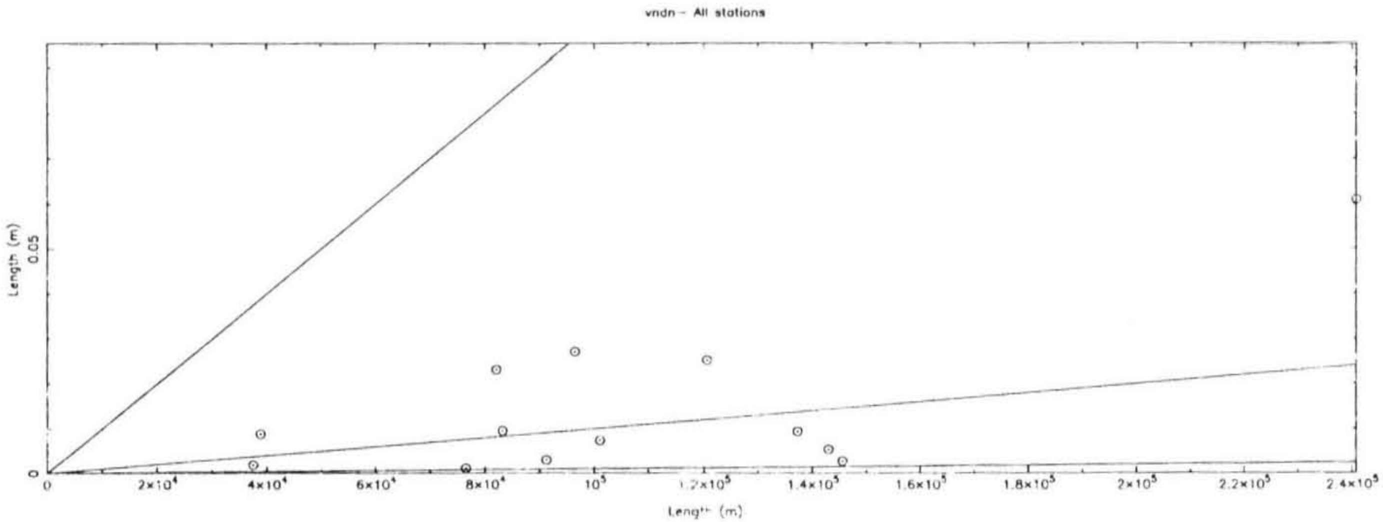
vndn– All stations
Length (m)
0
0.05
0
2×10⁴
4×10⁴
6×10⁴
8×10⁴
10⁵
1.2×10⁵
1.4×10⁵
1.6×10⁵
1.8×10⁵
2×10⁵
2.2×10⁵
2.4×10⁵
Length (m)

Fig. 2-5b (cont.)

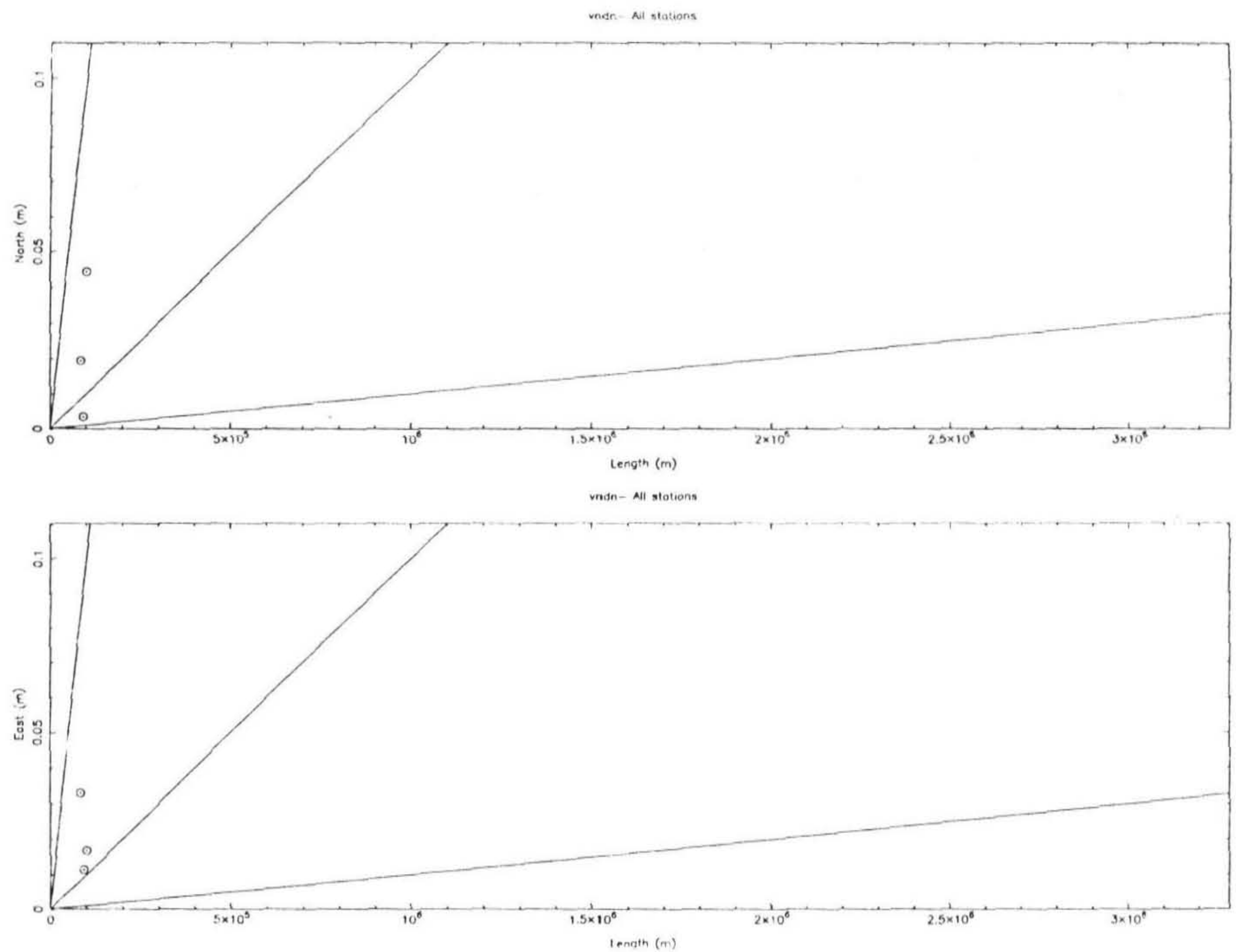


Fig. 2-5c SEP87

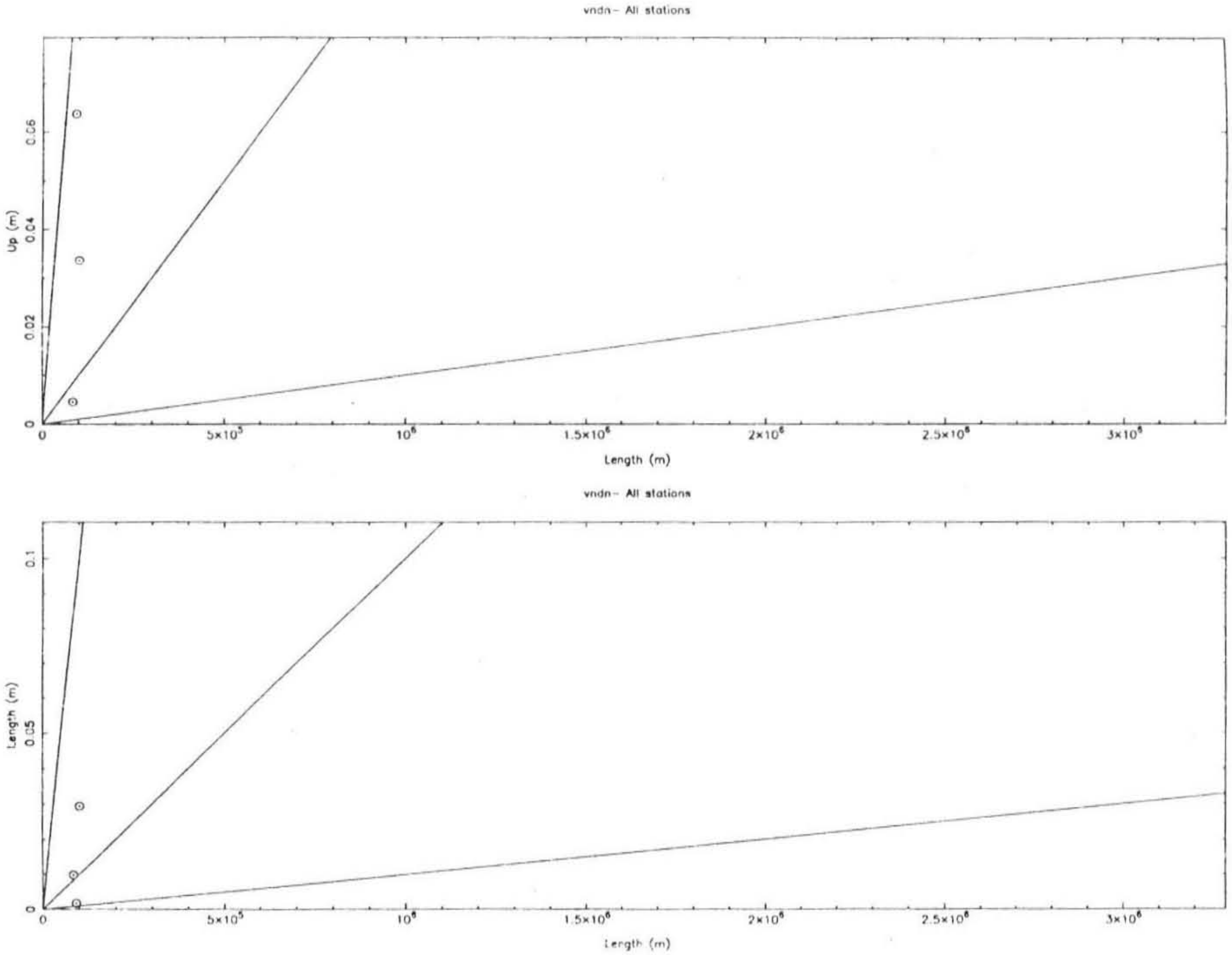
vndn- All stations
Up (m)
0
0.02
0.04
0.06
0
5×10^5
10^6
1.5×10^6
2×10^6
2.5×10^6
3×10^6
Length (m)
vndn- All stations
Length (m)
0
0.05
0.1
0
5×10^5
10^6
1.5×10^6
2×10^6
2.5×10^6
3×10^6
Length (m)

Fig. 2-5c (cont.)

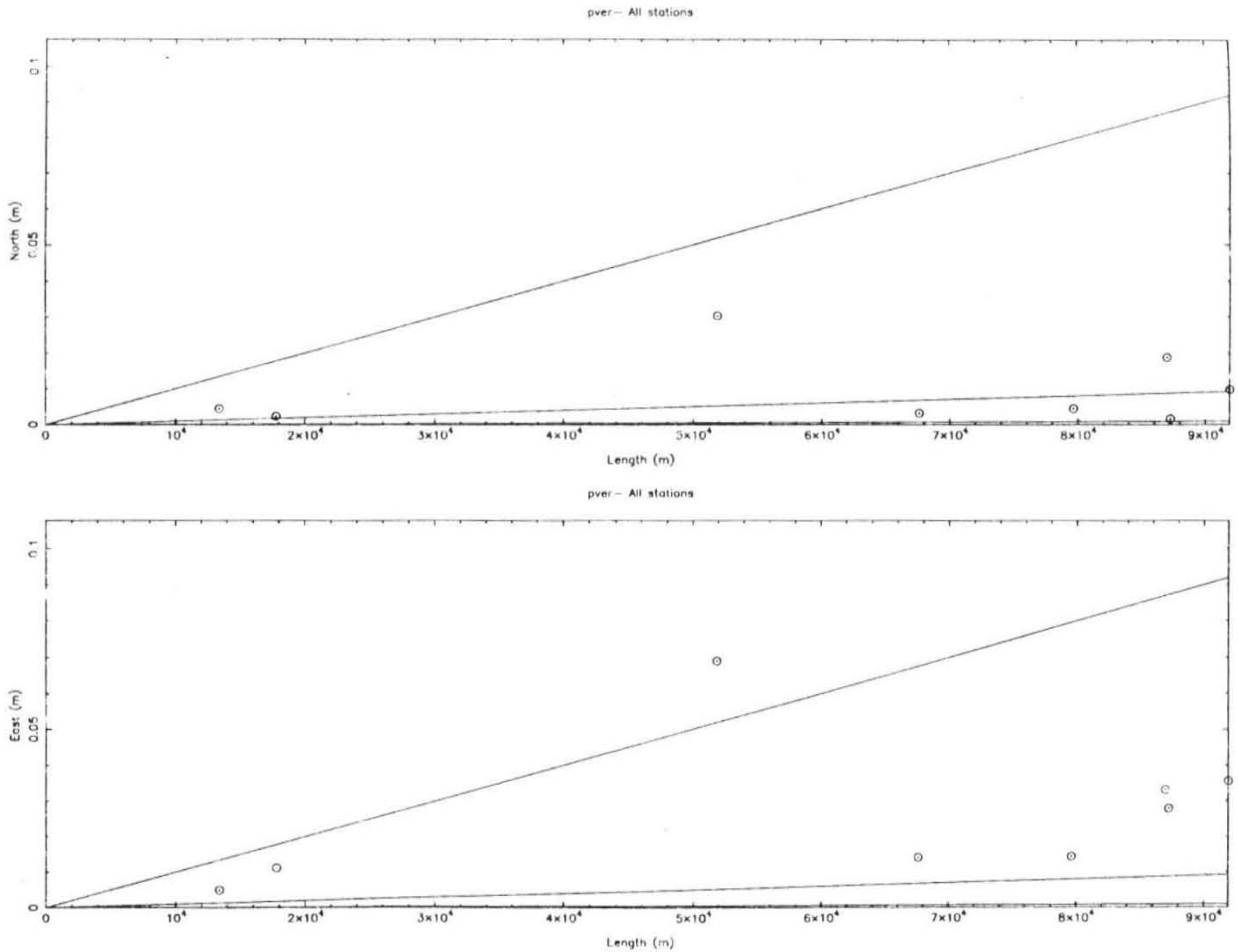


Fig. 2-5d OCT87

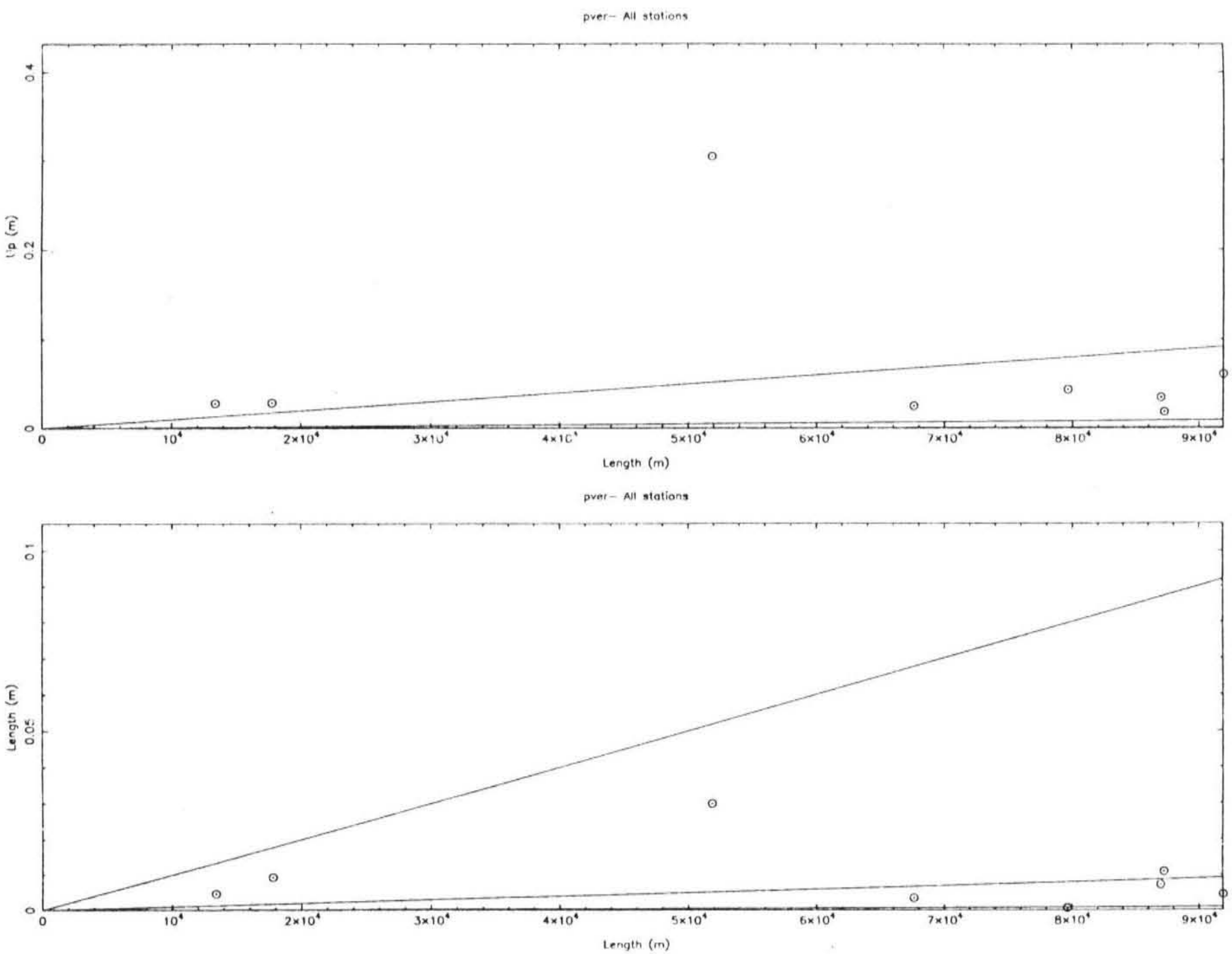
pver– All stations
Up (m)
0
0.2
0.4
Length (m)
0
10⁴
2×10⁴
3×10⁴
4×10⁴
5×10⁴
6×10⁴
7×10⁴
8×10⁴
9×10⁴
pver– All stations
Length (m)
0
0.05
0.1
Length (m)
0
10⁴
2×10⁴
3×10⁴
4×10⁴
5×10⁴
6×10⁴
7×10⁴
8×10⁴
9×10⁴

Fig. 2-5d (cont.)

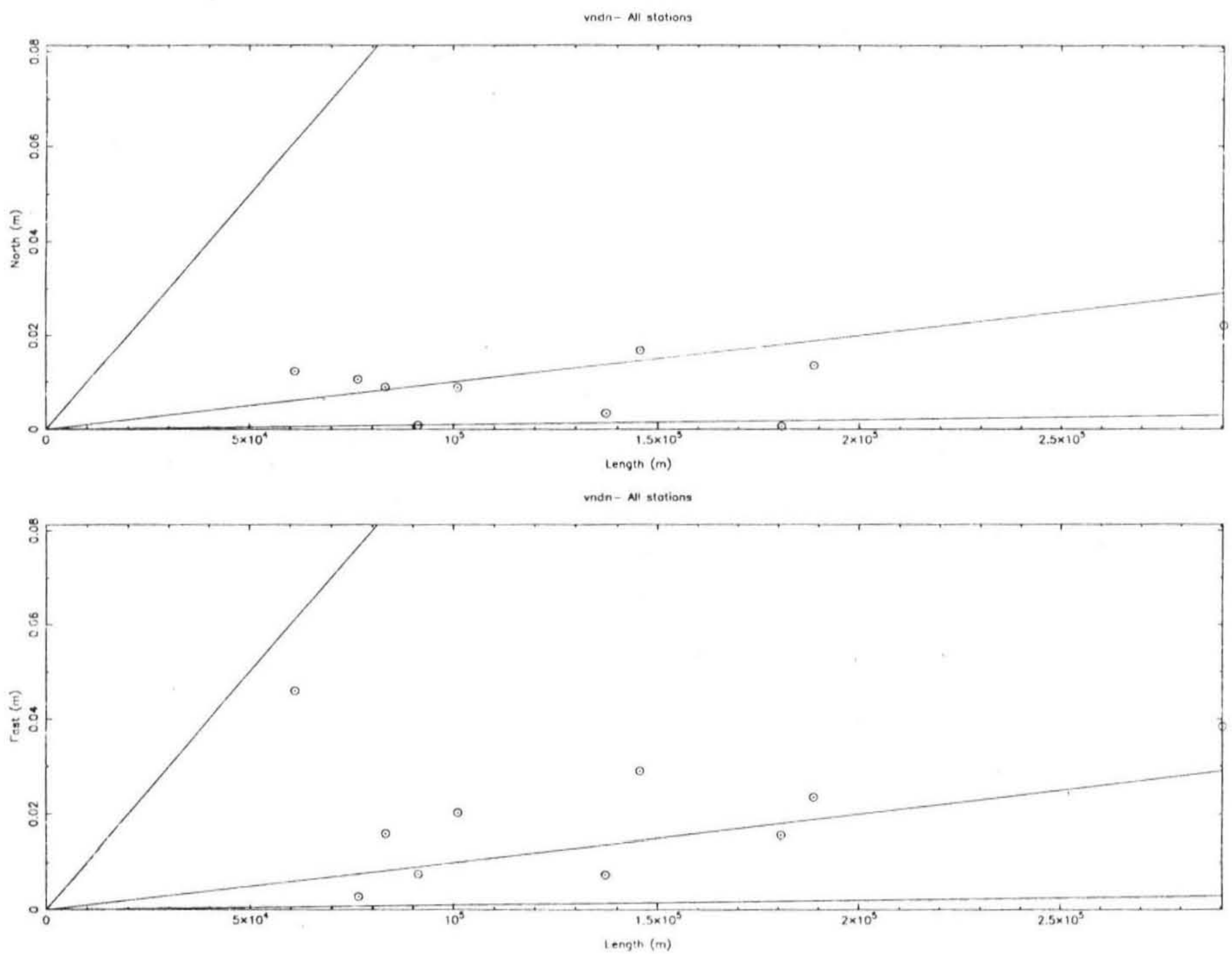


Fig. 2-5e MAR88

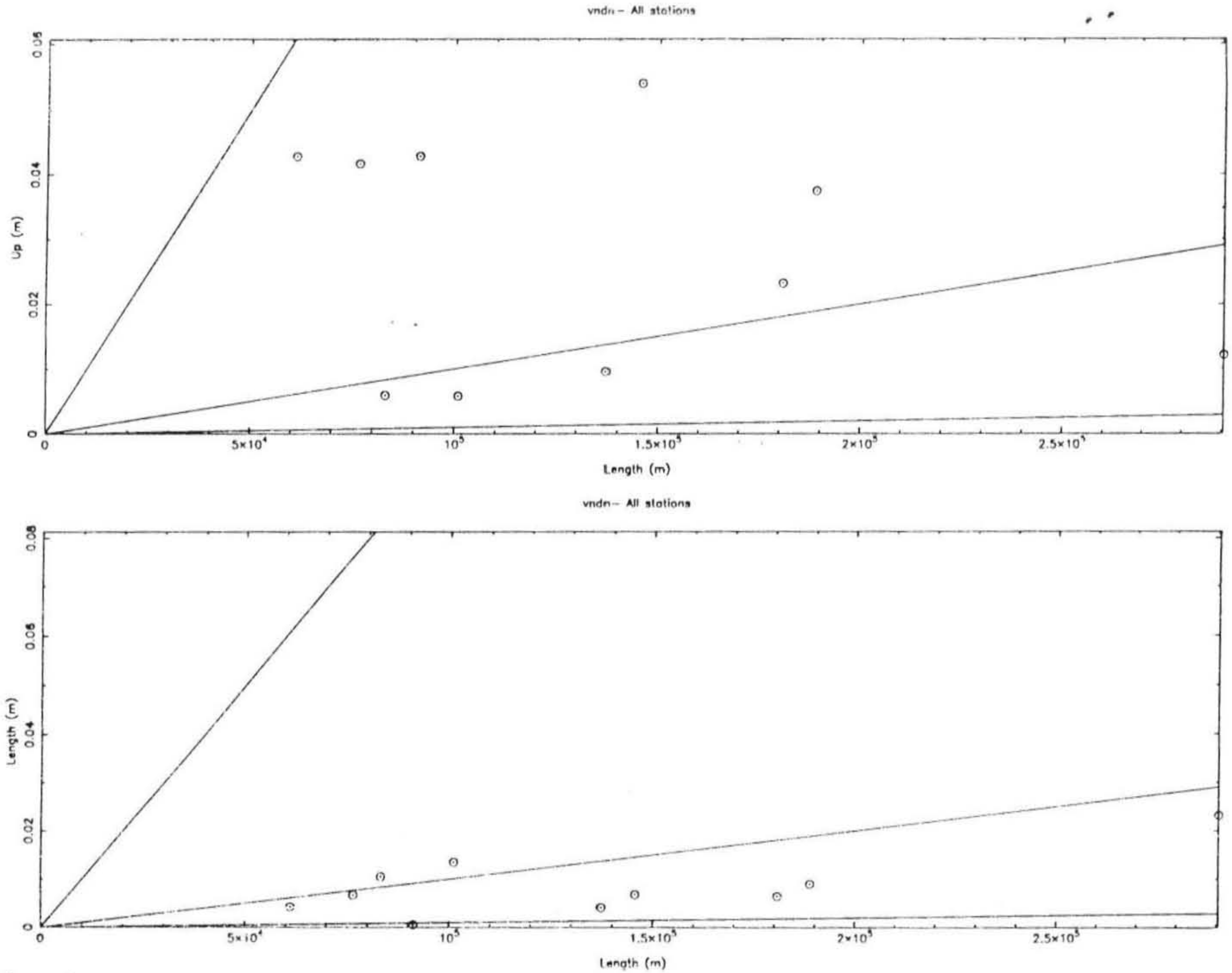

vndn – All stations
Up (m)
0
0.02
0.04
0.06
0
5×10^4
10^5
1.5×10^5
2×10^5
2.5×10^5
Length (m)
vndn – All stations
Length (m)
0
0.02
0.04
0.06
0.08
0
5×10^4
10^5
1.5×10^5
2×10^5
2.5×10^5
Length (m)


Fig. 2-5e (cont.)

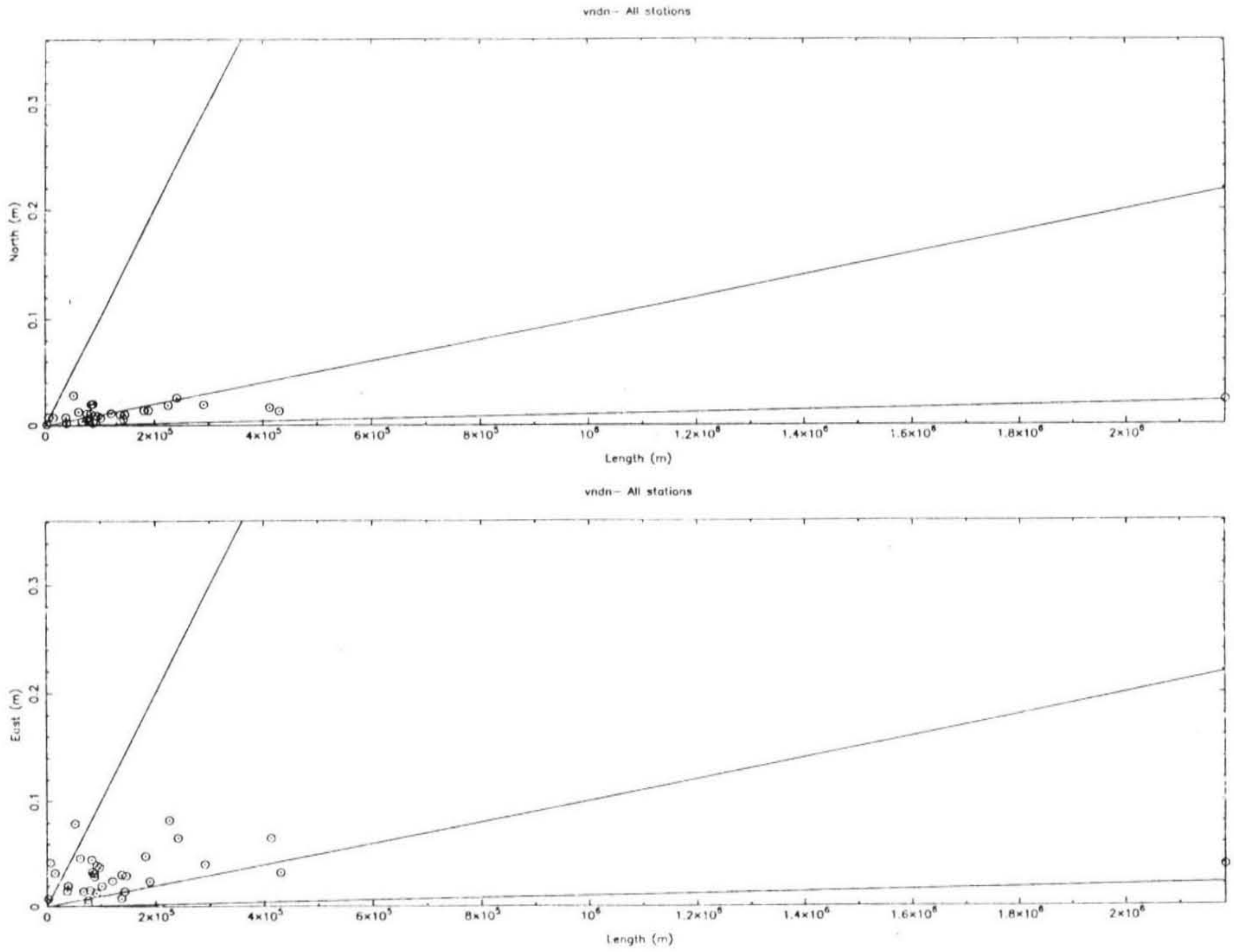


Fig. 2-5f All experiment baselines combined.

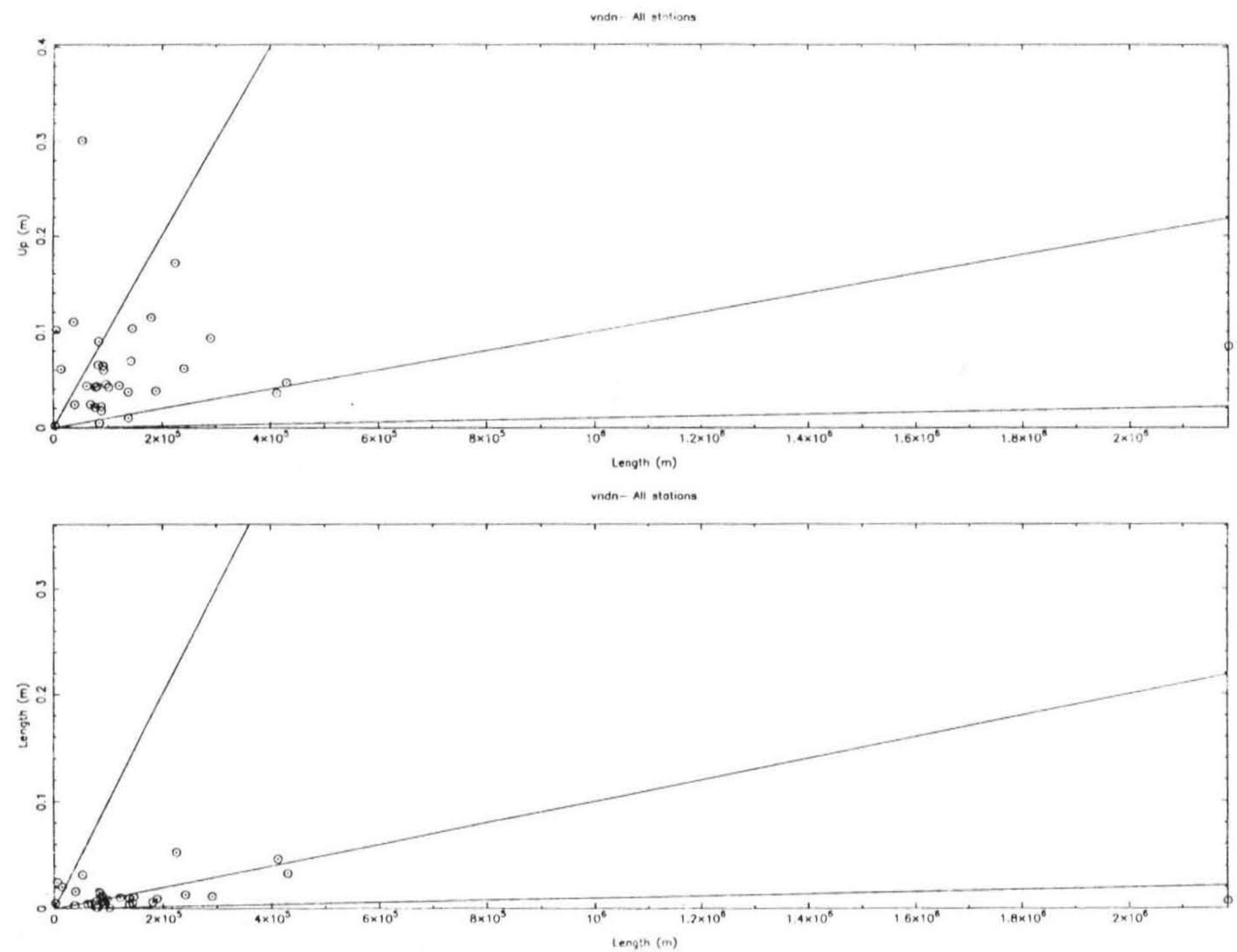
vndn - All stations
Up (m)
Length (m)
vndn - All stations
Length (m)
Length (m)

Fig. 2-5f (cont.)

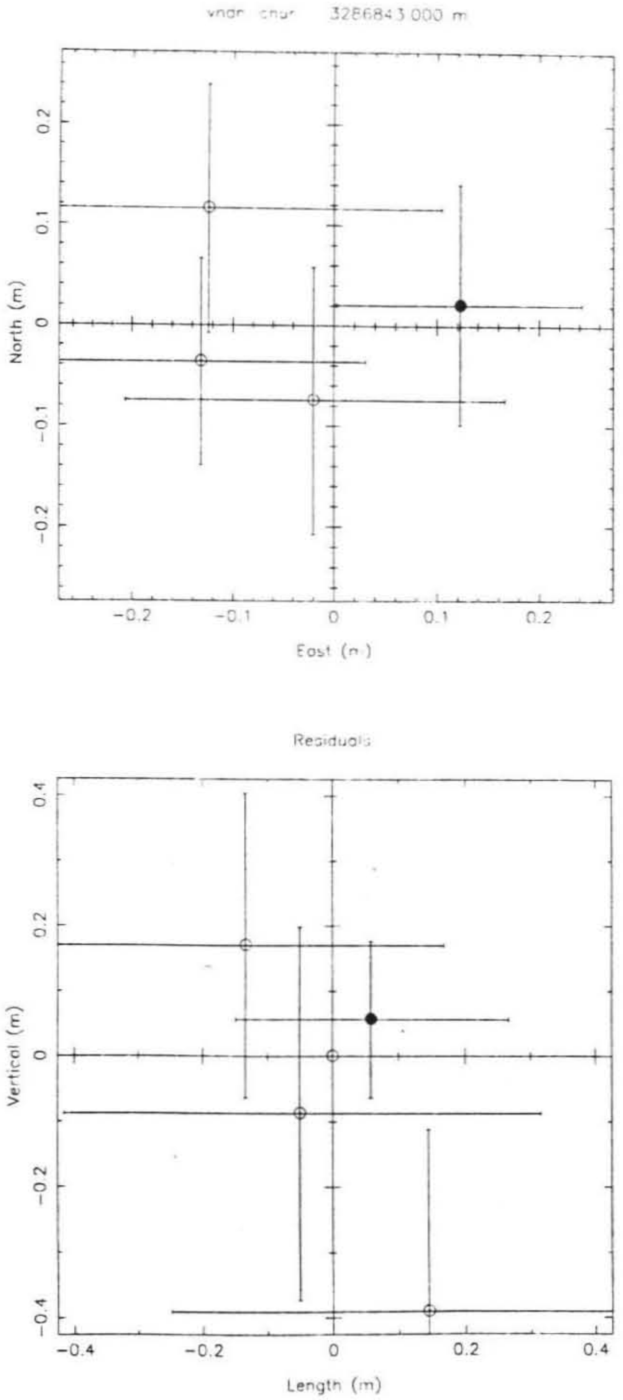


Figure 2-6. VNDN-CHUR vectors from SEP87 (open circles) plotted with SV3 VNDN-CHUR vector (solid circle) plotted against weighted mean in a) vertical and length, and b) north and east. Error bars are 2-sigma errors. SEP87 vector errors are weighted by the variance factor for the experiment. Scatter suggests several parts in $10^8$ to a few parts in $10^7$ agreement among data and reference frame, on this long (> 3200 km) baseline.

| Baseline | $days_{GPS}$ | length $_{GPS}$ (m) | $\Delta$ length $_{EDM-GPS}$ (m) | $\Delta$length (ppm) | number of EDM obs. |
|---|---|---|---|---|---|
| CHAF-SOLI | 1 | 1154.120 (0.007) | -0.004 (0.022) | 3.6 | 1 |
| ROAD-JACK | 2 | 1653.546 (0.025) | 0.002 (0.025) | 1.2 | 9 |

Table 2-3. Differences between mean GPS lengths for two short baselines and EDM lengths. EDM observations are from the REDEAM data set. Numbers in ( ) are the formal errors.

| Baseline | $days_{GPS}$ | length $_{SV3}$ (m) | Δ length $_{NSWC-SV3}$ (m) | Δlength (ppm) | Δ Azimuth |
|---|---|---|---|---|---|
| VNDN-BLHL | 3 | 91174.228 (0.010) | -0.009 (0.015) | 0.10 | 0.17 (0.10) |
| VNDN-CENT | 3 | 100986.581 (0.017) | 0.010 (0.014) | 0.10 | 0.10 (0.20) |
| VNDN-SCRW | 2 | 83674.818 (0.013) | 0.004 (0.015) | 0.05 | 0.02 (0.20) |
| VNDN-SCRE | 2 | 111637.919 (0.013) | -0.033 (0.014) | 0.30 | 0.18 (0.10) |

Table 2-4. Differences between NSWC orbits and SV3 adjusted NSWC orbits for SEP87 experiment. Values are based on multi-day vector adjustments for both the NSWC and SV3 orbit daily solutions. Azimuth difference is in micro radians of clockwise rotation. Numbers in ( ) are the formal errors..

| DOY $_{NSWC-SV3}$ | $\alpha$ | $\beta$ | $\varepsilon \parallel$ | $\varepsilon \perp$ | $\zeta$ | $\delta$ |
|---|---|---|---|---|---|---|
| 266 | 0.17 (0.09) | -30. (15.) | -0.16 (0.12) | 0.22 (0.12) | 57. (47.) | 0.18 (0.16) |
| 267 | 0.19 (0.08) | -50. (16.) | -0.16 (0.07) | 0.12 (0.14) | 50. (42.) | 0.13 (0.13) |
| 269 | 0.02 (0.10) | 56. (25.) | -0.12 (0.15) | 0.10 (0.12) | -163. ( 11.) | 0.25 (0.20) |

Table 2-5. Differences between NSWC orbits and SV3 adjusted NSWC orbits for three days during SEP87 experiment in terms of equivalent network μstrain. $\alpha$ is the clockwise network rotation in μradians, $\beta$ is the direction of minimum extension, $\varepsilon \parallel$ is the mstrain parallel to $\beta$, $\varepsilon \perp$ is the strain perpendicular to $\beta$, $\zeta$ is the direction of maximum tilt, $\delta$ is the tilt in μradians. Numbers in ( ) are the formal errors.

Table 2-6. Summary of GPS experiments.

| Experiment Name | Inclusive dates | Station days of data | Processing | Orbit source | $\sigma_0^2$ |
|---|---|---|---|---|---|
| *Major Campaigns* | | | | | |
| JUN86 | 16.JUN.86 - 19.JUN.86 | 48 | GPS22 | $NSWC_a$ | 11.9 |
| JAN87 | 29.DEC86 - 7.JAN.87 | 123 | GPS22 | $NSWC_a$ | 8.6 |
| SEP87 | 23.SEP.87 - 27.SEP.87 | 32 | GPS22 | $NSWC_a$ | 4.3 |
| OCT87 | 5.OCT.87 - 8.OCT.87 | 17 | GPS22 | $NSWC_a$ | 1.7 |
| MAR88 | 8.MAR.88 - 18.MAR.88 | 47 | GPS22 | $Broadcast_b$ | 3.0 |
| *GPS ties* | | | | | |
| Santa Barbara 2 1956 | 29.SEP.87 | 4 | GIPSY | $Broadcast_c$ | N/A |
| Chaffee 2 1923 | 4.OCT.87 | 4 | GPS22 | NSWC | N/A |
| Niguel 1884 | 11.OCT.87 | 2 | GPS22 | NSWC | N/A |
| MAY88 | | | | | |
| San Nicolas Island | 10.MAY.88 -11.MAY.88 | 6 | GIPSY/GPS22 | $Broadcast_c$ | 3.1 |
| San Clemente Island | 13.MAY-88 - 15.MAY.88 | 8 | GIPSY/GPS22 | $Broadcast_c$ | 2.5 |
| Santa Cruz Island | 17.MAY.88 - 19.MAY.88 | 11 | GIPSY/GPS22 | $Broadcast_c$ | 3.1 |

NSWC- Precise tabular orbits provided by NGS. Sixth order polynomial fit to 15 min. satellite state vectors for each satellite for each day of observations.

a- Adjusted daily orbits using fiducial stations held to SV3 coordinates.

b- Adjusted daily orbits using local stations whose positions were constrained to coordinates derived during previous experiments in the SV3 reference frame.

c-Broadcast orbits for GPS22 solutions derived from sixth order polynomial fit to broadcast ephemeris. GIPSY broadcast orbits derived from force modeling of satellite trajectories over several days of broadcast ephemerides.

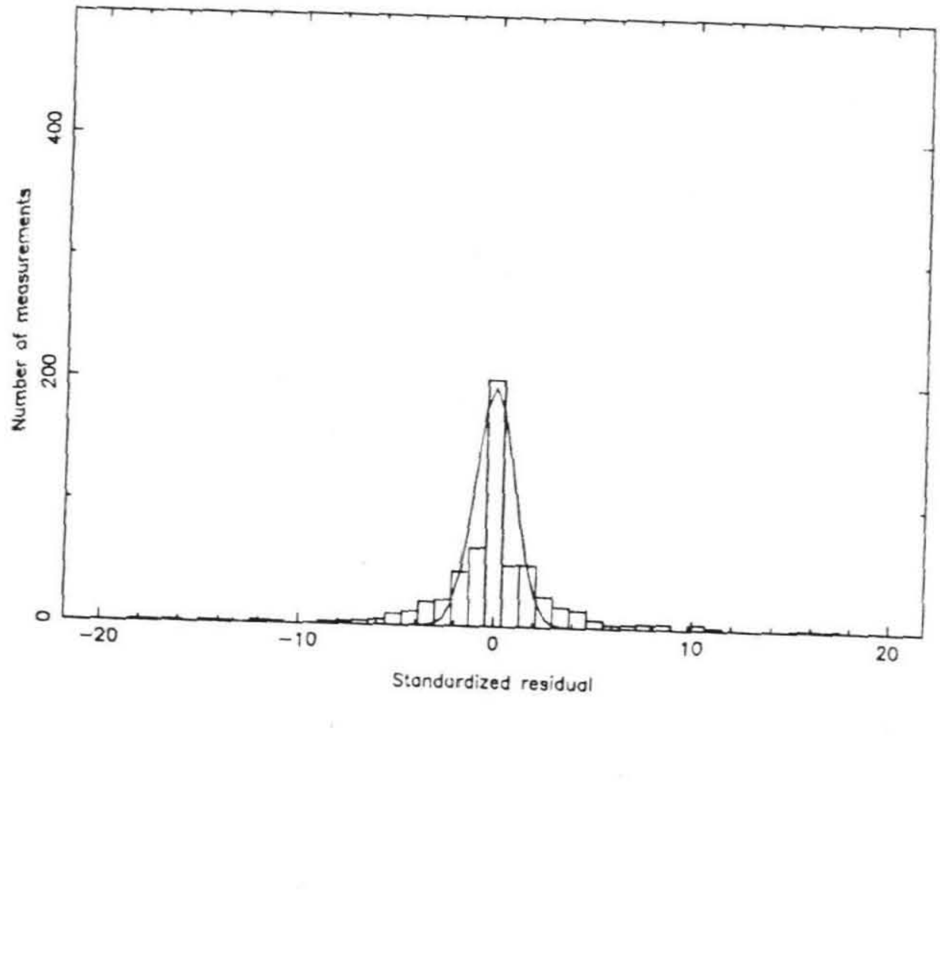


Figure 2-7. Histogram of the standardized residuals for the GPS adjustments is shown. The x-axis is in units of the standard error, $\sigma$, of the adjusted value. The solid line plotted on the histogram is a Gaussian distribution. The occurrence of values outside of the Gaussian distribution suggests that the formal errors of the adjustment under estimate the true error of the GPS vectors.

# Chapter 3

## Strain rate modeling

The purpose of this chapter is to quantify the strain rates in the offshore region of southern California from geodetic observations. In this study geodetic data collected since the late 1800's are used to calculate average rates of crustal strain across networks that extend from the offshore islands of southern California to the mainland. The geodetic data includes triangulation, trilateration, and GPS interstation vectors which have been combined to estimate strain rates averaged over the time period of the observations, from 15 to more than 115 years. The data types and their distribution were discussed in the previous chapter. In this chapter the strain rate modeling will be discussed, strain rates estimated for networks in the offshore region, and the quality of those strain estimates assessed. The heterogeneous nature of the data sets used requires that the estimated parameters be evaluated for reliability by common statistical tests and other, more qualitative means. By rating the estimates in this manner, the estimated parameters gain more realistic confidence estimates.

### 3.1 Introduction:

Geodetic data are widely used to measure crustal deformation in California. Several investigators have presented analyses of triangulation [Savage and Burford, 1973; Snay et al., 1987; Thatcher, 1975], trilateration [Lisowski and Prescott, 1981; Savage and Burford, 1973; Savage et al., 1987], and space-based geodetic observations

[Clark et al., 1987; Ryan, 1987; Sauber, 1989; Ward, 1988] that indicate strain rates in California on the order of 0.1 - 0.8 x $10^{-6}$/year . These types of observations can provide both reliable estimates of strain accumulation in seismically active areas [Savage, 1983] and critical information on the earthquake cycle, if the data are collected before and after fault rupture. Both types of observations can be used to test constitutive models of the crust that suggest time varying strain rates near faults during the earthquake cycle, if the data are of sufficient precision and quality.

After the 1906 San Francisco earthquake and the recognition of substantial ground displacements of survey monuments [Reid, 1910], the United States Coast and Geodetic Survey (USC&GS) initiated their triangulation campaign of the 1920's. The adjustment of the data from this campaign was used to evaluate the amount of deformation that had occurred since the first surveys in coastal California, 30 to 60 years earlier [Bowie, 1928]. Station displacements between this survey and the first surveys in the mid- to late- 1800's were interpreted to, possibly, be the result of tectonic motions along the coast. The results of these adjustments suggested a few meters of displacement in the coastal region relative to stations in northeastern and southern California. In northern California, the displacements are consistent with the geological sense of displacement for slip on the San Andreas fault. In the western part of southern California, though, these results indicate ~40 mm/yr of *left* lateral slip parallel to the San Andreas fault.

The direction of station displacements in southern California is opposite to that which has since been observed geodetically [Clark et al., 1987; Savage and Burford, 1973] and shown geologically [Crowell, 1981] along the San Andreas fault. It is unlikely that this contradiction of what is now understood about the sense of displacement on the San Andreas fault is real. More likely the calculated displacements are biased by the analysis of the data and the sparseness of the data set. Bowie's analysis used the adjusted positions of stations from only two observational epochs approximately

50 years apart, holding a number of stations on both sides of the San Andreas fault fixed with respect to each other. Bowie [1929, p.3] states that the maximum relative station displacement in southern California of 3.6 feet "..can easily be accounted for by the accumulation of accidental errors of triangulation" and [Bowie, 1929, p.20] " that there seems to be no method of differentiating the effects of [earth movements or accidental errors of observation] . . . "

Since then, numerous investigators have used geodetic observations to evaluate the present-day strain rates along geologically and seismically active faults [Savage and Burford, 1973; Thatcher, 1979a] and in other areas of suspected crustal disturbances [Snay, 1986; Zoback et al., 1985]. Many of these efforts have used existing geodetic data such as those collected periodically by the United States Coast and Geodetic Survey (USC&GS) and the National Geodetic Survey (NGS), while others have relied upon data collected explicitly for crustal deformation studies, such as those collected by the United States Geological Survey (USGS).

The crustal strain estimates presented here will be based on combinations of two types of measurements: Terrestrial and extraterrestrial. Prior to the development of GPS techniques for precise relative positioning, these geodetic data had never before been combined to evaluate crustal strain. This is now possible, because high precision extraterrestrial surveying, with relatively portable GPS receivers, has allowed for the reoccupation of these historical marks and the recovery of this temporally long data base. The significance of the relatively large uncertainties in the triangulation observations is diminished by the high precision of the GPS observations and the time that has passed since the triangulation surveys were performed.

Because the data used in this study have been collected by several agencies at irregular time intervals from different networks of stations, there are many temporal, spatial, and observational heterogeneities in the data set. The various networks have different numbers of observations spread over different time intervals. In addition to this, the data have been collected using techniques with very different precisions. Thus, the strain rate estimates for each network can not *a priori* be considered to be of equal quality, since each network has its own individual peculiarities.

3.2 Strain rate modeling from geodetic data:

The full displacement rate tensor has six components representing the displacement rate field in three dimensions. For the present study, these dimensions are in a local north, east, and up coordinate system. Because elevation changes have not been observed during the historical surveys, only the horizontal displacement rates can be estimated. In doing so, it is assumed that the vertical changes do not significantly affect the horizontal position of the stations. (Geologically rapid rates of uplift have been determined in the coastal region of Santa Barbara and Ventura [Lajoie et al., 1979], but leveling along this coastline suggests that these rates are low [Yerkes et al., 1980] and may be affected by oil withdrawal in the Ventura region [Buchanan-Banks et al., 1975].)

Let $\mathbf{u}_i(t)$ be the geodetic position in latitude, $\varphi$, and longitude, $\lambda$, of station i at time t.

$$\mathbf{u}_i(t) = \begin{bmatrix} \lambda_i(t) \\ \varphi_i(t) \end{bmatrix} \tag{3-1}$$

In the horizontal displacement rate model, the position of a station at time t, relative to an arbitrary reference time, $t_o$, is described by

$$\mathbf{u}_i(t) = \mathbf{u}_i(t_o) + \mathbf{L}[\mathbf{u}_i(t) - \mathbf{u}_o](t-t_o) \tag{3-2}$$

where the displacement rate matrix $\mathbf{L}$ is decomposed into symmetric and anti-symmetric matrices

$$\mathbf{L} = \mathbf{E} + \mathbf{W} \tag{3-3}$$

**E** is the symmetric strain rate tensor

$$\mathbf{E} = \begin{bmatrix} e_{11} & e_{12} \\ e_{12} & e_{22} \end{bmatrix} \tag{3-4}$$

in a north-east coordinate system with east directed along the 1-axis and north along the 2-axis and **W** is the rotation matrix

$$\mathbf{W} = \begin{bmatrix} 0 & w_{12} \\ -w_{12} & 0 \end{bmatrix} \tag{3-5}$$

Several deficiencies in the data set from the lack of accurate distance and azimuthal observations throughout the observational history prevent the unique determination of **L**. Even though azimuthal data have been collected at some of the triangulation stations, the accuracy of these data, >7 μradians [Snay et al., 1987], is too low to allow for the reliable estimation of network rotations. **W** is therefore indeterminable. Also, in most cases accurate length observations were not collected with the triangulation observations. In this case, all of the components of the strain rate tensor **E** can not be solved for explicitly. The data provide only enough information to solve for angular changes and, therefore, only the shear strains.

In order to account for these deficiencies when using triangulation data, it is common to use the parameterization

$$\gamma_1 = ( e_{11} - e_{22}) \tag{3-6}$$

$$\gamma_2 = 2e_{12} \tag{3-7}$$

called engineering shear strains. In this representation the maximum shear strain rate, $\gamma$, and its direction, $\Psi$, are given by

$$\gamma = \left(\gamma_1^2 + \gamma_2^2\right)^{\frac{1}{2}} \tag{3-8}$$

$$\psi = \frac{1}{2}\tan^{-1}\left(\frac{\gamma_1}{\gamma_2}\right) \tag{3-9}$$

and the direction of minimum extension, $\beta$, by

$$\beta = \frac{1}{2}\tan^{-1}\left(\frac{-\gamma_2}{\gamma_1}\right) = \psi \pm \frac{\pi}{4} \tag{3-10}$$

This parameterization can be thought of as representing pure or simple shear. The preferred representation is a matter of interpretation dependent on the individual geological setting, since these parameters are independent of the network rotation, **W**. Decreases in the right angle between lines oriented north and east are measured by $\gamma_2$ and increases in the right angle between lines oriented N45E and N45W are measured by $\gamma_1$. Right lateral shear across a vertical plane striking N45W is measured by $\gamma_1$ (or left lateral across a vertical plane striking N45E), and right lateral shear across a vertical plane striking N90E (or left lateral across a plane striking N00E) is measured by $\gamma_2$. Even though, the strain mechanism in a given area may not be by shear along vertical shear faults, these parameters provide quantitative estimates of the horizontal strain rate and direction for relative comparisons between different regions.

In these analyses two statistics will be reported: The standard deviations (formal errors) associated with the estimated parameters which are measures of the data strength of the estimated parameters, and the sigma of unit weight,

$$\sigma_o = \sqrt{\frac{\sum_{i=1}^{n}\left(\frac{x_i-\langle x_i\rangle}{\sigma_i}\right)^2}{(n-n_{par})}} \qquad (3\text{-}11)$$

where $x_i$, $\langle x_i\rangle$, and $\sigma_i$ are the *i* th observation, the estimate for the *i* th observation, and standard error of the estimate, n is the number of observations, and $n_{par}$ is the number of estimated parameters. This latter statistic is a measure of the normality of the post fit variance distribution. $\sigma_o^2$ is equivalent to a chi-squared over degrees of freedom statistic [Bevington, 1969; Snay, 1986; Vanicek and Krakiwsky, 1986]. Values of 1 suggest that the model variance distribution is normally distributed and that the *a priori* weights are a realistic estimation of the true error. Other values significantly different from 1 suggest that the model variance distribution is not normally distributed and/or the *a priori* weights are poor estimates of the the data uncertainty.

3.3 Methods:

The method used for the determination of strain rates from geodetic data depends on the type of geodetic data available. When estimating these strain rate parameters from data that are of one type, there are standard methods that are usually employed. For example, Frank's method [Frank, 1966] has been used widely for the analysis of strain rates from triangulation data. [Sauber, 1989; Thatcher, 1979a; Zoback et al., 1985]. With this method, angles, that have been repeatedly measured, are used to calculate the engineering shear strains $\gamma_1$ and $\gamma_2$. The change in the horizontal azimuth of an observed direction is modeled as

$$\Delta\alpha_{ij} = \Delta t \frac{1}{2}\left[\gamma_1 \left(\sin 2\theta_j - \sin 2\theta_i\right) + \gamma_2 \left(\cos 2\theta_j - \cos 2\theta_i\right)\right] \quad (3\text{-}12)$$

where the θ's are the azimuths to stations i and j, and $\Delta\alpha_{ij}$ is the observed angular change during some period, Δt. This technique could be employed in the analysis of the present data set that consists mostly of angles and interstation earth-centered and earth-fixed GPS vectors by reducing both to a common reference surface and calculating the angular changes. However, since there are other observations within the networks, than just those to the stations that have been repeated in time, this algorithm would not exploit all of the information in the data set.

Rather than reducing the GPS vectors to angles on an ellipsoid and comparing angles, the method of simultaneous reduction [Bibby, 1982] has been used. With this method, the data are used to solve for both station coordinates on a reference ellipsoid at each epoch and displacement rate parameters. Changes in station positions from one epoch to another are modeled by estimating both an average, network displacement-rate tensor and the station positions at each epoch. In doing this, stations, which are repeatedly occupied, provide information on the temporal changes in station positions. Other stations, which are occupied during only one epoch, provide strength to the positions at that epoch. This is preferable to Frank's method, because stations whose observations have not necessarily been repeated in time (and would be ignored by Frank's method) add strengthen to the positions of the other stations which may have been observed at other epochs. In these analyses, only triangulation observations from the primary triangulation stations within the GPS network are used.

A recent analysis of strain accumulation in the New York area using Frank's method suggested large amounts of right lateral shear strain [Zoback et al., 1985]. Subsequent analysis of a larger data set in the same region [Snay, 1986] using the method of simultaneous reduction found no statistically significant strain. It was shown that the analysis of strain using Frank's method does not allow one to evaluate the data for reliability and blunders, and may result in misinterpretation of data weaknesses and survey blunders as tectonic strain.

3.3.1 Implementation of simultaneous reduction technique:

Drew and Snay [1988; 1989] have developed a computer algorithm that implements simultaneous reduction for estimating the displacement-rate tensor from a set of geodetic data through a weighted least squares algorithm. Their program called DYNAP (DYNamic Adjustment Program) is a modification of the geodetic adjustment program ADJUST, authored by Milbert and Kass [1987]. The observational equations for the data can be found in Milbert and Kass [1987] and a matrix representation can be found in Drew and Snay [1989] and Feigl et al. [1990].

The displacement rate model of DYNAP is

$$\mathbf{u}(t) = \mathbf{u}(t_o) + \mathbf{C}[\mathbf{u}(t) - \mathbf{u}_o](t-t_o) \tag{3-13}$$

where $\mathbf{u}$ is the vector of station coordinates in latitude, $\varphi$, longitude, $\lambda$, and elevation, h, $\mathbf{C}$ is the displacement rate matrix,

$$\mathbf{C} = \begin{bmatrix} c_{\varphi\varphi} & c_{\varphi\lambda} \\ c_{\lambda\varphi} & c_{\lambda\lambda} \\ c_{h\varphi} & c_{h\lambda} \end{bmatrix} \tag{3-14}$$

$t_o$ is a reference time, and $\mathbf{u}_o$ is the origin. The components of $\mathbf{C}$ are related to the horizontal displacement rate matrix $\mathbf{L}$ via

$$\mathbf{L} = \begin{bmatrix} c_{\varphi\varphi} & \frac{r_m}{r_p} c_{\lambda\varphi} \\ \frac{r_p}{r_m} c_{\varphi\lambda} & c_{\lambda\lambda} \end{bmatrix} = \mathbf{E} + \mathbf{W} \tag{3-15}$$

and to the network tilt rate, $\tau$ , via

$$\tau = \begin{bmatrix} \tau_1 \\ \tau_2 \end{bmatrix} = \begin{bmatrix} \frac{-c_{h\varphi}}{r_p} \\ \frac{-c_{h\lambda}}{r_m} \end{bmatrix} \tag{3-16}$$

$$r_p = \frac{a}{w} \cos \varphi \tag{3-17}$$

$$r_m = \frac{a\left(1 - e^2\right)}{w^3} \tag{3-18}$$

$$w = \left(1 - e^2 \sin^2 \varphi\right)^{\frac{1}{2}} \tag{3-19}$$

where *a* and *e* are the radius and eccentricity, respectively, of the WGS-84 ellipsoid, and $\varphi$ is a reference latitude. In this model, crustal motion is assumed to be linear in both time and geodetic position, and homogeneous over the area of the network.

Inputs are initial preliminary positions, elevations, data, and constraints. Because the data sets lack sufficient information to determine all of the components of **C**, certain constraints had to be applied. For all of the networks, elevation observations at epochs other than the GPS epoch are unavailable, requiring that elevations be constrained to their GPS derived values and preventing the determination of the height dependent components of **C**. Azimuthal constraints were also applied to all of the networks, because no common, reliable observations, other than the GPS solutions, provide information on the orientation of the networks. One orientation between two stations was constrained to the GPS derived value for each network throughout the period of the observations. For the data sets with precision trilateration, this and the elevations were the only constraints necessary. For networks using only triangulation or triangulation and GPS vectors, in addition to the azimuthal and elevation constraints, a common scale needed to be defined throughout the period of the observations. This was accomplished by constraining a GPS vector between two stations over the time period of all the observations, thus introducing a constant scale and orientation to these data sets. The azimuth constraint precludes the determination of the network rotation rate, **W**, and the scale constraint results in an indeterminable dilatational strain rate, $(e_{11} + e_{22})$. These constraints do not bias the crustal motion parameter estimates, since no other information in the data set affects these free network parameters [Drew and Snay, 1989].

3.3.2 Data combinations:

Various station and data combinations have been used to estimate the strain rates over the networks: Triangulation -triangulation (TT), triangulation-GPS (TG), triangulation-trilateration (TL), trilateration-GPS (LG), and triangulation-trilateration-GPS (TLG). The combination used depends on the availability of that data. In Chapter 2, it was shown that some of the surveys have a few spurious points, outliers. Least squares techniques weight large outliers heavily [Menke, 1984; Press et al., 1987]. This can result in the erroneous estimation of the model parameters [Menke, 1984; Press et al., 1987]. The results discussed below are from the data set that excludes these outliers. Strain rates were calculated using both data sets (see Table 3-1) and the differences between the two were small. By estimating strain rates using these different data combinations, the strength and weakness of the estimates and data can be evaluated. Estimated parameters, that are independent of the data set used, are the most reliable averaged rates over those time periods, while estimates that depend strongly on the data combination used are the least reliable.

3.4 Network results:

Three regional networks have been defined based on the geological deformational style of each of these regions. These networks are subdivided into smaller networks, if the amount of data available will permit this and if the strain is thought to be heterogeneously distributed across the larger network. The sub-dividing allows the determination of strain over a smaller spatial and possibly more homogeneous region, however, with fewer observations. Table 3-1 summarizes the strain analyses for all of the networks and all of the data combinations.

The stations occupied span the offshore region from the Santa Barbara coast line to the Northern Channel Islands, and from the coast of Orange and San Diego counties west and north to the Northern Channel Islands. The three major networks are the Santa Barbara Channel and Oxnard Plain, the Northern Borderland between the northern channel islands and San Nicolas and Santa Barbara islands, and the Southern Borderland between San Nicolas island and the coast line of San Diego and Orange counties (Fig. 3-1).

From hundreds to tens of triangulation observations have been used, depending on the network. The channel network and the borderland networks differ in the quality of the data and the time span of the data available to each. The Santa Barbara Channel/Oxnard Plain networks have the largest number of observations, spread over the longest time period, while the northern and southern networks have triangulation data mostly from only one epoch in the mid 1900's.

3.4.1 Santa Barbara Channel and Oxnard Plain.

The geodetic networks in the western Transverse Ranges cover the Santa Barbara Channel and Oxnard Plain (Fig.3-2). The data set includes triangulation dating to the 1870's, precision trilateration, and GPS interstation vectors. There are over 475 directions in this network. The directions represent five epochs of observations with as many as 60-90 years between the first and last triangulation observations. Each sub-network has at least 3 epochs of observations with at least 50 years between the first and last triangulation observations. Of the observations, 60% are from the 1950's, 22% from the 1920's, and the rest are split between the 1870's, 1890's, and 1960's. In 1971, precision trilateration was performed across the channel to stations on the northern channel islands. These stations were occupied with GPS during the mid-1980's along with the GPS occupations of the triangulation stations.

The strain rate solution for the overall network from triangulation and GPS observations is consistent with generally north-south directed shortening. The rate of maximum shear strain ,$\gamma$, is $0.10 \pm 0.01$ μradians/year and the direction of minimum extension, $\beta$, is N05W $\pm$ 4 with $\sigma_0 = 1.18$. Subdivision of the network into a Santa Barbara Channel network (SBC) and an Oxnard Plain network (OP) (Figures 3-2a and 3-2b) suggests two different strain regimes. The SBC network is characterized by $\gamma = 0.24 \pm 0.02$ μradians/year and $\beta$ = N01W $\pm$ 2 with $\sigma_0 = 1.07$ and the Oxnard Plain network by $\gamma = 0.04 \pm 0.04$ μradians/year and $\beta$ = N43W $\pm$ 29 with $\sigma_0 = 1.21$.

3.4.1.1 Santa Barbara Channel Triangulation-GPS data sets:

The SBC network has been further subdivided into three smaller networks and the strain rates estimated using various combinations of the geodetic data to test the reliability of these estimates across the channel. The channel has been divided up into eastern Santa Barbara Channel (ESBC), central Santa Barbara Channel (CSBC), and western Santa Barbara Channel (WSBC) networks (Figures 3-2c, 3-2d, and 3-2e ). The strain rate estimates from these networks show that the generally north-south directed shortening of the overall network solution is also present in these smaller regions, but that the direction varies from N23W ± 7 in WSBC network to N10E ± 4 in the CSBC network and N19E ± 4 in the ESBC. The shear strain rates also changes from relatively low in the WSBC, 0.17 ± 0.04 μradians/year , intermediate in the CSBC, 0.26± 0.04 μradians/year, and high in the ESBC, 0.30 ± 0.05 μradians/year $\sigma_0$ for these estimates are 0.81, 1.00, and 0.55 for ESBC, CSBC, and WSBC, respectively.

The triangulation only solutions for the channel are substantially different from these triangulation-GPS solutions and have generally larger $\sigma_0$ 's (Table 3-1). This is most likely attributed to the generally shorter time period over which the triangulation only estimates are averaged combined with the larger uncertainties in the triangulation data.

Feigl et al. [1990] have reported that in 1942 ARGU was reset in a new location and that there exists no tie between the old location and the new location. Observations from ARGU were both included and excluded in the strain analyses, and were found to have no effect on the strain rates (see values in Table 3-1 for the WSBC). The good agreement between the analyses that include ARGU and those that exclude seems to suggest that the post 1942 position of ARGU is "close" to the pre-1942 position. A similar situation occurs at CHAF. The USC&GS site description for Chaffee states that in 1923 a new mark was set, Chaffee 2 1923, in "approximately the same position" as Chaffee 1867, the "old" survey mark. Bowie [1928] reports that the new mark at Chaffee "..was established as near as possible to the old one, and it is believed to be not more than 4 inches away from the old one. " The additional effect that this data has on the strain analysis is negligible. Unlike, with ARGU where the observations both before and after the movement of the mark were of the highest precision (first order), the late 1800's observations at Chaffee were third order. This, combined with the ± 4 inch uncertainty in its inferred position relative to the new mark, gives the data $^1/_9$ the weight of the post movement observations, and thus little effect on the solution.

3.4.1.2 Santa Barbara Channel GPS, Triangulation, and Trilateration data set:

Precision trilateration collected in 1971 covers most of the ESBC and CSBC networks with a few lines in the WSBC network (Fig. 3-3). In general the trilateration stations are co-located with the triangulation stations except for LACU on La Cumbre Peak and HIMT on Santa Cruz Island. The differences in network geometry between triangulation-GPS networks and trilateration-GPS networks are small. Therefore, the strain rate estimates from the two data types should be comparable, if strain rates are constant over the 15 and 100 year time scales.

Strain rates were estimated using three sub-sets of the trilateration-GPS data set. The networks are geometrically similar to the SBC, CSBC, and ESBC networks. Separate estimates were not calculated for the equivalent WSBC network, because the number of EDM lines was small and those lines did not cover the network evenly. The overall SBC network solution estimates $\gamma = 0.10 \pm 0.06$ μradians/year and $\beta =$ N43E $\pm$ 15 with $\sigma_o = 0.41$. The magnitude of the strain rate is indistinguishable from the triangulation-GPS only solution, but, with a $50^o$ difference in the direction of minimum extension. The ESBC network which had the highest shear strain rate at 0.37 μradians/year with $\beta =$ N20E has a very low shear strain rate, $\gamma = 0.07 \pm 0.08$ μradians/year with $\beta =$ N31E $\pm$ 35 and $\sigma_o = 0.44$. The CSBC network has a shear strain rate comparable to the triangulation-GPS solution of $\gamma = 0.24 \pm 0.14$ μradians/year with $\beta =$ N41E $\pm$ 13 and $\sigma_o = 0.36$.

Strain rates were estimated using the triangulation-trilateration data combination for the ESBC network. Since few of the triangulation stations are common to the trilateration stations, the triangulation observations were tied to the trilateration observations by connecting these sets of stations through the use of GPS vectors between the local triangulation and trilateration stations. These vectors were constrained to be invariant with time. These vector ties and the network are shown in Figure 3-4. The solution for this network has shear strain rates comparable to those of the ESBC network, $\gamma = 0.32 \pm 0.10$ μradians/year with $\beta =$ N22E $\pm$ 10 and $\sigma_o = 1.07$.

The source of these differences between both the triangulation-GPS and triangulation-trilateration solutions and the trilateration-GPS solutions has not yet been determined. The differences may represent real strain rate variation between the ~100 year average of the triangulation-GPS/trilateration observations and the 17 year average of the trilateration-GPS observations. Alternatively, systematic error in the reduction of the trilateration data and/or local monument instability may be causing the large difference in the direction of minimum extension between the triangulation-GPS and triangulation-trilateration and the trilateration-GPS estimates. Comparisons of trilateration derived strain rates with GPS derived strain rates have shown no appreciable difference between the two techniques in California [Prescott et al., 1988]. However, in those analyses, the agreement is based on frequent GPS and trilateration observations of 10-40 km baselines that had been collected over several years to months and not observation by each technique. With only the one epoch of trilateration, the low strain rate, and the short time period between the trilateration and GPS observations, small monument instabilities and observational blunders between the two surveys could have significant affects on the strain estimates.

All of the lines in the trilateration network were not observed with GPS and this may be the cause of the differences between the triangulation-GPS and the trilateration-GPS strain analyses. In particular, the line from DEVL to HIMT was estimated under less than ideal circumstances. HIMT was tied to the overall GPS network through a 2.5 day GPS experiment in May of 1988. During this experiment, data from continental fiducial stations were unusable, requiring that the baselines be estimated using broadcast orbits. This should not have resulted in large errors in the positions of the estimated stations (Chapter 2). However, an examination of the mark-to-mark distances among the trilateration stations suggests that the position of HIMT may be in error in its eastern component. All of the lines generally are consistent with a NNE contraction across the channel, except for the DEVL-HIMT line. The inferred GPS length for this line is 0.0739 m shorter than the 1971 EDM length, inconsistent with the NNE shortening implied by both the triangulation-trilateration and triangulation-GPS analyses. At this time it can not be determined if this inconsistency is real or the result of the data modeling, orbits, and/or set up error. Set up error may be unlikely. Independent estimates of these baselines by Larsen [1990] indicate large differences in the GPS estimates of the baselines that include HIMT (Table 3-2). The good agreement among the other GPS baselines suggest that the two different analyses, in general, provide consistent solutions, but that the analysis of the data from HIMT is spurious. This question can best be answered by a direct measurement of the DEVL-HIMT line.

The low $\sigma_o$ values for the trilateration-GPS estimates relative to $\sigma_o$ for the estimates that use triangulation data should not necessarily be interpreted as an indication that the trilateration-GPS estimates are more reliable. The data in these two data combinations are of different flavors for estimating the strain rates. The triangulation observations, while having greater uncertainty in each observation, have several epochs of observations with between 30 and 115 years between the GPS observations and the triangulation. Alternatively, the trilateration observations are few with only 15 years between them and the GPS observations, and, most importantly, only one epoch of trilateration. This lack of several observational epochs may be the cause of the much smaller $\sigma_o$'s for the trilateration-GPS, than for the triangulation combinations. This is because there is less variance when fitting two epochs of observations to a time dependent model than when fitting several epochs.

In order to average over the influence of this limited sampling, all of the data types have been combined to estimate the 3 components of the horizontal strain rate tensor, **E**, for the ESBC and CSBS networks. This combination for the two networks gives strain rate estimates consistent with the triangulation-GPS estimates in both direction of minimum extension $\beta$ and magnitude of maximum shear strain $\gamma$ (Table 3-1). The rates are slightly lower than those estimated with the triangulation-GPS data set alone. Since the trilateration provides a scale, the estimates of the three components of the strain tensor can provide information on the type of strain across the channel. For both of these networks, the strain components suggest approximately uniaxial strain across the channel. The maximum shortening strain rate is -0.20 μstrain/year directed N20E ± 4 for the ESBC network and -0.15 μstrain/year directed N15E ± 4 for the CSBC network. $\sigma_0$ for these two solutions are 0.76 and 0.85, respectively.

This reasonable agreement in the directions of minimum extension among the trilateration-triangulation, triangulation-GPS and trilateration-triangulation-GPS estimates suggests that these geodetically determined strain rates are reliable for both the 30-100 year and the 15 year averages. The disagreement in the magnitudes of the strain rates seem to suggest that the strain rates have decreased over the last 15 years.

### 3.4.2 Borderland:

The borderland networks include stations on Santa Rosa, Santa Cruz, San Nicolas, Santa Barbara, Catalina, and San Clemente islands and stations along the coast of Los Angeles, San Diego, and Orange counties. The data set consists of only triangulation observations and GPS vectors; no reliable trilateration data are available. The major triangulation stations that were occupied were established in the early 1940's and 1950's. Many stations were established in the late 1800's and early 1900's, but station destruction and lack of GPS observations to these stations makes them unusable for this study. The borderland has been divided up into two large networks: The Northern Borderland (NBL) and the Southern Borderland (SBL) networks. Almost all of the triangulation data in the borderland was collected during the surveys of the 1950's, with a few observations in the 1940's. These observations are too sparse and too closely spaced in time to allow for the determination of strain rates based only on the triangulation data set. The strain rate estimates are based on the combined triangulation-GPS data set. The lack of observations widely spaced in time and the apparently low data quality from closure problems during the collection of the 1950's data in the borderland (Chapter 2) limit the reliability of the estimates.

3.4.2.1 Northern Borderland

The extent of the NBL network is shown in Figure 3-5. Only the stations on Santa Rosa, Santa Cruz, San Nicolas, and Santa Barbara islands and Castro Peak are "co-located" triangulation-GPS stations. GPS observations were made to the triangulation stations Point Dume 1800 and Vicente 1951, but these observations were insufficient to test the repeatability of the GPS estimates and were not used to estimate their station positions. At each of these two sites, less than half a day of useful GPS data were obtained on days without tracking network data. Solutions can be obtained with this little data, but there are no ways, in the absence of more GPS data to determine if the solution is biased by the satellite geometry and/or field blunders. Field blunders have occurred during some of these experiments and were only noted, and recovered from, during the post-processing of the GPS observables, because of anomalously large daily repeatabilities.

Because there is only one epoch of triangulation observations, strain rates can not be estimated based on triangulation data alone and the strain rates have been estimated for three sub-sets of the triangulation-GPS data. These sub-sets compose three overlapping networks consisting of the overall network of triangulation-GPS stations and other triangulation stations (NBL), and two triangulation-GPS station networks (NBL-1, NBL-1a) (Fig. 3-5a, 3-5b, and 3-5c).

The solution for the overall NBL network is $\gamma = 0.04 \pm 0.03$ μradians/year and $\beta$ = N53W ± 36 with $\sigma_0$ = 0.97. This solution suggest that the strain rate averaged over the entire network is indistinguishable from zero. A similar result is obtained when the triangulation stations without GPS observations are eliminated and only data from the triangulation-GPS stations are used, NBL-1 network (Fig. 3-5b), with $\gamma = 0.06 \pm 0.05$ μradians/year $\beta$ = N80E ± 15 with $\sigma_0$ = 0.94. Network NBL-1A contains only triangulation-GPS stations that form a closed polygon (fig. 3-5c). The results for this solution are different from the previous two. While $\beta$ = N36W ± 7 is indistinguishable from the NBL network estimate with its low shear strain rate, the shear strain rate of NBL-1A of $\gamma = 0.17 \pm 0.06$ μradians/year with $\sigma_0 = 0.69$ suggests significant shear strain across the network.

The inconsistencies among these three solutions would seem to indicate that the strain is either not homogeneously distributed across the network or the strain is unresolvable with this limited data set. The only difference among the data sets is the presence of observations from triangulation stations at which there are no GPS observations. This would seem to suggest that, with this limited data set, the inclusion of these other observations is having a significant impact on the strain rate estimates. Since these observations should add strength to the station positions at the 1950 data epoch and the overall strain rate estimates, the estimates based on the overall network including all of the data should be the most reliable and representative of the strain rate across the northern Borderland.

But, a comparison of the residuals associated with each of these solutions suggests that these additional observations may be detracting from the solution. The NBL and NBL-1 solutions both have large (>3$\sigma$) standardized GPS residuals associated with station CTR3, and NBL has large (>3$\sigma$) standardized direction residuals associated with station CTR3. Data set NBL-1A represents the elimination of these data and data from LAG2 for which the ground survey tie between the GPS and triangulation stations is long (~8 km) and is considered to have the least suspect triangulation observations.

3.4.2.2 Southern Borderland

The SBL network is shown in Figure 3-6. The overall network has 163 triangulation observations from the 1940's and 1950's. Twenty-four observations from the 1940's are from among Santa Barbara, Santa Catalina, and San Clemente islands and 139 from the 1950's are from all of the other stations. Except for triangulation observations from stations Catalina Peak and San Pedro 1800, both of which have been destroyed and were not recovered with GPS, the data are from "co-located" triangulation-GPS observations. Station Niguel 1884 has also been destroyed, but GPS observations from its reference marks and ground surveys have allowed for recovery of this site with a somewhat large uncertainty (see Appendix A for discussion of the site tie). Since the two epochs of triangulation data are temporally close and the majority of triangulation data are from one epoch, the strain rate estimates are based solely on triangulation-GPS data sets with different combinations of data being used to test suspect strain rate estimates.

The estimates based on the entire data set, SBL, are $\gamma = 0.20 \pm 0.03$ microradians/year and $\beta$ = N16W $\pm$ 4 with $\sigma_0 = 1.11$. This estimate includes data from stations Catalina Peak and San Pedro at which no GPS observations were made. When these stations are eliminated from the solution, the estimates change significantly. For this smaller data set, SBL-1, of 76 directions, $\gamma = 0.07 \pm 0.04$ microradians/year and $\beta$ = N15W $\pm$ 15 with $\sigma_0 = 0.95$. To check for non-homogenous strain distribution, the region has been divided up into three sub-networks: inner (ISBL), intermediate (MSBL), and outer (OSBL) (Fig. 3-6b, 3-6c, and 3-6d). The ISBL network lacked sufficient data to solve for the strain rate parameters, so a fourth network I/MSBL that overlaps some of the area of the MSBL network was defined (Fig. 3-6e).

The OSBL network forms a triangle among San Nicolas, Santa Barbara, and San Clemente islands. Shear strain estimates for this network use 51 directions to triangulation-GPS sites. The estimates suggest strain indistinguishable from zero: $\gamma = 0.10 \pm 0.10$ $\mu$radians/year and $\beta$ = N64W $\pm$ 19 with $\sigma_0 = 0.96$. During the collection of the triangulation surveys in the 1950's, the observers apparently had problems with these data. The observations from Jackson 1951 on San Nicolas Island to stations on Santa Barbara and San Clemente islands were repeated many times on the same night and over several days. This type of observing is indicative of closure problems during the observations [Gossett, 1950]. The inability to close these figures may have been to due to a number of factors, such as horizontal refraction, and indicates that the observational accuracies are suspect (Chapter 2).

The MSBL network includes two nearly complete triangulation resurveys of the stations among Santa Barbara, Catalina, and San Clemente islands in the 1940's and 1950's. Catalina Peak is the only station for which there are not GPS observations in this network. Strain rate parameters were estimated both with and without directions from Catalina Peak. These estimates differ substantially from each other in the magnitude of the maximum shear strain rate. When Catalina Peak directions are included, $\gamma = 0.08 \pm 0.10$ microradians/year and $\beta$ = N05W ± 15 with $\sigma_0 = 1.30$, and, when those directions are excluded, $\gamma = 0.17 \pm 0.13$ microradians/year and $\beta$ = N01E ± 11 with $\sigma_0 = 1.11$. For the former solution, 66 directions were used as opposed to 23 for the later. Again, the additional information provided by the Catalina Peak observations would justify the preference of those solutions over the solutions without that additional data, however, large ($> 3\sigma$) standardized direction residuals associated with observations to Catalina Peak suggests that these data may not be reliable.

For the ISBL network, there are too few triangulation observations to determine the strain rate parameters based only on triangulation-GPS sites. Only two sets of directions exist among these three stations, WEST, NIGL, and SDAD, and all of these observations are from NIGL. Additionally, NIGL is tied through a ground survey to the GPS mark. The large uncertainty in this tie adds decimeters of uncertainty to 1980's position of NIGL. Strain rates were estimated, though, in a similar manner as the previous networks by including data from Catalina Peak and San Pedro. Figure 3-6d shows the triangulation data and GPS sites used. The estimates are $\gamma = 0.48 \pm 0.21$ microradians/year and $\beta$ = N09E ± 6 with $\sigma_0 = 1.40$. In order to get some data redundancy on strain rate estimates for this network, a fourth network, I/MSBL, is defined that includes the ISBL network and angles from stations within ISBL network and to stations within ISBL and MSBL networks. Both the shear strain rate estimate, $\gamma = 0.40 \pm 0.05$ μradians/year, and the direction of maximum shortening, $\beta$ = N17W ± 3, are close to the values for the ISBL network. Standardized direction residuals for directions to and from NIGL are large (>3$\sigma$). These observations represent 50% of the total directions and are dominating the strain rate estimates. The reliance of the strain rate estimates on directions from this one station and the poor fit of these observations to the model suggest that the estimated parameters are not representative of the average strain field across the network.

3.5 Relative Quality of the Strain rate estimates:

To test if these strain-rate estimates are significantly different from zero strain, the data were modeled under the assumption of no strain (i.e., C = 0 in Eq. 3-13). The F-test is used to test whether the two sample variances from these two models, one assuming deformation and the other assuming no deformation, are consistent. If the statistic F

$$F = \frac{\chi_2^2}{\chi_1^2} \qquad (3\text{-}21)$$

is <<1 or >>1, the two hypotheses are significantly different. The probability distribution of F is given by the incomplete beta function, I, [Bevington, 1969; Press et al., 1987] with the probability that the two variances, $n_1$ and $n_2$, are the same, P, given by

$$P = 2\,I\left(\frac{n_2}{2}, \frac{n_1}{2}, \frac{n_2}{(n_2 + n_1\,F)}\right) \tag{3-22}$$

$$I(a, b, x) = \frac{\int_0^x t^{a-1}(1-t)^{b-1}dt}{\int_0^1 t^{a-1}(1-t)^{b-1}dt} \tag{3-23}$$

Thus, the probability that the two distributions are different is given by 1-P. Low probabilities of significant differences implies a zero strain rate for that network, while high probabilities implies significant strain.

In order to reflect in the strain rate estimates variations in the data sets, a quality ranking for the estimated strain rate parameters is defined. This quality is a qualitative estimate of the relative reliabilities of the modeled parameters. Strain rate qualities are defined on a relative scale of A, B, C, D, and E. "A" qualities are the highest and "E" qualities the lowest. Several factors are considered necessary to accept the strain rate estimates for a region as reliable. Most important of these is whether or not the solutions pass the F-test for significance or insignificance of strain rates (Fig. 3-7). This statistic controls the initial ranking. Estimates are then degraded one category in quality for each of the following criteria that the solution fails: 1) At least two epochs of historical observations with greater than T years between them, where T is given by

$$T = \frac{\text{average historical observational uncertainty}}{\text{estimated strain rate}}$$

and 2) Reliable ground ties between GPS marks and the local triangulation station.

The results from the Santa Barbara Channel and Oxnard Plain networks are the most reliable and self consistent. The OP solution is consistent with zero strain and has a

2% probability of being different from the zero strain-rate solution. There are more than 60 years between the first and last triangulation surveys and reliable ground ties. But the network includes one ground tie of 8 km (COTR to LAG2) therefore, the OP network is ranked as B quality with zero strain rate. In the Santa Barbara Channel, the WSBC, CSBC, and ESBC networks all have strain rates that are significantly different from zero at the 90% confidence level, with reliable ground ties and 4 epochs of triangulation. These network strain estimates are, therefore, ranked as A quality.

For the borderland networks, the strain rate estimates are all of low quality consisting of only one epoch of observations (or two closely spaced epochs). Both the Northern Borderland and Southern Borderland regions have networks with zero strain and with indeterminable strain rates. NBL, and OSBL have model strain rates that are indistinguishable from zero with reliable ground ties. At the 90% confidence level, these solutions are indistinguishable from the zero strain solutions. However, because they have only one epoch of triangulation, they are ranked as B-quality estimates for zero strain rates. The MSBL network solutions for each of the data combinations are indistinguishable from zero at the 85% confidence level. Since this network only has one epoch of observations, it is ranked as a B-quality zero strain-rate estimate.

The ISBL and I/MSBL networks have only one epoch of observations and an unreliable ground tie at NIGL which is included in the majority of the observations. The triangulation station Niguel 1884, NIGL, was destroyed in 1986 leaving only two of its reference marks, NIGU and NIGB,that are both within 25 m of each other and ~400m from NIGL. Angles between NIGL and its reference marks were observed before the station was destroyed, but the distances were not. Because of this and the geometry of these marks, the data are insufficient to confidently recover the position of the triangulation station NIGL with respect to the GPS marks, NIGU and NIGB. This is an important station with respect to the strain-rate analysis. Without data from this station, the solution is singular. The strain rate estimates for these networks are ranked as D and

E qualities for indeterminant strain rates, because of P, the questionable ground tie, and the one epoch of triangulation data.

### 3.6 Summary

The strain rates in the offshore of southern California were determined by combining historical geodetic observations with GPS interstation vectors using a simultaneous reduction technique that averaged the strain over the area of several networks. Only triangulation observations and GPS interstation vectors were common to all of the networks. A limited set of trilateration observations spanned two networks in the Santa Barbara Channel. Strain rate estimates are based on combinations of all of the available data types for the networks and on subsets of available data when fewer than two reasonably spaced historical geodetic data epochs were available. The results indicate significant rates of strain in the Santa Barbara channel (SBC). Strain rates across the Oxnard Plain (OP), the Northern Continental Borderland (NBL), and the Outer Southern Continental Borderland (OSBL) are consistent with near zero strain.

Table 3-1. Shear strain rate estimates

| Network | Data types | $\gamma_1$ | $\gamma_2$ | $\gamma_{max}$ | $\beta$ | $\sigma_0^2$ | 1-P | Quality |
|---|---|---|---|---|---|---|---|---|
| *1 SBC/OP* | | | | | | | | |
| *a* | TG | 0.11 ± 0.02 | 0.02 ± 0.02 | 0.10 ± 0.01 | -5. ± 4 | 1.18 | 0.51 | E |
| | | (0.10 ± 0.01 | 0.02 ± 0.02 | 0.11 ± 0.01 | -6. ± 4 | 1.18 | 0.46 | E) |
| *b* | TT | -0.01 ± 0.05 | 0.10 ± 0.06 | 0.10 ± 0.06 | -46. ± 17 | 1.57 | 0.04 | B |
| | | (-0.08 ± 0.05 | 0.12 ± 0.06 | 0.14 ± 0.06 | -62. ± 11 | 2.42 | 0.06 | B) |
| *2 SBC* | | | | | | | | |
| *a* | TG | 0.23 ± 0.02 | 0.01 ± 0.02 | 0.24 ± 0.02 | -1. ± 2 | 1.07 | 0.80 | B |
| | | (0.22 ± 0.02 | 0.01 ± 0.02 | 0.22 ± 0.02 | -2. ± 2 | 1.40 | 0.92 | A) |
| *b* | LG | -0.01 ± 0.05 | -0.10 ± 0.05 | 0.10 ± 0.06 | 43. ± 15 | 0.19 | 0.87 | C |
| *c* | TLG | 0.20 ± 0.02 | 0.01 ± 0.02 | 0.20 ± 0.02 | -1. ± 2 | 1.13 | 0.93 | A |
| | | (0.20 ± 0.02 | 0.01 ± 0.02 | 0.20 ± 0.02 | -2. ± 3 | 1.45 | 0.87 | B) |
| *d* | TT | -0.22 ± 0.11 | -0.27 ± 0.10 | 0.35 ± 0.10 | -65. ± 10 | 1.78 | 0.24 | C |
| | | (-0.33 ± 0.11 | 0.33 ± 0.09 | 0.46 ± 0.09 | -68. ± 6 | 2.76 | 0.28 | C) |
| *e* | TG* | 0.19 ± 0.03 | -0.06 ± 0.02 | 0.20 ± 0.03 | 9. ± 3 | 0.69 | 0.92 | A |
| | | (0.21 ± 0.03 | -0.07 ± 0.02 | 0.22 ± 0.03 | 9. ± 3 | 0.94 | 0.89 | B) |
| *3 OP* | | | | | | | | |
| *a* | TG | 0.00 ± 0.04 | 0.04 ± 0.04 | 0.04 ± 0.04 | -43. ± 29 | 1.21 | 0.02 | B |
| | | (0.01 ± 0.04 | 0.06 ± 0.04 | 0.06 ± 0.04 | -41. ± 17 | 1.77 | 0.02 | B) |
| *b* | TT | 0.02 ± 0.08 | -0.01 ± 0.09 | 0.02 ± 0.08 | 18. ± 114 | 0.96 | 0.00 | B |
| | | (-0.01 ± 0.07 | -0.04 ± 0.09 | 0.04 ± 0.09 | 49. ± 56 | 1.72 | 0.00 | B) |
| *c* | TG* | 0.00 ± 0.04 | 0.03 ± 0.05 | 0.03 ± 0.05 | -48. ± 35 | 1.29 | 0.01 | B |
| | | (0.00 ± 0.04 | 0.05 ± 0.05 | 0.05 ± 0.05 | -44. ± 25 | 1.52 | 0.02 | B) |
| *4 ESBC* | | | | | | | | |
| *a* | TG | 0.28 ± 0.05 | -0.23 ± 0.04 | 0.37 ± 0.05 | 20. ± 3 | 0.76 | 0.99 | A |
| | | (0.24 ± 0.04 | -0.19 ± 0.04 | 0.30 ± 0.05 | 19. ± 4 | 0.81 | 0.89 | B) |
| *b* | LG | 0.03 ± 0.09 | -0.06 ± 0.07 | 0.07 ± 0.08 | 31. ± 35 | 0.16 | 0.97 | B |
| *c* | TLG | 0.20 ± 0.04 | -0.16 ± 0.04 | 0.26 ± 0.04 | 20. ± 4 | 0.83 | 0.97 | A |
| | | (0.19 ± 0.04 | -0.14 ± 0.04 | 0.24 ± 0.04 | 19. ± 4 | 0.86 | 0.83 | B) |
| *d* | TL | 0.23 ± 0.10 | -0.22 ± 0.12 | 0.32 ± 0.10 | 22. ± 10 | 1.28 | 0.59 | E |
| | | (0.19 ± 0.09 | -0.21 ± 0.11 | 0.29 ± 0.10 | 24. ± 10 | 1.37 | 0.21 | B) |
| *e* | TT | -0.11 ± 0.23 | 0.24 ± 0.25 | 0.26 ± 0.25 | -58. ± 25 | 1.60 | 0.03 | N/R |
| | | (-0.10 ± 0.21 | 0.05 ± 0.20 | 0.12 ± 0.23 | -77. ± 45 | 1.92 | 0.03 | N/R) |
| *f* | TG* | 0.40 ± 0.06 | -0.29 ± 0.05 | 0.49 ± 0.06 | 18. ± 3 | 0.65 | 1.00 | A |
| | | (0.32 ± 0.05 | -0.22 ± 0.05 | 0.39 ± 0.06 | 17. ± 3 | 0.75 | 0.94 | A) |
| *5 CSBC* | | | | | | | | |
| *a* | TG | 0.26 ± 0.04 | -0.10 ± 0.03 | 0.27 ± 0.04 | 10. ± 4 | 0.67 | 0.98 | A |
| | | (0.24 ± 0.04 | -0.11 ± 0.03 | 0.26 ± 0.04 | 12. ± 4 | 1.00 | 0.93 | A) |
| *b* | LG | 0.04 ± 0.10 | -0.24 ± 0.14 | 0.24 ± 0.14 | 41. ± 13 | 0.13 | 0.87 | C |
| *c* | TLG | 0.18 ± 0.03 | -0.11 ± 0.03 | 0.21 ± 0.03 | 16. ± 4 | 0.73 | 0.95 | A |
| | | (0.18 ± 0.03 | -0.13 ± 0.03 | 0.22 ± 0.03 | 18. ± 4 | 1.02 | 0.90 | A) |
| *d* | TT | 0.46 ± 0.21 | -0.06 ± 0.17 | 0.46 ± 0.21 | 4. ± 10 | 1.39 | 0.18 | B |
| | | (0.27 ± 0.18 | -0.03 ± 0.16 | 0.27 ± 0.18 | 3. ± 17 | 2.76 | 0.04 | A) |
| *e* | TG* | 0.16 ± 0.05 | -0.15 ± 0.04 | 0.22 ± 0.04 | 22. ± 6 | 0.30 | 1.00 | A |
| | | (0.16 ± 0.05 | -0.16 ± 0.03 | 0.23 ± 0.04 | 22. ± 6 | 0.66 | 0.95 | A) |
| *6 WSBC* | | | | | | | | |
| *a* | TG | 0.12 ± 0.04 | 0.12 ± 0.04 | 0.17 ± 0.04 | -23. ± 7 | 0.55 | 0.95 | A |
| *b* | TT | -0.10 ± 0.23 | -0.20 ± 0.15 | 0.22 ± 0.17 | 58. ± 27 | 0.63 | 0.20 | C |
| *c* | TG* | 0.11 ± 0.05 | 0.12 ± 0.04 | 0.16 ± 0.04 | -23. ± 8 | 0.15 | 1.00 | A |
| *7 NBL* | | | | | | | | |
| *a* | TG | -0.01 ± 0.04 | 0.04 ± 0.03 | 0.04 ± 0.03 | -53. ± 36 | 0.96 | 0.04 | B |
| | | (-0.02 ± 0.04 | 0.01 ± 0.03 | 0.02 ± 0.04 | -13. ± 36 | 1.53 | 0.01 | B) |
| *b* | TT | 0.16 ± 0.34 | 0.43 ± 0.28 | 0.46 ± 0.31 | -35. ± 9 | 1.12 | 0.10 | B |
| | | (0.16 ± 0.34 | 0.43 ± 0.28 | 0.46 ± 0.31 | -35. ± 9 | 1.12 | 0.10 | B) |
| *8 NBL-1* | | | | | | | | |
| | TG | -0.06 ± 0.05 | -0.02 ± 0.04 | 0.06 ± 0.05 | 80. ± 15 | 0.90 | 0.04 | B |

Table 3-1. Shear strain rate estimates

| Network | Data types | $\gamma_1$ | $\gamma_2$ | $\gamma_{max}$ | $\beta$ | $\sigma_0^2$ | 1-P | Quality |
|---|---|---|---|---|---|---|---|---|
| | | (-0.02 ± 0.04 | -0.04 ± 0.04 | 0.05 ± 0.04 | 59. ± 21 | 1.19 | 0.03 | B) |
| *9 NBL-1a* | | | | | | | | |
| | TG | 0.05 ± 0.05 | 0.17 ±0.05 | 0.17 ± 0.06 | -36. ±7 | 0.48 | 0.64 | E |
| | | (0.06 ± 0.05 | 0.11 ± 0.05 | 0.12 ± 0.06 | -30. ± 8 | 1.03 | 0.16 | C) |
| *10 SBL* | | | | | | | | |
| *a* | TG | 0.17 ± 0.03 | 0.11 ± 0.03 | 0.20 ± 0.03 | -16. ± 4 | 1.24 | 0.65 | E |
| | | (0.20 ± 0.03 | 0.11 ± 0.03 | 0.22 ± 0.03 | -14. ± 3 | 1.59 | 0.70 | E) |
| *b* | TG* | 0.06 ± 0.04 | 0.04 ± 0.04 | 0.07 ± 0.04 | -15. ± 15 | 0.92 | 0.11 | E |
| | | (0.12 ± 0.03 | 0.05 ± 0.04 | 0.13 ± 0.04 | -11. ± 8 | 1.12 | | E) |
| *11 OSBL* | | | | | | | | |
| | TG | -0.06 ± 0.06 | -0.08 ± 0.11 | 0.10 ±0.10 | 64. ± 19 | 0.95 | 0.09 | B |
| | | (-0.06 ± 0.06 | -0.04 ± 0.10 | 0.07 ± 0.08 | 73. ± 32 | 0.98 | 0.06 | B) |
| *12 MSBL* | | | | | | | | |
| *a* | TG | 0.08 ± 0.10 | 0.01 ± 0.05 | 0.08 ± 0.10 | -5. ± 15 | 1.69 | 0.15 | C |
| | | (0.18 ± 0.10 | 0.02 ± 0.05 | 0.20 ± 0.10 | -3. ± 7 | 2.12 | 0.12 | C) |
| *b* | TG* | 0.17 ± 0.13 | 0.00 ± 0.06 | 0.17 ± 0.13 | 1. ± 11 | 1.24 | 0.13 | C |
| | | (0.18 ± 0.12 | 0.00 ± 0.06 | 0.18 ± 0.12 | 1. ± 10 | 1.21 | 0.17 | C) |
| *13 ISBL* | | | | | | | | |
| | TG | 0.45 ± 0.18 | 0.15 ± 0.15 | 0.48 ± 0.21 | -9. ± 6 | 1.95 | 0.25 | E |
| *14 I/MSBL* | | | | | | | | |
| *a* | TG | 0.34 ± 0.05 | 0.22 ± 0.05 | 0.40 ± 0.05 | -17. ± 3 | 1.54 | 0.89 | D |
| | | (0.33 ± 0.04 | 0.20 ± 0.04 | 0.39 ± 0.04 | -16. ± 3 | 2.18 | 0.85 | D) |
| *b* | TG* | 0.25 ± 0.06 | 0.26 ± 0.09 | 0.36 ± 0.09 | -23. ± 5 | 1.02 | 0.59 | E |
| | | (0.26 ± 0.05 | 0.22 ± 0.07 | 0.33 ± 0.07 | -20. ± 5 | 1.44 | 0.64 | E) |

Table 3-1. Shear strain rate estimates for the various networks, subnetworks, and data types: triangulation (T), trilateration (L), and GPS (G). An asterisk (*) indicates that the analysis used contains a subset of the triangulation observations used in the previous analysis and contains data only from stations at which GPS measurements were made. P is the F-test probability of significantly different variances for the data fit to a strain model and a zero strain model. Quality is a relative ranking of the strain rate estimate with A being the highest and E the lowest.

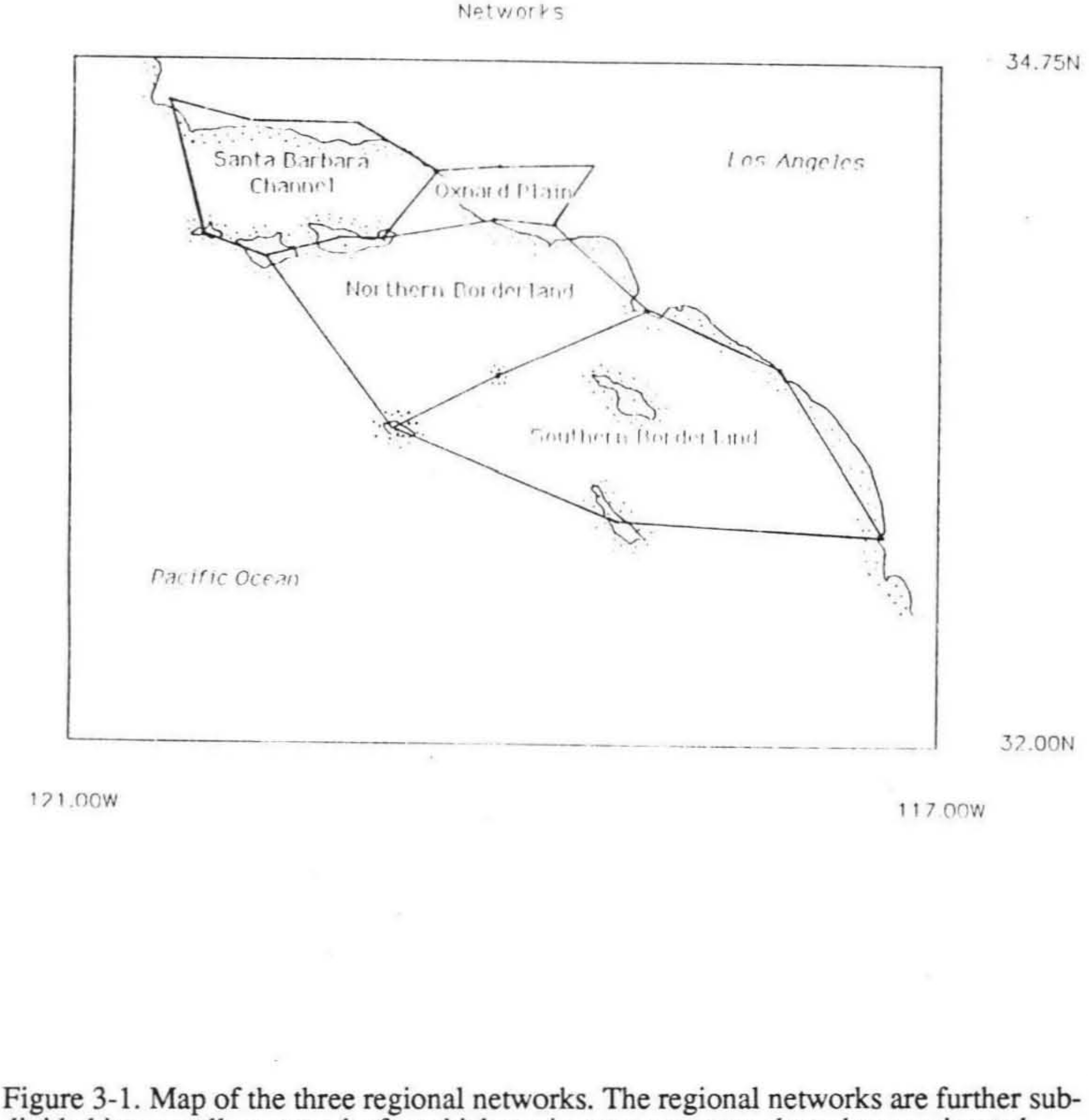


Figure 3-1. Map of the three regional networks. The regional networks are further sub-divided into smaller networks for which strain rate parameters have been estimated.

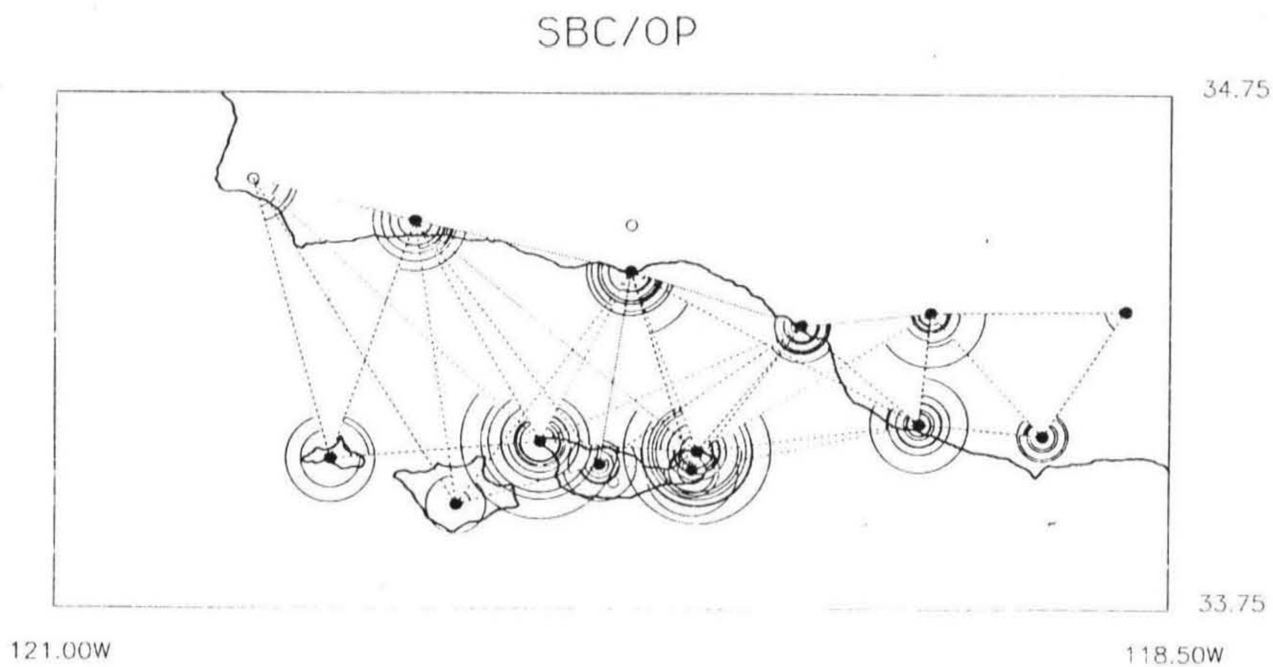


Figure 3-2. Maps of the Santa Barbara Channel and Oxnard plain networks geodetic networks showing triangulation observations. A solid circle indicates that the station is tied to the GPS network. The dotted lines and arcs indicate the observed directions. a) Santa Barbara Channel network

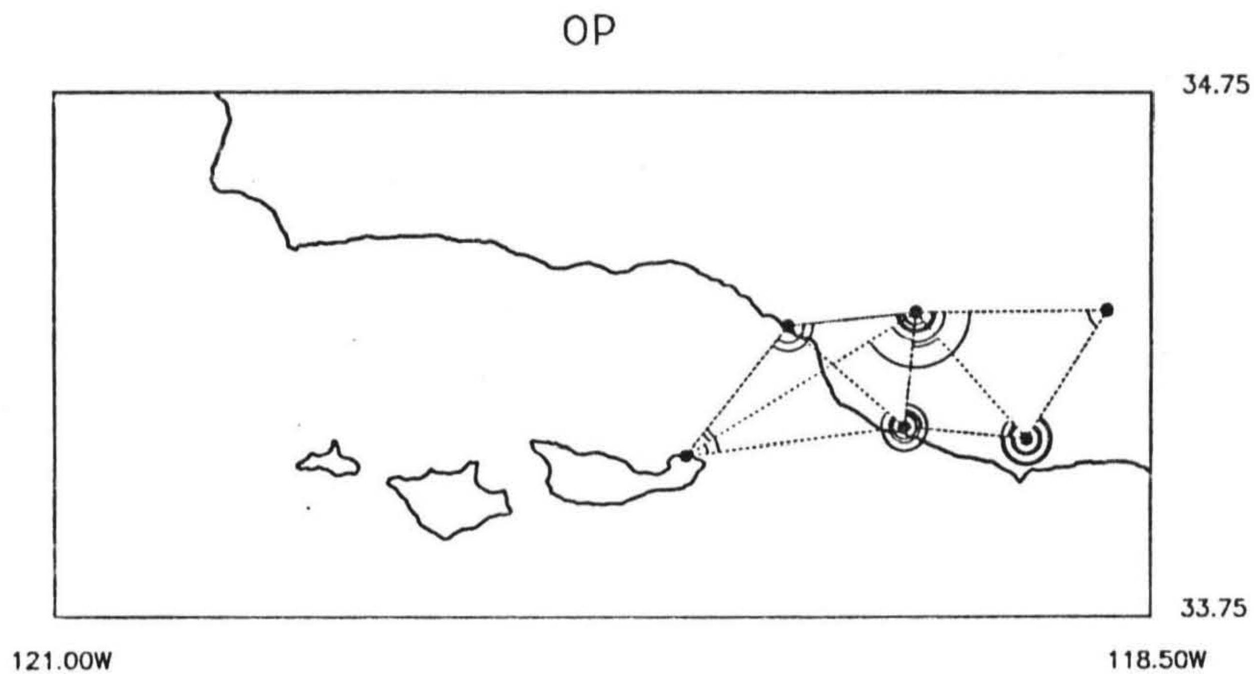


Figure 3-2b. Oxnard Plain network

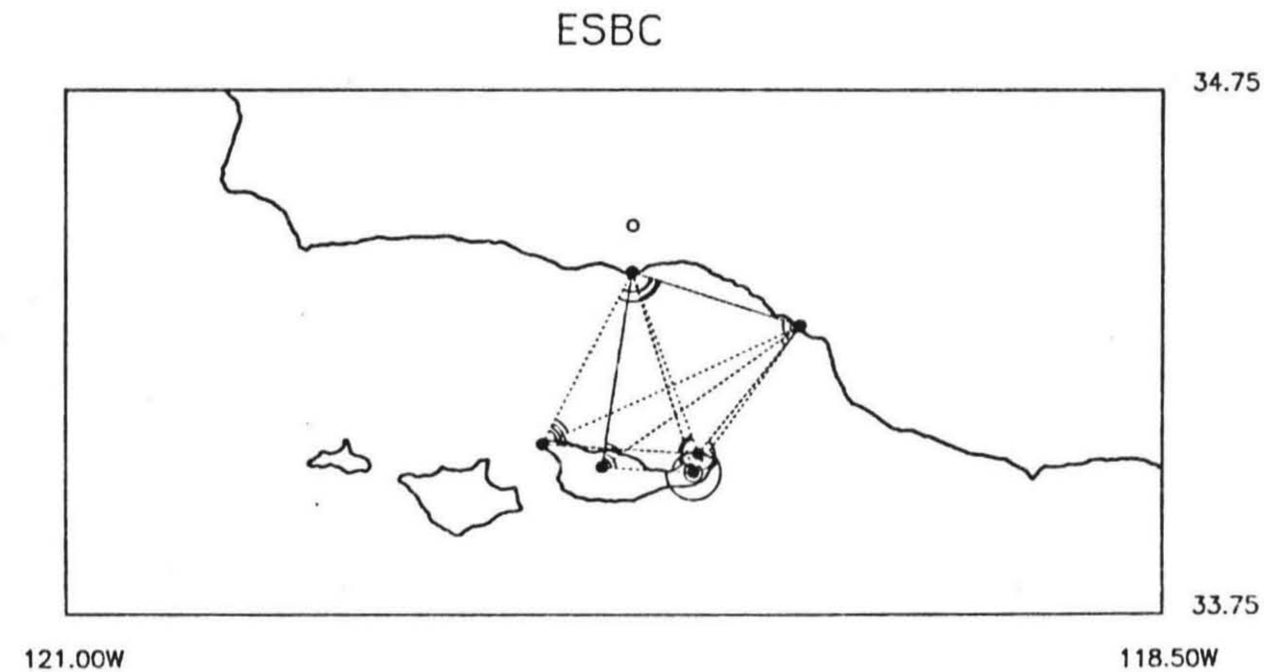


Figure 3-2c. Eastern Santa Barbara Channel network

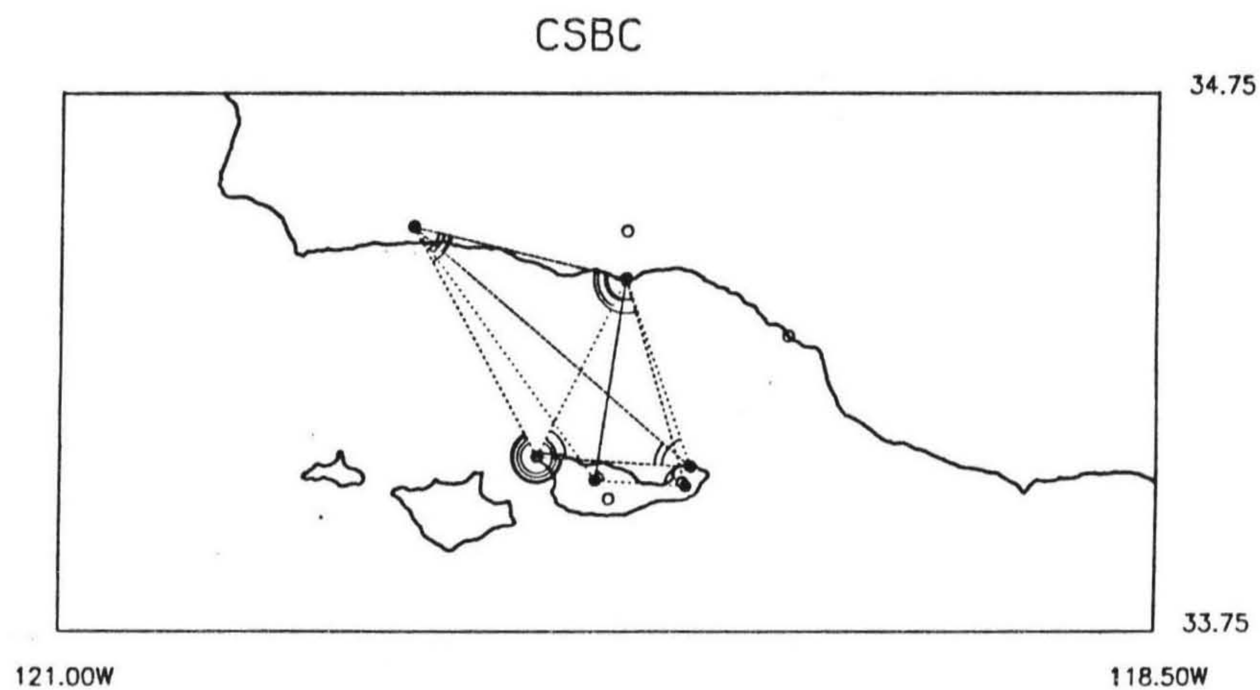


Figure 3-2d. Central Santa Barbara Channel network

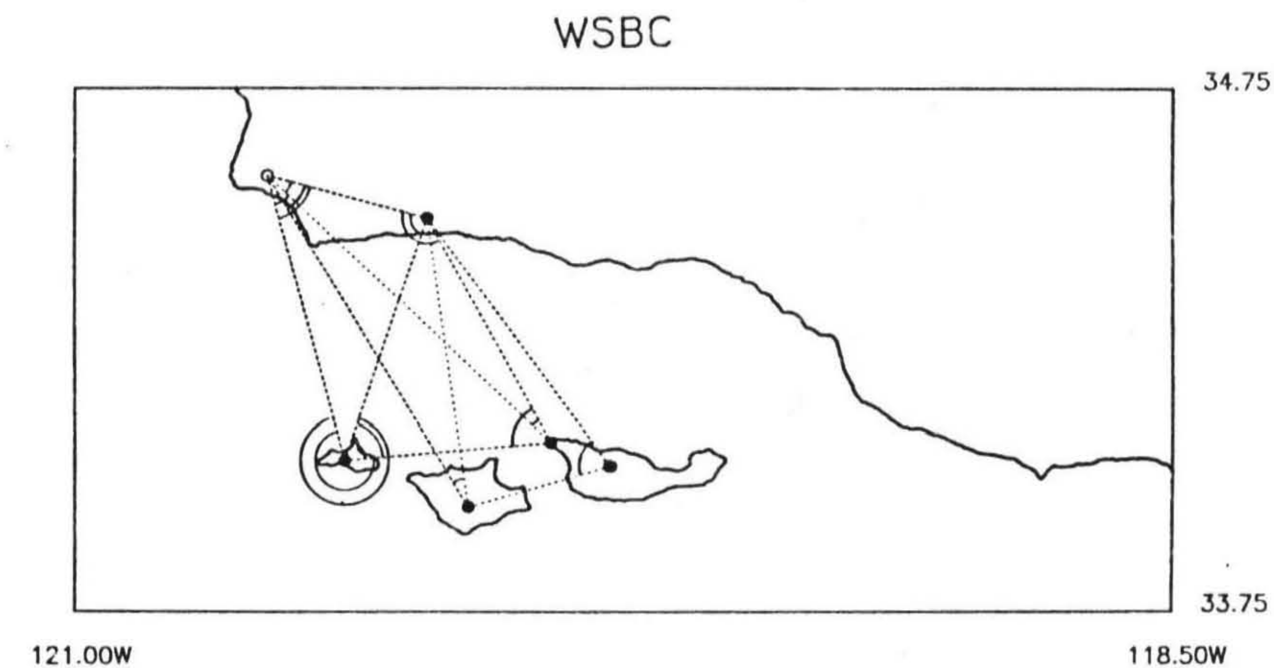


Figure 3-2e. Western Santa Barbara Channel network

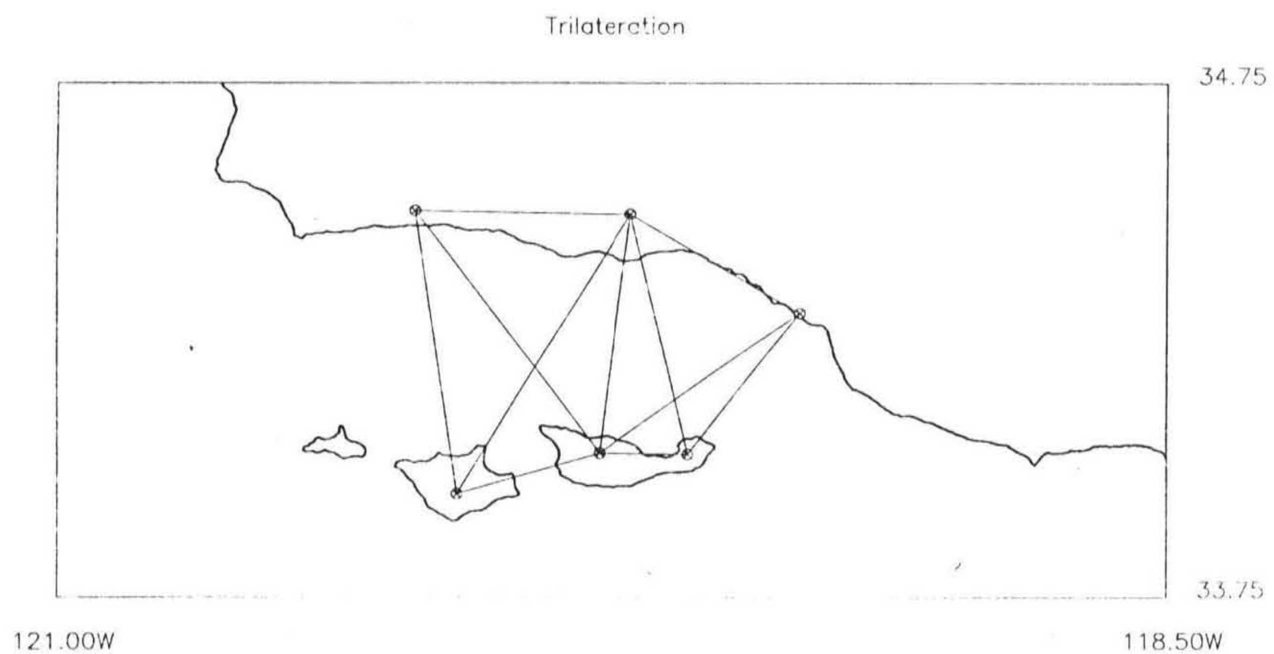


Figure 3-3. Map of precision trilateration observations collected across the Santa Barbara Channel in 1971.

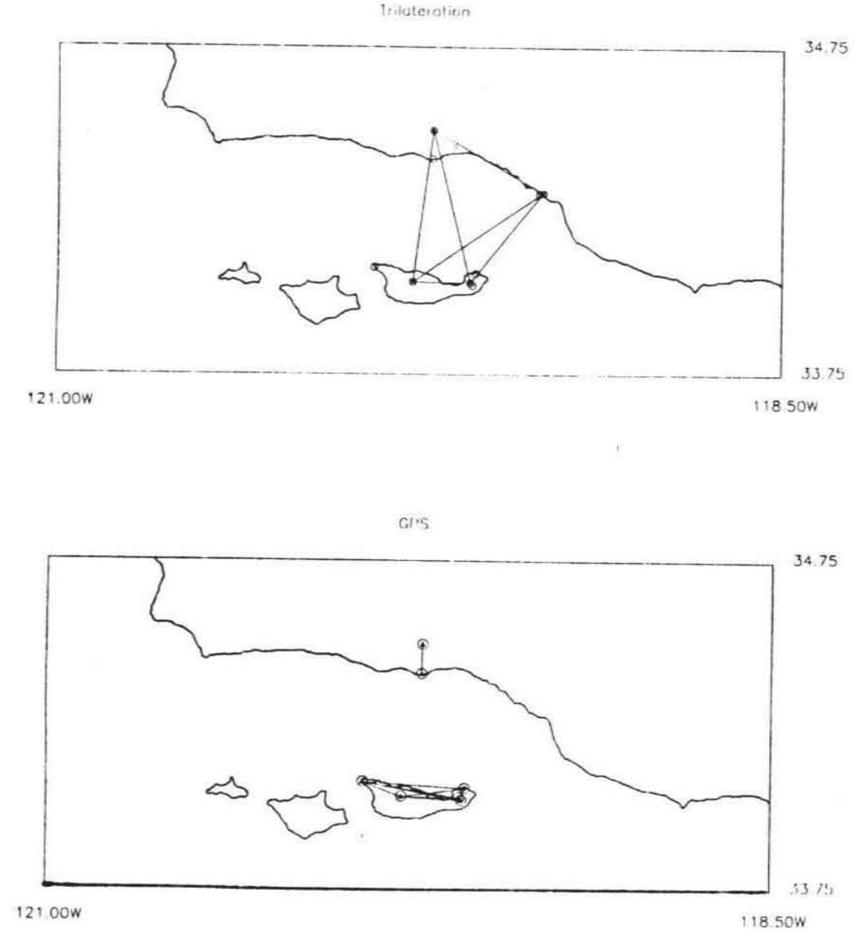


Figure 3-4. Maps of ESBC triangulation-trilateration network (TL) showing the trilateration lines and the GPS vectors. Because the same stations were not observed during the trilateration survey in 1971 as during the triangulation survey of the 1950's, the triangulation stations need to be tied to the trilateration stations in order to recover the data for the strain analysis. This is done with the GPS vectors shown on the lower map. These GPS vectors are time invariant vector ties between the triangulation stations and the local trilateration stations.

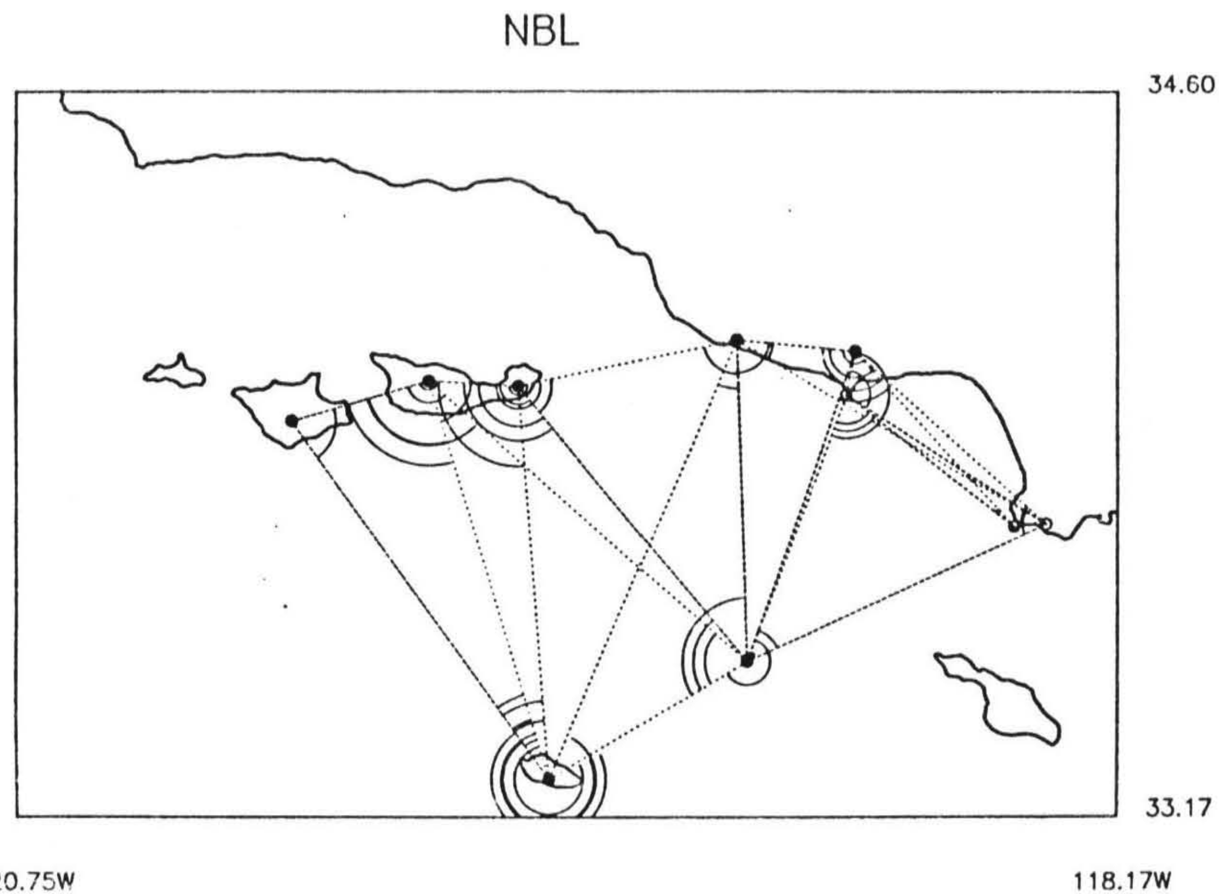


Figure 3-5. Maps of the Northern Borderland geodetic networks showing triangulation, and GPS observations. GPS vectors are not plotted a) Northern Borderland network, NBL, containing all of the observations

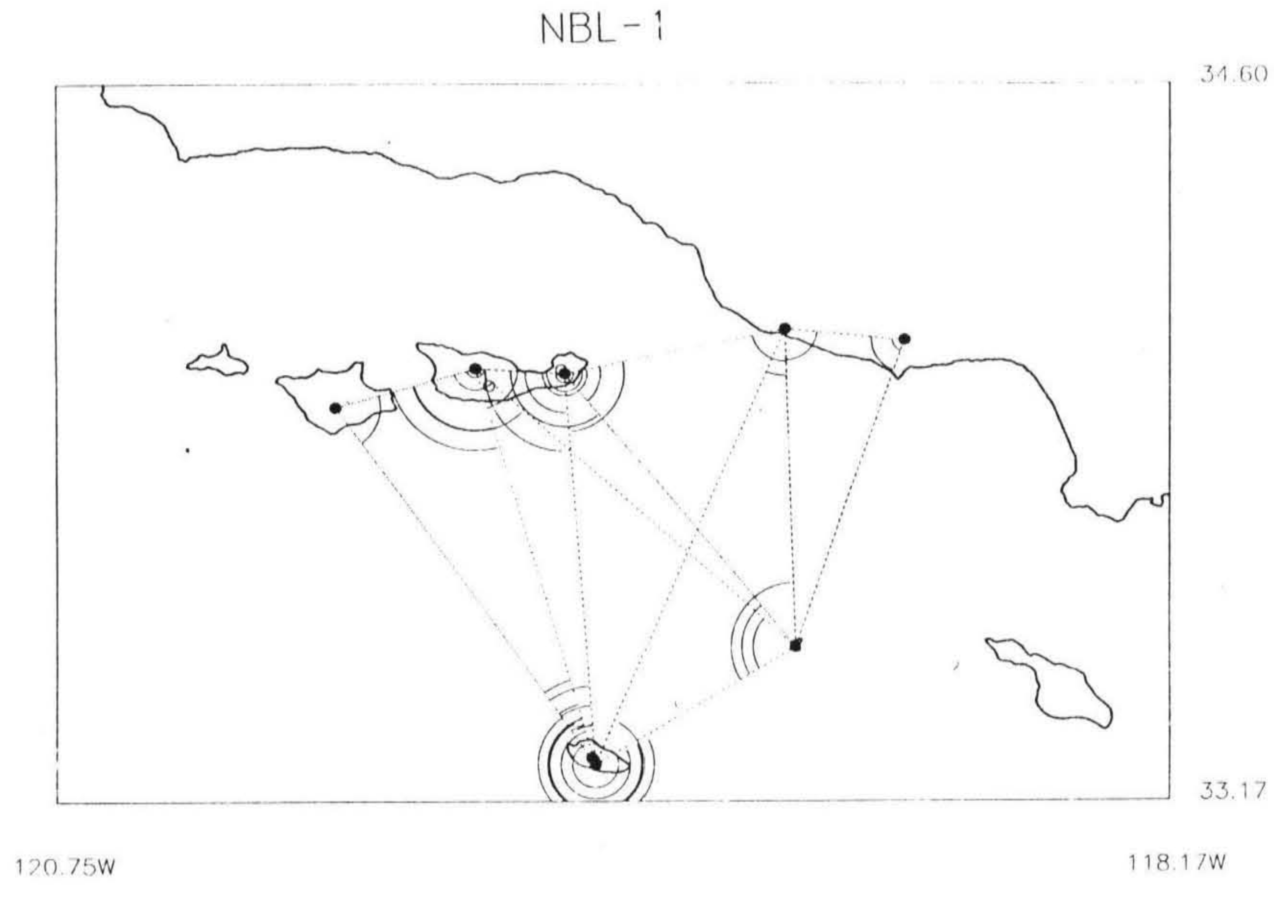


Figure 3-5b. Northern Borderland network, NBL-1,

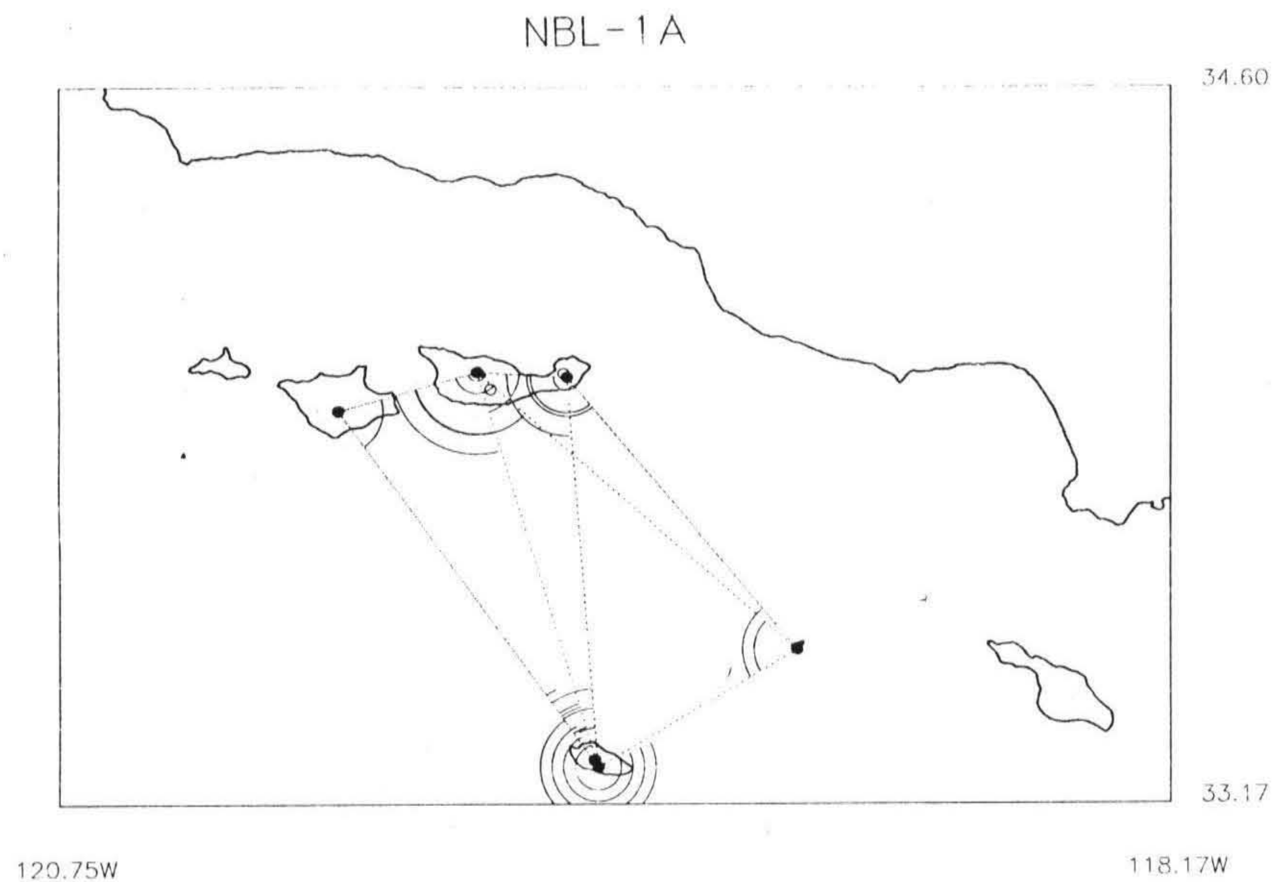


Figure 3-5c. Northern Borderland network, NBL-1A.

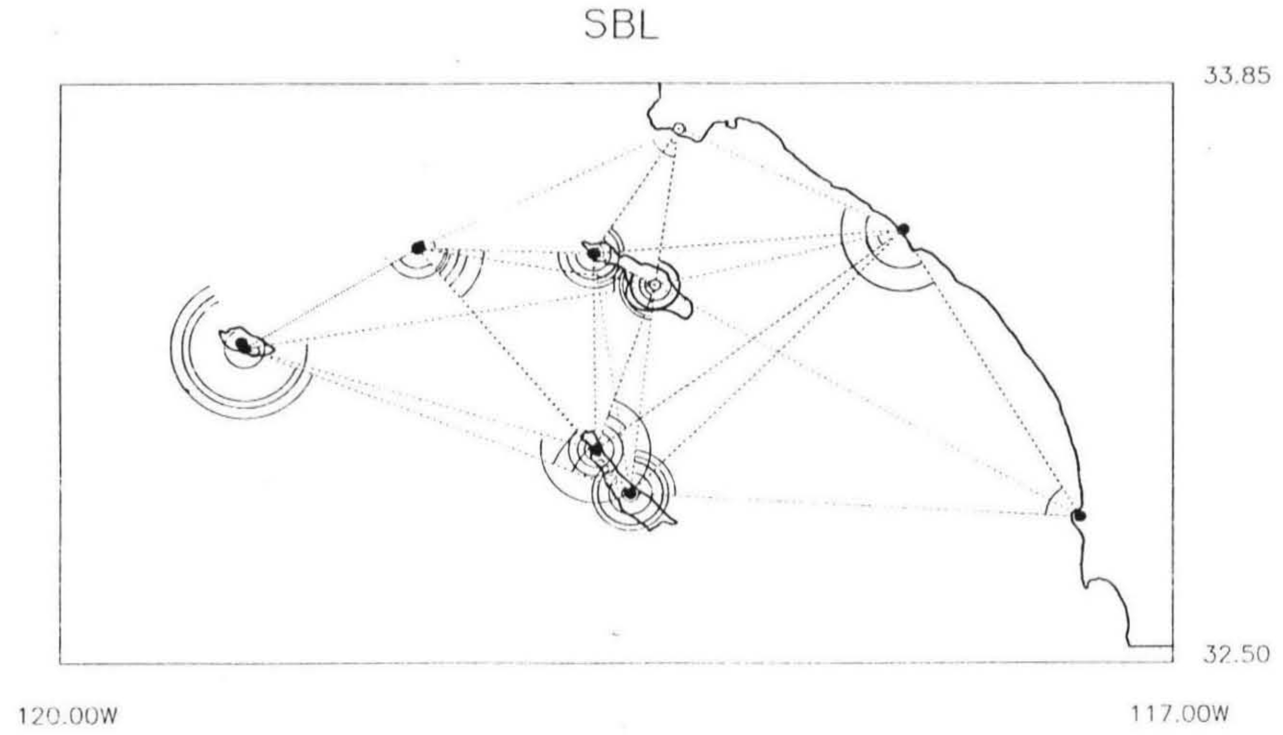


Figure 3-6. Maps of the Southern Borderland geodetic networks showing triangulation, and GPS observations. GPS vectors are not plotted a) Southern Borderland network

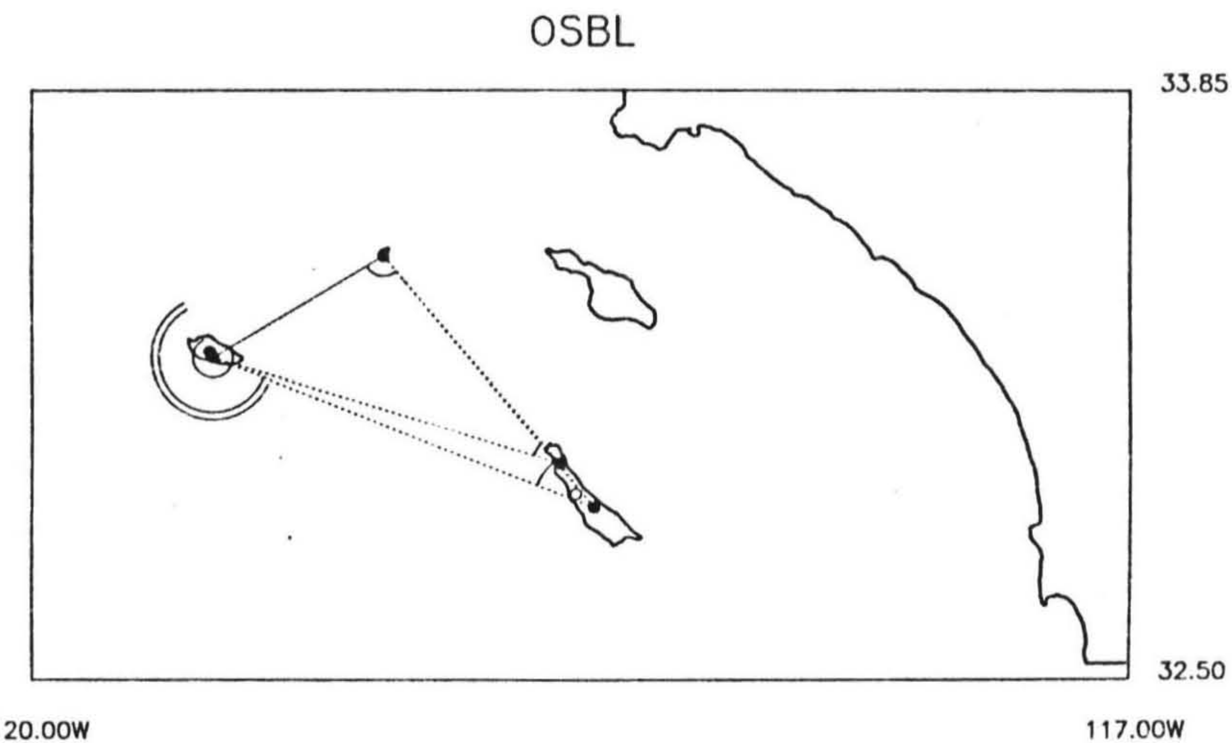


Figure 3-6b. Outer Southern Borderland network

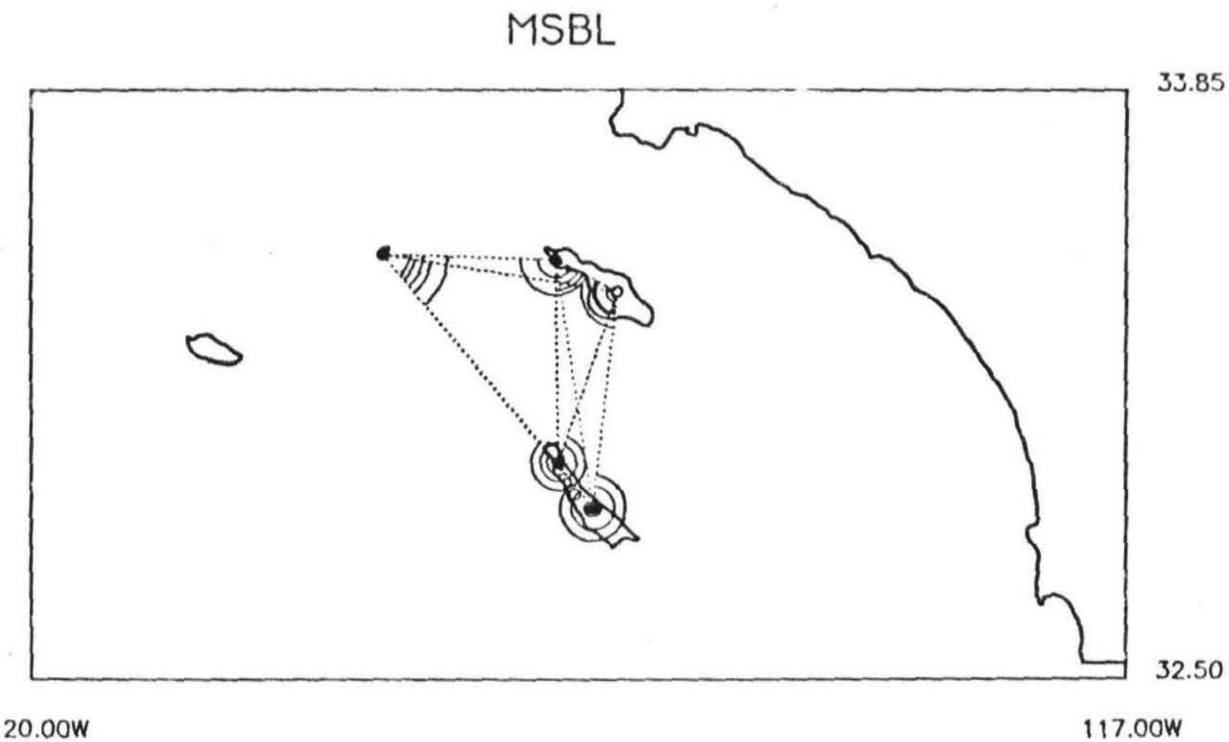


Figure 3-6c. Median Southern Borderland network

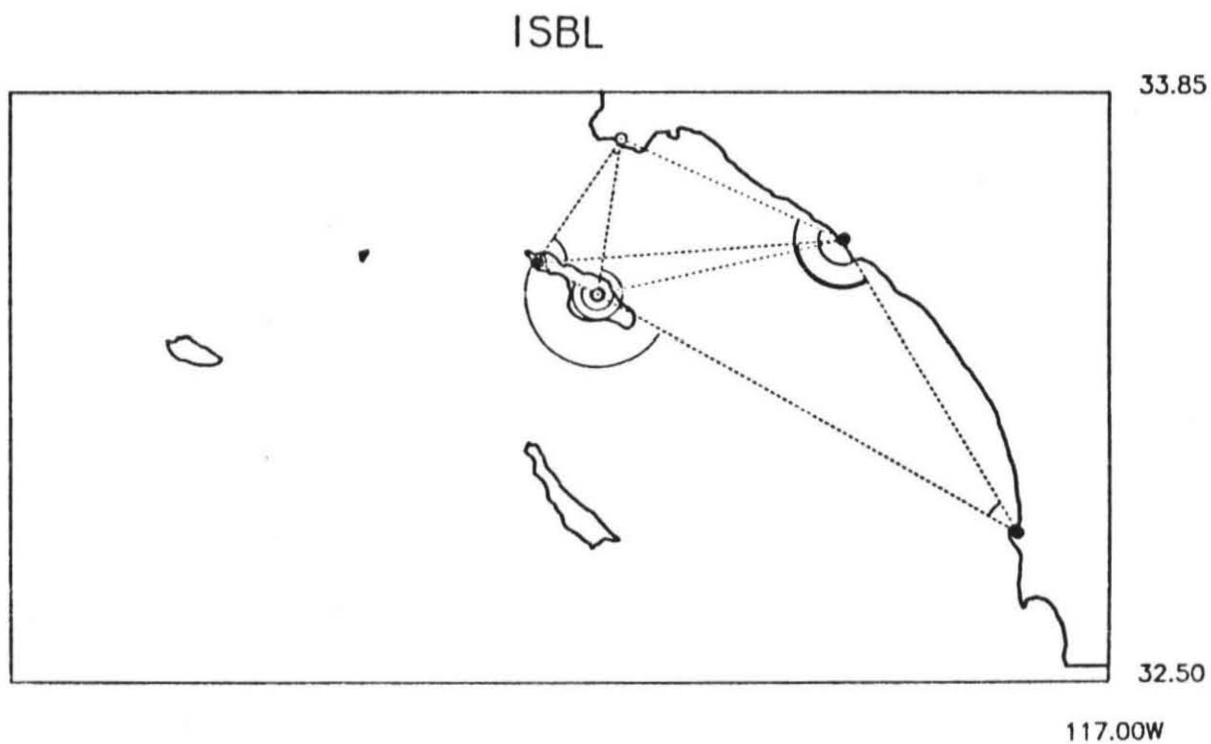


Figure 3-6d. Inner Southern Borderland network

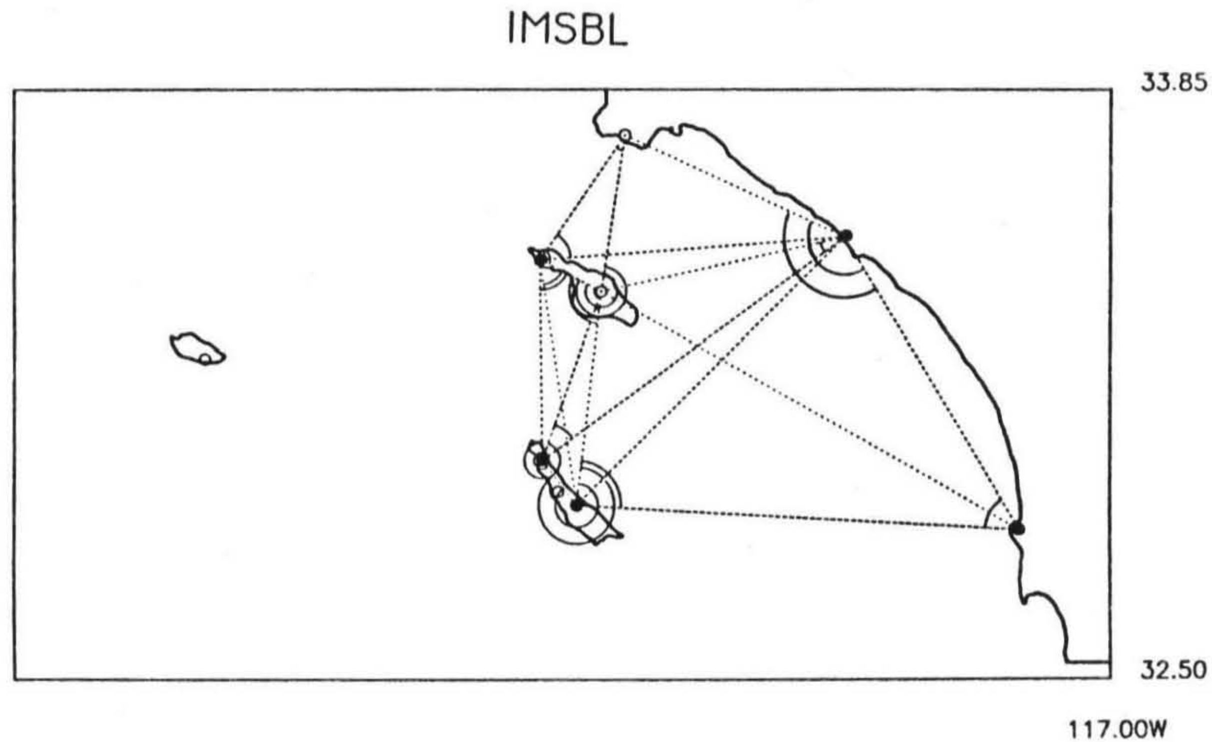


Figure 3-6e. Combined Inner and Median Southern Borderland network

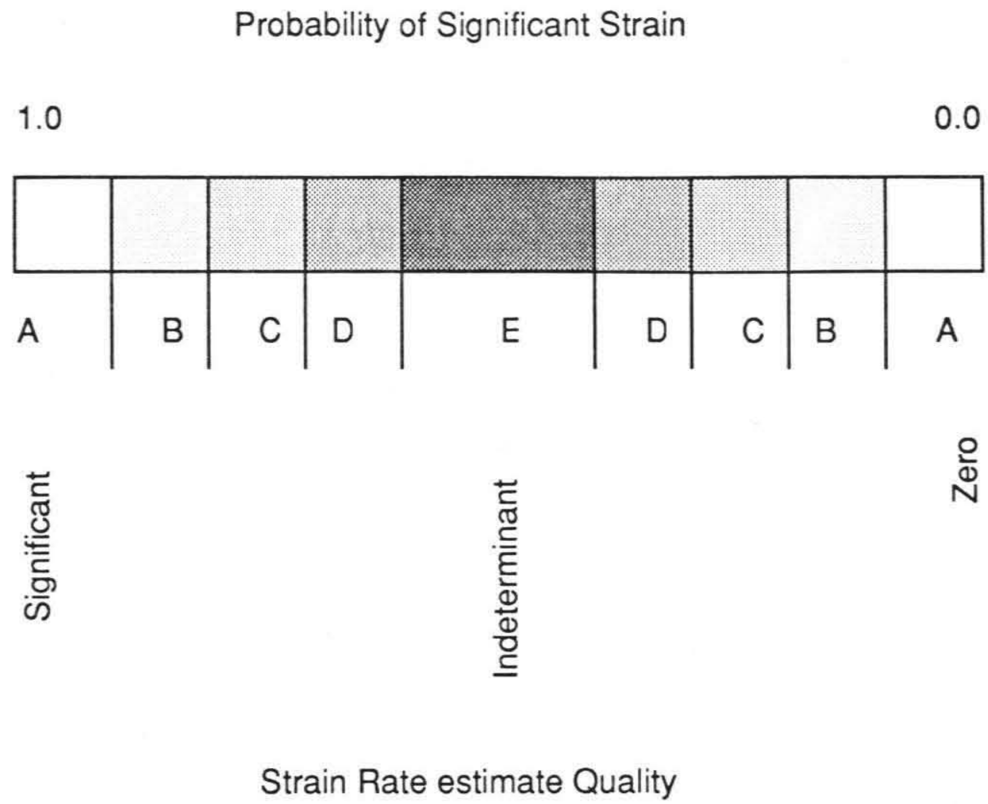


Figure 3-7. Strain estimate quality is based on the F-test for significantly different variances between the strain solution and the no strain solution. 1.0 indicates that variances are different and suggests that the strain-rate estimate is reliable; 0.0 indicates that variances are indistinguishable and the data fits a "no strain" solution equally well as the "strain" solution. High probabilities suggest significant strain rates and low probabilities suggest near zero strain rates. The qualities are ranked from "A" to "E" at increments of 0.1. "A" being the highest and "E" the lowest. "E" qualities indicate that no determination about the strain rate can be made.

| Baseline | $l_{EDM}$ | $l_{Larsen\ et\ al.}$ | $l_{Webb}$ | $l_{Webb} - l_{Larsen\ et\ al.}$ |
|---|---|---|---|---|
| CHAF-HIMT: | 38350.273 | -8.2 | -2.1 | 6.1 |
| LACU-HIMT: | 53282.202 | -7.2 | -6.6 | 0.6 |
| LACU-DEVL: | 52030.224 | -10.5 | -9.7 | 0.8 |
| CHAF-DEVL: | 51533.879 | -8.3 | -7.1 | 1.2 |
| GAVI-SOLE: | 61720.369 | 6.8 | 7.6 | 0.8 |
| GAVI-DEVL: | 64859.053 | 7.4 | 7.6 | 0.2 |
| DEVL-HIMT: | 18494.944 | -0.8 | -7.4 | -6.6 |
| DEVL-SOLE: | 30930.512 | -0.6 | 0.6 | 1.2 |
| LACU-SOLE: | 70287.175 | -7.3 | -5.6 | 1.7 |
| LACU-GAVI: | 44550.542 | 0.7 | 0.4 | -0.3 |
| LACU-CHAF: | 41268.926 | 1.3 | 2.4 | 1.1 |

Table 3-2. Showing differences between the observed Santa Barbara channel trilateration, $l_{EDM}$, and GPS estimates of those lengths by Larsen et al. [1990], $l_{Larsen\ et\ al.}$, and the GPS estimates presented here, $l_{Webb}$. $l_{EDM}$ is in meters, and $l_{Larsen\ et\ al.}$, $l_{Webb}$ and the GPS-GPS difference $l_{Webb} - l_{Larsen\ et\ al.}$ are in centimeters. If the lines including HIMT are excluded, the mean GPS-GPS difference is $8 \pm 6$ mm.

# Chapter 4.

# Geodetic results and their relationship to the geologic environment

## 4.1 Introduction:

The geodetic analyses of the previous chapter indicate regions of both significant strain and near zero strain for several networks in the offshore of southern California and provide quantitative estimates of the direction of maximum contraction and the strain rates averaged over several decades to more than a hundred years. In order to assess the long-term importance of these measurements for understanding the tectonics and kinematics of southern California, these strain rates will be evaluated against the style and rate of deformation recorded in the geological record. The geological direction of shortening can be inferred from the trends of mapped faults and fold axes for the geological time scale, and from focal mechanism studies for the geodetic and seismologic time scale. However, because both the most recent geological history of deformation in this region is incompletely known and the seismological record is limited, these data sets together can only be used to place constraints on the strain field for interpreting the significance of the geodetic strain rates as estimators of the long-term strain rate.

In this chapter, the evidence for the style and rate of deformation across the Santa Barbara Channel, Oxnard Plain, and Northern Borderland regions will be discussed and the geodetic estimates will be evaluated against this evidence. Strain estimates from the other networks are less reliably determinable and will not be discussed. Consistency between these long- and short-term indicators and the geodetic estimates would indicate that the geodetic strain rates are reliable estimates of the geologic strain field. Inconsistencies, though, may indicate that the strain fields are not necessarily constant in time or that the data, geologic and/or geodetic, are not strong enough to properly resolve the strain fields.

4.2 Geodetic strain-rate representation:

The strain-rate estimates based on the triangulation-GPS data set are used for the comparisons, because this is the only data set that is entirely common in observation type among all of the networks and spans the longest time period of observations with the most epoches (see Chapter 3). Because each network is a different size, shear-strain rate comparisons between the different networks are biased by the scale of the network. This scaling is removed by converting the strain-rates to length-dependent deformation rates. Since the primary mode of geological deformation in this part of the western Transverse Ranges is through crustal shortening [Dibblee, 1982d], the shear-strain rates have been reduced to equivalent uniaxial convergence rates across the networks, providing a useful quantity for comparison with geological slip rates.

Studies to the northeast [Eberhart-Phillips et al., 1990] and northwest [Feigl et al., 1990] of the Santa Barbara channel suggest non-uniaxial geodetic strain. However, these are in areas where both significant strike-slip faulting and north-northeast directed shortening are recorded in the geological record. Strike-slip faulting near and within the Santa Barbara channel networks has been recognized, but late Quaternary horizontal slip rates on these faults are considered to be low [Yerkes and Lee, 1987]. The highest rate is north of the channel networks on the east trending Santa Ynez fault, <10mm/yr. On the faults within the networks, the horizontal slip rates are on the order of 1mm/yr or less. This is an order of magnitude smaller than the geological contraction rates of 10-20 mm/yr [Davis and Namson, written communication, 1989] across the same areas. Other geodetic studies in the Santa Barbara channel [Larsen, 1990] indicate near uniaxial strain rates across the eastern channel and a combination of northwest-southeast extension and northeast-southwest contraction across the central channel, averaged over 17 years.

Uniaxial convergence is modeled by finding the uniaxial strain-rate, $\varepsilon$, in the direction of maximum contraction, $\beta$, derived from the shear-strain analyses. Let **U** be the uniaxial strain-rate tensor

$$\mathbf{U} = \begin{bmatrix} \varepsilon & 0 \\ 0 & 0 \end{bmatrix} \qquad (4\text{-}1)$$

that is related to the strain-rate tensor **E**

$$\mathbf{E} = \begin{bmatrix} e_{11} & e_{12} \\ e_{12} & e_{22} \end{bmatrix} \qquad (4\text{-}2)$$

in a north-east coordinate system, with east directed along the 1-axis and north along the 2-axis. **U** is related to **E** through a rotation **R** by

$$\mathbf{E} = \mathbf{R}\ \mathbf{U}\mathbf{R}^{T}. \qquad (4\text{-}3)$$

**R** is a rotation from the the uniaxial strain system in the direction of maximum contraction $\beta$, to the north-east system and has the form

$$\mathbf{R} = \begin{bmatrix} \cos\beta & -\sin\beta \\ \sin\beta & \cos\beta \end{bmatrix} \qquad (4\text{-}4)$$

The strain-rate tensor **E** can then be represented as

$$\mathbf{E} = \begin{bmatrix} \varepsilon\cos^2\beta & \varepsilon\sin\beta\cos\beta \\ \varepsilon\sin\beta\cos\beta & \varepsilon\sin^2\beta \end{bmatrix} \qquad (4\text{-}4)$$

Using the following relationships between the estimated shear-strain rates, $\gamma_1$ and $\gamma_2$, and the components of **E**:

$$\gamma_1 = (e_{11} - e_{22}) \tag{4-5}$$

$$\gamma_2 = 2e_{12} \tag{4-6}$$

$$\beta = \frac{1}{2}\tan^{-1}\left(\frac{-\gamma_2}{\gamma_1}\right). \tag{4-7}$$

the uniaxial strain-rate, $\varepsilon$, is given by

$$\varepsilon = \frac{\gamma_1}{\left(\cos^2\beta - \sin^2\beta\right)} \tag{4-8}$$

or

$$\varepsilon = \frac{\gamma_2}{2\sin\beta\cos\beta} \tag{4-9}$$

The relative convergence rate, v, for the motion of the average network-crossing length scale, l, in the direction of maximum contraction is given by

$$v = \varepsilon\, l \tag{4-10}$$

and tabulated in Table 4-1.

The geodetic data provide no information on network rotation. Therefore, in this model, network rotation is assumed to be zero. Regional geologic rotation rates in the Transverse Ranges over the last 15 Ma have been inferred from paleomagnetic data to be on the order of 5-10$^{\circ}$ / Ma [Hornafius et al., 1986]. These investigations indicate that the western Transverse Ranges has rotated clockwise as a block beginning in the Middle Miocene. The data show a decrease in the rotation rate in the western Transverse ranges from 10 Ma b.p. to the present. The average rotation rate over the last 5 Ma is 5$^{\circ}$ / Ma (0.09 μrad/yr). If this rotation is continuing at present at this rate, then the contribution to the network displacement rates would be on the order of a few mm/yr of block rotation of the networks spanning the Santa Barbara channel.

4.3 Tectonic setting:

The Santa Barbara Channel and Oxnard Plain are part of the western Transverse Ranges geomorphic province. The topography and structures of the Transverse Ranges cut across the general northwest-southeast structural grain of California by forming the only east trending mountain range in the state [Dibblee, 1982d]. Situated in the Big Bend region of of the San Andreas fault, the Transverse Ranges extend from east of the San Andreas to the coastline as a broad elevated mountains range. The Santa Ynez Mountains uplift and the Channel Islands uplift form the northern and southern boundaries, respectively, to the western Transverse Ranges. Between these two uplifts, the Santa Barbara Channel and Ventura basin form a deep sediment filled tectonic trough.

East of Ventura, the onshore extension of this depression narrows and is bounded to the south by the Oak Ridge uplift. The Oxnard Plain lies between the Oak Ridge uplift and the Santa Monica Mountains uplift to the south. North of the western Transverse Ranges, the structures include folds, faults, and sedimentary basins that trend west-northwest. This is intermediate in trend between the dominant northwest trend of the Coast Ranges and the west trend of the Transverse Ranges. To the south, deep northwest trending submerged fault bounded basins and ridges of the Continental Borderland abut abruptly against this west trend along the Santa Monica Mountains and Channel Islands uplifts [Dibblee, 1982d].

Several balanced cross sections constructed across the western Transverse Ranges by Davis and Namson [1988; 1989, written communication] represent the most complete synthesis of the available data on the subsurface structures and the deformational style. These sections, based on surface geological maps, seismic reflection profiles, and well data, suggest that the western Transverse Ranges are part of a fold and thrust belt that has experienced significant rates of shortening in the last 2-4 Ma. The shortening has been interpreted as the result of fault bend folding and blind thrusting along a 10-15 km deep decollemént, of a north over south thrust system. Most of the shortening has been interpreted as being consumed in folds and thrusts from the near shore northern channel platform, where the thrust system wedges back along south dipping back thrusts, to north of the Santa Ynez mountains. Some of the convergence is consumed in structures further offshore. From the restored sections, calculated average slip rates over the last 2-4 Ma indicate ~10-25 mm/yr of convergence across the western Transverse ranges [Davis and Namson, 1989, written communication ] (Table 4-2; Fig. 4-1). It is not possible to determine from the reconstructions which faults have been more active than others during the last 2-4 Ma.

4.3.1 Ventura Basin Tectonics:

Most of the information on the style, timing and rates of deformation during the last 2 Ma come from geologic investigations of structures in the Ventura Basin. Many of the structures there extend into the offshore along the north channel platform and in the coastal region between Santa Barbara and Ventura. The Ventura basin in the late Tertiary formed a broad west trending asymmetrical syncline. During the late Quaternary, in the eastern part of this structure, uplift of the Oak Ridge and southward thrusting of the north flank of the syncline over the basin severely narrowed this depositional trough [Dibblee, 1982c; Dibblee, 1982d]. This thick sequence (>10 km) of Pliocene to Pleistocene aged strata is bounded to the north and south by opposed reverse fault systems and is separated from the San Fernando basin to the east by the young Oak Ridge-Santa Susanna Mountains and Simi Hills uplifts.

Many of the structural trends of the Ventura Basin continue into the offshore west of Ventura. These include the Ventura-Rincon anticline, Pitas Point -Ventura fault, Javon Canyon fault, Oak Ridge fault, the Montalvo anticline and the Red Mountain fault

[Luyendyk et al., 1982; Yeats, 1983; Yerkes et al., 1980; Yerkes and Lee, 1979; Yerkes and Lee, 1987]. In addition to these structures, several east trending near shore folds and thrust faults occur between the Red mountain and Oak Ridge faults west of Ventura [Luyendyk et al., 1982]. Holocene vertical slip rates estimated on some of these faults indicate relatively low rates of vertical slip (< 1mm/yr) [Yerkes and Lee, 1987] in contrast to the relatively high uplift rates estimated from investigations of uplifted marine and stream terraces in the Ventura area ( ~10 mm/yr) [Lajoie et al., 1979]. This may suggest that folding and faulting along blind thrusts, and not slip on faults that break the surface, are the primary mode of vertical deformation, and crustal shortening.

Yeats [1983] concluded that decollemént tectonics began in the Ventura basin as recently as 2 Ma ago at relatively high rates. The convergence associated with this region has occurred through a combination of folding and thrust faulting. Across Ventura, north-south convergence has occurred during the last 0.2 Ma at a rate of 23 mm/yr based on stratigraphy and fold geometry. 20 mm/yr of this rate is consumed across the Ventura Anticline and Cañada Larga Syncline. Prior to this, the thrust faults under the Ventura Anticline were active between the last 1.3 Ma and 0.65 Ma, reaching a maximum slip rate of 2.8 mm/yr at 0.65 Ma b.p. [Yeats, 1983]. The spatial distribution of the deformation rate to the east is not well constrained. At least 12 mm/yr of convergence has been documented further to the east near Filmore [Yeats et al., 1988].

The Yeats [1983] estimate of 23 mm/yr of late Quaternary convergence across a 40 km section through Ventura agrees well with the average rate over the last 2-4 Ma of Namson and Davis [1988] of 17.6-26.5 mm/yr for their regional, 123 km-long cross-section, from the southern San Joaquin Basin to Ventura and with the 17 mm/yr estimate of Rockwell [1984], from Ojai to Ventura. But, 23 mm/yr exceeds the minimum slip rate solution of 8.8-15.9 mm/yr for the section from the Big Pine Fault to Ventura (Section 5 of Fig. 4-1). This, together with the change in the deformation rate on the Ventura Anticline, may imply that during the last 0.2 Ma the regional shortening was almost entirely being consumed in the folding of the Ventura Anticline and Cañada Larga Syncline and that prior to 0.2 Ma, the ~23 mm/yr of slip was being consumed along other structures. This would seem to indicate that the location of the active structures along which the regional shortening is being consumed can change on a time scale of < 0.5 Ma.

However, the cross-sections of Yeats [Yeats, 1983; Yeats et al., 1988] and of Namson and Davis [1988] interpret the deformation differently and the admissibility of each other's sections has been questioned [Namson and Davis, 1989a; Namson and Davis, 1989b; Weldon and Humphreys, 1989; Yeats and Huftile, 1989]. Because the cross-sections of Namson and Davis [1988] are demonstrably restorable and represent a minimum slip solution over a longer section than the sections of Yeats [Yeats, 1983; Yeats et al., 1988], the 2-4 Ma average minimum slip rate across this part of the western Transverse Ranges is probably best constrained to be between 8.8-15.9 mm/yr. The 23 mm/yr of Yeats [1983] across the Ventura Anticline for the last 0.2 Ma may represent an increase in the deformation rate in the Ventura region during the latest Quaternary, through a concentration of the regional shortening there.

## 4.4 Geological strain indicators within the geodetic networks :

### 4.4.1 Oxnard Plain:

The geodetic strain-rate estimate of zero significant strain across the OP network (0 ± 4 mm/yr) agrees well with the observed geological structures and inferred geological history of this area for the last 2-4 Ma [Dibblee, 1982b; Namson, 1987; Yeats, 1983]. This network which crosses relatively undeformed strata is bounded to the north by the Oak Ridge fault and to the south by the Malibu Coast fault (Fig. 4-2). Each of these trends has been active in the last 2-4 Ma [Dibblee, 1982b]. On the basis of stratigraphic well data, Yeats [1983] concluded that nearly all of the late Quaternary shortening across the Ventura basin occurs north of Oak Ridge, and thus north of the OP network.

Restored balanced cross-section across this part of the western Transverse ranges [Namson, 1987] interpret the Oxnard Plain to contain relatively undeformed strata and no active faults. The active structures wrap around the uplifted Oak Ridge-Simi Hills uplift, north of the network. Thrust faults and fold axes bend from a generally east west trend south of Ventura to *northeast* near Santa Paula, back to east-west north of the Oak Ridge-Simi Hills uplift. Some of these structures pass between station CHAF in the northwest corner of the network and the other stations, but the majority of the network lies in a geologically stable area.

4.4.2 Santa Barbara Channel networks:

The strain direction and deformation rate indicators for each of the three networks that cross the Santa Barbara channel are mainly derived from maps [Junger, 1979; Yerkes et al., 1980], seismic reflection profiles [Junger, 1979; Luyendyk et al., 1982], restored balanced cross sections [Davis and Namson, 1989, written communication], fault slip studies [Sarna-Wojcicki, et al., 1987; Keller et al., 1980; Yerkes et al., 1987], and marine terrace studies [Lajoie et al., 1979]. Two general structural trends that are contained within each of these networks are a zone of folding and thrust faulting along the northern channel platform and an antiformal uplift along the northern channel islands. Another major structural zone, the Mid-channel fault zone extends from Hueneme submarine canyon, near Oxnard, westward to Gaviota at a N70W trend with apparently north side up Quaternary slip [Junger, 1979]. In addition to the folds and faults, marine terraces record regional variations in the deformation rate.

The folds and faults along the northern channel platform [Vedder, et al., 1980; Luyendyk et al., 1982] indicate generally north directed shortening that has been active during the late Quaternary and Holocene. From seismic reflection profiles, several near shore east trending thrust faults and folds have been mapped [Vedder, et al., 1980; Luyendyk et al., 1982; Dibblee, 1982c]. Active thrust faulting has been suggested for some of these faults between Santa Barbara and Ventura on the basis of bathymetric breaks. Up to 10 m of south side up thrust faulting has been interpreted to break the sea floor and Holocene deposits along the Goleta-Rincon fault [Luyendyk et al., 1982], implying a vertical slip rate of >1 mm/yr. Further to the west, possible Holocene sea floor breaks less than 1 m were also recognized on the offshore extension of the south branch of the Santa Ynez Fault [Luyendyk et al., 1982], with minor amounts of left slip suggested on some of these faults [Dibblee, 1982c].

Discontinuous uplifted marine terraces from Ventura to Point Conception record large variations in rates of vertical deformation which may be indicative of spatial variation in convergence rates across the channel. Typical uplift rates along the southern California coast, south of the Transverse Ranges, are low, from ~0.1- 0.6 mm/yr, while along the east trending structures between Goleta and Ventura, uplift rates range from 4-10 mm/yr [Lajoie et al., 1979]. The most rapid uplift rates on the west coast of the conterminous United States are near Ventura (~10 mm/yr) on the foot wall of the Red Mountain Thrust . The uplift rate of marine terraces decreases to the west where at Point Conception it is within the range of typical values for southern California. If uplift is the result of crustal shortening due to folding or thrust faulting, as has been suggested for the Ventura area [Lajoie et al., 1979], this decrease would seem to suggest decreasing active convergence to the west. However, the sampling of marine terraces is discontinuous and limited to only three localities. Only a few, different onshore structures are overlain by terraces that have been studied and the along strike variation of deformation on a single structure has not been determined.

Less active, but more complex, deformation is indicated from marine terrace elevations and the trend and style of faulting along the generally west-northwest trending anticlinal Channel Islands uplift. The uplift extends from the mainland as part of the Santa Monica Mountains anticlinorium to the southwestern part of the Santa Barbara basin, where it terminates in a northwest plunge. It has an overall structural and physiographic trend that is intermediate between the trend of the Transverse Ranges and the Peninsular Ranges [Junger, 1979]. The lack of Pliocene deposits on the northern channel islands and in the Santa Monica Mountains has been interpreted as an indication that uplift of this west-northwest to west trending antiform began during the Pliocene [Dibblee, 1982a; Junger, 1979]. Little Pliocene or Quaternary activity has occurred on the north side of the antiform with the majority of the deformation occurring on the south side of the antiform in response to convergence between the east trending antiform and the northwest trending ridges of the Continental Borderland [Junger, 1979].

The preservation of several emergent marine terraces on the northern channel islands [Orr, 1960; Orr, 1968; Weaver, 1969] significantly above the height of the latest sea level high stand indicates that uplift of the islands has continued during Pleistocene time. Because the ages of the terraces and, thus, their correlation with the sea level record are not known, the uplift rates can not be calculated. It has been suggested [Patterson, 1979], based on geographic position and elevation, that the lowest terrace on Santa Cruz Island may be correlative with the Point Dumé terrace, to the east. The Point Dumé terrace has been correlated, on the basis of faunal assemblages in the terrace deposit [Lajoie et al., 1979] with the 120 ka sea level high stand. On this basis, the uplift rate of the northern channel islands may be quite low (< 0.6 mm/yr). This rate is within the typical range for uplifted marine terraces along the southern California coast, implying substantially less active deformation than to the north along the northern channel platform during the last 100 ka.

In addition to this young relatively slow uplift, two Pleistocene left-lateral strike-slip faults, the Santa Cruz Island fault and Santa Rosa Island fault, cut Santa Cruz and Santa Rosa islands roughly in half. Cumulative post-Miocene slip on these faults is considered to be low from the lack of offset on the channel islands platform [Junger, 1979]. Correlation of a seismically imaged fold axis with the Christi Anticline on Santa Cruz Island argues for 10 km of post Miocene slip on the Santa Cruz Island fault

[Luyendyk et al., 1982] implying an average maximum slip rate of ~2 mm/yr. Deflected stream channels across the Santa Cruz Island fault indicate late Quaternary left-lateral motion, however, no evidence of Holocene activity has been reported [Patterson, 1979].

The concentration of young folds, the offset of Pleistocene and Holocene deposits, the high 2-4 Ma convergence rates (10-25 mm/yr), and the high late-Pleistocene uplift rates (4-10 mm/yr) along the northern part of the channel indicate that the most active structures within the networks lie along the northern channel platform. Along the Channel Islands uplift, the lack of active late-Pleistocene and Holocene structures and the geologically low uplift (< 0.6 mm/yr) and slip rates (< 2 mm/yr) indicate substantially less active deformation than to the north. These later geological deformation rates are at the limit of the triangulation uncertainty (3 μradians/observation) given the ~100 years since the first triangulation surveys and the size of the networks (> 50 km). This suggests that the low deformation rate along the Channel Islands uplift is probably geodetically unresolvable.

#### 4.4.2.1 Eastern Santa Barbara Channel

The eastern Santa Barbara Channel network (ESBC) extends from Santa Cruz Island north across the channel to Ventura and Santa Barbara. The network spans the zone of deformation in the mid-channel, obliquely crossing the near shore folding and faulting between Ventura and Santa Barbara (Fig. 4-3a). The stations on Santa Cruz island pin the southern end of the network to the Channel Islands uplift north of the left slip faults along this trend. The geodetic convergence rate estimates across this network indicate 18 ± 5 mm/yr of N20E ± 3 directed convergence over the last ~110 years.

Some of the geological shortening recorded in the trends of late Quaternary and Holocene faults and fold axes within the network agree well with the geodetic direction of convergence. The offshore faults and folds within the ESBC network have two similar, but different trends, though. Most of the near shore faults and folds between the coastline and the Pitas Point fault are concave northward with trends that vary from N70E ($\beta$ = N20W) near Pitas Point to N90-80W ($\beta$ = N00-10E) near Santa Barbara. These faults include the south Rincon, Pitas Point, and Goleta-Rincon faults [Luyendyk et al., 1982], and the Rincon Anticline. Some faults and folds within this region have trends similar to those of faults and fold axes south of the Pitas Point fault with a N70-80W trend ($\beta$ = N10-20E). South of Pitas Point these include the Pitas Point fault, Oak Ridge fault, Montalvo Anticline, and Mid-Channel fault. The Mesa and Lavigia faults and the Montecito anticline which are north of the Goleta - Rincon fault have trends from N80W to N60W. These later trends imply a N10-30E direction of shortening, $\beta$, that is in good agreement with the geodetically estimated direction of N20E.

Active convergence is apparently taking place with a N20E direction of shortening along the Oak Ridge trend. The Oak Ridge structural-trend strikes N17E within the ESBC network. Paleontologic data from a well along the Oak Ridge trend indicate a mid-Holocene age for a reflector involved in the folding [Yeats, 1982]. In addition, active deformation is suggested by earthquake swarms that have occurred along the Oak Ridge trend several times during the instrumental record: June-August, 1968 [Hamilton et al., 1969], October-September 1983 [Henyey and Teng, 1985]. Focal mechanisms for only a few of these events [Henyey and Teng, 1985] have been published and indicate a N30E direction of maximum contraction .

The rates of convergence across these structures are difficult to assess, and must be inferred from deformation rates in the nearby onshore. As stated previously, convergence across this part of the western Transverse Ranges for the last 2-4 Ma has averaged 9-16mm/yr [Davis and Namson, 1989, written communication] and may be as high as 20 mm/yr during the last 0.2 Ma in the Ventura Basin [Yeats, 1983]. The westward continuation of these structures into the eastern Santa Barbara Channel and the presence of Holocene deformation in the channel seem to suggest that deformation within the ESBC network may be occurring at rates from 9-20 mm/yr, in good agreement with the geodetically determined rate of 18 ± 5 mm/yr.

The sum of the horizontal slip rates on faults within the network is significantly less than the geodetic convergence rate. The vertical and dip slip rate components have been determined for the onshore portions of the Javon Canyon, Red Mountain, and Pitas Point faults and are summarized in Morton and Yerkes [1987]. All of these slip rates are low (< 2 mm/yr) and are Holocene averages. When these slip rate components are converted into horizontal components, the horizontal rates sum to 1.5-3.0 mm/yr. In addition to these fault slip rates, the shortening across the onshore Oak Ridge structural trend has been estimated to be 12 mm/yr averaged over the last 100 ka [Yeats, et al., 1988].

Within the ESBC network, the sum of the horizontal slip on the faults and this part of the Oak Ridge trend is 13.5-16 mm/yr. This rate agrees with the geodetic convergence rate of 18 ± 5 mm/yr and is close to the 20 mm/yr of late Pleistocene convergence in the Ventura Basin. However, this sum does not include shortening due to folding on other structures nor does it include slip rates on all of the offshore faults. This would seem to suggest that slip on other faults and structures within the network may total to ~2-4 ± 5 mm/yr. This could be consumed through shortening on other faults and folds within the network which are consistent with a N20E direction of maximum shortening (e.g., the Mid-Channel fault, and the Montalvo Anticline), and/or through shortening and minor left slip along ~N90-70E trending structures (e.g., the Goleta-Rincon and Pitas Point faults).

4.4.2.2 Central Santa Barbara Channel:

Many of the same stations and geological structures in the ESBC network continue westward into the CSBC network (Fig. 4-3b). The stations on the southern edge of the Santa Barbara channel on Santa Cruz Island are common to both networks and sit along the Channel Islands uplift. On the northern edge of the channel only the station in Santa Barbara (SBAO) is common to both. GAVI of the CSBC network sits on a high peak in the Santa Ynez Mountains south of the Santa Ynez fault, and CHAF of the ESBC network sits on folded Pleistocene strata along the northern edge of the Ventura basin, near Ventura. The area over which these structures are spread in the ESBC network narrows westward into the CSBC network where they are confined to the northern channel platform. The geodetic convergence rate estimates across this network indicate 16 ± 2 mm/yr of N10E ± 4 directed convergence over the last ~100 years.

Fold and fault trends mapped along the northern channel platform in the CSBC network have trends that agree well with the geodetic direction of convergence, $\beta$, of N10E. These faults with late Pleistocene to Holocene offsets [Luyendyk et al., 1982; Yerkes and Lee, 1987] are south dipping with reverse slip and recognized sea floor offsets on the eastern edge of the network and in the ESBC network [Luyendyk et al., 1982]. Fault trends change from N70W ($\beta$ = N20E ) on the eastern edge of the network to N80-90W ($\beta$ = N00-10E ) in the central and western parts of the network. Only the late Pleistocene and younger faults along the northern channel platform have trends that agree with the geodetic direction of shortening. South of the Mid-Channel fault zone early to late Pleistocene faults trend N80-90E ($\beta$ = N00-10W ). Fold axis trends in the Pliocene Sisquoc offshore of Goleta [Dibblee, 1982c] are mostly N80-90W with a few N70W trends. These fold trends imply a N00-10E direction of maximum contraction, $\beta$, that is in good agreement with both the late Quaternary to Holocene direction of shortening indicated by the fault trends and the geodetically estimated direction of shortening of N10E.

Convergence rates from restored balanced cross sections [Davis and Namson, 1989, written communication] suggest 55.8 km of shortening in the last 2-4 Ma (14.0-25.4 mm/yr) from the San Andreas fault south to the Santa Barbara channel. At least 7.8 km (2-4 mm/yr) of this shortening is consumed in the offshore, south of the end of the section (Fig. 4-1). To agree with the geodetic data, 50-100% of the average shortening rate along the section would have to currently be occurring in the Santa Barbara Channel.

4.4.2.3 Western Santa Barbara Channel:

The WSBC network extends from San Miguel and Santa Rosa islands of the Channel Islands uplift to the western end of the Santa Ynez mountains uplift (Fig. 4-3c). Late Quaternary folds and faults within the area of the network are concentrated along the near shore platform of the north channel coastline and are the westward continuation of the zone of deformation along northern channel platform present in the ESBC and CSBC networks. The structures near and within this network suggests more complex deformation than in the other networks. The trends of fold axes and faults change from east to west across the network from generally N70W to N80E back to N70W along the northern channel platform, with some additional N35-55E trending faults. The mid-channel is devoid of faults with younger than early to late Pleistocene activity [Yerkes and Lee, 1987]. The geodetically modeled convergence rate across this network indicates 13 ± 4 mm/yr of convergence directed N23W ± 7.

The geodetically determined direction of maximum contraction differs significantly from most of the geological indicators within network. The westward continuation of the N80W trending structures of the CSBC network change trend at the offshore extension of the south branch of the Santa Ynez fault. There, structural trends of faults and folds along the north channel platform change from N80W to N70-90E. This implies a change in the direction of maximum contraction for the thrust faults and folds from N20E to N00-20W which agrees with the geodetically determined direction of maximum contraction of N23W ± 7. But, the extent of structures with this trend is limited to the region between Point Conception and Gaviota. The trends of onshore fold axes in the Pliocene Sisquoc formation north of Point Conception and the trends of offshore thrust faults between Point Conception and Point Arguello indicate a N00-35E direction of shortening.

The structures with trends consistent with the geodetically determined shortening direction occur near the offshore south branch of the Santa Ynez fault. This fault in the offshore has been interpreted from seismic sections and sea floor profiles as an oblique left slip thrust fault with 550 m of left slip and 950 m of reverse slip and a $60^{\circ}$ N dip [Yerkes et al., 1980]. The fault trends N30E, implying a direction of maximum contraction of N15W for pure strike slip faulting and of N60W for pure thrust faulting. The mean direction of maximum contraction, weighted by the relative amounts of strike-slip and dip slip motion on the fault, is N44W, significantly different from the geodetically determined direction that agrees with the direction of maximum contraction implied by pure strike-slip motion on the fault. In addition to these trends, several relatively short thrust faults with N35-55E trends cut across some of the approximately east-west trending folds suggesting a superposition of shortening in a N35-55W direction on the Pliocene to Pleistocene structures.

Convergence rates from restored balanced cross sections [Davis and Namson, 1989, written communication] suggest 10.5-19.0 mm/yr (41.8 km of shortening in the last 2-4 Ma) from the San Andreas fault southwest to the Santa Barbara channel (Fig. 4-1) along a section line oriented normal to the major structures at N20E across this part of the western Transverse Ranges. This section suggests that little of the deformation is consumed in the folds within the WSBC network.

4.4.2.4 Seismicity and stress:

There is agreement between the direction of maximum contraction from the geodetic data with the direction of compression indicated by seismicity studies. Seismicity in the western Transverse Ranges is consistent with active north-south convergence with several moderate to large historical earthquakes having occurred in and around the Santa Barbara Channel in 1812 ( magnitude 7+), 1925 ($M_L$ 6.3), 1941 ($M_L$ 6.0), 1973 ( $M_L$ 5.1) and 1978 ($M_L$ 5.1) [Yerkes and Lee, 1987]. Active north-south thrust and decollemént tectonics are indicated by low angle compressive earthquake focal mechanisms along a 12-15 km seismicity floor which has been interpreted to be a mid-crustal, sub-horizontal detachment [Hadley and Kanamori, 1977; Webb and Kanamori, 1985]. From the analysis of focal mechanisms from 200 events within the ESBC network with magnitudes from $M_L$ 2 to 6 from the period 1970 to 1975, it was concluded that the stress regime has near horizontal pressure axes directed N24E, approximately normal to the strike of the Big Bend segment of the San Andreas fault [Yerkes and Lee, 1987]. This compressive stress direction was inferred to be primarily the result of reverse displacement along the east-west trending Red Mountain-San Cayentano, Pitas Point-Ventura, Mid-Channel, and Anacapa-Santa Monica reverse faults [Yerkes and Lee, 1987]. This direction of compressive stress and the direction of minimum compressive stress from bore hole break outs of N24E in the Santa Barbara channel [Mount, 1989] agree well with the geodetic direction of shortening of N20E ± 3 for the ESBC network.

4.4.3 Northern Borderland:

The Northern Borderland network extends across the southern boundary between the western Transverse Ranges and the continental borderland. The geodetic strain-rate estimates are indistinguishable from a zero strain-rate solution (0 ± 2 mm/yr). The area covered by the network is structurally complex including northwest trending strike-slip faults of the Continental borderland, east trending thrust faults of the Channel islands uplift, and left lateral strike-slip faults of the northern channel islands [Junger, 1976; Junger and Wagner, 1977]. Seismicity studies suggest that the area just east of the network, offshore of Santa Monica, forms an active transition zone between the strike-slip faulting of the Borderland and the compressional tectonics of the Transverse Ranges [Hauksson and Saldivar, 1989]. Within the network, though, only a few Holocene and

Pleistocene fault offsets have been identified. These have been mapped along NW-SE striking faults between the Northern Channel islands and Santa Barbara and San Nicolas islands and along the eastern extension of the Santa Cruz Island fault [Greene and Kennedy, 1986]. The lack of young folds within the network argues for zero shortening between San Nicolas and Northern Channel islands, since the Pliocene [Junger, 1976].

### 4.4.4 Coseismic elastic strain release

The elastic strain released by two moderate earthquakes within the networks was insufficient to affect the strain-rate estimates. The 1978 $M_L$ 5.1 Santa Barbara and the 1981 $M_L$ 5.1 Santa Barbara island earthquakes [Corbett, 1984] occurred between the last historical observations and the first GPS observations near stations SBAO, of the SBC network, and SBIS, of the NBL network. The coseismic strain release was modeled as an elastic dislocation using the formulation of Okada [1985]. Fault plane orientation, width, depth, and coseismic slip were obtained from the analysis of Corbett [1984] and are summarized in Table 4-3. The parameters that would give the maximum surface displacements were chosen for the models. The elastic strain released by each of these events was $< 5$ cm of relative station displacement of the monuments. This is less than 0.6 μstrain which is five times smaller than the triangulation uncertainty and thus unresolvable by the strain analysis.

### 4.5 Summary:

The three networks that span the Santa Barbara Channel (ESBC, CSBC, and WSBC) indicate generally north-south convergence across the channel with the direction of maximum contraction changing from east to west along the channel from ~N20E to ~N20W. When scaled by the average network crossing length scale in this direction, a slight decrease in the convergence rate is indicated, from 18 mm/yr in the east to 13 mm/yr in the west. The geodetic direction of maximum contraction is agrees with at least some of the Holocene-Pleistocene structures in the channel. These structures are mainly thrust faults and fold axes that indicate generally N00E to N10E directions of shortening, β, with the highest concentration of structures in the eastern channel. The geologically youngest deformation seems to be concentrated along the northern channel platform. In the CSBC and ESBC networks, the agreement is with the majority of the Pleistocene and younger deformation. In the WSBC network, most of the structures agree better with the direction of maximum contraction implied by the geodesy and geology of the CSBC and ESBC network than with the direction of maximum contraction of the WSBC network. Some young structures, though, do agree with the N24W direction of maximum contraction of the WSBC network. These structures offset the older N00-10E structures, implying that the direction of shortening in this part of the channel may have changed during the most recent Quaternary to a more westerly direction than to the east. The geological record of deformation since the Pliocene in the Oxnard Plain and Northern Borderland networks are consistent with these strain-rate estimates of zero significant geodetic (0 ± 4 mm/yr).

Table 4-1
Uniaxial convergence rates

| Network | $\beta$ | $\varepsilon$ | $V_{min}$ | $V_{max}$ | $V_{ave}$ |
|---|---|---|---|---|---|
| SBC | -1.± 2 | - 0.23 ± 0.02 | 7 ± 2 | 17 ± 2 | 13 ± 2 |
| ESBC | 20 ± 3 | - 0.37 ± 0.07 | 15 ± 3 | 21 ± 4 | 18 ± 5 |
| CSBC | 10 ± 4 | - 0.28 ± 0.04 | 11 ± 2 | 21 ± 3 | 16 ± 2 |
| WSBC | -23 ± 7 | - 0.17 ± 0.06 | 9 ± 3 | 17 ± 6 | 13 ± 4 |

Table 4-1. Convergence rate estimates across the triangulation-GPS networks in the Santa Barbara Channel. $\beta$ is the azimuth of maximum shortening; $\varepsilon$ is the modeled uniaxial strain rate in µstrain/yr; $V_{min}$, $V_{max}$, and $V_{ave}$ are the minimum, maximum, and average network convergence rates, respectively, in mm/yr. These rates are calculated from the minimum, maximum, and average channel crossing length scale of the network in the direction of maximum contraction, $\beta$ .

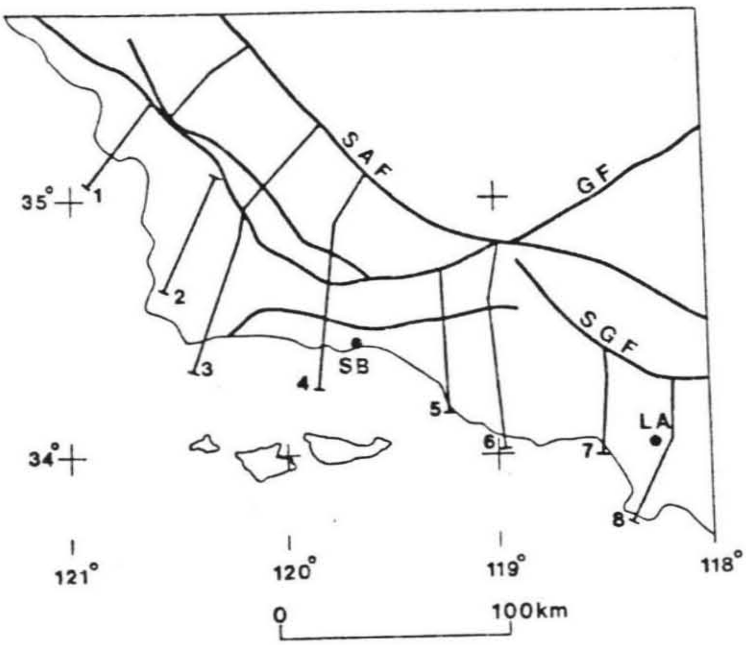


Figure 4-1 Map of southern and central California showing location of regional balanced cross sections of Davis and Namson [1989, written communication]. GF- Garlock fault, LA- Los Angeles, SAF- San Andreas fault, SB- Santa Barbara, SGF- San Gabriel fault.

Table 4-2

| Cross section | Total shortening (km) | slip rate (mm/yr) |
|---|---|---|
| 1 San Luis Obisbo | 26.8 | 6.7-17.2 |
| 2 Santa Maria Basin | 9.2 | 2.3-4.2 |
| 3 Point Conception | 41.8 | 10.5-19.0 |
| 4 Santa Barbara | 55.8 (7.8) | 14.0-25.4 |
| 5 Ventura Basin | 35 | 8.8-15.9 |
| 6 Santa Paula | 31 | 7.8-14.1 |
| 7 San Diego Fwy. | 12 | 5.5-3.0 |
| 8 Los Angeles | 21.4-29.7 | 5.4-13.5 |

Table 4-2. Average convergence rates for the last 2-4 Ma across balanced cross-sections in the western Transverse Ranges [Davis and Namson, 1989, written communication]. Numbers refer to cross sections in Figure 4-1.

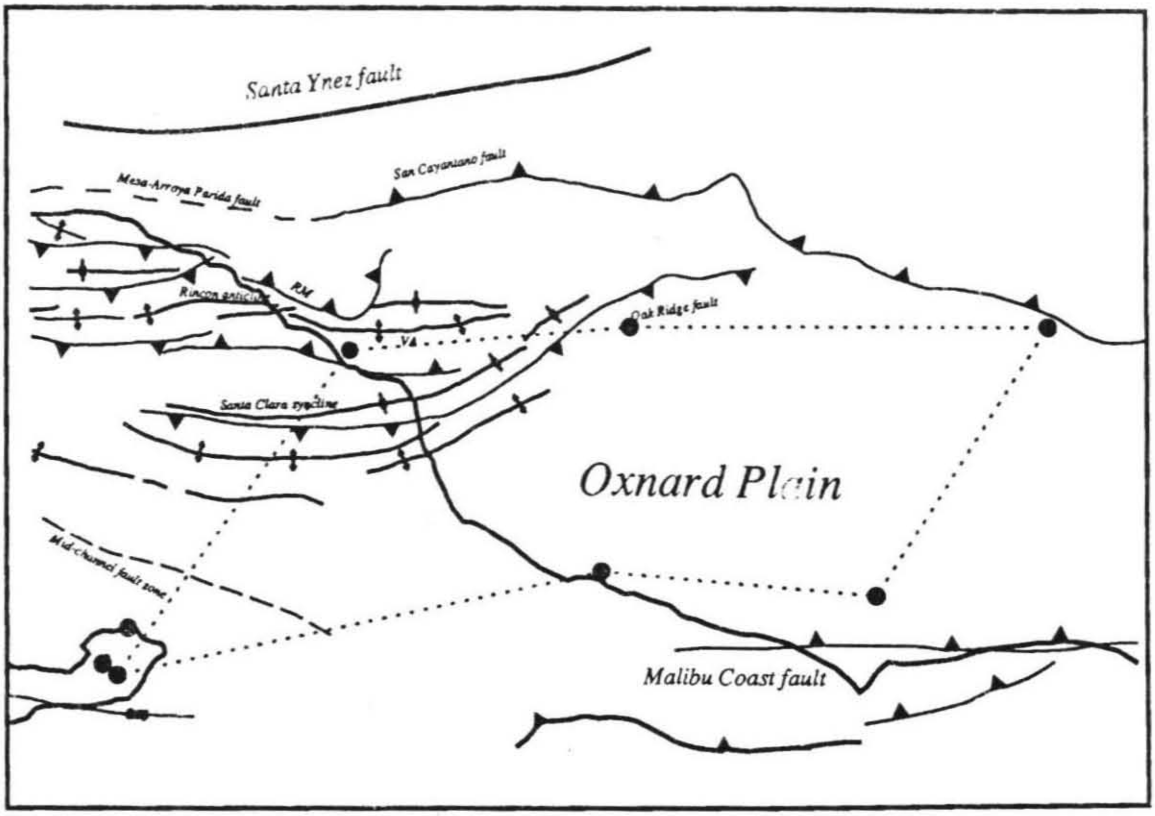


Figure 4-2. The strain rate for the Oxnard Plain network suggests zero strain across this region (0 ± 4 mm/yr). The structures shown are complied from published maps [Yerkes et al., 1980; Junger, 1979; Luyendyk et al., 1982; Dibblee, 1982b]. Thrust faults are shown with barbs on the hanging wall. Long dashed lines indicate that the fault is approximately located. Short dashes are for approximately located faults with early to late Pleistocene slip. The locations of the geodetic stations are indicated by the filled circles. VA- Ventura Anticline, RM- Red Mountain Thrust.

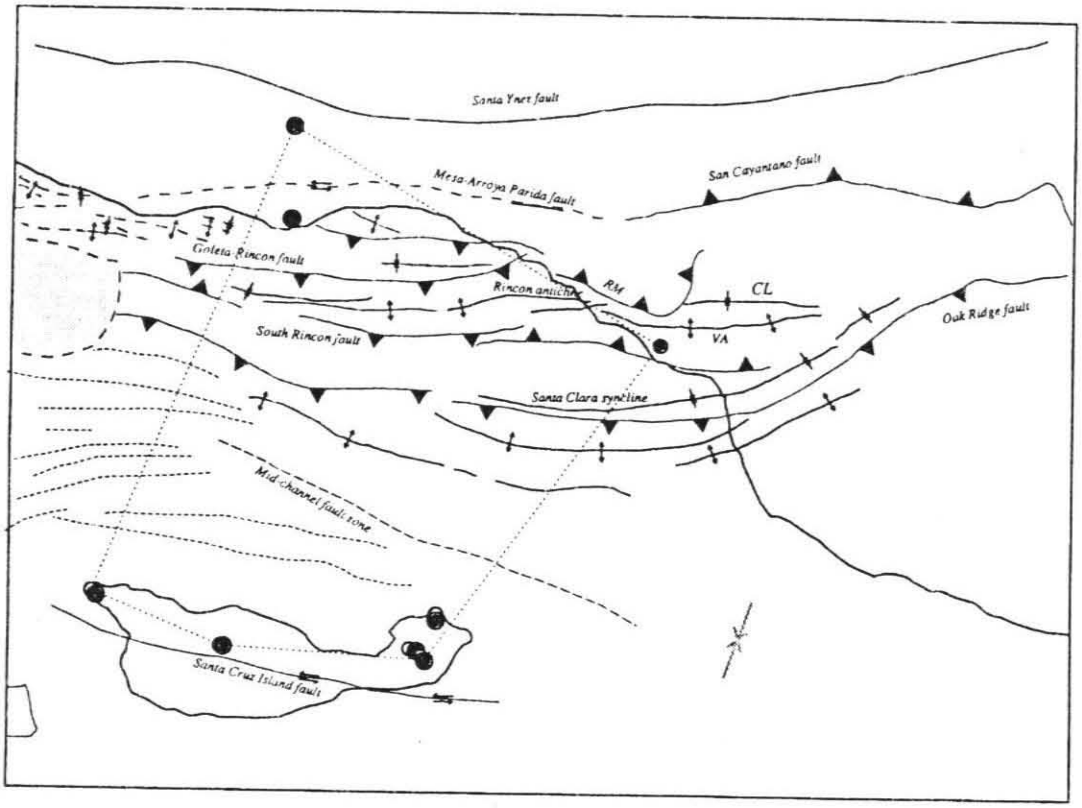


Figure 4-3. Maps of the three networks that span the Santa Barbara Channel (ESBC, CSBC, and WSBC) The geodetic direction of convergence is shown as the thick, shaded arrows on each map. The structures shown are compiled from published maps [Yerkes et al., 1980; Junger, 1979; Luyendyk et al., 1982; Dibblee, 1982b]. Thrust faults are shown with barbs on the hanging wall. Long dashed lines indicate that the fault is approximately located. Short dashes are for approximately located faults with early to late Pleistocene slip. The locations of the geodetic stations are indicated by the filled circles. a. Eastern Santa Barbara Channel network

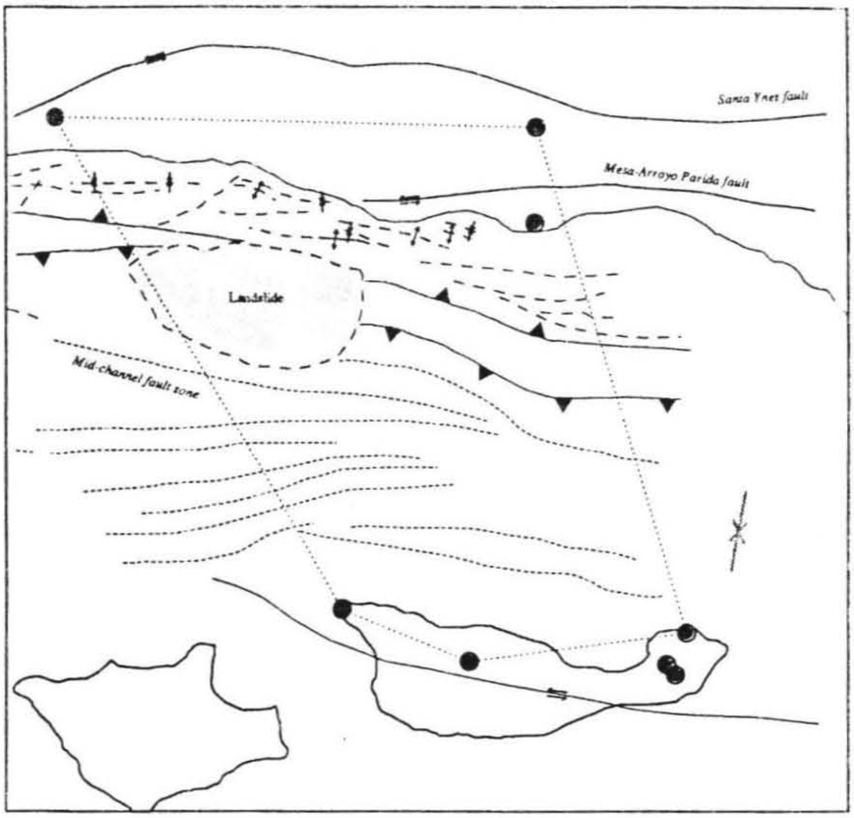


Figure 4-3b. Central Santa Barbara Channel network

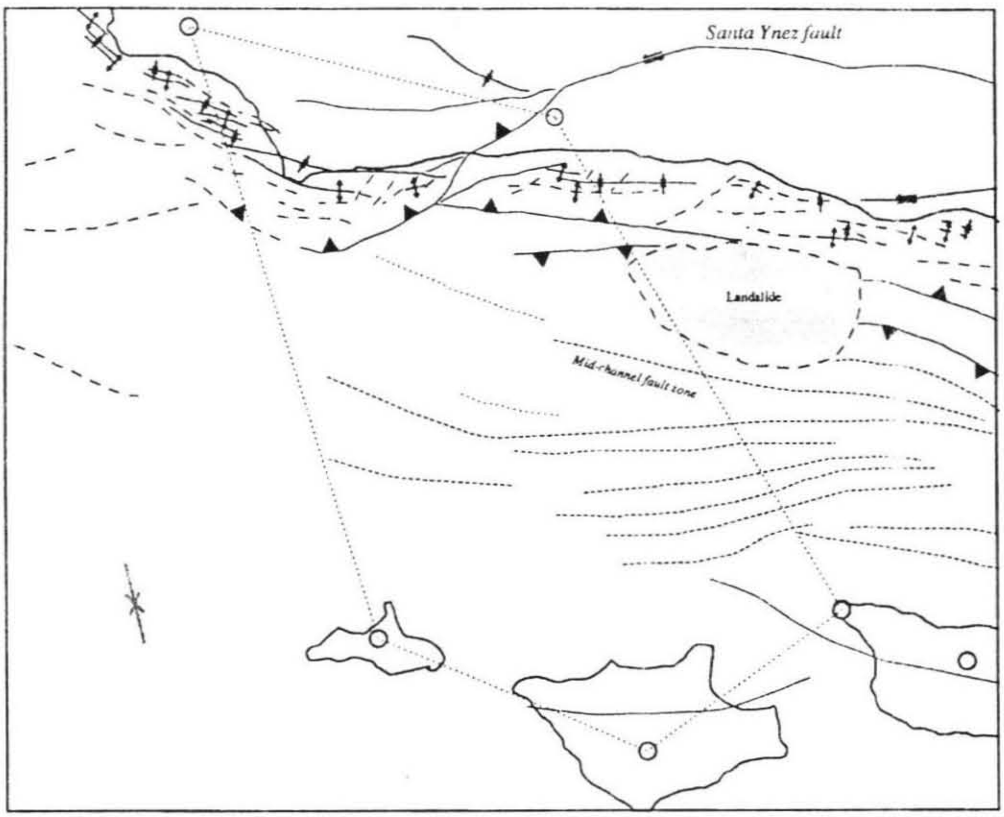


Figure 4-3c. Western Santa Barbara Channel network

Table 4-3

| Event | φ | λ | l | w | d | α | δ | slip (m) |
|---|---|---|---|---|---|---|---|---|
| a | 33.0 | 119.75 | 40 | 5 | 15 | 318 | 90.0 | 1 |
| b | 34.0 | 120.50 | 12 | 6 | 15 | 285 | 15.0 | 1 |

Table 4-3. Parameters used to calculate coseismic elastic-strain release from the Santa Barbara Island earthquake (a), and the Santa Barbara earthquake (b). Parameters are derived from Corbett [1984] to give the maximum possible slip using the formulations of Okada [1985]. φ and λ are the latitude and longitude of the corner of the fault plane; l, w, and d are the length, width, and depth of the fault plane in kilometers; α and δ are the strike and dip of the fault plane. The Santa Barbara Island earthquake was modeled as pure strike-slip and the Santa Barbara earthquake as pure thrust, both with 1 meter of slip.

# Chapter 5.

## Pacific-North American Plate motion from geodetic estimates of strain rates in the offshore of southern California.

### 5.1 Introduction:

In this chapter, the distribution of the motion between the Pacific and North American plates is addressed using space geodetic station velocities, and the geodetic strain rates estimated for the offshore of southern California in Chapter 3. These determinations of the offshore strain-rates suggest that the distribution and the magnitude of the Pacific-North American relative motion be re-evaluated. Specifically, previous models of the plate motion distribution across central and southern California [Bird and Rosenstock, 1984; DeMets et al., 1987; Minster and Jordan, 1984; Minster and Jordan, 1987; Weldon and Humphreys, 1986] which lacked specific knowledge of offshore deformation rates have made several assumptions and predictions of the deformation offshore that are inconsistent with the current data.

Rigid-plate models that have been developed over the last 15 years reasonably describe the motions of the plates from global inversions of marine magnetic anomaly patterns, transform fault trends, and seismicity [e.g., Chase, 1978; Minster and Jordan, 1978; DeMets et al., 1990]. These models form the framework on which other studies of plate interactions and geological investigations are based. However, substantial non-rigid plate behavior has been recognized where these plate boundaries lie within the continents or along their margins [e.g., Atwater, 1970]. Quaternary and older deformations in the western United States have been attributed to non-rigid plate interaction between the Pacific and North American plates resulting from the intra-continental nature of the plate boundary there [e.g., Minster and Jordan, 1984]. Estimates of plate motions from observations along this plate boundary must, therefore, be biased by this non-rigid behavior.

### 5.2 San Andreas Discrepancy

In California the San Andreas fault is generally recognized as the primary boundary between the Pacific and North American plates forming a 1000 km long intra-continental transform fault [e.g., Atwater, 1970; Minster and Jordan, 1984]. Geological and geodetical estimates of the slip rate on the San Andreas fault indicate that most of the relative plate motion can be accounted for by deformation along it [Savage and Burford, 1973; Weldon and Humphreys, 1986]. However, these observations can only account for ~65-75% of the average plate velocity for the last 2-4 Ma. Extension in the Basin and Ranges and faulting along the continental margin west of the San Andreas fault have been proposed to account for this missing motion, called the San Andreas "discrepancy" [Minster and Jordan, 1984]. But, the rate and direction of extension in the Basin and Ranges are insufficient to account for all of the missing motion, and the slip rates on the faults west of the San Andreas are poorly constrained [e.g., Minster and Jordan, 1984; Bird and Rosenstock, 1984; Weldon and Humphreys, 1986].

The discrepancy is defined as the difference between the observed deformation velocity, as indicated from geological and/or geodetical analyses, and the velocity predicted by global plate models. Attempts at resolving the discrepancy have focused on the comparison of the total velocity of the incomplete set of geodetically and/or geologically determined fault slip and deformation rates in the western United States with a global plate model vector. The discrepancy is then resolved by partitioning the discrepancy vector along faults of known Quaternary activity, but for which the slip rates are poorly constrained and/or unconstrained [e.g., Minster and Jordan, 1984; Bird and Rosenstock, 1984; Weldon and Humphreys, 1986; Minster and Jordan, 1987]. In these analyses, deformation rates that are averaged over time periods of from a few hundred to millions of years, geologically, and/or a few tens of years, geodetically, are compared with the global rate averaged over the last 2-4 Ma.

Since the discrepancy was first pointed out based on the RM-2 global plate model of Minster and Jordan [1978], a new global plate model, NUVEL-1, has been developed [DeMets et al., 1990]. The NUVEL-1 model uses a larger data set than RM-2 and contains more direct data on the relative Pacific-North American plate velocity than RM-2. In the NUVEL-1 model, 5 spreading rates determined from marine magnetic anomalies in the Gulf of California are used as direct measurements of Pacific-North American relative velocity. In contrast, only 1 was available and used in the RM-2 model, and that rate has since been found to be in error [Minster, public communication].

At the 95% confidence level, these models have essentially the same location for the Pacific-North American relative motion Euler pole. Thus, they give essentially the same direction of relative plate motion. The main difference is the magnitude of the relative motion. The NUVEL-1 model is slower than RM-2 by $0.07 \pm 0.03$ deg/m.y. (8% slower). When mapped to the linear plate velocity in California, this corresponds to a 15% decrease in the relative plate motion in California and implies that the magnitude and orientation of the San Andreas discrepancy is smaller than previously believed (Fig. 5-1) [DeMets, et al., 1987].

## 5.3 Previous Geodetic Studies

On a global scale, space-based geodetically determined rates agree well with rates averaged over a few millions of years, as estimated from global plate models. Satellite Laser Ranging (SLR) has been used to monitor plate motions since 1976. The results from these observations indicate good agreement between the SLR modeled station velocities, SL7.1, and the station velocities predicted by AM0-2 and NUVEL-1 [Smith et al., 1989a]. (AM0-2 is an absolute motion model based on the relative motion model RM-2). The linear correlation for the geodesic velocities of sites within the plate interiors between the SL7.1 and the AM0-2 and NUVEL-1 models are 0.999 and 1.031, respectively, indicating good agreement with both plate models [Smith et al., 1989a]. Previous preliminary analyses had a somewhat lower linear correlation of 0.61 with the RM-2 model [Christodoulidis et al., 1985]. These results yielded high relative plate rates [NASA, 1988] that were geologically unreasonable. The better agreement of the latest results is probably due to a combination of improved modeling, analysis techniques, and an increased number of observations spread over a longer time period.

Recent geodetic estimates of the velocity of stations in California based on the analysis of VLBI observations collected over the last 7 years suggest that the western most of these stations are moving at velocities that are within a few millimeters of the full NUVEL-1 velocity [Clark et al., 1987; Kroger et al., 1987; Sauber, 1989; Ward, 1988]. The velocity of the station at Vandenberg (VNDN) deviates insignificantly from the NUVEL-1 velocity for the Pacific plate. The VLBI station at Monument Peak (MONP), east of San Diego, is also close to the NUVEL-1 Pacific plate velocity. The velocity distribution across southern California from these VLBI analyses along with velocities derived from other geodetic stations has been interpreted to be consistent with distributed right lateral shear across southern California [Sauber, 1989; Ward, 1989].

VLBI observations have been used in global studies of plate motions. In these studies, the observed baseline evolution from stations around the world are used to invert for station velocities, in contrast to the regional studies mentioned above that only use data from baselines that span the San Andreas fault. Initially these global studies achieved results that were in good agreement with the RM-2 global plate model for Pacific-North American relative motion [NASA, 1988; Ryan, 1987]. With the availability of a few more years of data, inversion of these data have converged on agreement with the NUVEL-1 plate model. [Argus and Gordon, in prep; Ward, in press].

These analyses and the regional ones would seem to suggest: 1) that the Pacific-North American plate motion is distributed entirely onshore across southern California between Vandenberg and the San Andreas fault with additional motion being accommodated through Basin and Range extension [DeMets et al., 1990]; 2) that in California the crustal velocity field is most sensitive to the regional right-lateral shear of the plate motion rather than to the convergent deformation implied by structures that have formed over the last 0-4 Ma in parts of southern California; 3) that VNDN is part of the Pacific plate; and 4) that offshore of California, deformation rates are negligible.

But, these global VLBI analyses that agree well with the NUVEL-1 plate model [Argus and Gordon, in prep; Ward, in press] rely on the assumption that the VLBI station at VNDN is on the Pacific plate and that little or no deformation is occurring in the offshore of California, outboard of VNDN. In contrast, the geology of the offshore of southern California suggest active deformation during the last 2-4 Ma, and the triangulation-GPS strain-rate estimates suggest that deformation is occurring at a significant rate (Chapters 3 and 4). If the onshore and offshore geodetic deformation rates are added, then the geodetically determined velocity distribution across southern California exceeds the relative plate motion velocity predicted by the NUVEL-1 model.

5.4 Velocity path approach:

The distribution of strain across the Pacific-North American plate boundary can be evaluated by constructing velocity paths along which the known deformation rates are summed. Paths that start on the North American plate and end on the Pacific plate should sum to the relative plate velocity. This is true if all of the deformation is accurately accounted for along the path, the path actually begins and ends on these plates, and the plate model is applicable.

The velocity path approach has been employed by several investigators [Bird and Rosenstock, 1984; Minster and Jordan, 1984; Weldon and Humphreys, 1986; Minster and Jordan, 1987; Sauber, 1989; Humphreys and Weldon, in prep] to evaluate the Pacific-North American plate boundary strain distribution. Minster and Jordan [1984], Bird and Rosenstock [1984], and Weldon and Humphreys [1986] used existing geological data to estimate the misfit between the geological deformation observed onshore and the relative Pacific-North American motion predicted by RM-2. Similarly, Minster and Jordan [1987] and Sauber [1989] determined the discrepancy from the RM-2 and NUVEL-1 models, respectively, using ground based and space based geodetic data.

Both the geological and geodetic studies recognized four tectonic regions which their velocity paths must contain. Stable North America extends from the east coast of the United States to the Basin and Ranges. There, crustal extension of the non-rigid continental crust is occurring at significant rates through normal faulting from Arizona northward and from the Colorado Plateau west to the Sierra Nevada. The extension rate across the Basin and Ranges has been estimated to be $10.1 \pm 0.7$ at N63W $\pm$ 5, geologic, and $9.7 \pm 2$ at N56W $\pm$ 10, space-based geodetic [Minster and Jordan, 1987]. Extension across the southern Basin and Ranges between the Rio Grande Rift and San Andreas fault in southern California is considered to be 1-2 orders of magnitude less active than the northern Basin and Ranges, implying a negligible rate of 0.1-1.0 mm/yr [Humphreys and Weldon, in prep.]. West of the Basin and Ranges, the San Andreas fault is the primary plate boundary structure accommodating most of the relative plate motion through right lateral strike-slip faulting at a geologic and geodetic rate of $34 \pm 3$ mm/yr directed N41W $\pm$ 2 in central California [Minster and Jordan, 1984]. In southern California, south of the Transverse Ranges, right lateral strike-slip faulting is distributed on the San Andreas, San Jacinto, and Elsinore faults. The geologic velocity across each of these faults has been estimated to be $30 \pm 7$ mm/yr at N48W $\pm$ 5, $12 \pm 4$ mm/yr at N53W $\pm$ 7, and $5 \pm 3$ mm/yr at N49W $\pm$14, respectively, [Humphreys and Weldon, in prep]. Strain estimates from geodetic networks that cross these faults [Savage, 1983; Thatcher, 1979b] are consistent with these rates.

Finally, west of these faults active deformation in the offshore region along several faults has been recognized, but the strain rates across these structures are poorly constrained or unconstrained by geologic data. In central California, on the San Gregorio-Hosgri system, Hall [1975] has proposed 80-95 km of right lateral strike-slip displacement since the Pliocene, implying an average rate of 16-19 mm/yr directed ~N40W. Near San Simeon where part of this fault system comes ashore, late Quaternary slip rates have been estimated to be from 8-10 mm/yr [Weber, 1979] to 4 +6/-2 mm/yr [Hanson et al., 1987] on the San Simeon strand of the Hosgri system with an orientation of N40W ± 15. Pleistocene slip rates may be as high as 19 mm/yr [Weber, 1979]. In southern California, several active right lateral strike slip faults have been recognized in the continental borderland (e.g., Newport-Inglewood, Coronado Bank, and San Clemente Island faults) [Legg, 1985], however, no slip rates have been determined for these fault zones.

5.5 Offshore Geodetic Velocity path:

I have constructed a velocity path from stable North America to the Pacific plate by using VLBI station velocities of Sauber [1989] to connect the offshore networks to stable North America. (Other analyses such as Clark et al., [1987], Kroger et al., [1987], and Ward [1988] have results that are, within error, identical to those of Sauber [1989] for velocity VNDN and MONP with respect to North America). The networks that are connected to the mainland with determinable strain-rate estimates are limited to the Santa Barbara Channel and Northern Borderland regions. Three networks with different strain rates cross the channel. Two of these networks, the WSBC and ESBC, are "pinned" to the mainland near the VLBI stations VNDN and SANP, respectively, which can be used to connect the deformation path from North America out to San Nicolas Island through the Santa Barbara Channel and Northern Borderland networks. The strain estimates for the Northern Borderland suggest 0 ± 4 mm/yr of shortening across this network. Triangulation-GPS based strain-rate estimates in the southern Borderland are not considered reliable enough to connect a similar VLBI-triangulation-GPS path from MONP through the borderland to San Nicolas Island.

Both SANP and VNDN lie roughly along strike of an active zone of north-south crustal convergence in the western Transverse Ranges. SANP sits within this zone in the Ventura Basin and VNDN sits north of it in the Santa Maria Basin. Across this zone 10-15 mm/yr of crustal convergence has occurred during the last 2-4 Ma [Davis and Namson, written com., 1989] and as much as 20 mm/yr has occurred within the Ventura Basin [Yeats, 1983], with most of this convergence being interpreted to have occurred on structures that straddle the SANP VLBI site.

Sixty-three VLBI observations have been performed at VNDN over a 4 year period between 1983 and 1987. Baseline evolution between VNDN and the other VLBI stations observed [Ma et al., 1989] lie along well defined trends, indicating consistent and constant relative motions. On the other hand, only 4 experiments include SANP with observations between 1983 and 1987, and with the second experiment containing a large (~4 cm) outlier from the baseline evolution trend of the MOJAVE12 - SANP baseline. The large 2-sigma uncertainties on the SANP velocity suggest that the velocity of SANP is poorly determined and within error of the VNDN VLBI velocity.

Because of this, the limited set of VLBI observations at SANP, and the uncertain relationship of the SANP VLBI site to the active tectonics of the area, the mainland velocity path is chosen to end at VNDN. In doing so, the velocity path from North America includes Basin and Range extension, shear along the San Andreas fault, and Transverse range deformation north of VNDN, ending at the western part of the Santa Barbara Channel. There are four different networks solutions with which to cross the channel: SBC, WSBC, CSBC, and ESBC. The WSBC network would make the most sense, since this network contains stations in the area of VNDN. The velocity path then passes from stable North America, through VNDN, the western Santa Barbara Channel (WSBC), and the Northern Borderland (NBL) to San Nicolas island (Fig. 5-2). Figure 5-3 shows the velocity path plotted with the RM-2 and NUVEL-1 velocity models for central California Pacific-North American relative plate motion. Error ellipses are cumulative 1-sigma errors. This velocity path yields an end path velocity of $59 \pm 8$ mm/yr at N37W $\pm$ 7 which exceeds that predicted by NUVEL-1 by 23% and is coincidentally within error of the RM-2 velocity (Table 5-1).

5.6 Other velocity paths:

Other geodetically derived velocity paths can be estimated for the relative motion between these plates using results from VLBI and SLR solutions. The previously mentioned VLBI analyses are based on regional studies of VLBI baseline evolutions for stations in North America. VLBI analyses [e.g., Ma et al. 1989] and SLR analyses [e.g., Smith et al., 1989a] for stations within the plate interiors and along the plate boundaries can be used to estimate deformation across these boundary zones.

The SLR global solutions can be used to infer a velocity path from North America to Hawaii. As before, VLBI solutions are used to get from North America to the coast at Monument Peak, MONP. SLR velocities are then used to get from the coast to Hawaii, crossing the southern Borderland. SLR velocities are chosen to estimate the motion across this part of the path instead of VLBI, because there are no VLBI observations from MONP to stations on the Pacific plate, but there are SLR observations.

Smith et al. [1989b] and Robbins et al. [1989] present station geodesic velocities for several SLR stations on the North American and Pacific plates with respect to the absolute motion model AM0-2 of Minster and Jordan [1978]. The SLR geodesic velocities are with respect to stations Greenbelt, in Maryland, and Hawaii. Since Greenbelt and Hawaii are in the interiors of the North American and Pacific plates, respectively, they are not affected by plate boundary deformation. Velocities relative to them are equivalent to velocities relative to the North American (NOAM) and Pacific (PAC) plates, respectively.

In the SL7.1 solution, the station velocities of Mazatlan, Mexico, (MAZ) which was assumed to be on the NOAM plate, and Monument Peak (MONP), which was assumed to be on the PAC plate should not be moving with respect to the NOAM (i.e., Greenbelt) and PAC (i.e., Hawaii) plates, respectively. However, there is some residual motion between these two stations and the NOAM and PAC plates. MAZ moves at 7 ± 3 mm/yr directed N40W ± 16 with respect to NOAM, and MONP moves at 15 ± 2 mm/yr directed N23W ± 10. These deviations suggest non-rigid plate behavior between Greenbelt and Mazatlan and between Hawaii and Monument Peak.

By calling the former deviation continental deformation between Mazatlan and Greenbelt and adding it to the NUVEL-1 velocity at the mouth of the Gulf of California (23N 108W), the relative Pacific-North American velocity that includes the SLR derived deformation across North America is 57 ± 3 mm/yr at N52W ± 3. Similarly, by adding the SLR discrepancy at Monument Peak (MONP) to the VLBI velocity for MONP with respect to North America, the end velocity of 54 ± 7 mm/yr at N39W ± 6 is the Pacific-North American geodetic velocity at Monument Peak that includes deformation between Monument Peak and Hawaii. Both of these velocities exceed the magnitudes of their respective NUVEL-1 horizontal velocities by about 10%, but in the same direction as predicted by NUVEL-1 estimate. This is in good agreement with the previously determined VLBI-triangulation-GPS estimate for Pacific-North American relative plate motion in southern California at San Nicolas Island, which exceeds the NUVEL-1 estimate by about 20%.

VLBI has been used to estimate the motion between these plates by constructing a relative motion Euler pole from VLBI baseline evolution transverse and length rates for baselines that span the plate boundary [Argus and Gordon, in prep]. Argus and Gordon [in prep] used baselines from two stations on the North American plate, one at Fairbanks, Alaska, and the other at Fort Davis, Texas, and three stations on the Pacific plate, at Hawaii, Kwajalein in the western Pacific, and Vandenberg.

The time evolution of a VLBI baseline from station 1 to station 2 is defined in a length, **L**, transverse, **T**, and vertical, **V**, coordinate system, where

$$\mathbf{L} = \mathbf{X}_2 - \mathbf{X}_1 \tag{5-1}$$

$$\mathbf{T} = \mathbf{L} \times \mathbf{X}_2 \tag{5-2}$$

$$\mathbf{V} = \mathbf{T} \times \mathbf{L} \tag{5-3}$$

and $\mathbf{X}_1$ and $\mathbf{X}_2$ are the geocentric vectors to the two stations.

Assuming that the two stations are on separate plates, the station velocities in the direction of the length and transverse components should be a measure of the relative plate motion. Argus and Gordon [in press] calculated a rotation pole, ω, describing the Pacific-North American relative motion. In the calculation, ω is related to $\dot{v}_i$ , the component of the velocity in the direction $\widehat{v_i}$ (length or transverse) and the station position, $\mathbf{X}_2$, by

$$\dot{v}_i = \left[ \left( \omega \times \mathbf{X}_2 \right), \widehat{v_i} \right] \tag{5-4}$$

This analysis assumed that there is no deformation occurring in the offshore region of California (i.e., Vandenberg is assumed to be on the Pacific plate). However, the triangulation-GPS strain rates seem to suggests significant rates of deformation VLBI observations from VNDN to Hawaii and Kwajalein, on the Pacific Plate, indicate relative motion between VNDN and these stations. The error in their analysis could allow for 5 ± 7 mm/yr of motion along the plate boundary [Argus and Gordon, in prep].

5.7 Discussion:

Previous path integral formulations across the Pacific-North American plate boundary have relied upon unknown deformation rates in the offshore of southern and central California and have been constructed to close on an assumed relative plate-motion vector, resulting in the so called San Andreas discrepancy vector. This discrepancy vector is then distributed as deformation along tectonic boundaries. Some of these previous models recognized offshore faulting as a possible source of the discrepancy [Bird and Rosenstock, 1984; Minster and Jordan, 1984; Weldon and Humphreys, 1986] while others have explicitly or implicitly rejected this possibility [Argus and Gordon, in prep; DeMets et al., 1987; Ward, 1988].

The mean of the VLBI-triangulation-GPS and SLR-VLBI velocity paths indicate active deformation in the offshore and gives an estimate of the relative Pacific-North American motion of 56 ± 4 mm/yr at N38W ± 4. Slip rates on the offshore faults can be estimated as the difference between this rate and the onshore VLBI velocity. For the faults outboard of VNDN, such as along the San Gregorio-Hosgri system, this would amount to 13 mm/yr of motion directed N23W. If this is projected onto the strike of this fault zone, N40W ± 15, it would amount to 12 mm/yr of strike-slip motion with 4 mm/yr of convergent motion. The strike-slip rate agrees within error with the late Quaternary estimates of the slip rate on the San Simeon strand of the Hosgri system of 4-13 mm/yr [Hall, 1981; Hanson et al., 1987].

The deformation rate in the Continental Borderland between Monument Peak and San Nicolas Island would be 17 mm/yr at N22W. This segment of the path crosses several active right lateral strike slip fault zones [Legg, 1985] for which good fault orientation information exists, but no reliable rate information is available. Humphreys and Weldon [in prep] estimate the velocity across this part of southern California from the Elsinore fault, just east of Monument Peak to the San Clemente Island fault zone, to be 15 ± 13 mm/yr at N23W +9/-25, values that agree with the geodetic estimate. If the geodetic velocity is projected onto the mean strike of these faults, N37W. This implies 16 mm/yr of strike slip motion and 4 mm/yr of convergent motion.

The difference between the velocity paths presented here for southern California and the Gulf of California, and the NUVEL-1 global plate model velocity suggests that the 2-4 Ma average velocity of NUVEL-1 may underestimate the magnitude of the relative motion between the Pacific and North American plates as derived from the 10-110 year average of the geodetic model. The geodetic rate coincidentally agrees well with the RM-2 model rate. This agreement with the RM-2 rate is not an indication that the RM-2 model is preferable, but an indication that the NUVEL-1 model underestimates the geodetic rate of relative motion between the Pacific and North American plates by an amount equivalent to the difference between the RM-2 and NUVEL-1 rotation rates, ~15%.

5.8 Summary:

The offshore deformation vector implies relatively high rates of motion on the offshore fault systems of ~12-16 mm/yr. The combination of this estimates from geodetic data with VLBI and SLR velocities from stations on the mainland of southern California and Hawaii suggest that the integrated geodetic velocity from the North American plate to the Pacific plate exceeds the NUVEL-1 velocity by 8 mm/yr. A similar discrepancy is also present at mouth of the Gulf of California when the NUVEL-1 Pacific-North American relative velocity there is added to the geodetic SLR velocity of Mazatlan. These differences between the geodetic velocity and the NUVEL-1 plate model seem to suggest that the global plate model under estimates the geodetic rate of relative motion between the Pacific and North American plates by ~15%.

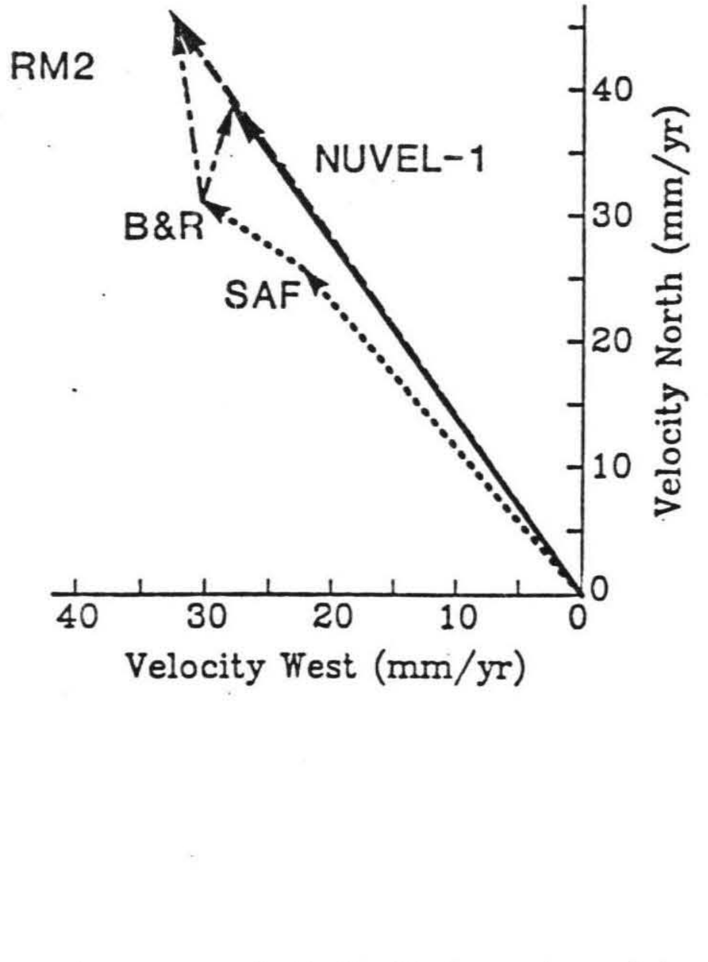


Figure 5-1. Linear velocity vectors for Pacific-North American relative plate motion at 36°N 120.6°W [after DeMets et al., 1990]. The NUVEL-1 and RM-2 models are shown as the solid and dashed lines, respectively. SAF and B&R are slip rates for the San Andreas fault and Basin and Range, respectively.The dash-dotted lines are the discrepancy vectors for Pacific-North American relative plate motion The RM-2 discrepancy is 14 mm/yr directed N08W and the NUVEL-1 discrepancy is 8 mm/yr directed N18E.

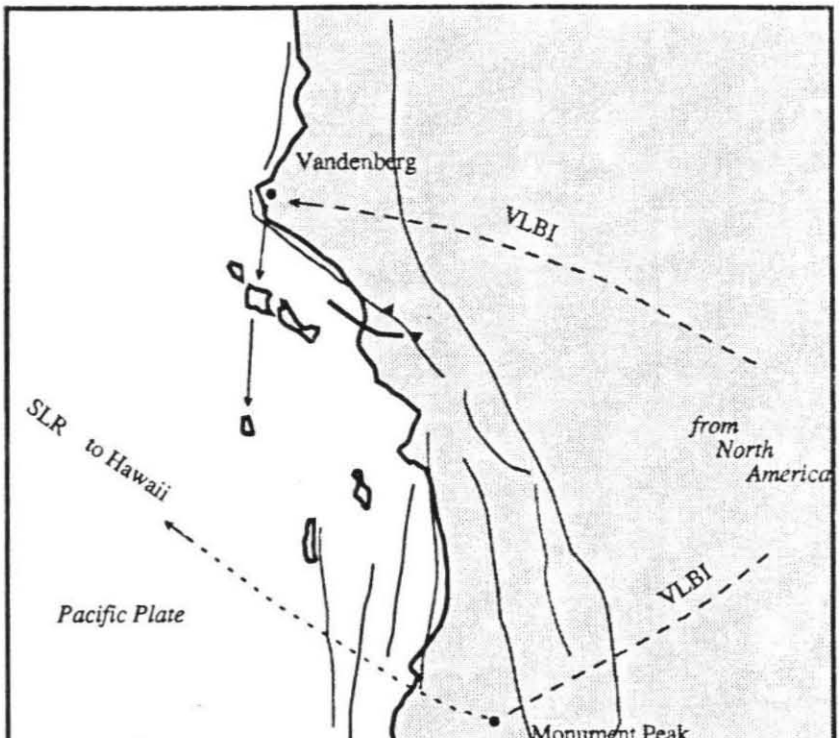


Figure 5-2. Velocity paths from stable North America with VLBI to the coastline at VNDN, across the Santa Barbara Channel through the WSBC network and out to San Nicolas Island (SNI) through the NBL network. Also shown is another path from North America to SNI through MONP VLBI to the Pacific Plate with SLR.

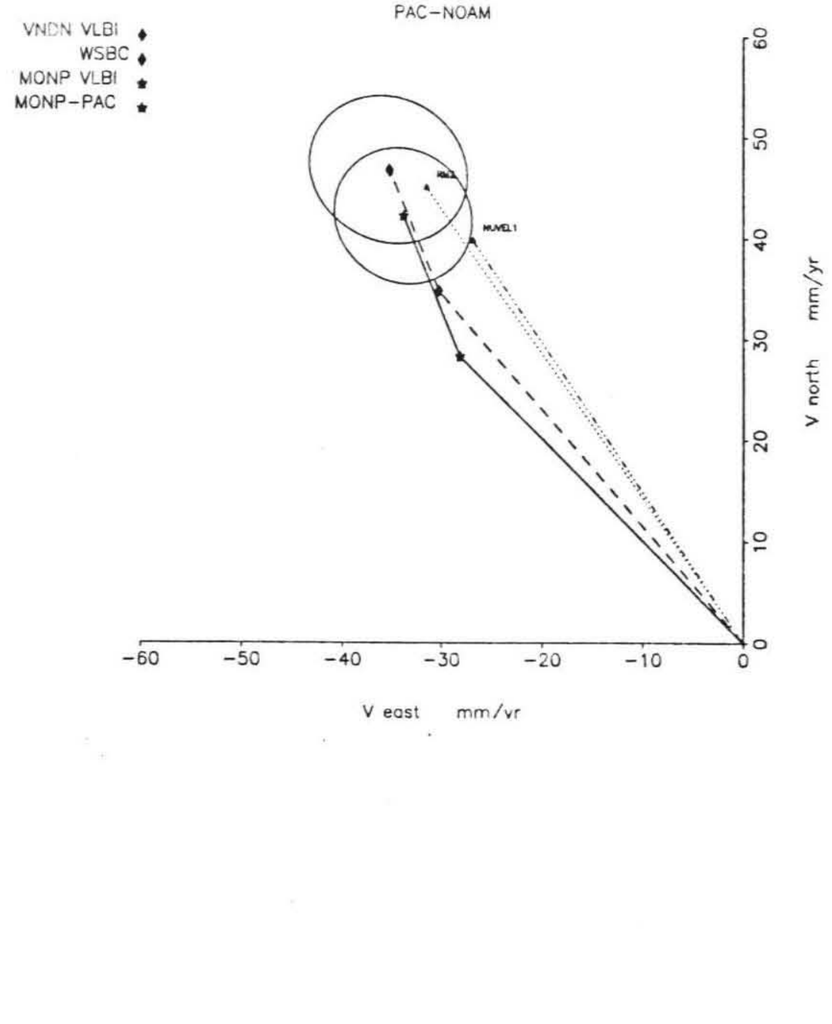


Figure 5-3. Velocity path from stable North America to the California Continental borderland using offshore strain rate estimates from Chapter 4. Also plotted is the VLBI-SLR Pacific-North American relative motion vector at MONP (see text for discussion).

Table 5-1

| Path | Velocity | Azimuth | $\sigma_a$ | $\sigma_b$ | $\zeta_b$ |
|---|---|---|---|---|---|
| NOAM-PAC$_{VNDN-SNI}$ | 58.6 | -37.0 | 8.1 | 7.1 | 26.0 |
| NOAM-PAC$_{MONP}$ | 54.1 | -38.8 | 7.1 | 6.5 | 33.9 |
| NOAM-PAC$_{mean}$ | 56.4 | -37.9 | 4.5 | 3.8 | 16.2 |
| NOAM-PAC$_{MAZ}$ | 57.1 | -51.8 | 2.6 | 2.0 | 23.0 |

Table 5-1. Geodetic velocities (in mm/yr) for Pacific-North American motion in southern California. NOAM- North American Plate, PAC- Pacific plate, VNDN- Vandenberg, SNI- San Nicolas Island, MONP- Monument Peak, MAZ- Mazatlan, Mexico. $\sigma_a$ and $\sigma_b$, are the lengths of the semi-major and semi-minor axis of the error ellipse and $\zeta_b$ is the azimuth of the semi-minor axis.

References

Agnew, D. C., Bock, Y., Jordan, T. H., King, R. W., Dixon, T. H., Hager, B. H., Jackson, D. D., Prescott, W. H., Stowell, J. L., Schutz, B. E., and Strange, W. E., 1988, GPS measurements in central and southern California: EOS Transactions of the American Geophysical Union, v. 68, p. 282.

Argus, D. F., and Gordon, R. G., 1990, Comparison of Pacific-North America plate motion determined from Very Long Baseline Interferometry with that determined from magnetic anomalies, transform faults, and earthquake slip vectors: Journal of Geophysical Research, in press.

Atwater, T., 1970, Implications of plate tectonics for the Cenozoic tectonic evolution of western North America: Geological Society of America, v. 81, pp. 3513-3536.

Beckmann, A., Larisch, H., and Schuster, O., 1988, Determination of azimuths from GPS measurements and comparison with common methods, in E. Groten and R. Strauss, *GPS-Techniques Applied to Geodesy and Surveying*: Heidelberg, Springer-Verlag, 459-465 pp.

Bevington, P. R., 1969, Data Reduction and Error Analysis for the Physical Sciences: New York, MacGraw-Hill, 336 pp.

Bibby, H. M., 1982, Unbiased estimate of strain from triangulation data using simultaneous reduction: Tectonophysics, v. 82, pp. 161-174.

Bird, P., and Rosenstock, R. W., 1984, Kinematics of present crust and mantle flow in southern California: Geological Society of America Bulletin, v. 95, pp. 946-957.

Blewitt, G., 1989, Carrier phase ambiguity resolution for the Global Positioning System applied to geodetic baselines up to 2000 km: Journal of Geophysical Research, no. 94, pp. 10187-10203.

Blewitt, G., Melbourne, W. G., Bertiger, W. I., Dixon, T. H., Kroger, pp. M., Lichten, S. M., Meehan, T. K., Neilan, R. E., Skrumeda, L. L., Thornton, C. L., Wu, S. C., and Young, L. E., 1988, GPS geodesy with centimeter accuracy, in E. Groten and R. Strauss, *GPS-Techniques Applied to Geodesy and Surveying*: Heidelberg, Springer-Verlag, 30-40 pp.

Bomford, G., 1980, Geodesy: Oxford University Press, 855 pp.

Bowie, W., 1928, Comparison of old and new triangulation in California: U. S. Coast and Geodetic Survey Special Publication 151, pp. 50.

Buchanan-Banks, J. M., Castle, R. O., and Ziony, J. I., 1975, Elevation changes in the central Transverse Ranges near Ventura, California: Tectonophysics, v. 29, pp. 113-125.

Chase, C. G., 1978, Plate kinematics: The Americas, East Africa, and the rest of the world: Earth and Planetary Science Letters, v. 37, pp. 355-368.

Chrisrodoulidis, D. C., Smith, D. E., Kolenkiewicz, R., Klosko, S. M., Torrence, M. H., and Dunn, pp. J., 1985, Observing tectonic plate motions and deformations from satellite laser ranging: Journal of Geophysical Research, v. 90, pp. 9249-9263.

Clark, T. A., Gordon, D., Himwich, W. E., Ma, C., Mallama, A., and Ryan, J. W., 1987, Determination of relative site motions in the western United States using Mark II very long baseline radio interferometry.: Journal of Geophysics Research, v. 92, pp. 12,741-12,750.

Corbett, E. J., 1984, Seismicity and crustal structure studies of southern California: Tectonic implications from improved earthquake locations: California Institute of Technology, Ph. D. thesis.

Crouch, J. K., Bachman, S. B., and Shay, J. T., 1984, Post-Miocene tectonics along the central California coast, in J. K. Crouch and S. B. Bachman, *Tectonics and Sedimentation along the California Margin*: Pacific Section S. E. pp. M., 37-54 pp.

Crowell, J. C., 1981, An outline of the tectonic history of southeastern California, in W. G. Ernst, *The Geotectonic development of California*: N.J., Prentice-Hall, 583-600 pp.

Davis, J. L., Prescott, W. H., Svarc, J. L., and Wendt, K. J., 1989a, Assessment of the Global Positioning System Measurement for Studies of Crustal Deformation: Journal of Geophysical Research, v. 94, pp. 13,635-13,650.

Davis, T. L., Namson, J., and Yerkes, R. F., 1989b, A cross section of the Los Angeles area: Seismically active fold and thrust belt, the 1987 Whitter Narrows earthquake, and earthquake hazard: Journal of Geophysical Research, v. 94, no. B7, pp. 9644-9664.

DeMets, C., Gordon, R. G., Argus, D. F., and Stein, S., 1990, Current plate motions: Geophysical Journal International, v. in press,

DeMets, C., Stein, S., and Argus, D. F., 1987, A revised estimate of Pacific-North America motion and implications for western North America plate boundary zone tectonics.: Geophysics Research Letter, v. 14, pp. 911-914.

Dibblee, T. W., 1982a, Geology of the Channel Islands, southern California, in D. L. Fife and J. A. Minch, *Geology and Mineral Wealth of the California Transverse Ranges*: Santa Ana, Calif., South Coast Geological Society, 27-39 pp.

Dibblee, T. W., 1982b, Geology of the Santa Monica Mountains and Simi Hills, southern California, in D. L. Fife and J. A. Minch, *Geology and Mineral Wealth of the California Transverse Ranges*: Santa Ana, Calif., South Coast Geological Society, 94-130 pp.

Dibblee, T. W., 1982c, Geology of the Santa Ynez-Topatopa mountains, southern California, in D. L. Fife and J. A. Minch, *Geology and Mineral Wealth of the California Transverse Ranges*: Santa Ana, Calif., South Coast Geological Society, 44-56 pp.

Dibblee, T. W., 1982d, Regional geology of the Transverse Ranges province of southern California, in D. L. Fife and J. A. Minch, *Geology and Mineral Wealth of the California Transverse Ranges*: Santa Ana, Calif., South Coast Geological Society, 7-25 pp.

Dong, D., and Bock, Y., 1989, GPS network analysis with phase ambiguity resolution applied to crustal deformation studies in California: Journal of Geophysical Research, v. 94, pp. 3949-3966.

Drew, A. R., and Snay, R. A., 1988, The Crustal Dynamics Adjustment Program (DYNAP), NGS, Rockville, Md.

Drew, A. R., and Snay, R. A., 1989, DYNAP: Software for estimating crustal deformation from geodetic data: Tectonophysics, v. 162, pp. 331-343.

Eberhart-Phillips, D., M. Lisowski, and M. D. Zoback. (1990). "Crustal strain near the Big Bend of the San Andreas fault: Analysis of the Los Padres-Tehachapi trilateration network, California." J. Geophys. Res. v. 95(B2): 1139-1154.

Feigl, K., King, R. W., and Jordan, T. H., in press, Geodetic measurement of tectonic deformation in the Santa Maria fold and thrust belt, California: Journal of Geophysical Research, v 95, pp. 2679-2700.

Frank, F. C., 1966, Deduction of strains from survey data: Bulletin of the Seismological Society of America, v. 56, pp. 35-42.

Gergen, J. G., 1975, The new adjustment of the North American Datum: The observables: ACSM Bull., v. 51, no. Nov. 9, pp. 9.

Gossett, F. R., 1950, Manual of Geodetic Triangulation: v. 247, pp. 344.

Greene, H. G., and Kennedy, M. P., 1986, Map of the Geology of the mid-southern California Continental Margin: California Division of Mines and Geology,

Hall, C. A., Jr., 1975, San Simeon-Hosgri fault system, coastal California: economic and environmental implications: Science, v. 190, pp. 1291-1294.

Hall, C. A., Jr., 1981, San Luis Obispo transform fault and middle Miocene rotation of the western Transverse Ranges, California: Journal of Geophysical Research, v. 86, pp. 1015-1031.

Hanson, K. L., Lettis, W. R., Mezger, E. L., and Weber, G. E., 1987, Late Pleistocene deformation along the San Simeon fault zone near San Simeon, California: Geol. Soc. Amer. Cordillerean Sec. 83rd Ann Meet., Abst. with Prog., pp. 386.

Hauksson, E., and Saldivar, G. V., 1989, Seismicity and active compressional tectonics in the Santa Monica Bay, southern California: Journal of Geophysical Research, v. 94, no. B7, pp. 9591-9606.

Henyey, T. L., and Teng, T.-L., 1985, Seismic studies of the Dos Cuadras and Beta offshore oil fields, southern California, Univ. of. So. Cal., Univ. of. So. Cal. Geophy. Lab. Tech. Report, 85-2

Hornafius, J. S., Luyendyk, B. P., Terres, R. R., and Kamerling, M. J., 1986, Timing and extent of Neogene tectonic rotation in the western Transverse Ranges, California, Geol. Soc. Am. Bull, v. 97, pp. 1476-1487.

Humphreys, E., and Weldon, R., 1989, Kinematic constraints on the rifting of Baja California.: AAPG Memoir on the Gulf of California.,in press,

Humphreys, G., and Weldon, R. J., in prep, Deformation across southern California: A local estimate of Pacific-North American relative plate motion.

Junger, A., 1976, Tectonics of the southern California borderland, in D. G. Howell, *Aspects of the geologic history of the California Continental Borderland*: American Association of Petroleum Geologists, Pacific Section, 486-498 pp.

Junger, A., 1979, Maps and seismic profiles showing the Northern Channel Islands Platform, Continental Borderland, California, U. S. Geol. Surv. Misc. Field. Stud. Map, MFS-991

Junger, A., and Wagner, H. C., 1977, Geology of the Santa Monica and San Pedro basins, California Continental Borderland, U. S. Geol. Surv. Misc. Field. Stud. Map, MF-850

King, R., Masters, W. E. G., Rizos, C., Stolz, A., and Collins, J., 1985, Surveying with GPS: Kensington, Australia, School of Surveying, University of New South Wales.

Kolenskiewcz, R., C., M., Torrence, M. H., and Dunn, pp. J., 1989, A comparison of SLR and VLBI coordinates and geodesic rates: v. 70, no. 43, pp. 1052.

Kroger, P. M., Lyzenga, G. A., Wallace, K. S., and Davidson, J. M., 1987, Tectonic motion in the western United States inferred from Very Long Baseline Interferometry measurements, 1980-1986: Journal of Geophysical Research, v. 92, no. B13, pp. 14151-14163.

Lajoie, K. R., Kern, J. pp., Wehmiller, J. F., Kennedy, G. L., Mathieson, S. A., Sarna-Wojcicki, A. M., Yerkes, R. F., and McCrory, pp. F., 1979, Quaternary marine shorelines and crustal deformation, San Diego to Santa Barbara, California, in pp. L. Abbott, *Geological Excursions in the Southern California Area*: Boulder, Colo., Geological Society of America, 3-15 pp.

Larsen, S., Agnew, D. C., and Hager, B. H., 1988, Strain accumulation in the Santa Barbara channel: 1971-1987: presented at the AGU Chapman Conference on GPS Positioning, Ft. Lauderdale, Florida, September 1988.

Larson, K. M., 1990, Precision, accuracy, and tectonics from the Global Positioning System: University of California at San Diego, Ph. D. thesis.

Legg, M., 1985, Geologic structure and tectonics of the inner Continental Borderland offshore northern Baja California, Mexico: University of California at Santa Barbara, Ph. D. thesis.

Legg, M., Luyendyk, B. pp., Mammerickx, J., and de Moustier, C., 1989, Sea Beam survey of an active strike-slip fault: The San Clemente fault in the California Continental Borderland: Journal of Geophysical Research, v. 94, no. B2, pp. 1727-1744.

Lisowski, M., and Prescott, W. H., 1981, Short-range distance measurements along the San Andres fault in central California, 1975 to 1979.: Bulletin of the Seismological Society of America, v. 71, pp. 607-1624.

Lorenzetti, E., and Tullis, T. E., 1989, Geodetic predictions of a strike-slip fault model: Implications for intermediate- and short-term earthquake prediction: Journal of Geophysical Research, v. 94, no. B9, pp. 12343-12361.

Luyendyk, B. P., Hajic, E. J., Crippen, R. E., and Simonett, D. S., 1982, Side-scan sonar and high-resolution reflection maps of the Santa Barbara Channel seafloor, University of California, Santa Barbara, California Sea Grant College Program, T-CSGCP-006.

Ma, C., Ryan, J. W., and Caprette, D., 1989, Crustal Dynamics Project data analysis - 1988: VLBI geodetic results 1979-87.: NASA Technical Memorandum, TM 100723.

Mader, G. L., 1986, GPS22: GPS Observable Processing Software, NGS, Rockville, Md.

Malys, S., and Jensen, P. A., 1989, Geodetic point positioning with GPS carrier beat phase data from the CASA UNO experiment: EOS Transactions of the American Geophysical Union, v. 70, no. 43, pp. 1053.

Menke, W., 1984, Geophysical Data Analysis: Discrete Inverse Theory: San Diego, Harcourt Brace Jovanovich, 268 pp.

Milbert, D. G., and Kass, W. G., 1987, ADJUST: The horizontal observation adjustment program, National Oceanic and Atmospheric Administration, Technical Memorandum, NOS NGS-47.

Minster, J. B., and Jordan, T. H., 1984, Vector constraints on Quaternary deformation of the western United States east and west of the San Andreas Fault, in J. K. Crouch and S. B. Bachman, *Tectonics and Sedimentation along the California Margin*: S. E. pp. M, Pacific Section, 1-16 pp.

Minster, J. B., and Jordan, T. H., 1987, Vector constraints on western U,S. deformation from space geodesy, neotectonics and plate motions: Journal of Geophysics Research, v. 92, pp. 4798-4804.

Minster, J. B., and T.H., J., 1978, Present-day plate motions: Journal of Geophysics Research, v. 83, pp. 5331-5354.

Morton, D. M., and Yerkes, R. F., 1987, Recent reverse faulting in the Transverse Ranges: U. S. Geological Survey Professional Paper 1339, pp. 1-5.

Mount, V., and Suppe, J., 1987, State of stress near the San Andreas fault: Implications for wrench tectonics: Geology, v. 15, pp. 1143-1146.

Murray, M., and King, R. W., 1988, SV3 coordinates of GPS Receivers, MIT, Internal Memorandum.

Namson, J., 1987, Structural transect through the Ventura basin and the western Transverse Ranges, in T. Davis and J. Namson, *Structural Evolution of the western Transverse Ranges*: Los Angeles, California, Pacific Section of the Society of Economic Paleontologists and Mineralogists, 29-42 pp.

Namson, J., and Davis, T., 1988, Structural transect of the western Transverse Ranges, California: Implications for lithospheric kinematics and seismic risk evaluation: Geology, v. 16, pp. 675-679.

Namson, J., and Davis, T., 1989a, Reply to Yeats, R. S. and Huftile, G. J. : Comment on "Structural transect of the western Transverse Ranges, California: Implications for lithospheric kinematics and seismic risk evaluation": Geology, pp. 772-773.

Namson, J., and Davis, T., 1989b, Reply to: Weldon, R. J. and Humphreys, G., Comment on "Structural transect of the western Transverse Ranges, California: Implications for lithospheric kinematics and seismic risk evaluation": Geology, pp. 770-771.

NASA, 1988, NASA geodynamics program summary report: 1979-1987, National Aeronautics and Space Administration, NASA Technical Memorandum, TM 4065.

NGS, 1988, Input Formats and Specifications of the National Geodetic Survey Data Base: Rockville, Md., Federal Geodetic Control Committee.

Okada, Y., 1985, Surface deformation due to shear and tensile faults in a half-space: Bulletin of the Seismological Society of America, v. 75, no. 4, pp. 1135-1154.

Orr, P. C., 1960, Late Pleistocene marine terraces on Santa Rosa island, California: v. 71, no. 7, pp. 1113-1119.

Orr, P. C., 1968, Prehistory of Santa Rosa Island, Santa Barbara County: Santa Barbara Museum of Natural History, 235 pp.

Patterson, R., 1979, Geology of the Santa Cruz Island fault: University of California at Santa Barbara, M. S. thesis.

Prescott, W. H., Davis, J. L., Svarc, J. L., and Wendt, K. J., 1988, Repeated Global Positioning System measurements: Results at scales from 5 to 200 km: EOS Transactions of the American Geophysical Union, v. 69, no. 44, pp. 1150.

Prescott, W. H., King, N. E., and Gu, G., 1984, Preseismic, coseismic, and postseismic deformation associated with the 1984 Morgan Hill, California earthquake: California Division of Mines and Geology Special Publication 68, v. 68, pp. 137-148.

Press, W. H., Flannery, B. pp., Teukolsky, S. A., and Vetterling, W. T., 1987, Numerical Recipes: The Art of Scientific Computing: Cambridge, Cambridge University Press, 818 pp.

Reid, H. F., 1910, The mechanics of the earthquake, The California Earthquake of April 18, 1906: State Earthquake Investigation Committee Report II, Carnegie Inst. of Washington, pp. 192.

Remondi, B. W., and Hofmann-Wellenhof, B., 1989, GPS broadcast orbits versus precise orbits: a comparison study: GPS Bulletin, v. 2, no. 6, pp. 8-20.

Rocken, C., 1988, The Global Positioning System: A new tool for tectonic studies: University of Colorado, Boulder, Ph. D. thesis.

Rockwell, T. K., Keller, E. A., Clark, M. N., and Johnson, D. L., 1984, Chronology and rates of faulting of Ventura River terraces, California: Geological Society of America Bulletin, v. 95, pp. 1466-1474.

Ryan, J. W., 1987, NASA/Crustal Dynamics result: Station motions from global scale VLBI baselines: EOS Transactions of the American Geophysical Union, v. 68, pp. 284.

Sauber, J., 1989, Geodetic measurement of deformation in California, NASA Technical Memorandum, TM-1000732.

Savage, J. C., 1983, Strain accumulation in the western United States: Annual Review of Earth Planetary Science, v. 11, pp. 11-43.

Savage, J. C., and Burford, R. O., 1973, Geodetic determination of relative motion in central California.: Journal of Geophysical Research, pp. 832-845.

Savage, J. C., Prescott, W. H., and Lisowski, M., 1987, Deformation along the San Andreas fault 1982-1986 as indicated by frequent Geodelite measurements: Journal of Geophysical Research, v. 78, pp. 6001-6007.

Smith, D. E., Douglas, N. B., Williamson, R. G., Torrence, M. H., Robbins, J. W., Klosko, S. M., Dunn, P. J., and Fricke, S. K., 1989a, Global plate motions latest results from LAGEOS laser ranging, ed., presented at the 16th Crustal Dynamics Principal Investigator's Meeting.

Smith, D. E., Kolenskiewcz, R., Dunn, P. J., Torrence, M. H., Klosko, S. M., Robbins, J. W., Williamson, R. G., Pavlis, E. C., Douglas, N. B., and Fricke, S. K., 1989b, Present-day tectonic motions from laser ranging to LAGEOS, ed., presented at the16th Crustal Dynamics Principal Investigator's Meeting.

Snay, R. A., 1986, Horizontal deformation in New York and Connecticut: Examining contradictory results from the geodetic evidence: Journal of Geophysical Research, v. 91, pp. 12695-12702.

Snay, R. A., Cline, M. W., and Timmerman, E. L., 1987, Project REDEAM: models for historical deformation, NOAA Tech. Rep., NOS 125 NGS 42.

Sovers, O. J., and Border, J. S., 1987, Observation Model and Parameter Partials for the JPL Geodetic GPS Modeling Software "GPSOMC", Jet Propulsion Laboratory, JPL 87-21.

Stock, J., and Molnar, P., 1988, Uncertainties and implications of the late Cretaceous and Tertiary position of North America relative to the Farallon, Kula, and Pacific plates: Tectonics, v. 7, no. 6, pp. 1339-1384.

Thatcher, W., 1975, Strain accumulation and release mechanism of the 1906 San Francisco earthquake: Journal of Geophysics Research, v. 80, no. 35, pp. 4862-4880.

Thatcher, W., 1979a, Horizontal crustal deformation from historic geodetic measurements in southern California: Journal of Geophysics Research, v. 84, no. B5, pp. 2351-2370.

Thatcher, W., 1979b, Systematic inversion of geodetic data in central California: Journal of Geophysics Research, v. 84, pp. 2283-2295.

Thatcher, W., and Lisowski, M., 1987, Long-term seismic potential of the San Andreas fault southeast of San Francisco, California: Journal of Geophysics Research, v. 92, no. B6, pp. 4771-4784.

Vanicek, P., and Krakiwsky, E., 1986, Geodesy: The Concepts: North-Holland, p. 697.

Vedder, J. G., Beyer, L. A., Junger, A., Moore, G. W., Roberts, A. E., Taylor, J. C., and Wagner, H. C., 1974, Preliminary report on the geology of the Continental Borderland of southern California, U. S. Geol. Surv. Misc. Field. Stud. Map, MF-624.

Ward, S. N., 1988, North America-Pacific plate boundary, an elastic-plastic megashear: evidence from very long baseline interferometry: Journal of Geophysical Research, v. 93, pp. 7716-7728.

Ward, S. N., 1989, Pacific-North American plate motions: New results from Very Long Baseline interferometry: EOS Transactions of the American Geophysical Union, v. 70, no. 43, pp. 1052.

Ward, S. N., in press, Pacific North American plate motions: New results from very long baseline interferometry: Journal of Geophysical Research,

Weaver, D. W., 1969, Geology of the northern Channel Islands: Pac Secs. A.A.P.G. and S.E.P.M., p. 199.

Webb, T. H., and Kanamori, H., 1985, Earthquake focal mechanisms in the eastern Transverse Ranges and San Emigdio mountains, southern California, and evidence for a regional decollement: Bulletin of the Seismological Society of America, v. 75, pp. 737-758.

Weber, G. E., 1979, Geologic investigation of the marine terraces of the San Simeon region and Pleistocene activity on the San Simeon fault zone, San Luis Obispo County, California, U. S. G. S., Final Technical Report, Contract No.14-08-0001-18230

Weldon, R., and Humphreys, G., 1986, A kinematic model of southern California: Tectonics, v. 5, pp.33-48.

Weldon, R. J., and Humphreys, G., 1989, Comment on "Structural transect of the western Transverse Ranges, California: Implications for lithospheric kinematics and seismic risk evaluation": Geology, pp. 769-770.

Wells, D., Beck, N., Delikaraolou, D., Kleusberg, A., Krakiwsky, E. J., Lachapelle, G., Langley, R. B., Nakiboglu, M., Schwartz, K., Tranquilla, J. M., and Vanicek, P., 1986, Guide to GPS Positioning: Fredricton, N. B., Canada, Canadian GPS Associates.

Yeats, R. S., 1981, Quaternary flake tectonics of the California Transverse Ranges: Geology, v. 9, pp. 16-20.

Yeats, R. S., 1982, Low-shake faults of the Ventura basin, California: Neotectonics in southern California, 78th Annual Meeting of the Geological Society of America Cordilleran Section, pp. 3-15.

Yeats, R. S., 1983, Large-scale Quaternary detachments in the Ventura basin, southern California: Journal of Geophysical Research, v. 88, no. B1, pp. 569-583.

Yeats, R. S., and Huftile, G. J., 1989, Comment on "Structural transect of the western Transverse Ranges, California: Implications for lithospheric kinematics and seismic risk evaluation": Geology, pp. 770-772.

Yeats, R. S., Huftile, G. J., and Grigsby, F. B., 1988, Oak Ridge fault, Ventura fold belt, and Sisar decollement, Ventura basin, California: Geology, v. 16, pp. 1112-1116.

Yerkes, R. F., Greene, H. G., Tinsley, J. C., and Lajoie, K. R., 1980, Seismotectonic setting of the Santa Barbara Channel area, southern California, U. S. Geol. Surv. Misc. Field Stud., MF-1169

Yerkes, R. F., and Lee, W. H. K., 1979, Maps showing faults and fault activity and epicenters, focal depths and focal mechanisms for 1970-1975 earthquakes, western Transverse Ranges, U. S. Geol. Surv. Misc. Field Studies Map, MF-1032.

Yerkes, R. F., and Lee, W. H. K., 1987, Late Quaternary deformation in the western Transverse Ranges: U. S. Geological Survey Professional Paper 1339, pp. 71-82.

Yerkes, R. F., Sarna-Wojcicki, A. M., and Lajoie, K. R., 1987, Geology and Quaternary deformation of the Ventura area: U. S. Geological Survey Professional Paper 1339, pp. 169-178.

Zoback, M. D., Prescott, W. H., and Krueger, S. W., 1985, Evidence for lower crustal ductile strain localization in southern New York: Nature, v. 317, pp. 705-707.

# Appendix A

## Local ties between GPS stations and Triangulation marks

Several of the triangulation stations were unrecoverable with GPS. The stations had either been destroyed or were unsuitable for GPS observations. This required that the GPS observations be made from eccentric marks and that the triangulation marks be tied into the larger GPS network through a local tie. The eccentric marks were original reference marks, other horizontal control marks, or newly established GPS marks. The local ties were made using GPS, local ground surveys conducted by the author, and/or local ground survey data proided by the NGS in the station descriptions (also known as the USC&GS/NGS Horizontal Control Data recovery notes, available from the NGS). The azimuths, distances and angles were then adjusted to obtain the best position offsets between the GPS mark and the triangulation station(s). During the adjustment, station elevations are held to their *a priori* values, unless vertical angle observations are available and the elevations can be solved for. The local geodetic coordinates, **g**, were then transformed from the WGS-84 ellipsoid into earth-centered and earth-fixed (ECEF) coordinates, **v**, at the latitude, φ, and longitude, λ, of the station using

$$\mathbf{A}\ \mathbf{g} = \mathbf{v} \quad \begin{bmatrix} -\sin\phi\cos\lambda & -\sin\lambda & \cos\phi\cos\lambda \\ -\sin\phi\sin\lambda & \cos\lambda & \cos\phi\sin\lambda \\ \cos\phi & 0 & \sin\phi \end{bmatrix} \begin{bmatrix} dn \\ de \\ du \end{bmatrix} = \begin{bmatrix} dx \\ dy \\ dz \end{bmatrix}$$

[Milbert and Kass, 1987]. The ties were treated in the later data adjustment as ECEF vectors with *a priori* sigmas as calculated from the adjustment of the tie observations. If a limited amount of ground survey data was available, the *a priori* sigmas of the tie were conservatively assumed to be 0.05 m. In cases with only horizontal observations, the vertical differences between markers are assumed to be zero.

Differences in the orientation of the local surveys with respect to the overall GPS network and its geodetic reference frame are a potential source of error in the positions of the tied bench marks. The orientations in the local geodetic reference frame were calculated from astronomical azimuths in the REDEAM data base and/or from observed and adjusted azimuths in the site descriptions. Laplace corrections were applied to the observed azimuths. Comparisons of observed Laplace azimuths with azimuths derived from GPS coordinates suggest that the GPS reference frame is locally rotated counter-clockwise $2.2 \pm 3.7$ arc seconds from the geodetic reference frame of the Laplace azimuths (Table A-1). This amount of angular difference corresponds to < .001 m for tie networks up to 100 m in dimensions.

The data available for the ties varied from site to site. Some sites had many angles, horizontal distances, and azimuths, while others only had one horizontal distance and azimuth. Each tie will be discussed below. The ECEF offsets are reported in units of meters.

A.1 San Miguel Island:

The triangulation mark New San Miguel 1873 and its reference marks were searched for. Only the reference mark New San Miguel RM2 1934 was found and was used for GPS observations during the MAR88 experiment. This mark is tied to the triangulation station through an observed azimuth, $37^{o}$ 21' 57.58" S, and a taped horizontal distance of 7.3455 m from the NGS recovery note of 1934. The ECEF vector assuming that both marks are at the same elevation and nominal 0.05 m measurement uncertainties, is :

| To - From | X | Y | Z |
|---|---|---|---|
| SMIG-NSMI | -5.4986 (0.0573) | -0.5640 (0.0011) | -4.8377 (0.0414) |

A.2 Santa Cruz Island:

The primary GPS mark on Santa Cruz Island is CENT. This is a USC&GS mark set in 1923. It is not part of the primary triangulation network, but is easily accessed on the island for GPS observations. The triangulation stations DEVL, SCRW, and SCRE have been tied into the GPS network during the JAN87 and SEP87 campaigns. Two other stations were tied to the GPS network via GPS observations in MAY88. The primary triangulation marks and the GPS marks are listed below:

| Designation | Name | Type of tie | Occupation |
|---|---|---|---|
| SCRW | Santa Cruz West RM1 1924 | GPS | SEP87 |
| SCW1 | Santa Cruz West 1874 | Ground | Destroyed |
| SCW2 | Santa Cruz West 2 1951 | Ground | (exists, not occupied) |
| HIGH | High 1951 | GPS | MAY88 |
| HIMT | High Mount 1951 | GPS | MAY88 |
| DEVL | Devils Peak 1951 | GPS | JAN87 |
| SCRE | Santa Cruz East 1898 | GPS | SEP87 |

CENT has been occupied during several campaigns and is confidently tied to the regional GPS network. During the SEP87 campaign, SCRW, Santa Cruz West RM1 1924, was occupied for two days during a large campaign in Central California that also included the occupation of CENT. These data have allowed SCRW to be tied into the GPS network. SCRW is a reference mark set in 1924 with ties to both SCW1 and

SCW2. The tie to each of these stations consisted of one horizontal distance and one local astronomical azimuth. The local ground ties used are reported in the USC&GS Horizontal Control Data recovery notes of 1861, 1934, and 1956. SCRW is 9.446 m in azimuth 199$^o$ 23 ' S from SCW1 and 9.296 m in azimuth 199$^o$ 55' 1.5" from SCW2 The vectors, assuming all the marks are at the elevation of SCRW and nominal 0.05 m north and east measurement uncertainties, are:

| To - From | X | Y | Z |
|---|---|---|---|
| SCRW-SCR2 | 5.1811 (0.0573) | 2.6700 (0.0011) | 7.2420 (0.0414) |
| SCRW-SCR1 | 5.2072 (0.0573) | 2.7635 (0.0011) | 7.3812 (0.0414) |

Stations HIGH and HIMT were tied to the GPS network during a three station GPS campaign in MAY88. These data were analyzed using GIPSY with broadcast orbits. The orientation of the baselines in the GPS reference frame was checked for biases by adjusting 359 direction measurements from 54 triangulation stations on Santa Cruz Island that included HIGH and HIMT. In this adjustment, the azimuth and distance between SCW2, CENT, and DEVL were constrained to their GPS values. The adjusted values for the azimuth between HIGH and HIMT were found to be within 0.1 arc second of the MAY88 GPS tie solutions, suggesting no significant orientation bias in the MAY88 solution.

A.3 Laguna Niguel:

The triangulation station at Niguel 1884 (NIGL), was destroyed shortly before the JUN86 experiment. Two reference marks, Niguel 1884 A (NIGU), and Niguel 1884 B (NIGB), still exist. NIGU, the primary GPS mark, is tied into the GPS network by many days of observations during several campaigns. NIGB and NIGU were simultaneously occupied for one day in OCT87. The tie between NIGL and NIGU uses data from the NGS recovery note for 1981. These data include several angles between all three of these stations and one other, 18 LSB69. Mark-to-mark distances were only available between NIGU, NIGB, and 18 LSB69. The tie was acquired using the GPS vector and the local ground tie distances and angles, constraining the station elevations to be their *a priori* values (Fig. A-1). The ECEF vectors with *a posteriori* scaled sigmas, assuming all the marks are at the elevation of NIGU, are:

| To - From | X | Y | Z |
|---|---|---|---|
| NIGU-NIGL | 377.5454 (0.3768) | -56.5097 (0.0505) | 189.7310 (0.3341) |
| NIGB-NIGL | 364.9135 (0.3799) | -78.2278 (0.0524) | 151.3927 (0.3345) |

A.4 Castro Peak:

Castro Peak has been used for triangulation observations since the late 1800's. Since then, two stations on the peak have been used for triangulation: Castro Peak 1898 (CTRO), and Castro Peak RM3 (CTR3). CTRO is unsuitable for GPS observations and CTR3 has been destroyed. The GPS mark, CATO, is a Los Angeles City survey control mark stamped SOSTICE CYN B2 AUX 1 LAC. This mark is tied to the triangulation stations using local ground survey information from the NGS site recovery notes of 1898, 1923, 1951, 1963, and 1975, and a survey performed by A. Donnellan and myself. The surveys included two azimuths, several taped and EDM horizontal distances. These data were adjusted and the adjusted positions were used to compute ECEF vector offsets from the GPS mark.

| To - From | X | Y | Z |
|---|---|---|---|
| CTR1-CATO | 13.7223 (0.0108) | -15.4697 (0.0013) | -10.2711 (0.0080) |
| CTR3-CATO | -12.1343 (0.0108) | 4.2322 (0.0013) | -3.1535 (0.0080) |
| CTRO-CATO | 2.0084 (0.0108) | -9.1950 (0.0013) | -10.4798 (0.0080) |

| | | | |
|---|---|---|---|
| CTR4-CATO | 20.0525 (0.0108) | -7.0117 (0.0013) | 5.1881 (0.0080) |
| CTAZ-CATO | -1135.7302 (0.0577) | 1554.2145 (0.0033) | 1204.0544 (0.04369) |

A.5 Santa Barbara 2 1956:

Poor sky visibility at the triangulation station Santa Barbara 2 1956 (SBAO), and its reference marks required that GPS observations be made from a temporary GPS set up in a field west of the triangulation station. This temporary station, SBA2, was surveyed to the triangulation stations by N. King and myself using a TOPCON GTS-38 total station. These observations and observations from the NGS recovery notes of 1956, 1959, 1972, and directions in the REDEAM data set from Santa Barbara 2 1956 to Santa Barbara 2 1956 RM5 (SBA5), Santa Barbara 2 1956 RM6 (SBA6), and Santa Barbara 2 AZ MK were used to calculate the north, east, and up offsets from the GPS antenna to the triangulation marks. The adjusted offsets were used to calculate ECEF vectors among the stations. The ECEF interstation vectors including elevation differences between the stations with 1-sigma *a posteriori* uncertainties are :

| To - From | X | Y | Z |
|---|---|---|---|
| SBAO-SBA2 | 45.6240 (0.0140) | -60.5497 (0.0117) | -30.5065 (0.0249) |
| SBA5-SBA2 | 31.8990 (0.0140) | -52.2874 (0.0117) | -29.5580 (0.0249) |
| SBA6-SBA2 | 54.6334 (0.0175) | -61.5388 (0.0177) | -25.2432 (0.0350) |

A.6 San Fernando 1898:

San Fernando 1898 (SAFO) was not recovered and a nearby Los Angeles County survey control marker, Pico L-9C (SAFE),was occupied with GPS. Horizontal angles, mark-to-mark distances, and elevations from the NGS recovery notes of 1952, 1956, 1959, 1963, and 1971, and adjusted azimuths from the Los Angeles County Survey

Control notes for Pico L-9 were used to calculate the north and east offsets between the GPS mark SAFE, and the triangulation marks. The ECEF vectors with *a posteriori* 1-sigma uncertainties are:

| To - From | X | Y | Z |
|---|---|---|---|
| SAF3-L_9A | -13.7781 (0.0091) | 39.7420 (0.0022) | 50.3369 (0.0055) |
| SAFO-L_9A | -16.6325 (0.0094) | 31.4151 (0.0017) | 28.4103 (0.0064) |
| L_92-L_9A | -4.9359 (0.0172) | 72.9992 (0.0040) | 90.3892 (0.0089) |
| SAF2-L_9A | -3.0562 (0.0108) | 9.1229 (0.0013) | 18.4879 (0.0080) |
| SAFE-L_9A | -23.6467 (0.0076) | 86.2845 (0.0014) | 84.1930 (0.0088) |

A.7 Laguna 2 1951:

Laguna 2 1951 (LAG2) is on Pacific Missile Test Center property and is unsuited for GPS observations. Station Mugu Cotar (COTR) on the PMTC was occupied with GPS during the JAN87 experiment. The tie between COTAR and LAG2 is a first order survey adjustment of the PMTC network [Rich Dixon of the PMTC, written com.] in the WGS-84 system. The WGS-84 latitude, longitude and elevations (m) are

| | | | |
|---|---|---|---|
| COTR | 34 07 12.63528 | 119 09 14.32436 | -34.561 |
| LAG2 | 34 06 30.76108 | 119 03 54.49855 | 404.657 |

The PMTC station coordinates were converted into an ECEF vector. First order surveys have a precision of several ppm [Gosset, 1951]. A conservative 10 ppm positional error was assigned to each component of the vector.

| To - From | X | Y | Z |
|---|---|---|---|
| COTR-LAG2 | -6632.3524 (0.0830) | -4937.4258 (0.0830) | -821.8911 (0.0830) |

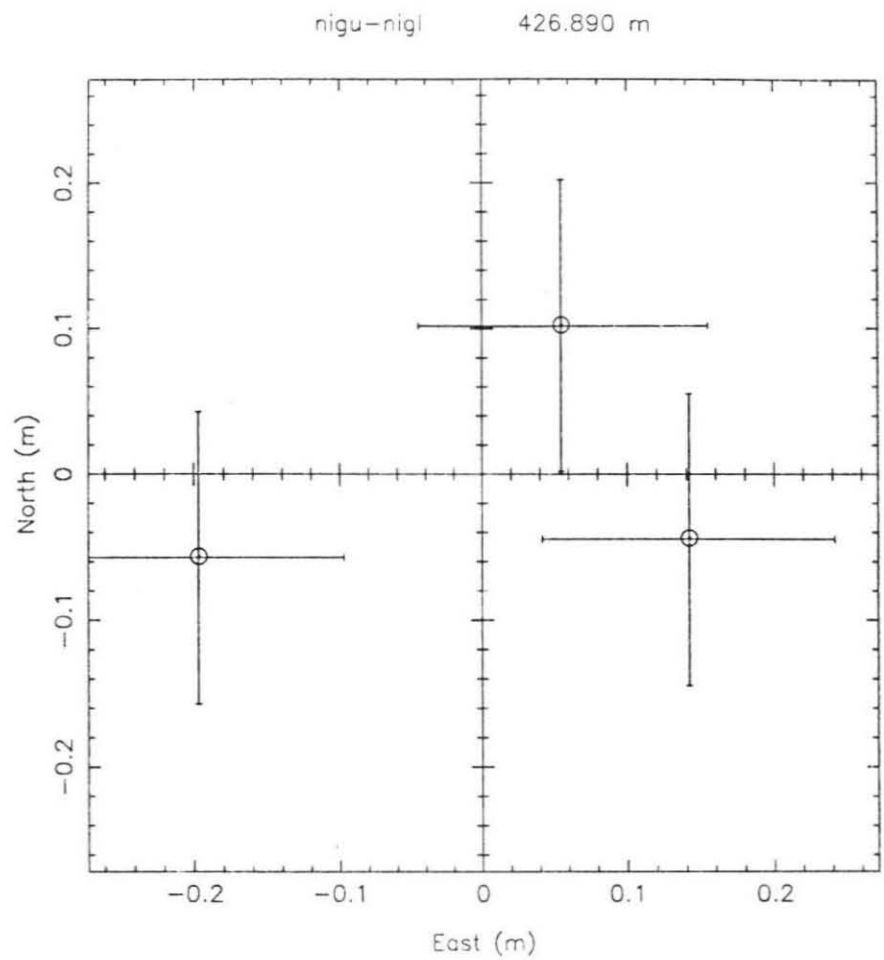


Figure A-1. North-east position scatter of separate solutions based on triangulation from NIGU, NIGB, and NIGL plotted about the best fit position.

| Stations | $\eta$ (arc sec) | $\alpha_{Laplace}$ | $\alpha_{GPS}$ | $\alpha_{Laplace} - \alpha_{GPS}$ | Year |
|---|---|---|---|---|---|
| CTRO-SCLA | 4.7E | 138 47 54.8 | 138 47 57.8 | -3.0 | 1923.83 |
| CHAF-LAG2 | 7.5E | 310 56 15.5 | 310 56 19.4 | -3.9 | 1970.83 |
| GAVI-SBAO | 8.9E | 238 35 04.8 | 238 35 08.5 | -3.7 | 1971.00 |
| HARB-BOUL | 4.8E | 322 23 22.9 | 322 23 24.1 | -1.2 | 1878. |
| LAG2-CHAF | 12.6E | 131 05 08.0 | 131 05 17.3 | -9.3 | 1960.17 |
| LAG2-CHAF | 12.6E | 131 05 09.2 | 131 05 17.3 | -8.1 | 1970.92 |
| ROAD-SBIS | 4.9E | 240 56 38.0 | 240 56 39.5 | -1.5 | 1971.00 |
| SAFO-SCLA | 4.6E | 089 28 28.4 | 089 28 30.1 | -2.7 | 1923.75 |
| SBIS-LAG2 | 2.7E | 178 12 43.3 | 173 12 43.7 | -0.4 | 1971.00 |
| SBAO-CHAF | 6.6E | 287 51 13.2 | 287 51 16.1 | -2.9 | 1970.92 |
| SCRE-GAVI | 1.7W | 130 31 20.9 | 130 31 17.7 | 3.2 | 1924.92 |
| SCRE-GAVI | 1.7W | 130 31 20.6 | 130 31 17.7 | 2.9 | 1874.17 |
| HARB-WEST | 4.8E | 179 17 37.2 | 179 17 33.9 | 3.3 | 1908.17 |

Table A-1. Geodetic azimuths from the south for several stations in the triangulation-GPS network. $\eta$ is the deflection of the vertical used to calculate the Laplace azimuth from the observed astronomical azimuth from the first station to the second. $\eta$ is calculated from the difference between the astronomical position and the GPS position at the observing station. Differences are reported in arc seconds. Mean difference is $-2.2 \pm 3.7$ arc seconds.

| Observation type | from | to | date | observation | s.e. | source |
|---|---|---|---|---|---|---|
| HD | 1 | 3 | 1981 8 7 | 0 0 0.00 | 0.70 | NGS |
| HD | 1 | 2 | | 303 33 58.80 | 0.70 | NGS |
| HD | 1 | 4 | | 328 8 48.50 | 0.70 | NGS |
| HD | 2 | 3 | 1981 8 7 | 0 0 0.00 | 0.70 | NGS |
| HD | 2 | 4 | | 17 75 23.20 | 0.70 | NGS |
| HD | 2 | 1 | | 118 80 37.00 | 0.70 | NGS |
| HD | 3 | 1 | 1981 8 7 | 0 0 0.00 | 0.70 | NGS |
| HD | 3 | 4 | | 4 42 7.70 | 0.70 | NGS |
| HD | 3 | 2 | | 5 52 6.00 | 0.70 | NGS |
| SD | 1 | 4 | 1981 8 7 | 54.8670 | 3.0 | NGS |
| SD | 2 | 4 | 1981 8 7 | 23.1180 | 3.0 | NGS |
| SD | 2 | 1 | 1981 8 7 | 45.7901 | 3.0 | NGS |
| ID | 1 | nigu Niguel_A | | 33 30 5.232926 117 43 4.908335 233.69 | | |
| ID | 2 | nigb Niguel_B | | 33 30 5.084147 117 43 4.912492 233.69 | | |
| ID | 3 | nigl Niguel_1884 | | 33 30 4.493877 117 44 0.307559 233.71 | | |
| ID | 4 | mk18 Mark 18 lsb69 | | 33 30 5.072576 117 43 5.000833 233.69 | | |

Table A-2. Observations used in the determination of the NIGU ground tie. HD = horizontal direction, SD = mark-to-mark distance in meters, ID = station name and *a priori* latitude, longitude and elevation. Standard errors (s.e.) are in arc seconds (HD) and millimeters (SD). All data are from NGS Horizontal Control site description recovery notes of 1981.

| Observation type | from | to | date | observation | s.e. | |
|---|---|---|---|---|---|---|
| HD | 401 | 46 | 1971 4 27 | 82 21 1.90 | 1.20 | |
| HD | 401 | 43 | | 92 25 55.90 | 1.20 | |
| HD | 401 | 201 | | 182 25 19.00 | 1.20 | |
| HD | 47 | 406 | 1963 3 15 | 0 0 0.00 | 1.20 | |
| HD | 47 | 407 | | 2 25 27.00 | 1.20 | |
| HD | 47 | 43 | | 234 44 25.00 | 1.20 | |
| HD | 43 | 406 | 1963 3 15 | 43 34 22.20 | 1.20 | |
| HD | 43 | 407 | | 66 65 18.00 | 1.20 | |
| HD | 43 | 47 | | 95 51 36.40 | 1.20 | |
| HD | 43 | 401 | 1971 3 17 | 0 0 0.00 | 1.20 | |
| HD | 43 | 46 | | 160 3 53.80 | 1.20 | |
| SD | 46 | 201 | | 123.1177 | 20.0 | |
| SD | 401 | 201 | | 23.6340 | 20.0 | |
| SD | 401 | 43 | | 52.6370 | 20.0 | |
| SD | 401 | 46 | | 116.4740 | 20.0 | |
| SD | 46 | 43 | | 65.5170 | 10.0 | |
| SD | 46 | 47 | | 45.4230 | 10.0 | |
| SD | 43 | 47 | | 23.2210 | 10.0 | |
| SD | 43 | 407 | | 45.8010 | 10.0 | |
| SD | 47 | 407 | | 27.6360 | 10.0 | |
| GA | 201 | 46 | 1974 1 1 | 329 93 4.60 | 1.50 | LACO |
| GA | 47 | 406 | 1974 1 1 | 301 13 35.50 | 1.50 | LACO |
| GA | 43 | 406 | 1974 1 1 | 304 44 57.70 | 1.50 | LACO |
| ID | 43 | saf3 3 | | 34 19 4.799976 118 36 0.362230 113.80 | | |
| ID | 46 | l9_a | | 34 19 4.612187 118 36 0.240385 108.78 | | |
| ID | 47 | safo | | 34 19 4.725005 118 36 0.353275 108.60 | | |
| ID | 201 | safe | | 34 19 4.956141 118 36 0.483515 103.05 | | |
| ID | 401 | l9_2 | | 34 19 4.967087 118 36 0.391385 108.78 | | |
| ID | 406 | azimuth mark | | 34 19 4.166400 118 35 5.264400 108.78 | | |
| ID | 407 | saf2 | | 34 19 4.671462 118 36 0.270015 113.80 | | |

Table A-3. Observations used in the determination of the SAFE ground tie. HD = horizontal direction, GA = geodetic azimuth, SD = mark-to-mark distance in meters, ID = station name and *a priori* latitude, longitude and elevation. Standard errors (s.e.) are in arc seconds (HD and GA) and millimeters (SD). Data are from NGS Horizontal Control site description recovery notes of 1981. Mark: l9_2 = PICO L-9 aux 2 ecc 1 LAC 1971, saf2 = SAN FERNANDO 1898 RM 2, azimuth mark = azimuth mark of the NGS Horizontal Control site description recovery notes of 1981.

| Observation type | from | to | date | observation | | | s.e. | source |
|---|---|---|---|---|---|---|---|---|
| HD | 4 | 8 | 1987 10 1 | 0 | 0 | 0.00 | 0.60 | CIT |
| HD | 4 | 1 | | 126 | 65 | 45.25 | 0.60 | CIT |
| HD | 4 | 8 | 1987 10 1 | 0 | 0 | 0.00 | 0.60 | CIT |
| HD | 4 | 1 | | 126 | 65 | 51.00 | 0.60 | CIT |
| HD | 4 | 8 | 1987 10 1 | 0 | 0 | 0.00 | 0.60 | CIT |
| HD | 4 | 2 | | 10 | 1 | 34.00 | 0.60 | CIT |
| HD | 4 | 1 | 1987 10 1 | 0 | 0 | 0.00 | 0.60 | CIT |
| HD | 4 | 8 | | 233 | 30 | 15.00 | 0.60 | CIT |
| HD | 4 | 2 | 1987 10 1 | 0 | 0 | 0.00 | 0.60 | CIT |
| HD | 4 | 8 | | 349 | 94 | 14.00 | 0.60 | CIT |
| HD | 4 | 3 | 1987 10 1 | 0 | 0 | 0.00 | 0.60 | CIT |
| HD | 4 | 8 | | 243 | 32 | 53.00 | 0.60 | CIT |
| HD | 1 | 2 | 1969 3 1 | 0 | 0 | 0.00 | 0.60 | CIT |
| HD | 1 | 3 | | 138 | 85 | 17.00 | 0.60 | CIT |
| HD | 1 | 2 | 1969 3 1 | 0 | 0 | 0.00 | 0.60 | CIT |
| HD | 1 | 3 | | 138 | 85 | 55.00 | 0.60 | CIT |
| HD | 4 | 8 | 1987 10 1 | 0 | 0 | 0.00 | 0.60 | CIT |
| HD | 4 | 3 | | 116 | 63 | 23.00 | 0.60 | CIT |
| HD | 1 | 3 | 1969 3 1 | 0 | 0 | 0.00 | 0.60 | CIT |
| HD | 1 | 2 | | 221 | 10 | 3.00 | 0.60 | CIT |
| VA | 4 | 8 | 1987 10 1 | 95 | 54 | 14.00 | 1.00 | CIT |
| VA | 4 | 1 | 1987 10 1 | 89 | 94 | 29.00 | 3.00 | CIT |
| VA | 4 | 8 | 1987 10 1 | 95 | 54 | 18.00 | 1.00 | CIT |
| VA | 4 | 8 | 1987 10 1 | 95 | 54 | 17.00 | 1.00 | CIT |
| VA | 4 | 1 | 1987 10 1 | 89 | 94 | 18.50 | 3.00 | CIT |
| VA | 4 | 8 | 1987 10 1 | 95 | 54 | 20.00 | 1.00 | CIT |
| VA | 4 | 2 | 1987 10 1 | 86 | 65 | 56.00 | 1.00 | CIT |
| VA | 4 | 2 | 1987 10 1 | 86 | 65 | 32.00 | 1.00 | CIT |
| VA | 4 | 3 | 1987 10 1 | 89 | 94 | 53.50 | 1.00 | CIT |
| VA | 4 | 3 | 1987 10 1 | 89 | 94 | 57.50 | 1.00 | CIT |
| VA | 4 | 3 | 1987 10 1 | 89 | 94 | 58.50 | 1.00 | CIT |
| SD | 4 | 8 | | | 73.1650 | | 3.0 | CIT |
| SD | 4 | 1 | | | 12.7590 | | 3.0 | CIT |
| SD | 4 | 8 | | | 73.1650 | | 3.0 | CIT |
| SD | 4 | 1 | | | 12.7600 | | 3.0 | CIT |
| SD | 4 | 8 | | | 73.1650 | | 3.0 | CIT |
| SD | 4 | 2 | | | 5.5510 | | 3.0 | CIT |
| SD | 4 | 3 | | | 22.7840 | | 3.0 | CIT |
| SD | 4 | 2 | | | 5.5590 | | 3.0 | CIT |
| SD | 4 | 3 | | | 22.7840 | | 3.0 | CIT |
| SD | 1 | 2 | | | 16.0170 | | 3.0 | CIT |
| SD | 1 | 3 | | | 10.4830 | | 3.0 | CIT |
| SD | 1 | 2 | | | 16.0410 | | 3.0 | CIT |
| SD | 1 | 3 | | | 10.4900 | | 3.0 | CIT |
| SD | 1 | 2 | | | 16.0500 | | 3.0 | CIT |
| SD | 1 | 3 | | | 10.4850 | | 3.0 | CIT |
| GA | 1 | 3 | 1956 10 0 | 52 | 23 | 14.20 | 0.70 | NGS |
| GA | 1 | 3 | 1956 10 10 | 52 | 23 | 52.50 | 0.70 | NGS |
| GA | 1 | 2 | 1956 10 10 | 273 | 33 | 54.20 | 0.70 | NGS |
| GA | 1 | 2 | 1956 10 10 | 273 | 33 | 32.50 | 0.70 | NGS |

| Observation type | from | to | date | observation | s.e. | source |
|---|---|---|---|---|---|---|
| ID | 1 | sbao | | 34 24 1.658695 119 42 5.924460 | | |
| ID | 2 | sba5 | | 34 24 1.661866 119 42 5.987134 | | |
| ID | 3 | sba6 | | 34 24 1.679406 119 42 5.891928 | | |
| ID | 4 | Temp inst | | 34 24 1.648308 119 42 5.972818 | | |
| ID | 8 | SBA2 | | 34 24 1.795381 119 43 0.195833 | | |

Table A-4. Observations used in the determination of the SBA2 ground tie. HD = horizontal direction, VA = vertical angle, GA = geodetic azimuth, SD = mark-to-mark distance in meters, ID = station name and *a priori* latitude, longitude and elevation. Standard errors (s.e.) are in arc seconds (HD, VA, and GA) and millimeters (SD). Data are from NGS Horizontal Control site description recovery notes of 1981. sba6 = SANTA BARBARA 2 1956 RM6, sba5 = SANTA BARBARA 2 1956 RM5, sbao = SANTA BARBARA 2 1956

# Appendix B

The triangulation observations for both of the data sets derived in Chapter 2 are listed in the following tables in the NGS Blue Book format. Figure B-1 describes the Blue-Book format for horizontal observations. Station serial numbers correspond to those listed in Table 2-1. Table B-1 contains all of the horizontal direction observations. Table B-2 contains the subset set of the horizontal directions that has been edited for possible data blunders, as explained in Chapter 2. The trilateration observations are contained in Table B-3. Table B-4 lists the components, and the uncertainties, of the interstation GPS vectors estimated for each experiment day. The SV3 fiducial coordinates are listed in Table B-5.

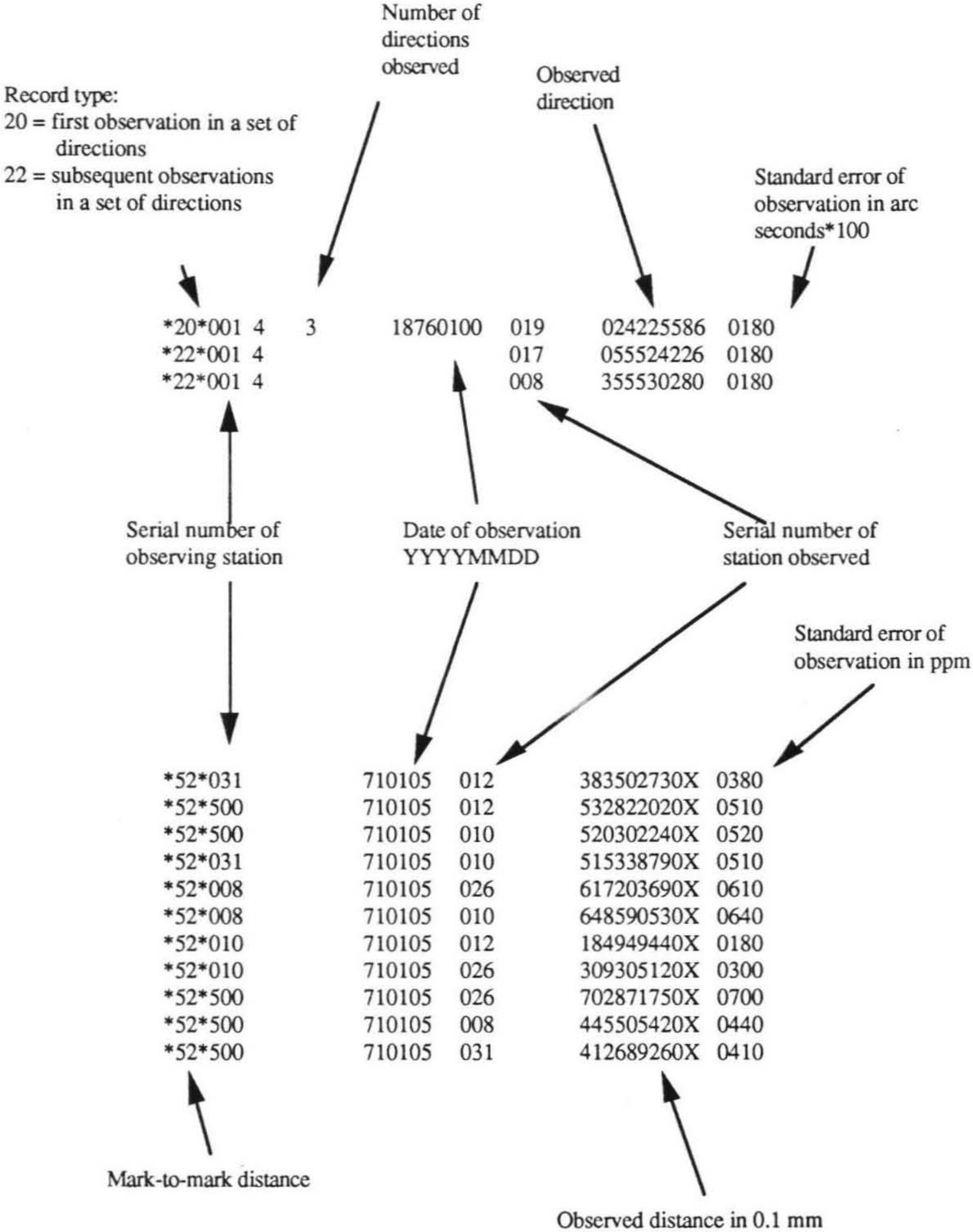


Figure. B-1. Description of NGS Blue Book format

Table B-1

| | | | | | | |
|---|---|---|---|---|---|---|
| *22*022 | 17 | | | 041 | 177594140 | 0209 |
| *22*022 | 17 | | | 042 | 190385009 | 0209 |
| *22*022 | 17 | | | 005 | 270362117 | 0209 |
| *22*022 | 17 | | | 023 | 288530408 | 0209 |
| *20*042 | 9 | 004 | 18770100 | 005 | 160490952 | 0209 |
| *22*042 | 9 | | | 023 | 200215417 | 0209 |
| *22*042 | 9 | | | 022 | 220135125 | 0209 |
| *22*042 | 9 | | | 041 | 343274324 | 0209 |
| *20*039 | 1 | 002 | 18780100 | 023 | 234515608 | 0209 |
| *22*039 | 1 | | | 005 | 265522417 | 0180 |
| *20*005 | 1 | 003 | 18780100 | 023 | 026442444 | 0209 |
| *22*005 | 1 | | | 022 | 033563345 | 0209 |
| *22*005 | 1 | | | 042 | 074342629 | 0209 |
| *20*001 | 3 | 003 | 18760100 | 019 | 024225586 | 0180 |
| *22*001 | 3 | | | 017 | 055524226 | 0180 |
| *22*001 | 3 | | | 008 | 355530280 | 0180 |
| *20*008 | 13 | 005 | 18750100 | 002 | 033445062 | 0180 |
| *22*008 | 13 | | | 025 | 060243890 | 0180 |
| *22*008 | 13 | | | 019 | 081382020 | 0180 |
| *22*008 | 13 | | | 017 | 128562273 | 0180 |
| *22*008 | 13 | | | 001 | 215264732 | 0180 |
| *20*017 | 1 | 003 | 18730100 | 019 | 042582659 | 0209 |
| *22*017 | 1 | | | 001 | 303052946 | 0209 |
| *22*017 | 1 | | | 008 | 336352894 | 0209 |
| *20*019 | 2 | 005 | 18740100 | 017 | 000000000 | 0209 |
| *22*019 | 2 | | | 001 | 048372232 | 0209 |
| *22*019 | 2 | | | 008 | 066190531 | 0209 |
| *22*019 | 2 | | | 002 | 121373598 | 0209 |
| *22*019 | 2 | | | 025 | 188142720 | 0209 |
| *20*029 | 10 | 002 | 18980100 | 034 | 000000000 | 0180 |
| *22*029 | 10 | | | 050 | 316541632 | 0180 |
| *20*051 | 1 | 004 | 18980100 | 050 | 007172850 | 0209 |
| *22*051 | 1 | | | 025 | 094453351 | 0209 |
| *22*051 | 1 | | | 002 | 164333164 | 0209 |
| *22*051 | 1 | | | 034 | 320231000 | 0209 |
| *20*050 | 1 | 005 | 18980100 | 029 | 000000000 | 0209 |
| *22*050 | 1 | | | 025 | 167125362 | 0209 |
| *22*050 | 1 | | | 002 | 203220325 | 0209 |
| *22*050 | 1 | | | 051 | 215305210 | 0209 |
| *22*050 | 1 | | | 034 | 270042478 | 0180 |
| *20*002 | 11 | 005 | 18980100 | 008 | 013311926 | 0180 |
| *22*002 | 11 | | | 051 | 197423901 | 0180 |
| *22*002 | 11 | | | 050 | 208174678 | 0180 |
| *22*002 | 11 | | | 025 | 250014601 | 0180 |
| *22*002 | 11 | | | 019 | 296431693 | 0180 |
| *20*034 | 36 | 004 | 18980100 | 050 | 000000000 | 0180 |
| *22*034 | 36 | | | 025 | 052414348 | 0180 |
| *22*034 | 36 | | | 051 | 078320847 | 0180 |
| *22*034 | 36 | | | 029 | 313011526 | 0180 |
| *20*025 | 7 | 006 | 18980100 | 019 | 000000000 | 0209 |
| *22*025 | 7 | | | 008 | 036505946 | 0209 |
| *22*025 | 7 | | | 002 | 066414176 | 0209 |
| *22*025 | 7 | | | 051 | 124343916 | 0209 |
| *22*025 | 7 | | | 034 | 144215258 | 0209 |
| *22*025 | 7 | | | 050 | 168483978 | 0209 |
| *20*001 | 7 | 3 | 19240930 | 008 | 061430872 | 0060 |
| *22*001 | 7 | | | 019 | 090125991 | 0060 |
| *22*001 | 7 | | | 017 | 121424468 | 0060 |
| *20*001 | 8 | 3 | 19240930 | 008 | 061430982 | 0080 |

| | | | | | | |
|---|---|---|---|---|---|---|
| *22*001 | 8 | | | 019 | 090130000 | 0080 |
| *22*001 | 8 | | | 017 | 121424373 | 0100 |
| *20*001 | 9 | 2 | 19240930 | 008 | 061430880 | 0060 |
| *22*001 | 9 | | | 019 | 090130029 | 0060 |
| *20*001 | 10 | 3 | 19241102 | 008 | 061430534 | 0060 |
| *22*001 | 10 | | | 019 | 090125727 | 0060 |
| *22*001 | 10 | | | 017 | 121424415 | 0060 |
| *20*001 | 13 | 3 | 19241102 | 008 | 061430798 | 0060 |
| *22*001 | 13 | | | 019 | 090125936 | 0060 |
| *22*001 | 13 | | | 017 | 121424462 | 0060 |
| *20*029 | 12 | 4 | 19230301 | 047 | 000000000 | 0060 |
| *22*029 | 12 | | | 038 | 099560896 | 0060 |
| *22*029 | 12 | | | 050 | 243355632 | 0060 |
| *22*029 | 12 | | | 034 | 286413841 | 0060 |
| *20*029 | 13 | 3 | 19230302 | 038 | 099560860 | 0060 |
| *22*029 | 13 | | | 050 | 243355583 | 0060 |
| *22*029 | 13 | | | 034 | 286413796 | 0060 |
| *20*008 | 1 | 3 | 19251113 | 002 | 178180366 | 0060 |
| *22*008 | 1 | | | 025 | 204575108 | 0060 |
| *22*008 | 1 | | | 019 | 226113179 | 0060 |
| *20*008 | 15 | 5 | 19241105 | 002 | 000000000 | 0060 |
| *22*008 | 15 | | | 025 | 026394481 | 0060 |
| *22*008 | 15 | | | 019 | 047532531 | 0060 |
| *22*008 | 15 | | | 017 | 095112722 | 0060 |
| *22*008 | 15 | | | 001 | 181415550 | 0240 |
| *20*008 | 16 | 4 | 19241106 | 002 | 000000000 | 0170 |
| *22*008 | 16 | | | 025 | 026394355 | 0060 |
| *22*008 | 16 | | | 019 | 047532573 | 0070 |
| *22*008 | 16 | | | 001 | 181415410 | 0240 |
| *20*008 | 17 | 3 | 19241107 | 002 | 000000000 | 0060 |
| *22*008 | 17 | | | 017 | 095112652 | 0060 |
| *22*008 | 17 | | | 001 | 181415411 | 0060 |
| *20*008 | 18 | 2 | 19241119 | 002 | 000000000 | 0060 |
| *22*008 | 18 | | | 001 | 181415610 | 0060 |
| *20*008 | 19 | 2 | 19241119 | 002 | 000000000 | 0060 |
| *22*008 | 19 | | | 001 | 181415590 | 0060 |
| *20*008 | 22 | 5 | 19241120 | 002 | 000000000 | 0060 |
| *22*008 | 22 | | | 025 | 026394419 | 0060 |
| *22*008 | 22 | | | 019 | 047532556 | 0060 |
| *22*008 | 22 | | | 017 | 095112687 | 0060 |
| *22*008 | 22 | | | 001 | 181415528 | 0060 |
| *20*050 | 3 | 4 | 19231105 | 029 | 089553295 | 0060 |
| *22*050 | 3 | | | 038 | 114592435 | 0060 |
| *22*050 | 3 | | | 025 | 257082812 | 0060 |
| *22*050 | 3 | | | 002 | 293173764 | 0060 |
| *20*050 | 4 | 4 | 19231106 | 029 | 089553321 | 0060 |
| *22*050 | 4 | | | 038 | 114592444 | 0060 |
| *22*050 | 4 | | | 025 | 257082822 | 0060 |
| *22*050 | 4 | | | 002 | 293173658 | 0060 |
| *20*017 | 2 | 3 | 19241108 | 008 | 000000000 | 0240 |
| *22*017 | 2 | | | 019 | 066225650 | 0240 |
| *22*017 | 2 | | | 001 | 326295907 | 0080 |
| *20*017 | 3 | 2 | 19241108 | 008 | 000000000 | 0060 |
| *22*017 | 3 | | | 019 | 066225855 | 0120 |
| *20*017 | 4 | 3 | 19241108 | 008 | 000000000 | 0060 |
| *22*017 | 4 | | | 019 | 066225844 | 0060 |
| *22*017 | 4 | | | 001 | 326300064 | 0060 |
| *20*017 | 5 | 3 | 19241113 | 008 | 000000000 | 0060 |
| *22*017 | 5 | | | 019 | 066225716 | 0060 |
| *22*017 | 5 | | | 001 | 326295930 | 0060 |
| *20*017 | 6 | 3 | 19241113 | 008 | 000000000 | 0060 |

| | | | | | |
|---|---|---|---|---|---|
| *22*017 6 | | | 019 | 066225789 | 0060 |
| *22*017 6 | | | 001 | 326295965 | 0060 |
| *20*047 13 | 3 | 19231027 | 038 | 056024798 | 0070 |
| *22*047 13 | | | 029 | 109021728 | 0060 |
| *22*047 13 | | | 034 | 166181619 | 0060 |
| *20*047 93 | 3 | 19231027 | 038 | 056024814 | 0060 |
| *22*047 93 | | | 029 | 109021716 | 0060 |
| *22*047 93 | | | 034 | 166181645 | 0060 |
| *20*038 15 | 2 | 19231018 | 029 | 241020121 | 0060 |
| *22*038 15 | | | 047 | 268062939 | 0070 |
| *20*038 16 | 2 | 19231019 | 029 | 241020202 | 0060 |
| *22*038 16 | | | 047 | 268062877 | 0060 |
| *20*038 17 | 2 | 19231017 | 029 | 000000000 | 0060 |
| *22*038 17 | | | 047 | 027042761 | 0060 |
| *20*002 1 | 3 | 19251110 | 019 | 099003664 | 0060 |
| *22*002 1 | | | 008 | 175483886 | 0060 |
| *22*002 1 | | | 008 | 175484095 | 0060 |
| *20*002 11 | 3 | 19241111 | 050 | 000000000 | 0070 |
| *22*002 11 | | | 025 | 041435825 | 0060 |
| *22*002 11 | | | 019 | 088252864 | 0060 |
| *20*002 12 | 3 | 19241110 | 050 | 000000000 | 0070 |
| *22*002 12 | | | 025 | 041435871 | 0060 |
| *22*002 12 | | | 019 | 088252862 | 0060 |
| *20*034 38 | 4 | 19231107 | 047 | 000000000 | 0060 |
| *22*034 38 | | | 029 | 049254224 | 0060 |
| *22*034 38 | | | 050 | 096242823 | 0060 |
| *22*034 38 | | | 025 | 149061219 | 0060 |
| *20*034 39 | 2 | 19231108 | 029 | 049254196 | 0060 |
| *22*034 39 | | | 050 | 096242782 | 0060 |
| *20*025 10 | 3 | 19241112 | 034 | 019471183 | 0110 |
| *22*025 10 | | | 050 | 044135914 | 0110 |
| *22*025 10 | | | 002 | 302070109 | 0090 |
| *20*025 11 | 3 | 19241112 | 034 | 000000000 | 0110 |
| *22*025 11 | | | 050 | 024264528 | 0090 |
| *22*025 11 | | | 002 | 282194861 | 0080 |
| *20*025 12 | 5 | 19241113 | 034 | 019471296 | 0070 |
| *22*025 12 | | | 050 | 044135997 | 0070 |
| *22*025 12 | | | 019 | 235251861 | 0060 |
| *22*025 12 | | | 008 | 272161768 | 0060 |
| *22*025 12 | | | 002 | 302070042 | 0060 |
| *20*025 13 | 3 | 19241114 | 034 | 019471232 | 0070 |
| *22*025 13 | | | 008 | 272161828 | 0060 |
| *22*025 13 | | | 019 | 235251792 | 0060 |
| *20*025 14 | 5 | 19241114 | 034 | 019471247 | 0070 |
| *22*025 14 | | | 050 | 044135918 | 0070 |
| *22*025 14 | | | 019 | 235251826 | 0240 |
| *22*025 14 | | | 008 | 272161798 | 0240 |
| *22*025 14 | | | 002 | 302070075 | 0060 |
| *20*019 1 | 3 | 19251115 | 008 | 017414254 | 0060 |
| *22*019 1 | | | 002 | 073001458 | 0060 |
| *22*019 1 | | | 025 | 139370535 | 0060 |
| *20*019 4 | 4 | 19241115 | 025 | 000000000 | 0060 |
| *22*019 4 | | | 008 | 238043744 | 0060 |
| *22*019 4 | | | 002 | 293230664 | 0060 |
| *22*019 4 | | | 001 | 220225503 | 0060 |
| *20*019 5 | 5 | 19241115 | 025 | 000000000 | 0060 |
| *22*019 5 | | | 017 | 171453232 | 0060 |
| *22*019 5 | | | 001 | 220225431 | 0070 |
| *22*019 5 | | | 008 | 238043759 | 0080 |
| *22*019 5 | | | 002 | 293230752 | 0080 |
| *20*019 6 | 4 | 19241115 | 025 | 000000000 | 0240 |

| | | | | | | |
|---|---|---|---|---|---|---|
| *22*019 | 6 | | | 001 | 220225482 | 0060 |
| *22*019 | 6 | | | 008 | 238043745 | 0060 |
| *22*019 | 6 | | | 002 | 293230693 | 0060 |
| *20*002 | 29 | 2 | 19241119 | 031 | 000000000 | 0070 |
| *22*002 | 29 | | | 008 | 175484119 | 0060 |
| *20*002 | 30 | 2 | 19241119 | 031 | 000000000 | 0070 |
| *22*002 | 30 | | | 008 | 175484050 | 0060 |
| *20*041 | 2 | 003 | 19401106 | 022 | 000000000 | 0070 |
| *22*041 | 2 | | | 004 | 313415770 | 0070 |
| *22*041 | 2 | | | 042 | 315530881 | 0070 |
| *20*041 | 3 | 002 | 19401105 | 022 | 000000000 | 0070 |
| *22*041 | 3 | | | 042 | 315530338 | 0070 |
| *20*041 | 4 | 002 | 19401105 | 022 | 000000000 | 0070 |
| *22*041 | 4 | | | 042 | 315530608 | 0070 |
| *20*022 | 1 | 003 | 19401023 | 041 | 249063586 | 0070 |
| *22*022 | 1 | | | 042 | 261454646 | 0070 |
| *22*022 | 1 | | | 004 | 341425364 | 0070 |
| *20*042 | 2 | 002 | 19401105 | 041 | 000000000 | 0070 |
| *22*042 | 2 | | | 022 | 236460391 | 0070 |
| *20*042 | 3 | 004 | 19401027 | 004 | 000000000 | 0070 |
| *22*042 | 3 | | | 023 | 039323641 | 0070 |
| *22*042 | 3 | | | 022 | 059243073 | 0070 |
| *22*042 | 3 | | | 041 | 182382845 | 0070 |
| *20*004 | 1 | 004 | 19401030 | 023 | 210020172 | 0070 |
| *22*004 | 1 | | | 022 | 217142359 | 0070 |
| *22*004 | 1 | | | 042 | 257525274 | 0070 |
| *22*004 | 1 | | | 041 | 258201015 | 0070 |
| *20*023 | 1 | 002 | 19400319 | 042 | 061535450 | 0070 |
| *22*023 | 1 | | | 004 | 154303466 | 0070 |
| *20*023 | 2 | 004 | 19401022 | 022 | 000000000 | 0070 |
| *22*023 | 2 | | | 041 | 054035738 | 0070 |
| *22*023 | 2 | | | 042 | 061535632 | 0070 |
| *22*023 | 2 | | | 004 | 154303508 | 0070 |
| *20*001 | 2 | 2 | 19511202 | 008 | 000000000 | 0060 |
| *22*001 | 2 | | | 026 | 043574213 | 0060 |
| *20*041 | 5 | 2 | 19511018 | 042 | 000000000 | 0060 |
| *22*041 | 5 | | | 022 | 044065606 | 0060 |
| *20*041 | 6 | 4 | 19511022 | 004 | 000000000 | 0060 |
| *22*041 | 6 | | | 042 | 002111030 | 0060 |
| *22*041 | 6 | | | 022 | 046180399 | 0060 |
| *22*041 | 6 | | | 024 | 331314679 | 0060 |
| *20*041 | 7 | 3 | 19511022 | 004 | 000000000 | 0060 |
| *22*041 | 7 | | | 042 | 002111004 | 0060 |
| *22*041 | 7 | | | 024 | 331314743 | 0060 |
| *20*041 | 8 | 2 | 19511208 | 022 | 000000000 | 0060 |
| *22*041 | 8 | | | 030 | 038154570 | 0060 |
| *20*041 | 9 | 2 | 19511210 | 022 | 000000000 | 0060 |
| *22*041 | 9 | | | 009 | 086140953 | 0060 |
| *20*041 | 10 | 2 | 19511210 | 022 | 000000000 | 0060 |
| *22*041 | 10 | | | 009 | 086140610 | 0060 |
| *20*041 | 11 | 3 | 19511210 | 022 | 000000000 | 0060 |
| *22*041 | 11 | | | 030 | 038154853 | 0060 |
| *22*041 | 11 | | | 009 | 086140562 | 0060 |
| *20*041 | 12 | 3 | 19511202 | 042 | 000000000 | 0060 |
| *22*041 | 12 | | | 022 | 044065341 | 0060 |
| *22*041 | 12 | | | 030 | 082224091 | 0060 |
| *20*041 | 13 | 2 | 19511207 | 042 | 000000000 | 0060 |
| *22*041 | 13 | | | 030 | 082224423 | 0060 |
| *20*029 | 4 | 2 | 19521117 | 034 | 000000000 | 0060 |
| *22*029 | 4 | | | 047 | 073182184 | 0060 |
| *20*029 | 5 | 2 | 19560604 | 034 | 043062255 | 0060 |

| | | | | | | |
|---|---|---|---|---|---|---|
| *22*029 | 5 | | | 038 | 216205318 | 0060 |
| *20*029 | 6 | 3 | 19560605 | 033 | 000000000 | 0060 |
| *22*029 | 6 | | | 047 | 116244263 | 0060 |
| *22*029 | 6 | | | 038 | 216205010 | 0060 |
| *20*029 | 7 | 4 | 19560605 | 033 | 000000000 | 0060 |
| *22*029 | 7 | | | 034 | 043062020 | 0060 |
| *22*029 | 7 | | | 047 | 116244197 | 0060 |
| *22*029 | 7 | | | 038 | 216205005 | 0060 |
| *20*029 | 8 | 3 | 19560607 | 033 | 000000000 | 0060 |
| *22*029 | 8 | | | 034 | 043062087 | 0060 |
| *22*029 | 8 | | | 047 | 116244248 | 0060 |
| *20*029 | 9 | 2 | 19560607 | 033 | 000000000 | 0060 |
| *22*029 | 9 | | | 034 | 043062076 | 0060 |
| *20*029 | 10 | 3 | 19560606 | 033 | 000000000 | 0060 |
| *22*029 | 10 | | | 034 | 043061929 | 0060 |
| *22*029 | 10 | | | 047 | 116244103 | 0060 |
| *20*028 | 1 | 3 | 19510814 | 016 | 059343922 | 0100 |
| *22*028 | 1 | | | 033 | 143383504 | 0060 |
| *22*028 | 1 | | | 034 | 186464086 | 0060 |
| *20*028 | 2 | 2 | 19510816 | 033 | 000000000 | 0060 |
| *22*028 | 2 | | | 016 | 275560346 | 0060 |
| *20*028 | 3 | 2 | 19510816 | 033 | 000000000 | 0080 |
| *22*028 | 3 | | | 016 | 275560238 | 0080 |
| *20*028 | 4 | 3 | 19510820 | 016 | 000000000 | 0060 |
| *22*028 | 4 | | | 033 | 084035663 | 0060 |
| *22*028 | 4 | | | 038 | 300252158 | 0060 |
| *20*028 | 5 | 3 | 19511023 | 038 | 000000000 | 0060 |
| *22*028 | 5 | | | 021 | 005392063 | 0060 |
| *22*028 | 5 | | | 016 | 059344092 | 0060 |
| *20*028 | 6 | 2 | 19511023 | 038 | 000000000 | 0120 |
| *22*028 | 6 | | | 029 | 343053460 | 0140 |
| *20*028 | 7 | 3 | 19511025 | 038 | 000000000 | 0060 |
| *22*028 | 7 | | | 021 | 005392033 | 0060 |
| *22*028 | 7 | | | 004 | 067115054 | 0060 |
| *20*028 | 8 | 3 | 19511025 | 038 | 000000000 | 0060 |
| *22*028 | 8 | | | 021 | 005392052 | 0060 |
| *22*028 | 8 | | | 004 | 067114988 | 0060 |
| *20*028 | 10 | 3 | 19591109 | 004 | 000000000 | 0060 |
| *22*028 | 10 | | | 033 | 076264301 | 0060 |
| *22*028 | 10 | | | 029 | 275535910 | 0140 |
| *20*028 | 11 | 2 | 19591109 | 033 | 013274202 | 0060 |
| *22*028 | 11 | | | 004 | 297005791 | 0060 |
| *20*022 | 4 | 2 | 19511010 | 038 | 000000000 | 0060 |
| *22*022 | 4 | | | 030 | 068324985 | 0060 |
| *20*022 | 5 | 3 | 19511010 | 038 | 000000000 | 0060 |
| *22*022 | 5 | | | 030 | 068325318 | 0060 |
| *22*022 | 5 | | | 041 | 177594094 | 0060 |
| *20*022 | 6 | 3 | 19511013 | 023 | 000000000 | 0060 |
| *22*022 | 6 | | | 038 | 071065612 | 0060 |
| *22*022 | 6 | | | 041 | 249063563 | 0060 |
| *20*022 | 7 | 2 | 19511013 | 023 | 000000000 | 0060 |
| *22*022 | 7 | | | 038 | 071065592 | 0060 |
| *20*022 | 8 | 3 | 19511014 | 041 | 000000000 | 0060 |
| *22*022 | 8 | | | 023 | 110532176 | 0060 |
| *22*022 | 8 | | | 038 | 182001705 | 0060 |
| *20*022 | 9 | 2 | 19511018 | 023 | 000000000 | 0060 |
| *22*022 | 9 | | | 004 | 341425324 | 0060 |
| *20*022 | 10 | 3 | 19511019 | 004 | 000000000 | 0060 |
| *22*022 | 10 | | | 023 | 018170619 | 0060 |
| *22*022 | 10 | | | 038 | 089240148 | 0060 |
| *20*022 | 11 | 3 | 19511022 | 042 | 000000000 | 0060 |

| | | | | | |
|---|---|---|---|---|---|
| *22*022 11 | | | 004 | 079570724 | 0060 |
| *22*022 11 | | | 023 | 098141340 | 0060 |
| *20*022 12 | 3 | 19511026 | 023 | 000000000 | 0060 |
| *22*022 12 | | | 030 | 139394620 | 0060 |
| *22*022 12 | | | 009 | 181422904 | 0060 |
| *20*022 13 | 3 | 19511027 | 023 | 000000000 | 0120 |
| *22*022 13 | | | 024 | 323484627 | 0140 |
| *22*022 13 | | | 004 | 341425340 | 0120 |
| *20*022 15 | 3 | 19511028 | 024 | 000000000 | 0060 |
| *22*022 15 | | | 004 | 017540720 | 0060 |
| *22*022 15 | | | 023 | 036111190 | 0060 |
| *20*022 16 | 3 | 19511028 | 024 | 000000000 | 0060 |
| *22*022 16 | | | 004 | 017540708 | 0060 |
| *22*022 16 | | | 023 | 036111304 | 0060 |
| *20*031 3 | 3 | 19510808 | 034 | 000000000 | 0060 |
| *22*031 3 | | | 033 | 046555101 | 0060 |
| *22*031 3 | | | 011 | 131552165 | 0060 |
| *20*031 5 | 2 | 19510813 | 034 | 000000000 | 0060 |
| *22*031 5 | | | 033 | 046555113 | 0060 |
| *20*031 6 | 2 | 19510813 | 034 | 000000000 | 0060 |
| *22*031 6 | | | 033 | 046555375 | 0060 |
| *20*031 7 | 2 | 19511025 | 034 | 000000000 | 0060 |
| *22*031 7 | | | 033 | 046555135 | 0060 |
| *20*031 8 | 2 | 19511107 | 011 | 020174609 | 0060 |
| *22*031 8 | | | 010 | 038434264 | 0060 |
| *20*031 9 | 2 | 19511107 | 011 | 020174605 | 0060 |
| *22*031 9 | | | 010 | 038434018 | 0060 |
| *20*031 10 | 2 | 19511113 | 010 | 038434126 | 0060 |
| *22*031 10 | | | 002 | 092324757 | 0060 |
| *20*031 11 | 2 | 19511113 | 010 | 038434136 | 0060 |
| *22*031 11 | | | 002 | 092324566 | 0060 |
| *20*031 12 | 2 | 19510100 | 034 | 000000000 | 0060 |
| *22*031 12 | | | 025 | 134222517 | 0070 |
| *20*031 13 | 2 | 19560612 | 034 | 000000000 | 0060 |
| *22*031 13 | | | 003 | 204035081 | 0070 |
| *20*031 14 | 3 | 19560613 | 034 | 000000000 | 0060 |
| *22*031 14 | | | 033 | 046555100 | 0060 |
| *22*031 14 | | | 025 | 134222384 | 0060 |
| *20*031 15 | 3 | 19560613 | 034 | 000000000 | 0060 |
| *22*031 15 | | | 018 | 161092268 | 0080 |
| *22*031 15 | | | 003 | 204035174 | 0060 |
| *20*031 16 | 2 | 19560613 | 034 | 000000000 | 0060 |
| *22*031 16 | | | 003 | 204034925 | 0060 |
| *20*031 17 | 2 | 19560614 | 033 | 000000000 | 0060 |
| *22*031 17 | | | 018 | 114132910 | 0060 |
| *20*031 18 | 2 | 19560614 | 033 | 000000000 | 0090 |
| *22*031 18 | | | 018 | 114132920 | 0090 |
| *20*031 19 | 3 | 19560620 | 033 | 000000000 | 0060 |
| *22*031 19 | | | 025 | 087263202 | 0060 |
| *22*031 19 | | | 003 | 157075966 | 0060 |
| *20*031 20 | 2 | 19591030 | 033 | 000000000 | 0060 |
| *22*031 20 | | | 003 | 157075900 | 0060 |
| *20*031 21 | 2 | 19591030 | 033 | 000000000 | 0060 |
| *22*031 21 | | | 003 | 157075752 | 0060 |
| *20*031 22 | 3 | 19591109 | 033 | 000000000 | 0060 |
| *22*031 22 | | | 011 | 084593176 | 0060 |
| *22*031 22 | | | 010 | 103252498 | 0060 |
| *20*031 23 | 3 | 19591109 | 033 | 000000000 | 0060 |
| *22*031 23 | | | 011 | 084593127 | 0060 |
| *22*031 23 | | | 010 | 103252346 | 0060 |
| *20*031 24 | 2 | 19591109 | 011 | 020174457 | 0060 |

| | | | | | | |
|---|---|---|---|---|---|---|
| *22*031 | 24 | | | 010 | 038433755 | 0070 |
| *20*031 | 25 | 2 | 19591110 | 010 | 103252091 | 0060 |
| *22*031 | 25 | | | 003 | 157075636 | 0060 |
| *20*031 | 26 | 2 | 19591110 | 010 | 038434046 | 0060 |
| *22*031 | 26 | | | 033 | 295181666 | 0060 |
| *20*010 | 3 | 5 | 19511106 | 002 | 000000000 | 0060 |
| *22*010 | 3 | | | 031 | 045263114 | 0060 |
| *22*010 | 3 | | | 011 | 084441619 | 0060 |
| *22*010 | 3 | | | 004 | 123014756 | 0060 |
| *22*010 | 3 | | | 024 | 154465162 | 0070 |
| *20*010 | 4 | 4 | 19511106 | 002 | 000000000 | 0060 |
| *22*010 | 4 | | | 031 | 045263073 | 0060 |
| *22*010 | 4 | | | 011 | 084441742 | 0060 |
| *22*010 | 4 | | | 004 | 123014732 | 0060 |
| *20*010 | 5 | 4 | 19511111 | 011 | 000000000 | 0060 |
| *22*010 | 5 | | | 004 | 038172994 | 0070 |
| *22*010 | 5 | | | 024 | 070023303 | 0070 |
| *22*010 | 5 | | | 026 | 160230406 | 0060 |
| *20*010 | 6 | 2 | 19511117 | 026 | 004442481 | 0060 |
| *22*010 | 6 | | | 008 | 075011088 | 0060 |
| *20*010 | 7 | 2 | 19511117 | 026 | 004442442 | 0060 |
| *22*010 | 7 | | | 008 | 075010978 | 0060 |
| *20*010 | 8 | 3 | 19591104 | 026 | 000000000 | 0060 |
| *22*010 | 8 | | | 003 | 114484013 | 0060 |
| *22*010 | 8 | | | 011 | 199365296 | 0060 |
| *20*010 | 9 | 2 | 19591104 | 026 | 000000000 | 0060 |
| *22*010 | 9 | | | 011 | 199365078 | 0060 |
| *20*010 | 10 | 6 | 19591105 | 026 | 000000000 | 0060 |
| *22*010 | 10 | | | 003 | 114484104 | 0060 |
| *22*010 | 10 | | | 031 | 160190490 | 0060 |
| *22*010 | 10 | | | 011 | 199365272 | 0060 |
| *22*010 | 10 | | | 004 | 237542553 | 0060 |
| *22*010 | 10 | | | 024 | 269392896 | 0060 |
| *20*010 | 11 | 3 | 19591106 | 031 | 000000000 | 0060 |
| *22*010 | 11 | | | 011 | 039174590 | 0060 |
| *22*010 | 11 | | | 024 | 109202163 | 0060 |
| *20*010 | 12 | 3 | 19591106 | 031 | 000000000 | 0060 |
| *22*010 | 12 | | | 011 | 039174497 | 0060 |
| *22*010 | 12 | | | 024 | 109202304 | 0060 |
| *20*010 | 13 | 3 | 19591105 | 026 | 000000000 | 0060 |
| *22*010 | 13 | | | 011 | 199365542 | 0060 |
| *22*010 | 13 | | | 024 | 269392983 | 0090 |
| *20*008 | 2 | 2 | 19511115 | 002 | 000000000 | 0060 |
| *22*008 | 2 | | | 026 | 068285277 | 0060 |
| *20*008 | 3 | 2 | 19511115 | 002 | 000000000 | 0060 |
| *22*008 | 3 | | | 026 | 068285152 | 0060 |
| *20*008 | 4 | 2 | 19511116 | 002 | 000000000 | 0060 |
| *22*008 | 4 | | | 001 | 181420132 | 0060 |
| *20*008 | 5 | 3 | 19511126 | 002 | 000000000 | 0060 |
| *22*008 | 5 | | | 010 | 040200141 | 0060 |
| *22*008 | 5 | | | 001 | 181415595 | 0060 |
| *20*008 | 7 | 3 | 19560612 | 003 | 000000000 | 0060 |
| *22*008 | 7 | | | 018 | 047482560 | 0060 |
| *22*008 | 7 | | | 001 | 181365100 | 0060 |
| *20*008 | 8 | 2 | 19560612 | 003 | 000000000 | 0060 |
| *22*008 | 8 | | | 018 | 047482727 | 0060 |
| *20*008 | 9 | 2 | 19560619 | 025 | 128454319 | 0060 |
| *22*008 | 9 | | | 018 | 149592454 | 0070 |
| *20*008 | 10 | 2 | 19560619 | 025 | 128454263 | 0060 |
| *22*008 | 10 | | | 018 | 149592463 | 0060 |
| *20*008 | 13 | 2 | 19560620 | 003 | 000000000 | 0060 |

| | | | | | | |
|---|---|---|---|---|---|---|
| *22*008 | 13 | | | 018 | 047482258 | 0060 |
| *20*042 | 5 | 2 | 19511006 | 004 | 000000000 | 0060 |
| *22*042 | 5 | | | 022 | 059243216 | 0060 |
| *20*042 | 6 | 2 | 19511006 | 004 | 000000000 | 0060 |
| *22*042 | 6 | | | 041 | 182382536 | 0060 |
| *20*042 | 7 | 4 | 19511007 | 022 | 000000000 | 0060 |
| *22*042 | 7 | | | 030 | 034082829 | 0060 |
| *22*042 | 7 | | | 041 | 123135303 | 0060 |
| *22*042 | 7 | | | 024 | 268005198 | 0060 |
| *20*042 | 8 | 3 | 19511008 | 024 | 000000000 | 0060 |
| *22*042 | 8 | | | 004 | 032343667 | 0060 |
| *22*042 | 8 | | | 022 | 091590692 | 0060 |
| *20*011 | 1 | 3 | 19511102 | 031 | 052254622 | 0060 |
| *22*011 | 1 | | | 033 | 094331448 | 0060 |
| *22*011 | 1 | | | 010 | 290092663 | 0060 |
| *20*011 | 3 | 5 | 19511103 | 002 | 000000000 | 0060 |
| *22*011 | 3 | | | 004 | 157131396 | 0060 |
| *22*011 | 3 | | | 024 | 192160536 | 0060 |
| *22*011 | 3 | | | 033 | 094331578 | 0060 |
| *22*011 | 3 | | | 010 | 290092730 | 0060 |
| *20*011 | 5 | 6 | 19591107 | 010 | 000000000 | 0060 |
| *22*011 | 5 | | | 003 | 069450675 | 0060 |
| *22*011 | 5 | | | 031 | 122161942 | 0060 |
| *22*011 | 5 | | | 033 | 164234695 | 0060 |
| *22*011 | 5 | | | 004 | 227034479 | 0060 |
| *22*011 | 5 | | | 024 | 262063503 | 0060 |
| *20*011 | 6 | 3 | 19591107 | 010 | 000000000 | 0060 |
| *22*011 | 6 | | | 003 | 069450702 | 0060 |
| *22*011 | 6 | | | 024 | 262063542 | 0060 |
| *20*024 | 1 | 2 | 19510829 | 013 | 028073687 | 0070 |
| *22*024 | 1 | | | 004 | 115152575 | 0060 |
| *20*024 | 2 | 2 | 19510829 | 013 | 028073758 | 0070 |
| *22*024 | 2 | | | 004 | 115152664 | 0060 |
| *20*024 | 3 | 3 | 19511102 | 013 | 000000000 | 0070 |
| *22*024 | 3 | | | 004 | 087075008 | 0060 |
| *22*024 | 3 | | | 041 | 139170099 | 0060 |
| *20*024 | 4 | 3 | 19511103 | 013 | 000000000 | 0070 |
| *22*024 | 4 | | | 011 | 023440782 | 0060 |
| *22*024 | 4 | | | 004 | 087074850 | 0060 |
| *20*024 | 5 | 3 | 19511106 | 013 | 000000000 | 0080 |
| *22*024 | 5 | | | 010 | 011400252 | 0070 |
| *22*024 | 5 | | | 004 | 087074782 | 0070 |
| *20*024 | 6 | 4 | 19511111 | 013 | 000000000 | 0070 |
| *22*024 | 6 | | | 010 | 011395897 | 0090 |
| *22*024 | 6 | | | 011 | 023440474 | 0070 |
| *22*024 | 6 | | | 004 | 087074862 | 0060 |
| *20*024 | 7 | 4 | 19511115 | 013 | 000000000 | 0070 |
| *22*024 | 7 | | | 011 | 023440571 | 0060 |
| *22*024 | 7 | | | 004 | 087074982 | 0060 |
| *22*024 | 7 | | | 026 | 352591299 | 0060 |
| *20*024 | 8 | 3 | 19511115 | 013 | 000000000 | 0070 |
| *22*024 | 8 | | | 004 | 087074909 | 0060 |
| *22*024 | 8 | | | 026 | 352591430 | 0060 |
| *20*024 | 9 | 4 | 19511117 | 013 | 000000000 | 0070 |
| *22*024 | 9 | | | 004 | 087074933 | 0060 |
| *22*024 | 9 | | | 022 | 108451587 | 0060 |
| *22*024 | 9 | | | 042 | 134432061 | 0060 |
| *20*024 | 10 | 3 | 19511117 | 013 | 000000000 | 0070 |
| *22*024 | 10 | | | 004 | 087074820 | 0060 |
| *22*024 | 10 | | | 042 | 134432016 | 0060 |
| *20*024 | 11 | 5 | 19591105 | 026 | 000000000 | 0060 |

| | | | | | | |
|---|---|---|---|---|---|---|
| *22*024 | 11 | | | 013 | 007004846 | 0070 |
| *22*024 | 11 | | | 010 | 018405003 | 0070 |
| *22*024 | 11 | | | 011 | 030445336 | 0060 |
| *22*024 | 11 | | | 004 | 094083610 | 0120 |
| *20*024 | 12 | 4 | 19591106 | 026 | 000000000 | 0060 |
| *22*024 | 12 | | | 010 | 018404684 | 0060 |
| *22*024 | 12 | | | 011 | 030445312 | 0060 |
| *22*024 | 12 | | | 004 | 094083514 | 0060 |
| *20*024 | 13 | 4 | 19591106 | 010 | 000000000 | 0060 |
| *22*024 | 13 | | | 033 | 039141201 | 0060 |
| *22*024 | 13 | | | 004 | 075274814 | 0060 |
| *22*024 | 13 | | | 026 | 341191039 | 0060 |
| *20*033 | 1 | 2 | 19510808 | 028 | 089512896 | 0090 |
| *22*033 | 1 | | | 031 | 305252775 | 0060 |
| *20*033 | 2 | 3 | 19510813 | 034 | 000000000 | 0060 |
| *22*033 | 2 | | | 028 | 089512807 | 0060 |
| *22*033 | 2 | | | 031 | 305252602 | 0060 |
| *20*033 | 4 | 2 | 19510813 | 034 | 000000000 | 0060 |
| *22*033 | 4 | | | 028 | 089512938 | 0080 |
| *20*033 | 5 | 3 | 19511022 | 031 | 022324866 | 0060 |
| *22*033 | 5 | | | 028 | 166585049 | 0060 |
| *22*033 | 5 | | | 004 | 249393085 | 0060 |
| *20*033 | 6 | 2 | 19511022 | 028 | 000000000 | 0060 |
| *22*033 | 6 | | | 004 | 082404086 | 0060 |
| *20*033 | 7 | 2 | 19511105 | 011 | 000000000 | 0060 |
| *22*033 | 7 | | | 031 | 052530428 | 0060 |
| *20*033 | 8 | 2 | 19560605 | 034 | 000000000 | 0060 |
| *22*033 | 8 | | | 029 | 089522493 | 0060 |
| *20*033 | 9 | 2 | 19560605 | 034 | 000000000 | 0060 |
| *22*033 | 9 | | | 029 | 089522303 | 0060 |
| *20*033 | 10 | 2 | 19560606 | 034 | 000000000 | 0060 |
| *22*033 | 10 | | | 029 | 089522505 | 0060 |
| *20*033 | 11 | 3 | 19560612 | 034 | 000000000 | 0060 |
| *22*033 | 11 | | | 038 | 114562294 | 0060 |
| *22*033 | 11 | | | 031 | 305252879 | 0060 |
| *20*033 | 12 | 3 | 19560612 | 034 | 000000000 | 0060 |
| *22*033 | 12 | | | 025 | 257060177 | 0060 |
| *22*033 | 12 | | | 031 | 305252681 | 0060 |
| *20*033 | 13 | 3 | 19560612 | 034 | 000000000 | 0060 |
| *22*033 | 13 | | | 025 | 257060173 | 0060 |
| *22*033 | 13 | | | 031 | 305252884 | 0060 |
| *20*033 | 14 | 3 | 19560613 | 025 | 257055974 | 0060 |
| *22*033 | 14 | | | 003 | 293114708 | 0070 |
| *22*033 | 14 | | | 031 | 305252595 | 0060 |
| *20*033 | 15 | 4 | 19560613 | 034 | 000000000 | 0060 |
| *22*033 | 15 | | | 025 | 257055905 | 0060 |
| *22*033 | 15 | | | 003 | 293114798 | 0080 |
| *22*033 | 15 | | | 031 | 305252769 | 0060 |
| *20*033 | 16 | 2 | 19560615 | 034 | 000000000 | 0060 |
| *22*033 | 16 | | | 025 | 257060038 | 0060 |
| *20*033 | 17 | 2 | 19560615 | 034 | 000000000 | 0070 |
| *22*033 | 17 | | | 025 | 257060145 | 0070 |
| *20*033 | 19 | 5 | 19591107 | 004 | 082403856 | 0060 |
| *22*033 | 19 | | | 024 | 107334091 | 0060 |
| *22*033 | 19 | | | 011 | 162405228 | 0060 |
| *22*033 | 19 | | | 003 | 203202020 | 0060 |
| *22*033 | 19 | | | 031 | 215335701 | 0060 |
| *20*033 | 20 | 3 | 19591107 | 011 | 005594532 | 0060 |
| *22*033 | 20 | | | 003 | 046391261 | 0060 |
| *22*033 | 20 | | | 031 | 058525007 | 0060 |
| *20*033 | 21 | 2 | 19591110 | 011 | 005594566 | 0060 |

| | | | | | |
|---|---|---|---|---|---|
| *22*033 21 | | | 031 | 058524807 | 0060 |
| *20*030 2 | 5 | 19511007 | 009 | 000000000 | 0060 |
| *22*030 2 | | | 042 | 084563366 | 0060 |
| *22*030 2 | | | 022 | 108421064 | 0060 |
| *22*030 2 | | | 023 | 117064622 | 0060 |
| *22*030 2 | | | 038 | 146150510 | 0060 |
| *20*030 4 | 3 | 19511009 | 042 | 000000000 | 0060 |
| *22*030 4 | | | 022 | 023453952 | 0060 |
| *22*030 4 | | | 038 | 061183307 | 0060 |
| *20*030 5 | 5 | 19511202 | 009 | 000000000 | 0060 |
| *22*030 5 | | | 041 | 076244130 | 0060 |
| *22*030 5 | | | 022 | 108421098 | 0060 |
| *22*030 5 | | | 023 | 117064562 | 0080 |
| *22*030 5 | | | 038 | 146150301 | 0060 |
| *20*030 6 | 2 | 19511206 | 009 | 000000000 | 0060 |
| *22*030 6 | | | 041 | 076244120 | 0060 |
| *20*016 2 | 3 | 19510829 | 004 | 000000000 | 0060 |
| *22*016 2 | | | 028 | 171132523 | 0080 |
| *22*016 2 | | | 038 | 282323298 | 0110 |
| *20*016 3 | 2 | 19510830 | 004 | 000000000 | 0060 |
| *22*016 3 | | | 028 | 171132692 | 0100 |
| *20*016 4 | 3 | 19511018 | 028 | 000000000 | 0070 |
| *22*016 4 | | | 038 | 111190848 | 0070 |
| *22*016 4 | | | 004 | 188463357 | 0070 |
| *20*016 5 | 2 | 19511018 | 028 | 000000000 | 0080 |
| *22*016 5 | | | 038 | 111190824 | 0080 |
| *20*016 6 | 2 | 19511022 | 004 | 000000000 | 0070 |
| *22*016 6 | | | 028 | 171132350 | 0070 |
| *20*016 7 | 2 | 19511024 | 021 | 000000000 | 0060 |
| *22*016 7 | | | 004 | 072125060 | 0060 |
| *20*016 8 | 2 | 19511024 | 021 | 000000000 | 0060 |
| *22*016 8 | | | 004 | 072125155 | 0060 |
| *20*016 9 | 2 | 19511127 | 028 | 000000000 | 0070 |
| *22*016 9 | | | 038 | 111190746 | 0070 |
| *20*047 2 | 2 | 19521116 | 029 | 000000000 | 0060 |
| *22*047 2 | | | 034 | 057155928 | 0060 |
| *20*047 3 | 2 | 19560605 | 029 | 109021895 | 0060 |
| *22*047 3 | | | 034 | 166181859 | 0060 |
| *20*047 7 | 2 | 19560607 | 029 | 109021883 | 0060 |
| *22*047 7 | | | 034 | 166181737 | 0060 |
| *20*047 9 | 2 | 19560628 | 038 | 056024891 | 0060 |
| *22*047 9 | | | 029 | 109021837 | 0060 |
| *20*047 10 | 3 | 19560628 | 038 | 000000000 | 0060 |
| *22*047 10 | | | 029 | 052592795 | 0060 |
| *22*047 10 | | | 034 | 110152870 | 0060 |
| *20*038 2 | 2 | 19511013 | 023 | 025391983 | 0060 |
| *22*038 2 | | | 028 | 123385928 | 0060 |
| *20*038 3 | 3 | 19511018 | 022 | 000000000 | 0060 |
| *22*038 3 | | | 023 | 025392045 | 0060 |
| *22*038 3 | | | 016 | 114324794 | 0060 |
| *20*038 4 | 4 | 19511019 | 022 | 000000000 | 0060 |
| *22*038 4 | | | 023 | 025392241 | 0060 |
| *22*038 4 | | | 016 | 114324700 | 0240 |
| *22*038 4 | | | 028 | 123385866 | 0060 |
| *20*038 5 | 2 | 19511019 | 022 | 000000000 | 0170 |
| *22*038 5 | | | 023 | 025392160 | 0170 |
| *20*038 6 | 3 | 19511022 | 022 | 000000000 | 0070 |
| *22*038 6 | | | 004 | 056391503 | 0090 |
| *22*038 6 | | | 016 | 114324703 | 0070 |
| *20*038 7 | 2 | 19511023 | 022 | 000000000 | 0060 |
| *22*038 7 | | | 028 | 123390226 | 0060 |

| | | | | | | |
|---|---|---|---|---|---|---|
| *20*038 | 8 | 2 | 19511025 | 030 | 000000000 | 0060 |
| *22*038 | 8 | | | 028 | 197332437 | 0060 |
| *20*038 | 9 | 2 | 19511025 | 030 | 000000000 | 0060 |
| *22*038 | 9 | | | 028 | 197332423 | 0060 |
| *20*038 | 10 | 2 | 19511103 | 023 | 000000000 | 0120 |
| *22*038 | 10 | | | 004 | 030595110 | 0120 |
| *20*038 | 11 | 2 | 19560531 | 030 | 089142878 | 0060 |
| *22*038 | 11 | | | 029 | 286481542 | 0060 |
| *20*038 | 12 | 4 | 19560531 | 030 | 089142864 | 0060 |
| *22*038 | 12 | | | 029 | 286481554 | 0140 |
| *22*038 | 12 | | | 047 | 313524380 | 0060 |
| *22*038 | 12 | | | 047 | 313524391 | 0060 |
| *20*038 | 14 | 2 | 19560605 | 047 | 000000000 | 0060 |
| *22*038 | 14 | | | 029 | 332553345 | 0060 |
| *20*004 | 4 | 3 | 19511018 | 016 | 000000000 | 0060 |
| *22*004 | 4 | | | 038 | 044390676 | 0060 |
| *22*004 | 4 | | | 023 | 071233316 | 0060 |
| *20*004 | 6 | 3 | 19511019 | 023 | 000000000 | 0060 |
| *22*004 | 6 | | | 022 | 007122191 | 0060 |
| *22*004 | 6 | | | 024 | 147405019 | 0060 |
| *20*004 | 7 | 5 | 19511022 | 033 | 000000000 | 0060 |
| *22*004 | 7 | | | 023 | 093253405 | 0060 |
| *22*004 | 7 | | | 022 | 100375925 | 0060 |
| *22*004 | 7 | | | 041 | 141434189 | 0080 |
| *22*004 | 7 | | | 024 | 241062829 | 0060 |
| *20*004 | 8 | 3 | 19511025 | 028 | 000000000 | 0060 |
| *22*004 | 8 | | | 016 | 001092489 | 0060 |
| *22*004 | 8 | | | 038 | 045482871 | 0060 |
| *20*004 | 9 | 3 | 19511025 | 028 | 000000000 | 0060 |
| *22*004 | 9 | | | 016 | 001092181 | 0060 |
| *22*004 | 9 | | | 038 | 045483045 | 0060 |
| *20*004 | 11 | 3 | 19511027 | 016 | 000000000 | 0060 |
| *22*004 | 11 | | | 041 | 119414077 | 0060 |
| *22*004 | 11 | | | 024 | 219042685 | 0060 |
| *20*004 | 12 | 3 | 19511027 | 022 | 000000000 | 0060 |
| *22*004 | 12 | | | 041 | 041054523 | 0060 |
| *22*004 | 12 | | | 024 | 140282880 | 0060 |
| *20*004 | 13 | 3 | 19511028 | 022 | 000000000 | 0060 |
| *22*004 | 13 | | | 042 | 040382708 | 0060 |
| *22*004 | 13 | | | 041 | 041054545 | 0060 |
| *20*004 | 14 | 3 | 19511028 | 022 | 000000000 | 0060 |
| *22*004 | 14 | | | 042 | 040382752 | 0060 |
| *22*004 | 14 | | | 041 | 041054678 | 0060 |
| *20*004 | 16 | 4 | 19511103 | 024 | 000000000 | 0070 |
| *22*004 | 16 | | | 010 | 072471941 | 0070 |
| *22*004 | 16 | | | 011 | 081333478 | 0070 |
| *22*004 | 16 | | | 033 | 118532939 | 0070 |
| *20*004 | 18 | 4 | 19591108 | 024 | 000000000 | 0060 |
| *22*004 | 18 | | | 010 | 072471916 | 0060 |
| *22*004 | 18 | | | 011 | 081333548 | 0060 |
| *22*004 | 18 | | | 033 | 118533016 | 0060 |
| *20*002 | 4 | 2 | 19511113 | 031 | 000000000 | 0070 |
| *22*002 | 4 | | | 010 | 080443103 | 0140 |
| *20*002 | 5 | 3 | 19511114 | 031 | 000000000 | 0060 |
| *22*002 | 5 | | | 011 | 055191688 | 0060 |
| *22*002 | 5 | | | 010 | 080442766 | 0060 |
| *20*002 | 6 | 3 | 19511114 | 031 | 000000000 | 0060 |
| *22*002 | 6 | | | 011 | 055191836 | 0060 |
| *22*002 | 6 | | | 010 | 080442964 | 0060 |
| *20*002 | 7 | 3 | 19511115 | 010 | 000000000 | 0060 |
| *22*002 | 7 | | | 026 | 026575291 | 0060 |

| | | | | | | |
|---|---|---|---|---|---|---|
| *22*002 | 7 | | | 008 | 095041238 | 0060 |
| *20*002 | 8 | 3 | 19511115 | 010 | 000000000 | 0060 |
| *22*002 | 8 | | | 026 | 026575410 | 0060 |
| *22*002 | 8 | | | 008 | 095041229 | 0060 |
| *20*003 | 1 | 2 | 19560612 | 025 | 052193798 | 0060 |
| *22*003 | 1 | | | 018 | 099050057 | 0060 |
| *20*003 | 2 | 3 | 19560612 | 031 | 000000000 | 0060 |
| *22*003 | 2 | | | 025 | 052193479 | 0240 |
| *22*003 | 2 | | | 018 | 099050003 | 0060 |
| *20*003 | 3 | 3 | 19560613 | 031 | 000000000 | 0060 |
| *22*003 | 3 | | | 025 | 052193754 | 0060 |
| *22*003 | 3 | | | 018 | 099050074 | 0060 |
| *20*003 | 4 | 3 | 19560613 | 031 | 000000000 | 0060 |
| *22*003 | 4 | | | 033 | 010382360 | 0060 |
| *22*003 | 4 | | | 025 | 052193633 | 0060 |
| *20*003 | 6 | 3 | 19560614 | 031 | 000000000 | 0060 |
| *22*003 | 6 | | | 025 | 052193656 | 0060 |
| *22*003 | 6 | | | 018 | 099045918 | 0060 |
| *20*003 | 7 | 4 | 19560620 | 031 | 000000000 | 0060 |
| *22*003 | 7 | | | 025 | 052193618 | 0060 |
| *22*003 | 7 | | | 018 | 099050171 | 0060 |
| *22*003 | 7 | | | 008 | 176001586 | 0060 |
| *20*003 | 8 | 3 | 19560620 | 031 | 000000000 | 0060 |
| *22*003 | 8 | | | 018 | 099050204 | 0060 |
| *22*003 | 8 | | | 008 | 176001512 | 0060 |
| *20*003 | 9 | 2 | 19560702 | 018 | 000000000 | 0060 |
| *22*003 | 9 | | | 008 | 076551514 | 0060 |
| *20*003 | 10 | 3 | 19591022 | 031 | 000000000 | 0060 |
| *22*003 | 10 | | | 010 | 080470379 | 0060 |
| *22*003 | 10 | | | 026 | 107480581 | 0060 |
| *20*003 | 11 | 3 | 19591022 | 031 | 000000000 | 0060 |
| *22*003 | 11 | | | 010 | 080470324 | 0060 |
| *22*003 | 11 | | | 026 | 107480423 | 0060 |
| *20*003 | 12 | 3 | 19591023 | 031 | 000000000 | 0060 |
| *22*003 | 12 | | | 011 | 055202165 | 0060 |
| *22*003 | 12 | | | 010 | 080470330 | 0060 |
| *20*003 | 13 | 3 | 19591023 | 031 | 000000000 | 0120 |
| *22*003 | 13 | | | 011 | 055201970 | 0120 |
| *22*003 | 13 | | | 010 | 080470025 | 0120 |
| *20*003 | 14 | 2 | 19591030 | 031 | 000000000 | 0060 |
| *22*003 | 14 | | | 033 | 010382395 | 0060 |
| *20*003 | 15 | 4 | 19591123 | 031 | 000000000 | 0060 |
| *22*003 | 15 | | | 033 | 010382377 | 0060 |
| *22*003 | 15 | | | 011 | 055202035 | 0060 |
| *22*003 | 15 | | | 010 | 080470153 | 0060 |
| *20*003 | 16 | 4 | 19591123 | 011 | 000000000 | 0060 |
| *22*003 | 16 | | | 010 | 025264153 | 0060 |
| *22*003 | 16 | | | 031 | 304393586 | 0060 |
| *22*003 | 16 | | | 033 | 315180158 | 0060 |
| *20*034 | 4 | 2 | 19510808 | 033 | 000000000 | 0060 |
| *22*034 | 4 | | | 031 | 078293958 | 0060 |
| *20*034 | 5 | 3 | 19510813 | 028 | 000000000 | 0060 |
| *22*034 | 5 | | | 033 | 047002696 | 0060 |
| *22*034 | 5 | | | 031 | 125300590 | 0060 |
| *20*034 | 6 | 2 | 19510917 | 033 | 001094434 | 0070 |
| *22*034 | 6 | | | 031 | 079392026 | 0060 |
| *20*034 | 7 | 2 | 19511112 | 033 | 000000000 | 0060 |
| *22*034 | 7 | | | 031 | 078293691 | 0060 |
| *20*034 | 9 | 2 | 19521117 | 047 | 028233054 | 0060 |
| *22*034 | 9 | | | 029 | 077491266 | 0060 |
| *20*034 | 11 | 2 | 19560510 | 031 | 000000000 | 0060 |

| | | | | | |
|---|---|---|---|---|---|
| *22*034 11 | | | 033 | 281302179 | 0060 |
| *20*034 12 | 2 | 19560510 | 031 | 000000000 | 0060 |
| *22*034 12 | | | 033 | 281302169 | 0060 |
| *20*034 13 | 3 | 19560510 | 031 | 000000000 | 0060 |
| *22*034 13 | | | 029 | 234290456 | 0060 |
| *22*034 13 | | | 033 | 281302040 | 0100 |
| *20*034 14 | 2 | 19560510 | 031 | 000000000 | 0060 |
| *22*034 14 | | | 029 | 234290584 | 0060 |
| *20*034 17 | 2 | 19560604 | 029 | 000000000 | 0060 |
| *22*034 17 | | | 033 | 047011914 | 0060 |
| *20*034 18 | 2 | 19560604 | 029 | 000000000 | 0060 |
| *22*034 18 | | | 033 | 047011782 | 0060 |
| *20*034 19 | 3 | 19560604 | 029 | 000000000 | 0060 |
| *22*034 19 | | | 033 | 047011548 | 0060 |
| *22*034 19 | | | 047 | 310341789 | 0060 |
| *20*034 20 | 5 | 19560605 | 047 | 000000000 | 0060 |
| *22*034 20 | | | 029 | 049254337 | 0060 |
| *22*034 20 | | | 033 | 096265829 | 0060 |
| *22*034 20 | | | 029 | 049254527 | 0060 |
| *22*034 20 | | | 033 | 096270093 | 0060 |
| *20*034 21 | 3 | 19560607 | 047 | 000000000 | 0060 |
| *22*034 21 | | | 029 | 049253993 | 0060 |
| *22*034 21 | | | 033 | 096265633 | 0060 |
| *20*034 22 | 2 | 19560612 | 033 | 000000000 | 0060 |
| *22*034 22 | | | 031 | 078293740 | 0060 |
| *20*034 23 | 3 | 19560613 | 033 | 000000000 | 0060 |
| *22*034 23 | | | 025 | 052391475 | 0070 |
| *22*034 23 | | | 031 | 078293710 | 0060 |
| *20*034 24 | 3 | 19560614 | 033 | 000000000 | 0060 |
| *22*034 24 | | | 025 | 052391252 | 0070 |
| *22*034 24 | | | 031 | 078293815 | 0060 |
| *20*034 25 | 3 | 19560614 | 033 | 000000000 | 0060 |
| *22*034 25 | | | 025 | 052391401 | 0060 |
| *22*034 25 | | | 031 | 078293744 | 0060 |
| *20*034 27 | 2 | 19590428 | 031 | 079392304 | 0070 |
| *22*034 27 | | | 047 | 264424522 | 0070 |
| *20*025 2 | 5 | 19560614 | 018 | 000000000 | 0060 |
| *22*025 2 | | | 003 | 066353703 | 0060 |
| *22*025 2 | | | 031 | 124344074 | 0060 |
| *22*025 2 | | | 034 | 144215312 | 0070 |
| *22*025 2 | | | 033 | 168484860 | 0240 |
| *20*025 3 | 2 | 19560612 | 018 | 000000000 | 0070 |
| *22*025 3 | | | 033 | 168484415 | 0070 |
| *20*025 4 | 3 | 19560615 | 018 | 000000000 | 0060 |
| *22*025 4 | | | 031 | 124343770 | 0060 |
| *22*025 4 | | | 033 | 168484310 | 0060 |
| *20*025 5 | 2 | 19560619 | 018 | 000000000 | 0060 |
| *22*025 5 | | | 008 | 036505455 | 0060 |
| *20*025 6 | 2 | 19560619 | 018 | 000000000 | 0060 |
| *22*025 6 | | | 008 | 036505585 | 0060 |
| *20*025 8 | 5 | 19560620 | 018 | 000000000 | 0060 |
| *22*025 8 | | | 003 | 066353538 | 0060 |
| *22*025 8 | | | 031 | 124343680 | 0060 |
| *22*025 8 | | | 034 | 144214888 | 0070 |
| *22*025 8 | | | 033 | 168484079 | 0060 |
| *20*018 1 | 2 | 19560612 | 003 | 154210918 | 0060 |
| *22*018 1 | | | 025 | 221000916 | 0060 |
| *20*018 2 | 2 | 19560613 | 003 | 000000000 | 0090 |
| *22*018 2 | | | 031 | 038003171 | 0090 |
| *20*018 3 | 3 | 19560614 | 003 | 000000000 | 0060 |
| *22*018 3 | | | 031 | 038003414 | 0060 |

| | | | | | | |
|---|---|---|---|---|---|---|
| *22*018 | 3 | | | 025 | 066390146 | 0060 |
| *20*018 | 4 | 3 | 19560614 | 003 | 000000000 | 0060 |
| *22*018 | 4 | | | 031 | 038003477 | 0060 |
| *22*018 | 4 | | | 025 | 066390118 | 0060 |
| *20*018 | 5 | 3 | 19560620 | 008 | 000000000 | 0060 |
| *22*018 | 5 | | | 003 | 055162415 | 0060 |
| *22*018 | 5 | | | 025 | 121552632 | 0060 |
| *20*026 | 2 | 2 | 19511115 | 010 | 000000000 | 0060 |
| *22*026 | 2 | | | 024 | 070584847 | 0060 |
| *20*026 | 3 | 2 | 19511115 | 008 | 000000000 | 0060 |
| *22*026 | 3 | | | 002 | 043245585 | 0060 |
| *20*026 | 4 | 2 | 19511202 | 001 | 038154069 | 0060 |
| *22*026 | 4 | | | 008 | 061045573 | 0060 |
| *20*026 | 5 | 2 | 19511202 | 001 | 038153887 | 0060 |
| *22*026 | 5 | | | 008 | 061045541 | 0060 |
| *20*026 | 6 | 2 | 19591022 | 003 | 000000000 | 0060 |
| *22*026 | 6 | | | 010 | 038101754 | 0060 |
| *20*026 | 7 | 2 | 19591022 | 003 | 000000000 | 0060 |
| *22*026 | 7 | | | 010 | 038101751 | 0060 |
| *20*026 | 8 | 2 | 19591022 | 010 | 000000000 | 0070 |
| *22*026 | 8 | | | 024 | 070584953 | 0070 |
| *20*026 | 9 | 2 | 19591023 | 010 | 000000000 | 0060 |
| *22*026 | 9 | | | 024 | 070584779 | 0060 |
| *20*009 | 6 | 2 | 19511007 | 022 | 000000000 | 0060 |
| *22*009 | 6 | | | 030 | 029151729 | 0060 |
| *20*009 | 7 | 2 | 19511207 | 022 | 000000000 | 0090 |
| *22*009 | 7 | | | 030 | 029151833 | 0090 |
| *20*009 | 8 | 2 | 19511207 | 041 | 000000000 | 0060 |
| *22*009 | 8 | | | 030 | 055371887 | 0060 |
| *20*009 | 9 | 2 | 19511207 | 041 | 000000000 | 0060 |
| *22*009 | 9 | | | 030 | 055371800 | 0070 |
| *20*021 | 1 | 2 | 19511025 | 016 | 000000000 | 0060 |
| *22*021 | 1 | | | 028 | 009305929 | 0060 |
| *20*021 | 2 | 2 | 19511025 | 016 | 000000000 | 0060 |
| *22*021 | 2 | | | 028 | 009305957 | 0060 |
| *20*023 | 4 | 3 | 19511102 | 038 | 000000000 | 0060 |
| *22*023 | 4 | | | 022 | 083133978 | 0060 |
| *22*023 | 4 | | | 004 | 237441360 | 0060 |
| *20*023 | 5 | 3 | 19511102 | 038 | 000000000 | 0060 |
| *22*023 | 5 | | | 022 | 083133845 | 0060 |
| *22*023 | 5 | | | 004 | 237441230 | 0060 |
| *20*023 | 6 | 3 | 19511202 | 038 | 000000000 | 0060 |
| *22*023 | 6 | | | 030 | 051180280 | 0060 |
| *22*023 | 6 | | | 022 | 083133985 | 0060 |
| *20*023 | 7 | 3 | 19511205 | 038 | 000000000 | 0060 |
| *22*023 | 7 | | | 030 | 051175978 | 0060 |
| *22*023 | 7 | | | 022 | 083133848 | 0060 |
| *20*038 | 18 | 2 | 19511018 | 022 | 000000000 | 0060 |
| *22*038 | 18 | | | 021 | 077020363 | 0060 |
| *20*038 | 19 | 2 | 19511019 | 022 | 000000000 | 0170 |
| *22*038 | 19 | | | 021 | 077020670 | 0240 |
| *20*038 | 20 | 2 | 19511025 | 030 | 000000000 | 0060 |
| *22*038 | 20 | | | 021 | 150562980 | 0060 |
| *20*038 | 21 | 2 | 19511025 | 030 | 000000000 | 0060 |
| *22*038 | 22 | | | 021 | 150562991 | 0060 |
| *20*038 | 30 | 2 | 19511106 | 021 | 000000000 | 0060 |
| *22*038 | 30 | | | 023 | 308371704 | 0060 |
| *20*038 | 31 | 2 | 19511106 | 021 | 000000000 | 0080 |
| *22*038 | 31 | | | 023 | 308371620 | 0090 |
| *20*038 | 32 | 2 | 19511126 | 021 | 000000000 | 0060 |
| *22*038 | 32 | | | 028 | 046365528 | 0060 |

| | | | | | | |
|---|---|---|---|---|---|---|
| *20*038 | 33 | 2 | 19511126 | 021 | 000000000 | 0060 |
| *22*038 | 33 | | | 028 | 046365782 | 0060 |
| *20*021 | 22 | 2 | 19511025 | 016 | 000000000 | 0060 |
| *22*021 | 22 | | | 038 | 137144468 | 0060 |
| *20*021 | 23 | 2 | 19511025 | 016 | 000000000 | 0060 |
| *22*021 | 23 | | | 038 | 137144442 | 0060 |
| *20*031 | 32 | 2 | 19560612 | 034 | 000000000 | 0060 |
| *22*031 | 32 | | | 033 | 046555505 | 0060 |
| *20*031 | 33 | 2 | 19560612 | 034 | 000000000 | 0070 |
| *22*031 | 33 | | | 003 | 204035508 | 0070 |
| *20*031 | 37 | 2 | 19560614 | 033 | 000000000 | 0060 |
| *22*031 | 37 | | | 025 | 087263475 | 0060 |
| *20*008 | 31 | 2 | 19560612 | 003 | 000000000 | 0060 |
| *22*008 | 31 | | | 001 | 181364970 | 0060 |
| *20*033 | 31 | 2 | 19560604 | 034 | 000000000 | 0060 |
| *22*033 | 31 | | | 029 | 089521932 | 0060 |
| *20*018 | 14 | 2 | 19560619 | 008 | 000000000 | 0060 |
| *22*018 | 14 | | | 025 | 121552087 | 0060 |
| *20*018 | 15 | 2 | 19560619 | 008 | 000000000 | 0060 |
| *22*018 | 15 | | | 025 | 121552161 | 0060 |
| *20*018 | 16 | 2 | 19560620 | 008 | 000000000 | 0060 |
| *22*018 | 16 | | | 031 | 093165508 | 0110 |
| *20*028 | 12 | 002 | 19630628 | 034 | 000000000 | 0060 |
| *22*028 | 12 | | | 043 | 073181887 | 0060 |
| *20*028 | 13 | 002 | 19630628 | 034 | 000000000 | 0060 |
| *22*028 | 13 | | | 043 | 073181706 | 0060 |
| *20*028 | 17 | 002 | 19640518 | 033 | 000000000 | 0070 |
| *22*028 | 17 | | | 034 | 043080526 | 0070 |
| *20*028 | 1 | 002 | 19640518 | 033 | 000000000 | 0070 |
| *22*028 | 1 | | | 034 | 043080411 | 0070 |
| *20*033 | 18 | 002 | 19600100 | 031 | 021350903 | 0120 |
| *22*033 | 18 | | | 034 | 076094243 | 0070 |
| *20*033 | 22 | 002 | 19640521 | 034 | 000000000 | 0070 |
| *22*033 | 22 | | | 028 | 089512839 | 0070 |
| *20*033 | 23 | 002 | 19640521 | 034 | 000000000 | 0070 |
| *22*033 | 23 | | | 028 | 089512791 | 0070 |
| *20*043 | 1 | 002 | 19630627 | 028 | 131094468 | 0060 |
| *22*043 | 1 | | | 034 | 188230036 | 0060 |
| *20*043 | 2 | 002 | 19630627 | 028 | 131094473 | 0060 |
| *22*043 | 2 | | | 034 | 188225968 | 0060 |
| *20*034 | 26 | 002 | 19601103 | 033 | 000000000 | 0070 |
| *22*034 | 26 | | | 031 | 078293856 | 0120 |
| *20*034 | 30 | 002 | 19630628 | 043 | 028213059 | 0060 |
| *22*034 | 30 | | | 028 | 077495925 | 0060 |
| *20*034 | 31 | 002 | 19630628 | 043 | 028213128 | 0060 |
| *22*034 | 31 | | | 028 | 077500019 | 0060 |
| *20*034 | 33 | 002 | 19630717 | 043 | 028213146 | 0060 |
| *22*034 | 33 | | | 028 | 077500097 | 0060 |
| *20*034 | 34 | 002 | 19640520 | 028 | 000000000 | 0070 |
| *22*034 | 34 | | | 033 | 047002696 | 0070 |
| *20*034 | 35 | 002 | 19640520 | 028 | 000000000 | 0070 |
| *22*034 | 35 | | | 033 | 047002751 | 0070 |

Table B-2

| | | | | | | |
|---|---|---|---|---|---|---|
| *20*029 | 11 | 3 | 18980100 | 034 | 000000000 | 0180 |
| *22*029 | 11 | | | 047 | 073182096 | 0180 |
| *22*029 | 11 | | | 050 | 316541632 | 0180 |
| *20*050 | 2 | 4 | 18980100 | 029 | 000000000 | 0209 |
| *22*050 | 2 | | | 025 | 167125362 | 0209 |
| *22*050 | 2 | | | 002 | 203220325 | 0209 |
| *22*050 | 2 | | | 034 | 270042478 | 0180 |
| *20*047 | 12 | 2 | 18980100 | 029 | 000000000 | 0180 |
| *22*047 | 12 | | | 034 | 057155927 | 0180 |
| *20*002 | 10 | 4 | 18980100 | 008 | 013311926 | 0180 |
| *22*002 | 10 | | | 050 | 208174678 | 0180 |
| *22*002 | 10 | | | 025 | 250014601 | 0180 |
| *22*002 | 10 | | | 019 | 296431693 | 0180 |
| *20*034 | 37 | 4 | 18980100 | 050 | 000000000 | 0180 |
| *22*034 | 37 | | | 025 | 052414348 | 0180 |
| *22*034 | 37 | | | 047 | 263353253 | 0180 |
| *22*034 | 37 | | | 029 | 313011526 | 0180 |
| *20*025 | 9 | 5 | 18980100 | 019 | 000000000 | 0209 |
| *22*025 | 9 | | | 008 | 036505946 | 0209 |
| *22*025 | 9 | | | 002 | 066414176 | 0209 |
| *22*025 | 9 | | | 034 | 144215258 | 0209 |
| *22*025 | 9 | | | 050 | 168483978 | 0209 |
| *20*001 | 4 | 3 | 18760100 | 019 | 024225586 | 0180 |
| *22*001 | 4 | | | 017 | 055524226 | 0180 |
| *22*001 | 4 | | | 008 | 355530280 | 0180 |
| *20*008 | 14 | 5 | 18750100 | 002 | 033445062 | 0180 |
| *22*008 | 14 | | | 025 | 060243890 | 0180 |
| *22*008 | 14 | | | 019 | 081382020 | 0180 |
| *22*008 | 14 | | | 017 | 128562273 | 0180 |
| *22*008 | 14 | | | 001 | 215264732 | 0180 |
| *20*017 | 1 | 3 | 18730100 | 019 | 042582659 | 0209 |
| *22*017 | 1 | | | 001 | 303052946 | 0209 |
| *22*017 | 1 | | | 008 | 336352894 | 0209 |
| *20*019 | 3 | 4 | 18740100 | 017 | 000000000 | 0209 |
| *22*019 | 3 | | | 001 | 048372232 | 0209 |
| *22*019 | 3 | | | 008 | 066190531 | 0209 |
| *22*019 | 3 | | | 025 | 188142720 | 0209 |
| *20*001 | 7 | 003 | 19240930 | 008 | 061430872 | 0060 |
| *22*001 | 7 | | | 019 | 090125991 | 0060 |
| *22*001 | 7 | | | 017 | 121424468 | 0060 |
| *20*001 | 8 | 003 | 19240930 | 008 | 061430982 | 0080 |
| *22*001 | 8 | | | 019 | 090130000 | 0080 |
| *22*001 | 8 | | | 017 | 121424373 | 0100 |
| *20*001 | 9 | 002 | 19240930 | 008 | 061430880 | 0060 |
| *22*001 | 9 | | | 019 | 090130029 | 0060 |
| *20*001 | 10 | 003 | 19241102 | 008 | 061430534 | 0060 |
| *22*001 | 10 | | | 019 | 090125727 | 0060 |
| *22*001 | 10 | | | 017 | 121424415 | 0060 |
| *20*001 | 13 | 003 | 19241102 | 008 | 061430798 | 0060 |
| *22*001 | 13 | | | 019 | 090125936 | 0060 |
| *22*001 | 13 | | | 017 | 121424462 | 0060 |
| *20*029 | 12 | 004 | 19230301 | 047 | 000000000 | 0060 |
| *22*029 | 12 | | | 038 | 099560896 | 0060 |
| *22*029 | 12 | | | 050 | 243355632 | 0060 |
| *22*029 | 12 | | | 034 | 286413841 | 0060 |
| *20*029 | 13 | 003 | 19230302 | 038 | 099560860 | 0060 |
| *22*029 | 13 | | | 050 | 243355583 | 0060 |
| *22*029 | 13 | | | 034 | 286413796 | 0060 |
| *20*008 | 1 | 003 | 19251113 | 002 | 178180366 | 0060 |

| | | | | | |
|---|---|---|---|---|---|
| *22*008 1 | | | 025 | 204575108 | 0060 |
| *22*008 1 | | | 019 | 226113179 | 0060 |
| *20*008 15 | 005 | 19241105 | 002 | 000000000 | 0060 |
| *22*008 15 | | | 025 | 026394481 | 0060 |
| *22*008 15 | | | 019 | 047532531 | 0060 |
| *22*008 15 | | | 017 | 095112722 | 0060 |
| *22*008 15 | | | 001 | 181415550 | 0240 |
| *20*008 16 | 004 | 19241106 | 002 | 000000000 | 0170 |
| *22*008 16 | | | 025 | 026394355 | 0060 |
| *22*008 16 | | | 019 | 047532573 | 0070 |
| *22*008 16 | | | 001 | 181415410 | 0240 |
| *20*008 17 | 003 | 19241107 | 002 | 000000000 | 0060 |
| *22*008 17 | | | 017 | 095112652 | 0060 |
| *22*008 17 | | | 001 | 181415411 | 0060 |
| *20*008 18 | 002 | 19241119 | 002 | 000000000 | 0060 |
| *22*008 18 | | | 001 | 181415610 | 0060 |
| *20*008 19 | 002 | 19241119 | 002 | 000000000 | 0060 |
| *22*008 19 | | | 001 | 181415590 | 0060 |
| *20*008 22 | 005 | 19241120 | 002 | 000000000 | 0060 |
| *22*008 22 | | | 025 | 026394419 | 0060 |
| *22*008 22 | | | 019 | 047532556 | 0060 |
| *22*008 22 | | | 017 | 095112687 | 0060 |
| *22*008 22 | | | 001 | 181415528 | 0060 |
| *20*050 3 | 004 | 19231105 | 029 | 089553295 | 0060 |
| *22*050 3 | | | 038 | 114592435 | 0060 |
| *22*050 3 | | | 025 | 257082812 | 0060 |
| *22*050 3 | | | 002 | 293173764 | 0060 |
| *20*050 4 | 004 | 19231106 | 029 | 089553321 | 0060 |
| *22*050 4 | | | 038 | 114592444 | 0060 |
| *22*050 4 | | | 025 | 257082822 | 0060 |
| *22*050 4 | | | 002 | 293173658 | 0060 |
| *20*017 2 | 003 | 19241108 | 008 | 000000000 | 0240 |
| *22*017 2 | | | 019 | 066225650 | 0240 |
| *22*017 2 | | | 001 | 326295907 | 0080 |
| *20*017 3 | 002 | 19241108 | 008 | 000000000 | 0060 |
| *22*017 3 | | | 019 | 066225855 | 0120 |
| *20*017 4 | 003 | 19241108 | 008 | 000000000 | 0060 |
| *22*017 4 | | | 019 | 066225844 | 0060 |
| *22*017 4 | | | 001 | 326300064 | 0060 |
| *20*017 5 | 003 | 19241113 | 008 | 000000000 | 0060 |
| *22*017 5 | | | 019 | 066225716 | 0060 |
| *22*017 5 | | | 001 | 326295930 | 0060 |
| *20*017 6 | 003 | 19241113 | 008 | 000000000 | 0060 |
| *22*017 6 | | | 019 | 066225789 | 0060 |
| *22*017 6 | | | 001 | 326295965 | 0060 |
| *20*047 13 | 003 | 19231027 | 038 | 056024798 | 0070 |
| *22*047 13 | | | 029 | 109021728 | 0060 |
| *22*047 13 | | | 034 | 166181619 | 0060 |
| *20*047 93 | 003 | 19231027 | 038 | 056024814 | 0060 |
| *22*047 93 | | | 029 | 109021716 | 0060 |
| *22*047 93 | | | 034 | 166181645 | 0060 |
| *20*038 15 | 002 | 19231018 | 029 | 241020121 | 0060 |
| *22*038 15 | | | 047 | 268062939 | 0070 |
| *20*038 16 | 2 | 19231019 | 029 | 241020202 | 0060 |
| *22*038 16 | | | 047 | 268062877 | 0060 |
| *20*038 17 | 002 | 19231017 | 029 | 000000000 | 0060 |
| *22*038 17 | | | 047 | 027042761 | 0060 |
| *20*002 11 | 003 | 19241111 | 050 | 000000000 | 0070 |
| *22*002 11 | | | 025 | 041435825 | 0060 |
| *22*002 11 | | | 019 | 088252864 | 0060 |
| *20*002 12 | 003 | 19241110 | 050 | 000000000 | 0070 |

| | | | | | |
|---|---|---|---|---|---|
| *22*002 12 | | | 025 | 041435871 | 0060 |
| *22*002 12 | | | 019 | 088252862 | 0060 |
| *20*034 38 | 004 | 19231107 | 047 | 000000000 | 0060 |
| *22*034 38 | | | 029 | 049254224 | 0060 |
| *22*034 38 | | | 050 | 096242823 | 0060 |
| *22*034 38 | | | 025 | 149061219 | 0060 |
| *20*034 39 | 002 | 19231108 | 029 | 049254196 | 0060 |
| *22*034 39 | | | 050 | 096242782 | 0060 |
| *20*025 10 | 003 | 19241112 | 034 | 019471183 | 0110 |
| *22*025 10 | | | 050 | 044135914 | 0110 |
| *22*025 10 | | | 002 | 302070109 | 0090 |
| *20*025 11 | 003 | 19241112 | 034 | 000000000 | 0110 |
| *22*025 11 | | | 050 | 024264528 | 0090 |
| *22*025 11 | | | 002 | 282194861 | 0080 |
| *20*025 12 | 005 | 19241113 | 034 | 019471296 | 0070 |
| *22*025 12 | | | 050 | 044135997 | 0070 |
| *22*025 12 | | | 019 | 235251861 | 0060 |
| *22*025 12 | | | 008 | 272161768 | 0060 |
| *22*025 12 | | | 002 | 302070042 | 0060 |
| *20*025 13 | 003 | 19241114 | 034 | 019471232 | 0070 |
| *22*025 13 | | | 008 | 272161828 | 0060 |
| *22*025 13 | | | 019 | 235251792 | 0060 |
| *20*025 14 | 005 | 19241114 | 034 | 019471247 | 0070 |
| *22*025 14 | | | 050 | 044135918 | 0070 |
| *22*025 14 | | | 019 | 235251826 | 0240 |
| *22*025 14 | | | 008 | 272161798 | 0240 |
| *22*025 14 | | | 002 | 302070075 | 0060 |
| *20*019 1 | 003 | 19251115 | 008 | 017414254 | 0060 |
| *22*019 1 | | | 002 | 073001458 | 0060 |
| *22*019 1 | | | 025 | 139370535 | 0060 |
| *20*019 4 | 004 | 19241115 | 025 | 000000000 | 0060 |
| *22*019 4 | | | 008 | 238043744 | 0060 |
| *22*019 4 | | | 002 | 293230664 | 0060 |
| *22*019 4 | | | 001 | 220225503 | 0060 |
| *20*019 5 | 005 | 19241115 | 025 | 000000000 | 0060 |
| *22*019 5 | | | 017 | 171453232 | 0060 |
| *22*019 5 | | | 001 | 220225431 | 0070 |
| *22*019 5 | | | 008 | 238043759 | 0080 |
| *22*019 5 | | | 002 | 293230752 | 0080 |
| *20*019 6 | 004 | 19241115 | 025 | 000000000 | 0240 |
| *22*019 6 | | | 001 | 220225482 | 0060 |
| *22*019 6 | | | 008 | 238043745 | 0060 |
| *22*019 6 | | | 002 | 293230693 | 0060 |
| *20*041 2 | 003 | 19401106 | 022 | 000000000 | 0070 |
| *22*041 2 | | | 004 | 313415770 | 0070 |
| *22*041 2 | | | 042 | 315530881 | 0070 |
| *20*041 4 | 002 | 19401105 | 022 | 000000000 | 0070 |
| *22*041 4 | | | 042 | 315530608 | 0070 |
| *20*022 1 | 003 | 19401023 | 041 | 249063586 | 0070 |
| *22*022 1 | | | 042 | 261454646 | 0070 |
| *22*022 1 | | | 004 | 341425364 | 0070 |
| *20*042 2 | 002 | 19401105 | 041 | 000000000 | 0070 |
| *22*042 2 | | | 022 | 236460391 | 0070 |
| *20*042 3 | 004 | 19401027 | 004 | 000000000 | 0070 |
| *22*042 3 | | | 023 | 039323641 | 0070 |
| *22*042 3 | | | 022 | 059243073 | 0070 |
| *22*042 3 | | | 041 | 182382845 | 0070 |
| *20*004 1 | 004 | 19401030 | 023 | 210020172 | 0070 |
| *22*004 1 | | | 022 | 217142359 | 0070 |
| *22*004 1 | | | 042 | 257525274 | 0070 |
| *22*004 1 | | | 041 | 258201015 | 0070 |

| | | | | | | |
|---|---|---|---|---|---|---|
| *20*023 | 1 | 002 | 19400319 | 042 | 061535450 | 0070 |
| *22*023 | 1 | | | 004 | 154303466 | 0070 |
| *20*023 | 2 | 004 | 19401022 | 022 | 000000000 | 0070 |
| *22*023 | 2 | | | 041 | 054035738 | 0070 |
| *22*023 | 2 | | | 042 | 061535632 | 0070 |
| *22*023 | 2 | | | 004 | 154303508 | 0070 |
| *20*001 | 2 | 2 | 19511202 | 008 | 000000000 | 0060 |
| *22*001 | 2 | | | 026 | 043574213 | 0060 |
| *20*041 | 5 | 2 | 19511018 | 042 | 000000000 | 0060 |
| *22*041 | 5 | | | 022 | 044065606 | 0060 |
| *20*041 | 6 | 4 | 19511022 | 004 | 000000000 | 0060 |
| *22*041 | 6 | | | 042 | 002111030 | 0060 |
| *22*041 | 6 | | | 022 | 046180399 | 0060 |
| *22*041 | 6 | | | 024 | 331314679 | 0060 |
| *20*041 | 7 | 3 | 19511022 | 004 | 000000000 | 0060 |
| *22*041 | 7 | | | 042 | 002111004 | 0060 |
| *22*041 | 7 | | | 024 | 331314743 | 0060 |
| *20*041 | 9 | 2 | 19511210 | 022 | 000000000 | 0060 |
| *22*041 | 9 | | | 009 | 086140953 | 0060 |
| *20*041 | 11 | 2 | 19511210 | 022 | 000000000 | 0060 |
| *22*041 | 11 | | | 030 | 038154853 | 0060 |
| *20*041 | 12 | 2 | 19511202 | 022 | 044065341 | 0060 |
| *22*041 | 12 | | | 030 | 082224091 | 0060 |
| *20*041 | 13 | 2 | 19511207 | 042 | 000000000 | 0060 |
| *22*041 | 13 | | | 030 | 082224423 | 0060 |
| *20*029 | 4 | 2 | 19521117 | 034 | 000000000 | 0060 |
| *22*029 | 4 | | | 047 | 073182184 | 0060 |
| *20*029 | 5 | 2 | 19560604 | 034 | 043062255 | 0060 |
| *22*029 | 5 | | | 038 | 216205318 | 0060 |
| *20*029 | 6 | 3 | 19560605 | 033 | 000000000 | 0060 |
| *22*029 | 6 | | | 047 | 116244263 | 0060 |
| *22*029 | 6 | | | 038 | 216205010 | 0060 |
| *20*029 | 7 | 4 | 19560605 | 033 | 000000000 | 0060 |
| *22*029 | 7 | | | 034 | 043062020 | 0060 |
| *22*029 | 7 | | | 047 | 116244197 | 0060 |
| *22*029 | 7 | | | 038 | 216205005 | 0060 |
| *20*029 | 8 | 3 | 19560607 | 033 | 000000000 | 0060 |
| *22*029 | 8 | | | 034 | 043062087 | 0060 |
| *22*029 | 8 | | | 047 | 116244248 | 0060 |
| *20*029 | 9 | 2 | 19560607 | 033 | 000000000 | 0060 |
| *22*029 | 9 | | | 034 | 043062076 | 0060 |
| *20*029 | 10 | 3 | 19560606 | 033 | 000000000 | 0060 |
| *22*029 | 10 | | | 034 | 043061929 | 0060 |
| *22*029 | 10 | | | 047 | 116244103 | 0060 |
| *20*028 | 1 | 3 | 19510814 | 016 | 059343922 | 0100 |
| *22*028 | 1 | | | 033 | 143383504 | 0060 |
| *22*028 | 1 | | | 034 | 186464086 | 0060 |
| *20*028 | 2 | 2 | 19510816 | 033 | 000000000 | 0060 |
| *22*028 | 2 | | | 016 | 275560346 | 0060 |
| *20*028 | 3 | 2 | 19510816 | 033 | 000000000 | 0080 |
| *22*028 | 3 | | | 016 | 275560238 | 0080 |
| *20*028 | 4 | 3 | 19510820 | 016 | 000000000 | 0060 |
| *22*028 | 4 | | | 033 | 084035663 | 0060 |
| *22*028 | 4 | | | 038 | 300252158 | 0060 |
| *20*028 | 5 | 3 | 19511023 | 038 | 000000000 | 0060 |
| *22*028 | 5 | | | 021 | 005392063 | 0060 |
| *22*028 | 5 | | | 016 | 059344092 | 0060 |
| *20*028 | 7 | 3 | 19511025 | 038 | 000000000 | 0060 |
| *22*028 | 7 | | | 021 | 005392033 | 0060 |
| *22*028 | 7 | | | 004 | 067115054 | 0060 |
| *20*028 | 8 | 3 | 19511025 | 038 | 000000000 | 0060 |

| | | | | | |
|---|---|---|---|---|---|
| *22*028 | 8 | | | 021 | 005392052 | 0060 |
| *22*028 | 8 | | | 004 | 067114988 | 0060 |
| *20*028 | 10 | 2 | 19591109 | 004 | 000000000 | 0060 |
| *22*028 | 10 | | | 033 | 076264301 | 0060 |
| *20*028 | 11 | 2 | 19591109 | 033 | 013274202 | 0060 |
| *22*028 | 11 | | | 004 | 297005791 | 0060 |
| *20*022 | 4 | 2 | 19511010 | 038 | 000000000 | 0060 |
| *22*022 | 4 | | | 030 | 068324985 | 0060 |
| *20*022 | 6 | 3 | 19511013 | 023 | 000000000 | 0060 |
| *22*022 | 6 | | | 038 | 071065612 | 0060 |
| *22*022 | 6 | | | 041 | 249063563 | 0060 |
| *20*022 | 7 | 2 | 19511013 | 023 | 000000000 | 0060 |
| *22*022 | 7 | | | 038 | 071065592 | 0060 |
| *20*022 | 9 | 2 | 19511018 | 023 | 000000000 | 0060 |
| *22*022 | 9 | | | 004 | 341425324 | 0060 |
| *20*022 | 10 | 3 | 19511019 | 004 | 000000000 | 0060 |
| *22*022 | 10 | | | 023 | 018170619 | 0060 |
| *22*022 | 10 | | | 038 | 089240148 | 0060 |
| *20*022 | 11 | 3 | 19511022 | 042 | 000000000 | 0060 |
| *22*022 | 11 | | | 004 | 079570724 | 0060 |
| *22*022 | 11 | | | 023 | 098141340 | 0060 |
| *20*022 | 12 | 2 | 19511026 | 023 | 000000000 | 0060 |
| *22*022 | 12 | | | 030 | 139394620 | 0060 |
| *20*022 | 13 | 3 | 19511027 | 023 | 000000000 | 0120 |
| *22*022 | 13 | | | 024 | 323484627 | 0140 |
| *22*022 | 13 | | | 004 | 341425340 | 0120 |
| *20*022 | 15 | 3 | 19511028 | 024 | 000000000 | 0060 |
| *22*022 | 15 | | | 004 | 017540720 | 0060 |
| *22*022 | 15 | | | 023 | 036111190 | 0060 |
| *20*022 | 16 | 3 | 19511028 | 024 | 000000000 | 0060 |
| *22*022 | 16 | | | 004 | 017540708 | 0060 |
| *22*022 | 16 | | | 023 | 036111304 | 0060 |
| *20*031 | 3 | 3 | 19510808 | 034 | 000000000 | 0060 |
| *22*031 | 3 | | | 033 | 046555101 | 0060 |
| *22*031 | 3 | | | 011 | 131552165 | 0060 |
| *20*031 | 5 | 2 | 19510813 | 034 | 000000000 | 0060 |
| *22*031 | 5 | | | 033 | 046555113 | 0060 |
| *20*031 | 7 | 2 | 19511025 | 034 | 000000000 | 0060 |
| *22*031 | 7 | | | 033 | 046555135 | 0060 |
| *20*031 | 8 | 2 | 19511107 | 011 | 020174609 | 0060 |
| *22*031 | 8 | | | 010 | 038434264 | 0060 |
| *20*031 | 9 | 2 | 19511107 | 011 | 020174605 | 0060 |
| *22*031 | 9 | | | 010 | 038434018 | 0060 |
| *20*031 | 10 | 2 | 19511113 | 010 | 038434126 | 0060 |
| *22*031 | 10 | | | 002 | 092324757 | 0060 |
| *20*031 | 11 | 2 | 19511113 | 010 | 038434136 | 0060 |
| *22*031 | 11 | | | 002 | 092324566 | 0060 |
| *20*031 | 12 | 2 | 19510100 | 034 | 000000000 | 0060 |
| *22*031 | 12 | | | 025 | 134222517 | 0070 |
| *20*031 | 13 | 2 | 19560612 | 034 | 000000000 | 0060 |
| *22*031 | 13 | | | 003 | 204035081 | 0070 |
| *20*031 | 14 | 3 | 19560613 | 034 | 000000000 | 0060 |
| *22*031 | 14 | | | 033 | 046555100 | 0060 |
| *22*031 | 14 | | | 025 | 134222384 | 0060 |
| *20*031 | 15 | 3 | 19560613 | 034 | 000000000 | 0060 |
| *22*031 | 15 | | | 018 | 161092268 | 0080 |
| *22*031 | 15 | | | 003 | 204035174 | 0060 |
| *20*031 | 16 | 2 | 19560613 | 034 | 000000000 | 0060 |
| *22*031 | 16 | | | 003 | 204034925 | 0060 |
| *20*031 | 17 | 2 | 19560614 | 033 | 000000000 | 0060 |
| *22*031 | 17 | | | 018 | 114132910 | 0060 |

| | | | | | |
|---|---|---|---|---|---|
| *20*031 18 | 2 | 19560614 | 033 | 000000000 | 0090 |
| *22*031 18 | | | 018 | 114132920 | 0090 |
| *20*031 19 | 3 | 19560620 | 033 | 000000000 | 0060 |
| *22*031 19 | | | 025 | 087263202 | 0060 |
| *22*031 19 | | | 003 | 157075966 | 0060 |
| *20*031 20 | 2 | 19591030 | 033 | 000000000 | 0060 |
| *22*031 20 | | | 003 | 157075900 | 0060 |
| *20*031 21 | 2 | 19591030 | 033 | 000000000 | 0060 |
| *22*031 21 | | | 003 | 157075752 | 0060 |
| *20*031 22 | 3 | 19591109 | 033 | 000000000 | 0060 |
| *22*031 22 | | | 011 | 084593176 | 0060 |
| *22*031 22 | | | 010 | 103252498 | 0060 |
| *20*031 23 | 3 | 19591109 | 033 | 000000000 | 0060 |
| *22*031 23 | | | 011 | 084593127 | 0060 |
| *22*031 23 | | | 010 | 103252346 | 0060 |
| *20*031 24 | 2 | 19591109 | 011 | 020174457 | 0060 |
| *22*031 24 | | | 010 | 038433755 | 0070 |
| *20*031 25 | 2 | 19591110 | 010 | 103252091 | 0060 |
| *22*031 25 | | | 003 | 157075636 | 0060 |
| *20*031 26 | 2 | 19591110 | 010 | 038434046 | 0060 |
| *22*031 26 | | | 033 | 295181666 | 0060 |
| *20*010 3 | 2 | 19511106 | 002 | 000000000 | 0060 |
| *22*010 3 | | | 024 | 154465162 | 0070 |
| *20*010 4 | 3 | 19511106 | 002 | 000000000 | 0060 |
| *22*010 4 | | | 031 | 045263073 | 0060 |
| *22*010 4 | | | 011 | 084441742 | 0060 |
| *20*010 5 | 3 | 19511111 | 004 | 038172994 | 0070 |
| *22*010 5 | | | 024 | 070023303 | 0070 |
| *22*010 5 | | | 026 | 160230406 | 0060 |
| *20*010 6 | 2 | 19511117 | 026 | 004442481 | 0060 |
| *22*010 6 | | | 008 | 075011088 | 0060 |
| *20*010 7 | 2 | 19511117 | 026 | 004442442 | 0060 |
| *22*010 7 | | | 008 | 075010978 | 0060 |
| *20*010 8 | 3 | 19591104 | 026 | 000000000 | 0060 |
| *22*010 8 | | | 003 | 114484013 | 0060 |
| *22*010 8 | | | 011 | 199365296 | 0060 |
| *20*010 10 | 6 | 19591105 | 026 | 000000000 | 0060 |
| *22*010 10 | | | 003 | 114484104 | 0060 |
| *22*010 10 | | | 031 | 160190490 | 0060 |
| *22*010 10 | | | 011 | 199365272 | 0060 |
| *22*010 10 | | | 004 | 237542553 | 0060 |
| *22*010 10 | | | 024 | 269392896 | 0060 |
| *20*010 11 | 3 | 19591106 | 031 | 000000000 | 0060 |
| *22*010 11 | | | 011 | 039174590 | 0060 |
| *22*010 11 | | | 024 | 109202163 | 0060 |
| *20*010 12 | 2 | 19591106 | 031 | 000000000 | 0060 |
| *22*010 12 | | | 024 | 109202304 | 0060 |
| *20*010 13 | 3 | 19591105 | 026 | 000000000 | 0060 |
| *22*010 13 | | | 011 | 199365542 | 0060 |
| *22*010 13 | | | 024 | 269392983 | 0090 |
| *20*008 2 | 2 | 19511115 | 002 | 000000000 | 0060 |
| *22*008 2 | | | 026 | 068285277 | 0060 |
| *20*008 3 | 2 | 19511115 | 002 | 000000000 | 0060 |
| *22*008 3 | | | 026 | 068285152 | 0060 |
| *20*008 5 | 3 | 19511126 | 002 | 000000000 | 0060 |
| *22*008 5 | | | 010 | 040200141 | 0060 |
| *22*008 5 | | | 001 | 181415595 | 0060 |
| *20*008 7 | 3 | 19560612 | 003 | 000000000 | 0060 |
| *22*008 7 | | | 018 | 047482560 | 0060 |
| *22*008 7 | | | 001 | 181365100 | 0060 |
| *20*008 9 | 2 | 19560619 | 025 | 128454319 | 0060 |

| | | | | | | |
|---|---|---|---|---|---|---|
| *22*008 | 9 | | | 018 | 149592454 | 0070 |
| *20*008 | 10 | 2 | 19560619 | 025 | 128454263 | 0060 |
| *22*008 | 10 | | | 018 | 149592463 | 0060 |
| *20*042 | 5 | 2 | 19511006 | 004 | 000000000 | 0060 |
| *22*042 | 5 | | | 022 | 059243216 | 0060 |
| *20*042 | 6 | 2 | 19511006 | 004 | 000000000 | 0060 |
| *22*042 | 6 | | | 041 | 182382536 | 0060 |
| *20*042 | 7 | 3 | 19511007 | 022 | 000000000 | 0060 |
| *22*042 | 7 | | | 030 | 034082829 | 0060 |
| *22*042 | 7 | | | 024 | 268005198 | 0060 |
| *20*042 | 8 | 3 | 19511008 | 024 | 000000000 | 0060 |
| *22*042 | 8 | | | 004 | 032343667 | 0060 |
| *22*042 | 8 | | | 022 | 091590692 | 0060 |
| *20*011 | 1 | 3 | 19511102 | 031 | 052254622 | 0060 |
| *22*011 | 1 | | | 033 | 094331448 | 0060 |
| *22*011 | 1 | | | 010 | 290092663 | 0060 |
| *20*011 | 3 | 5 | 19511103 | 002 | 000000000 | 0060 |
| *22*011 | 3 | | | 004 | 157131396 | 0060 |
| *22*011 | 3 | | | 024 | 192160536 | 0060 |
| *22*011 | 3 | | | 033 | 094331578 | 0060 |
| *22*011 | 3 | | | 010 | 290092730 | 0060 |
| *20*011 | 5 | 6 | 19591107 | 010 | 000000000 | 0060 |
| *22*011 | 5 | | | 003 | 069450675 | 0060 |
| *22*011 | 5 | | | 031 | 122161942 | 0060 |
| *22*011 | 5 | | | 033 | 164234695 | 0060 |
| *22*011 | 5 | | | 004 | 227034479 | 0060 |
| *22*011 | 5 | | | 024 | 262063503 | 0060 |
| *20*011 | 6 | 3 | 19591107 | 010 | 000000000 | 0060 |
| *22*011 | 6 | | | 003 | 069450702 | 0060 |
| *22*011 | 6 | | | 024 | 262063542 | 0060 |
| *20*024 | 1 | 2 | 19510829 | 013 | 028073687 | 0070 |
| *22*024 | 1 | | | 004 | 115152575 | 0060 |
| *20*024 | 2 | 2 | 19510829 | 013 | 028073758 | 0070 |
| *22*024 | 2 | | | 004 | 115152664 | 0060 |
| *20*024 | 3 | 3 | 19511102 | 013 | 000000000 | 0070 |
| *22*024 | 3 | | | 004 | 087075008 | 0060 |
| *22*024 | 3 | | | 041 | 139170099 | 0060 |
| *20*024 | 4 | 2 | 19511103 | 013 | 000000000 | 0070 |
| *22*024 | 4 | | | 004 | 087074850 | 0060 |
| *20*024 | 5 | 2 | 19511106 | 013 | 000000000 | 0080 |
| *22*024 | 5 | | | 004 | 087074782 | 0070 |
| *20*024 | 6 | 4 | 19511111 | 013 | 000000000 | 0070 |
| *22*024 | 6 | | | 010 | 011395897 | 0090 |
| *22*024 | 6 | | | 011 | 023440474 | 0070 |
| *22*024 | 6 | | | 004 | 087074862 | 0060 |
| *20*024 | 7 | 4 | 19511115 | 013 | 000000000 | 0070 |
| *22*024 | 7 | | | 011 | 023440571 | 0060 |
| *22*024 | 7 | | | 004 | 087074982 | 0060 |
| *22*024 | 7 | | | 026 | 352591299 | 0060 |
| *20*024 | 8 | 2 | 19511115 | 013 | 000000000 | 0070 |
| *22*024 | 8 | | | 004 | 087074909 | 0060 |
| *20*024 | 9 | 4 | 19511117 | 013 | 000000000 | 0070 |
| *22*024 | 9 | | | 004 | 087074933 | 0060 |
| *22*024 | 9 | | | 022 | 108451587 | 0060 |
| *22*024 | 9 | | | 042 | 134432061 | 0060 |
| *20*024 | 10 | 3 | 19511117 | 013 | 000000000 | 0070 |
| *22*024 | 10 | | | 004 | 087074820 | 0060 |
| *22*024 | 10 | | | 042 | 134432016 | 0060 |
| *20*024 | 11 | 5 | 19591105 | 026 | 000000000 | 0060 |
| *22*024 | 11 | | | 013 | 007004846 | 0070 |
| *22*024 | 11 | | | 010 | 018405003 | 0070 |

| | | | | | |
|---|---|---|---|---|---|
| *22*024 | 11 | | | 011 | 030445336 | 0060 |
| *22*024 | 11 | | | 004 | 094083610 | 0120 |
| *20*024 | 12 | 4 | 19591106 | 026 | 000000000 | 0060 |
| *22*024 | 12 | | | 010 | 018404684 | 0060 |
| *22*024 | 12 | | | 011 | 030445312 | 0060 |
| *22*024 | 12 | | | 004 | 094083514 | 0060 |
| *20*024 | 13 | 4 | 19591106 | 010 | 000000000 | 0060 |
| *22*024 | 13 | | | 033 | 039141201 | 0060 |
| *22*024 | 13 | | | 004 | 075274814 | 0060 |
| *22*024 | 13 | | | 026 | 341191039 | 0060 |
| *20*033 | 1 | 2 | 19510808 | 028 | 089512896 | 0090 |
| *22*033 | 1 | | | 031 | 305252775 | 0060 |
| *20*033 | 2 | 3 | 19510813 | 034 | 000000000 | 0060 |
| *22*033 | 2 | | | 028 | 089512807 | 0060 |
| *22*033 | 2 | | | 031 | 305252602 | 0060 |
| *20*033 | 4 | 2 | 19510813 | 034 | 000000000 | 0060 |
| *22*033 | 4 | | | 028 | 089512938 | 0080 |
| *20*033 | 5 | 3 | 19511022 | 031 | 022324866 | 0060 |
| *22*033 | 5 | | | 028 | 166585049 | 0060 |
| *22*033 | 5 | | | 004 | 249393085 | 0060 |
| *20*033 | 6 | 2 | 19511022 | 028 | 000000000 | 0060 |
| *22*033 | 6 | | | 004 | 082404086 | 0060 |
| *20*033 | 7 | 2 | 19511105 | 011 | 000000000 | 0060 |
| *22*033 | 7 | | | 031 | 052530428 | 0060 |
| *20*033 | 8 | 2 | 19560605 | 034 | 000000000 | 0060 |
| *22*033 | 8 | | | 029 | 089522493 | 0060 |
| *20*033 | 9 | 2 | 19560605 | 034 | 000000000 | 0060 |
| *22*033 | 9 | | | 029 | 089522303 | 0060 |
| *20*033 | 10 | 2 | 19560606 | 034 | 000000000 | 0060 |
| *22*033 | 10 | | | 029 | 089522505 | 0060 |
| *20*033 | 11 | 3 | 19560612 | 034 | 000000000 | 0060 |
| *22*033 | 11 | | | 038 | 114562294 | 0060 |
| *22*033 | 11 | | | 031 | 305252879 | 0060 |
| *20*033 | 12 | 3 | 19560612 | 034 | 000000000 | 0060 |
| *22*033 | 12 | | | 025 | 257060177 | 0060 |
| *22*033 | 12 | | | 031 | 305252681 | 0060 |
| *20*033 | 13 | 3 | 19560612 | 034 | 000000000 | 0060 |
| *22*033 | 13 | | | 025 | 257060173 | 0060 |
| *22*033 | 13 | | | 031 | 305252884 | 0060 |
| *20*033 | 14 | 2 | 19560613 | 025 | 257055974 | 0060 |
| *22*033 | 14 | | | 031 | 305252595 | 0060 |
| *20*033 | 15 | 4 | 19560613 | 034 | 000000000 | 0060 |
| *22*033 | 15 | | | 025 | 257055905 | 0060 |
| *22*033 | 15 | | | 003 | 293114798 | 0080 |
| *22*033 | 15 | | | 031 | 305252769 | 0060 |
| *20*033 | 16 | 2 | 19560615 | 034 | 000000000 | 0060 |
| *22*033 | 16 | | | 025 | 257060038 | 0060 |
| *20*033 | 17 | 2 | 19560615 | 034 | 000000000 | 0070 |
| *22*033 | 17 | | | 025 | 257060145 | 0070 |
| *20*033 | 19 | 5 | 19591107 | 004 | 082403856 | 0060 |
| *22*033 | 19 | | | 024 | 107334091 | 0060 |
| *22*033 | 19 | | | 011 | 162405228 | 0060 |
| *22*033 | 19 | | | 003 | 203202020 | 0060 |
| *22*033 | 19 | | | 031 | 215335701 | 0060 |
| *20*033 | 20 | 3 | 19591107 | 011 | 005594532 | 0060 |
| *22*033 | 20 | | | 003 | 046391261 | 0060 |
| *22*033 | 20 | | | 031 | 058525007 | 0060 |
| *20*033 | 21 | 2 | 19591110 | 011 | 005594566 | 0060 |
| *22*033 | 21 | | | 031 | 058524807 | 0060 |
| *20*030 | 2 | 5 | 19511007 | 009 | 000000000 | 0060 |
| *22*030 | 2 | | | 042 | 084563366 | 0060 |

| | | | | | |
|---|---|---|---|---|---|
| *22*030 | 2 | | | 022 | 108421064 | 0060 |
| *22*030 | 2 | | | 023 | 117064622 | 0060 |
| *22*030 | 2 | | | 038 | 146150510 | 0060 |
| *20*030 | 4 | 3 | 19511009 | 042 | 000000000 | 0060 |
| *22*030 | 4 | | | 022 | 023453952 | 0060 |
| *22*030 | 4 | | | 038 | 061183307 | 0060 |
| *20*030 | 5 | 5 | 19511202 | 009 | 000000000 | 0060 |
| *22*030 | 5 | | | 041 | 076244130 | 0060 |
| *22*030 | 5 | | | 022 | 108421098 | 0060 |
| *22*030 | 5 | | | 023 | 117064562 | 0080 |
| *22*030 | 5 | | | 038 | 146150301 | 0060 |
| *20*030 | 6 | 2 | 19511206 | 009 | 000000000 | 0060 |
| *22*030 | 6 | | | 041 | 076244120 | 0060 |
| *20*016 | 2 | 3 | 19510829 | 004 | 000000000 | 0060 |
| *22*016 | 2 | | | 028 | 171132523 | 0080 |
| *22*016 | 2 | | | 038 | 282323298 | 0110 |
| *20*016 | 3 | 2 | 19510830 | 004 | 000000000 | 0060 |
| *22*016 | 3 | | | 028 | 171132692 | 0100 |
| *20*016 | 4 | 3 | 19511018 | 028 | 000000000 | 0070 |
| *22*016 | 4 | | | 038 | 111190848 | 0070 |
| *22*016 | 4 | | | 004 | 188463357 | 0070 |
| *20*016 | 5 | 2 | 19511018 | 028 | 000000000 | 0080 |
| *22*016 | 5 | | | 038 | 111190824 | 0080 |
| *20*016 | 6 | 2 | 19511022 | 004 | 000000000 | 0070 |
| *22*016 | 6 | | | 028 | 171132350 | 0070 |
| *20*016 | 7 | 2 | 19511024 | 021 | 000000000 | 0060 |
| *22*016 | 7 | | | 004 | 072125060 | 0060 |
| *20*016 | 8 | 2 | 19511024 | 021 | 000000000 | 0060 |
| *22*016 | 8 | | | 004 | 072125155 | 0060 |
| *20*016 | 9 | 2 | 19511127 | 028 | 000000000 | 0070 |
| *22*016 | 9 | | | 038 | 111190746 | 0070 |
| *20*047 | 2 | 2 | 19521116 | 029 | 000000000 | 0060 |
| *22*047 | 2 | | | 034 | 057155928 | 0060 |
| *20*047 | 3 | 2 | 19560605 | 029 | 109021895 | 0060 |
| *22*047 | 3 | | | 034 | 166181859 | 0060 |
| *20*047 | 7 | 2 | 19560607 | 029 | 109021883 | 0060 |
| *22*047 | 7 | | | 034 | 166181737 | 0060 |
| *20*047 | 9 | 2 | 19560628 | 038 | 056024891 | 0060 |
| *22*047 | 9 | | | 029 | 109021837 | 0060 |
| *20*047 | 10 | 3 | 19560628 | 038 | 000000000 | 0060 |
| *22*047 | 10 | | | 029 | 052592795 | 0060 |
| *22*047 | 10 | | | 034 | 110152870 | 0060 |
| *20*038 | 2 | 2 | 19511013 | 023 | 025391983 | 0060 |
| *22*038 | 2 | | | 028 | 123385928 | 0060 |
| *20*038 | 3 | 2 | 19511018 | 022 | 000000000 | 0060 |
| *22*038 | 3 | | | 016 | 114324794 | 0060 |
| *20*038 | 4 | 3 | 19511019 | 022 | 000000000 | 0060 |
| *22*038 | 4 | | | 023 | 025392241 | 0060 |
| *22*038 | 4 | | | 016 | 114324700 | 0240 |
| *20*038 | 5 | 2 | 19511019 | 022 | 000000000 | 0170 |
| *22*038 | 5 | | | 023 | 025392160 | 0170 |
| *20*038 | 6 | 3 | 19511022 | 022 | 000000000 | 0070 |
| *22*038 | 6 | | | 004 | 056391503 | 0090 |
| *22*038 | 6 | | | 016 | 114324703 | 0070 |
| *20*038 | 7 | 2 | 19511023 | 022 | 000000000 | 0060 |
| *22*038 | 7 | | | 028 | 123390226 | 0060 |
| *20*038 | 8 | 2 | 19511025 | 030 | 000000000 | 0060 |
| *22*038 | 8 | | | 028 | 197332437 | 0060 |
| *20*038 | 9 | 2 | 19511025 | 030 | 000000000 | 0060 |
| *22*038 | 9 | | | 028 | 197332423 | 0060 |
| *20*038 | 10 | 2 | 19511103 | 023 | 000000000 | 0120 |

| | | | | | |
|---|---|---|---|---|---|
| *22*038 10 | | | 004 | 030595110 | 0120 |
| *20*038 11 | 2 | 19560531 | 030 | 089142878 | 0060 |
| *22*038 11 | | | 029 | 286481542 | 0060 |
| *20*038 12 | 4 | 19560531 | 030 | 089142864 | 0060 |
| *22*038 12 | | | 029 | 286481554 | 0140 |
| *22*038 12 | | | 047 | 313524380 | 0060 |
| *22*038 12 | | | 047 | 313524391 | 0060 |
| *20*038 14 | 2 | 19560605 | 047 | 000000000 | 0060 |
| *22*038 14 | | | 029 | 332553345 | 0060 |
| *20*004 4 | 3 | 19511018 | 016 | 000000000 | 0060 |
| *22*004 4 | | | 038 | 044390676 | 0060 |
| *22*004 4 | | | 023 | 071233316 | 0060 |
| *20*004 6 | 3 | 19511019 | 023 | 000000000 | 0060 |
| *22*004 6 | | | 022 | 007122191 | 0060 |
| *22*004 6 | | | 024 | 147405019 | 0060 |
| *20*004 7 | 3 | 19511022 | 022 | 100375925 | 0060 |
| *22*004 7 | | | 041 | 141434189 | 0080 |
| *22*004 7 | | | 024 | 241062829 | 0060 |
| *20*004 8 | 2 | 19511025 | 028 | 000000000 | 0060 |
| *22*004 8 | | | 016 | 001092489 | 0060 |
| *20*004 9 | 2 | 19511025 | 028 | 000000000 | 0060 |
| *22*004 9 | | | 038 | 045483045 | 0060 |
| *20*004 11 | 3 | 19511027 | 016 | 000000000 | 0060 |
| *22*004 11 | | | 041 | 119414077 | 0060 |
| *22*004 11 | | | 024 | 219042685 | 0060 |
| *20*004 12 | 3 | 19511027 | 022 | 000000000 | 0060 |
| *22*004 12 | | | 041 | 041054523 | 0060 |
| *22*004 12 | | | 024 | 140282880 | 0060 |
| *20*004 13 | 3 | 19511028 | 022 | 000000000 | 0060 |
| *22*004 13 | | | 042 | 040382708 | 0060 |
| *22*004 13 | | | 041 | 041054545 | 0060 |
| *20*004 14 | 3 | 19511028 | 022 | 000000000 | 0060 |
| *22*004 14 | | | 042 | 040382752 | 0060 |
| *22*004 14 | | | 041 | 041054678 | 0060 |
| *20*004 16 | 4 | 19511103 | 024 | 000000000 | 0070 |
| *22*004 16 | | | 010 | 072471941 | 0070 |
| *22*004 16 | | | 011 | 081333478 | 0070 |
| *22*004 16 | | | 033 | 118532939 | 0070 |
| *20*004 18 | 4 | 19591108 | 024 | 000000000 | 0060 |
| *22*004 18 | | | 010 | 072471916 | 0060 |
| *22*004 18 | | | 011 | 081333548 | 0060 |
| *22*004 18 | | | 033 | 118533016 | 0060 |
| *20*002 4 | 2 | 19511113 | 031 | 000000000 | 0070 |
| *22*002 4 | | | 010 | 080443103 | 0140 |
| *20*002 5 | 3 | 19511114 | 031 | 000000000 | 0060 |
| *22*002 5 | | | 011 | 055191688 | 0060 |
| *22*002 5 | | | 010 | 080442766 | 0060 |
| *20*002 6 | 3 | 19511114 | 031 | 000000000 | 0060 |
| *22*002 6 | | | 011 | 055191836 | 0060 |
| *22*002 6 | | | 010 | 080442964 | 0060 |
| *20*002 7 | 3 | 19511115 | 010 | 000000000 | 0060 |
| *22*002 7 | | | 026 | 026575291 | 0060 |
| *22*002 7 | | | 008 | 095041238 | 0060 |
| *20*002 8 | 3 | 19511115 | 010 | 000000000 | 0060 |
| *22*002 8 | | | 026 | 026575410 | 0060 |
| *22*002 8 | | | 008 | 095041229 | 0060 |
| *20*003 1 | 2 | 19560612 | 025 | 052193798 | 0060 |
| *22*003 1 | | | 018 | 099050057 | 0060 |
| *20*003 2 | 3 | 19560612 | 031 | 000000000 | 0060 |
| *22*003 2 | | | 025 | 052193479 | 0240 |
| *22*003 2 | | | 018 | 099050003 | 0060 |

| | | | | | |
|---|---|---|---|---|---|
| *20*003 3 | 3 | 19560613 | 031 | 000000000 | 0060 |
| *22*003 3 | | | 025 | 052193754 | 0060 |
| *22*003 3 | | | 018 | 099050074 | 0060 |
| *20*003 4 | 3 | 19560613 | 031 | 000000000 | 0060 |
| *22*003 4 | | | 033 | 010382360 | 0060 |
| *22*003 4 | | | 025 | 052193633 | 0060 |
| *20*003 6 | 3 | 19560614 | 031 | 000000000 | 0060 |
| *22*003 6 | | | 025 | 052193656 | 0060 |
| *22*003 6 | | | 018 | 099045918 | 0060 |
| *20*003 7 | 4 | 19560620 | 031 | 000000000 | 0060 |
| *22*003 7 | | | 025 | 052193618 | 0060 |
| *22*003 7 | | | 018 | 099050171 | 0060 |
| *22*003 7 | | | 008 | 176001586 | 0060 |
| *20*003 8 | 3 | 19560620 | 031 | 000000000 | 0060 |
| *22*003 8 | | | 018 | 099050204 | 0060 |
| *22*003 8 | | | 008 | 176001512 | 0060 |
| *20*003 9 | 2 | 19560702 | 018 | 000000000 | 0060 |
| *22*003 9 | | | 008 | 076551514 | 0060 |
| *20*003 10 | 3 | 19591022 | 031 | 000000000 | 0060 |
| *22*003 10 | | | 010 | 080470379 | 0060 |
| *22*003 10 | | | 026 | 107480581 | 0060 |
| *20*003 11 | 3 | 19591022 | 031 | 000000000 | 0060 |
| *22*003 11 | | | 010 | 080470324 | 0060 |
| *22*003 11 | | | 026 | 107480423 | 0060 |
| *20*003 12 | 3 | 19591023 | 031 | 000000000 | 0060 |
| *22*003 12 | | | 011 | 055202165 | 0060 |
| *22*003 12 | | | 010 | 080470330 | 0060 |
| *20*003 13 | 3 | 19591023 | 031 | 000000000 | 0120 |
| *22*003 13 | | | 011 | 055201970 | 0120 |
| *22*003 13 | | | 010 | 080470025 | 0120 |
| *20*003 14 | 2 | 19591030 | 031 | 000000000 | 0060 |
| *22*003 14 | | | 033 | 010382395 | 0060 |
| *20*003 15 | 4 | 19591123 | 031 | 000000000 | 0060 |
| *22*003 15 | | | 033 | 010382377 | 0060 |
| *22*003 15 | | | 011 | 055202035 | 0060 |
| *22*003 15 | | | 010 | 080470153 | 0060 |
| *20*003 16 | 4 | 19591123 | 011 | 000000000 | 0060 |
| *22*003 16 | | | 010 | 025264153 | 0060 |
| *22*003 16 | | | 031 | 304393586 | 0060 |
| *22*003 16 | | | 033 | 315180158 | 0060 |
| *20*034 4 | 2 | 19510808 | 033 | 000000000 | 0060 |
| *22*034 4 | | | 031 | 078293958 | 0060 |
| *20*034 5 | 3 | 19510813 | 028 | 000000000 | 0060 |
| *22*034 5 | | | 033 | 047002696 | 0060 |
| *22*034 5 | | | 031 | 125300590 | 0060 |
| *20*034 6 | 2 | 19510917 | 033 | 001094434 | 0070 |
| *22*034 6 | | | 031 | 079392026 | 0060 |
| *20*034 7 | 2 | 19511112 | 033 | 000000000 | 0060 |
| *22*034 7 | | | 031 | 078293691 | 0060 |
| *20*034 9 | 2 | 19521117 | 047 | 028233054 | 0060 |
| *22*034 9 | | | 029 | 077491266 | 0060 |
| *20*034 11 | 2 | 19560510 | 031 | 000000000 | 0060 |
| *22*034 11 | | | 033 | 281302179 | 0060 |
| *20*034 12 | 2 | 19560510 | 031 | 000000000 | 0060 |
| *22*034 12 | | | 033 | 281302169 | 0060 |
| *20*034 13 | 3 | 19560510 | 031 | 000000000 | 0060 |
| *22*034 13 | | | 029 | 234290456 | 0060 |
| *22*034 13 | | | 033 | 281302040 | 0100 |
| *20*034 14 | 2 | 19560510 | 031 | 000000000 | 0060 |
| *22*034 14 | | | 029 | 234290584 | 0060 |
| *20*034 18 | 2 | 19560604 | 029 | 000000000 | 0060 |

| | | | | | |
|---|---|---|---|---|---|
| *22*034 18 | | | 033 | 047011782 | 0060 |
| *20*034 19 | 3 | 19560604 | 029 | 000000000 | 0060 |
| *22*034 19 | | | 033 | 047011548 | 0060 |
| *22*034 19 | | | 047 | 310341789 | 0060 |
| *20*034 20 | 2 | 19560605 | 029 | 049254337 | 0060 |
| *22*034 20 | | | 033 | 096265829 | 0060 |
| *20*034 22 | 2 | 19560612 | 033 | 000000000 | 0060 |
| *22*034 22 | | | 031 | 078293740 | 0060 |
| *20*034 23 | 3 | 19560613 | 033 | 000000000 | 0060 |
| *22*034 23 | | | 025 | 052391475 | 0070 |
| *22*034 23 | | | 031 | 078293710 | 0060 |
| *20*034 24 | 3 | 19560614 | 033 | 000000000 | 0060 |
| *22*034 24 | | | 025 | 052391252 | 0070 |
| *22*034 24 | | | 031 | 078293815 | 0060 |
| *20*034 25 | 3 | 19560614 | 033 | 000000000 | 0060 |
| *22*034 25 | | | 025 | 052391401 | 0060 |
| *22*034 25 | | | 031 | 078293744 | 0060 |
| *20*034 27 | 2 | 19590428 | 031 | 079392304 | 0070 |
| *22*034 27 | | | 047 | 264424522 | 0070 |
| *20*025 2 | 3 | 19560614 | 018 | 000000000 | 0060 |
| *22*025 2 | | | 031 | 124344074 | 0060 |
| *22*025 2 | | | 034 | 144215312 | 0070 |
| *20*025 3 | 2 | 19560612 | 018 | 000000000 | 0070 |
| *22*025 3 | | | 033 | 168484415 | 0070 |
| *20*025 4 | 2 | 19560615 | 018 | 000000000 | 0060 |
| *22*025 4 | | | 031 | 124343770 | 0060 |
| *20*025 6 | 2 | 19560619 | 018 | 000000000 | 0060 |
| *22*025 6 | | | 008 | 036505585 | 0060 |
| *20*025 8 | 4 | 19560620 | 003 | 066353538 | 0060 |
| *22*025 8 | | | 031 | 124343680 | 0060 |
| *22*025 8 | | | 034 | 144214888 | 0070 |
| *22*025 8 | | | 033 | 168484079 | 0060 |
| *20*018 1 | 2 | 19560612 | 003 | 154210918 | 0060 |
| *22*018 1 | | | 025 | 221000916 | 0060 |
| *20*018 2 | 2 | 19560613 | 003 | 000000000 | 0090 |
| *22*018 2 | | | 031 | 038003171 | 0090 |
| *20*018 3 | 3 | 19560614 | 003 | 000000000 | 0060 |
| *22*018 3 | | | 031 | 038003414 | 0060 |
| *22*018 3 | | | 025 | 066390146 | 0060 |
| *20*018 4 | 3 | 19560614 | 003 | 000000000 | 0060 |
| *22*018 4 | | | 031 | 038003477 | 0060 |
| *22*018 4 | | | 025 | 066390118 | 0060 |
| *20*018 5 | 3 | 19560620 | 008 | 000000000 | 0060 |
| *22*018 5 | | | 003 | 055162415 | 0060 |
| *22*018 5 | | | 025 | 121552632 | 0060 |
| *20*026 2 | 2 | 19511115 | 010 | 000000000 | 0060 |
| *22*026 2 | | | 024 | 070584847 | 0060 |
| *20*026 3 | 2 | 19511115 | 008 | 000000000 | 0060 |
| *22*026 3 | | | 002 | 043245585 | 0060 |
| *20*026 4 | 2 | 19511202 | 001 | 038154069 | 0060 |
| *22*026 4 | | | 008 | 061045573 | 0060 |
| *20*026 5 | 2 | 19511202 | 001 | 038153887 | 0060 |
| *22*026 5 | | | 008 | 061045541 | 0060 |
| *20*026 6 | 2 | 19591022 | 003 | 000000000 | 0060 |
| *22*026 6 | | | 010 | 038101754 | 0060 |
| *20*026 7 | 2 | 19591022 | 003 | 000000000 | 0060 |
| *22*026 7 | | | 010 | 038101751 | 0060 |
| *20*026 8 | 2 | 19591022 | 010 | 000000000 | 0070 |
| *22*026 8 | | | 024 | 070584953 | 0070 |
| *20*026 9 | 2 | 19591023 | 010 | 000000000 | 0060 |
| *22*026 9 | | | 024 | 070584779 | 0060 |

| | | | | | | |
|---|---|---|---|---|---|---|
| *20*009 | 6 | 2 | 19511007 | 022 | 000000000 | 0060 |
| *22*009 | 6 | | | 030 | 029151729 | 0060 |
| *20*009 | 7 | 2 | 19511207 | 022 | 000000000 | 0090 |
| *22*009 | 7 | | | 030 | 029151833 | 0090 |
| *20*009 | 8 | 2 | 19511207 | 041 | 000000000 | 0060 |
| *22*009 | 8 | | | 030 | 055371887 | 0060 |
| *20*009 | 9 | 2 | 19511207 | 041 | 000000000 | 0060 |
| *22*009 | 9 | | | 030 | 055371800 | 0070 |
| *20*021 | 1 | 2 | 19511025 | 016 | 000000000 | 0060 |
| *22*021 | 1 | | | 028 | 009305929 | 0060 |
| *20*021 | 2 | 2 | 19511025 | 016 | 000000000 | 0060 |
| *22*021 | 2 | | | 028 | 009305957 | 0060 |
| *20*023 | 4 | 3 | 19511102 | 038 | 000000000 | 0060 |
| *22*023 | 4 | | | 022 | 083133978 | 0060 |
| *22*023 | 4 | | | 004 | 237441360 | 0060 |
| *20*023 | 5 | 2 | 19511102 | 038 | 000000000 | 0060 |
| *22*023 | 5 | | | 004 | 237441230 | 0060 |
| *20*023 | 6 | 3 | 19511202 | 038 | 000000000 | 0060 |
| *22*023 | 6 | | | 030 | 051180280 | 0060 |
| *22*023 | 6 | | | 022 | 083133985 | 0060 |
| *20*023 | 7 | 2 | 19511205 | 030 | 051175978 | 0060 |
| *22*023 | 7 | | | 022 | 083133848 | 0060 |
| *20*038 | 19 | 2 | 19511019 | 022 | 000000000 | 0170 |
| *22*038 | 19 | | | 021 | 077020670 | 0240 |
| *20*038 | 20 | 2 | 19511025 | 030 | 000000000 | 0060 |
| *22*038 | 20 | | | 021 | 150562980 | 0060 |
| *20*038 | 21 | 2 | 19511025 | 030 | 000000000 | 0060 |
| *22*038 | 22 | | | 021 | 150562991 | 0060 |
| *20*038 | 30 | 2 | 19511106 | 021 | 000000000 | 0060 |
| *22*038 | 30 | | | 023 | 308371704 | 0060 |
| *20*038 | 32 | 2 | 19511126 | 021 | 000000000 | 0060 |
| *22*038 | 32 | | | 028 | 046365528 | 0060 |
| *20*021 | 22 | 2 | 19511025 | 016 | 000000000 | 0060 |
| *22*021 | 22 | | | 038 | 137144468 | 0060 |
| *20*021 | 23 | 2 | 19511025 | 016 | 000000000 | 0060 |
| *22*021 | 23 | | | 038 | 137144442 | 0060 |
| *20*031 | 37 | 2 | 19560614 | 033 | 000000000 | 0060 |
| *22*031 | 37 | | | 025 | 087263475 | 0060 |
| *20*028 | 12 | 2 | 19630628 | 034 | 000000000 | 0060 |
| *22*028 | 12 | | | 043 | 073181887 | 0060 |
| *20*028 | 13 | 2 | 19630628 | 034 | 000000000 | 0060 |
| *22*028 | 13 | | | 043 | 073181706 | 0060 |
| *20*028 | 17 | 2 | 19640518 | 033 | 000000000 | 0070 |
| *22*028 | 17 | | | 034 | 043080526 | 0070 |
| *20*028 | 18 | 2 | 19640518 | 033 | 000000000 | 0140 |
| *22*028 | 18 | | | 029 | 199265590 | 0200 |
| *20*033 | 18 | 2 | 19600100 | 031 | 021350903 | 0120 |
| *22*033 | 18 | | | 034 | 076094243 | 0070 |
| *20*033 | 22 | 2 | 19640521 | 034 | 000000000 | 0070 |
| *22*033 | 22 | | | 028 | 089512839 | 0070 |
| *20*033 | 23 | 2 | 19640521 | 034 | 000000000 | 0070 |
| *22*033 | 23 | | | 028 | 089512791 | 0070 |
| *20*043 | 1 | 2 | 19630627 | 028 | 131094468 | 0060 |
| *22*043 | 1 | | | 034 | 188230036 | 0060 |
| *20*043 | 2 | 2 | 19630627 | 028 | 131094473 | 0060 |
| *22*043 | 2 | | | 034 | 188225968 | 0060 |
| *20*034 | 26 | 2 | 19601103 | 033 | 000000000 | 0070 |
| *22*034 | 26 | | | 031 | 078293856 | 0120 |
| *20*034 | 30 | 2 | 19630628 | 043 | 028213059 | 0060 |
| *22*034 | 30 | | | 028 | 077495925 | 0060 |
| *20*034 | 31 | 2 | 19630628 | 043 | 028213128 | 0060 |

| | | | | | |
|---|---|---|---|---|---|
| *22*034 31 | | | 028 | 077500019 | 0060 |
| *20*034 33 | 2 | 19630717 | 043 | 028213146 | 0060 |
| *22*034 33 | | | 028 | 077500097 | 0060 |
| *20*034 34 | 2 | 19640520 | 028 | 000000000 | 0070 |
| *22*034 34 | | | 033 | 047002696 | 0070 |
| *20*034 35 | 2 | 19640520 | 028 | 000000000 | 0070 |
| *22*034 35 | | | 033 | 047002751 | 0070 |
| *20*029 24 | 2 | 19630314 | 027 | 087500480 | 0070 |
| *22*029 24 | | | 028 | 345002380 | 0070 |

Table B-3

| | | | | |
|---|---|---|---|---|
| *52*031 | 710105 | 012 | 383502730X | 0380 |
| *52*500 | 710105 | 012 | 532822020X | 0510 |
| *52*500 | 710105 | 010 | 520302240X | 0520 |
| *52*031 | 710105 | 010 | 515338790X | 0510 |
| *52*008 | 710105 | 026 | 617203690X | 0610 |
| *52*008 | 710105 | 010 | 648590530X | 0640 |
| *52*010 | 710105 | 012 | 184949440X | 0180 |
| *52*010 | 710105 | 026 | 309305120X | 0300 |
| *52*500 | 710105 | 026 | 702871750X | 0700 |
| *52*500 | 710105 | 008 | 445505420X | 0440 |
| *52*500 | 710105 | 031 | 412689260X | 0410 |

Table B-4

| Date | Baseline | X | $\sigma_x$ | Y | $\sigma_y$ | Z | $\sigma_z$ | L | $\sigma_l$ | ID | SW |
|---|---|---|---|---|---|---|---|---|---|---|---|
| 86 06 16 | pver-aust | -1781678.7467 | 0.0682 | 790607.7371 | 0.0688 | 322539.7092 | 0.0484 | 1975720.5304 | 0.1085 | e167 | gps22 |
| 86 06 16 | pver-west | 21959.4287 | 0.0899 | 8333.9244 | 0.0651 | 25986.1293 | 0.0552 | 35027.8421 | 0.1240 | e167 | gps22 |
| 86 06 16 | pver-boul | 30080.7521 | 0.0973 | 42898.3728 | 0.1246 | 78336.1641 | 0.0663 | 94242.6477 | 0.1717 | e167 | gps22 |
| 86 06 16 | pver-ftdv | -1201260.9823 | 0.0006 | 662024.0659 | 0.0006 | 290843.4646 | 0.0006 | 1402103.3244 | 0.0006 | e167 | gps22 |
| 86 06 16 | pver-hayo | -4017862.8923 | 0.0006 | -212745.4428 | 0.0006 | -773932.2116 | 0.0006 | 4097249.5546 | 0.0006 | e167 | gps22 |
| 86 06 16 | pver-monu | -139163.4255 | 0.0893 | 132310.9557 | 0.0663 | 78002.7784 | 0.0558 | 207260.9019 | 0.1246 | e167 | gps22 |
| 86 06 16 | pver-mojl | -169028.3791 | 0.0006 | -23422.1099 | 0.0006 | -145575.4559 | 0.0006 | 224302.0319 | 0.0006 | e167 | gps22 |
| 86 06 16 | pver-nigu | -48432.1720 | 0.0670 | 41938.8659 | 0.0539 | 21078.1488 | 0.0434 | 67445.0304 | 0.0961 | e167 | gps22 |
| 86 06 16 | pver-pnft | -155816.8324 | 0.0719 | 91289.1448 | 0.0570 | 11770.6492 | 0.0465 | 180972.7642 | 0.1029 | e167 | gps22 |
| 86 06 16 | pver-rich | -3486771.2077 | 0.0006 | 1004022.6567 | 0.0006 | 782321.5281 | 0.0006 | 3711827.3025 | 0.0006 | e167 | gps22 |
| 86 06 16 | pver-twin | 102677.3545 | 0.0756 | -20848.5277 | 0.0670 | 47290.9603 | 0.0527 | 114951.0120 | 0.1141 | e167 | gps22 |
| 86 06 17 | vndn-aust | -1934297.5335 | 0.0583 | 935191.8683 | 0.0558 | 397080.2569 | 0.0391 | 2184894.3931 | 0.0893 | g168 | gps22 |
| 86 06 17 | vndn-west | -130659.4283 | 0.0639 | 152917.8931 | 0.0515 | 100526.7145 | 0.0403 | 224858.5968 | 0.0918 | g168 | gps22 |
| 86 06 17 | vndn-monu | -291782.2099 | 0.0676 | 276894.9616 | 0.0564 | 152543.3413 | 0.0422 | 430205.9376 | 0.0980 | g168 | gps22 |
| 86 06 17 | vndn-nigu | -201050.9759 | 0.0632 | 186522.7822 | 0.0527 | 95618.7612 | 0.0403 | 290439.6507 | 0.0918 | g168 | gps22 |
| 86 06 17 | vndn-otay | -249359.9650 | 0.0694 | 274408.0570 | 0.0570 | 180265.6440 | 0.0428 | 412281.3072 | 0.0998 | g168 | gps22 |
| 86 06 17 | vndn-pnft | -308435.6550 | 0.0651 | 235873.2222 | 0.0564 | 86311.1775 | 0.0428 | 397766.7025 | 0.0961 | g168 | gps22 |
| 86 06 17 | vndn-sdad | -221687.4850 | 0.0682 | 243402.6616 | 0.0558 | 158259.5476 | 0.0422 | 365289.3114 | 0.0980 | g168 | gps22 |
| 86 06 17 | vndn-ftdv | -1353879.7801 | 0.0006 | 806607.9908 | 0.0006 | 365384.0826 | 0.0006 | 1617749.1888 | 0.0006 | g168 | gps22 |
| 86 06 17 | vndn-hayo | -4170481.6907 | 0.0006 | -68161.5180 | 0.0006 | -699391.5940 | 0.0006 | 4229268.5096 | 0.0006 | g168 | gps22 |
| 86 06 17 | vndn-rich | -3639390.0064 | 0.0006 | 1148606.5824 | 0.0006 | 856862.1459 | 0.0006 | 3911351.3569 | 0.0006 | g168 | gps22 |
| 86 06 17 | vndn-pver | -152618.7975 | 0.0006 | 144583.9253 | 0.0006 | 74540.6184 | 0.0006 | 223054.5059 | 0.0006 | g168 | gps22 |
| 86 06 17 | vndn-twin | -49941.4932 | 0.0651 | 123735.5497 | 0.0527 | 121831.5155 | 0.0415 | 180686.3502 | 0.0936 | g168 | gps22 |
| 86 06 17 | vndn-boul | -122538.1683 | 0.0936 | 187482.3746 | 0.0967 | 152876.7799 | 0.0583 | 271176.2403 | 0.1469 | g168 | gps22 |
| 86 06 17 | vndn-mojl | -321647.1770 | 0.0006 | 121161.8155 | 0.0006 | -71034.8385 | 0.0006 | 350974.4154 | 0.0006 | g168 | gps22 |
| 86 06 18 | vndn-aust | -1934297.5009 | 0.0564 | 935191.8526 | 0.0577 | 397080.2555 | 0.0403 | 2184894.3573 | 0.0905 | f169 | gps22 |
| 86 06 18 | vndn-bouc | -262494.7874 | 0.1166 | 231944.8536 | 0.0601 | 111498.9826 | 0.0589 | 367605.7013 | 0.1438 | f169 | gps22 |
| 86 06 18 | vndn-west | -130659.4466 | 0.0645 | 152917.7141 | 0.0484 | 100526.8537 | 0.0409 | 224858.5480 | 0.0905 | f169 | gps22 |
| 86 06 18 | vndn-lajl | -222616.4283 | 0.0732 | 241982.0941 | 0.0539 | 155966.7913 | 0.0459 | 363921.7609 | 0.1017 | f169 | gps22 |
| 86 06 18 | vndn-monu | -291782.2386 | 0.0663 | 276894.9827 | 0.0527 | 152543.3544 | 0.0422 | 430205.9753 | 0.0949 | f169 | gps22 |
| 86 06 18 | vndn-twin | -49941.4451 | 0.0725 | 123735.5554 | 0.0564 | 121831.5421 | 0.0490 | 180686.3588 | 0.1042 | f169 | gps22 |
| 86 06 18 | vndn-otay | -249360.0580 | 0.0701 | 274408.0796 | 0.0533 | 180265.6906 | 0.0434 | 412281.3989 | 0.0980 | f169 | gps22 |
| 86 06 18 | vndn-ftdv | -1353879.7803 | 0.0000 | 806607.9909 | 0.0000 | 365384.0820 | 0.0000 | 1617749.1888 | 0.0000 | f169 | gps22 |
| 86 06 18 | vndn-hayo | -4170481.6904 | 0.0000 | -68161.5178 | 0.0000 | -699391.5942 | 0.0000 | 4229268.5094 | 0.0000 | f169 | gps22 |
| 86 06 18 | vndn-pver | -152618.7972 | 0.0000 | 144583.9247 | 0.0000 | 74540.6174 | 0.0000 | 223054.5049 | 0.0000 | f169 | gps22 |
| 86 06 18 | vndn-rich | -3639390.0058 | 0.0000 | 1148606.5817 | 0.0000 | 856862.1455 | 0.0000 | 3911351.3560 | 0.0000 | f169 | gps22 |
| 86 06 18 | vndn-bluf | -119385.8749 | 0.0905 | 183426.8218 | 0.0936 | 150120.4809 | 0.0595 | 265395.0732 | 0.1426 | f169 | gps22 |
| 86 06 18 | vndn-mojl | -321647.1768 | 0.0000 | 121161.8150 | 0.0000 | -71034.8386 | 0.0000 | 350974.4151 | 0.0000 | f169 | gps22 |

| | | | | | | | | | | | |
|---|---|---|---|---|---|---|---|---|---|---|---|
| 86 06 19 | vndn-west | -130659.4320 | 0.0570 | 152917.5692 | 0.0434 | 100526.8917 | 0.0366 | 224858.4579 | 0.0806 | d170 | gps22 |
| 86 06 19 | vndn-cuya | -277820.5495 | 0.0645 | 266332.0497 | 0.0508 | 147361.0989 | 0.0415 | 412107.1607 | 0.0918 | d170 | gps22 |
| 86 06 19 | vndn-moj1 | -321647.1767 | 0.0006 | 121161.8152 | 0.0006 | -71034.8386 | 0.0006 | 350974.4151 | 0.0006 | d170 | gps22 |
| 86 06 19 | vndn-twin | -49941.4705 | 0.0620 | 123735.2080 | 0.0477 | 121831.6964 | 0.0403 | 180686.2319 | 0.0880 | d170 | gps22 |
| 86 06 19 | vndn-pver | -152618.7981 | 0.0006 | 144583.9251 | 0.0006 | 74540.6174 | 0.0006 | 223054.5058 | 0.0006 | d170 | gps22 |
| 86 06 19 | vndn-sant | -222192.7599 | 0.0577 | 185380.3401 | 0.0552 | 76699.3644 | 0.0415 | 299363.1332 | 0.0899 | d170 | gps22 |
| 86 06 19 | vndn-yuma | -481293.6054 | 0.0657 | 361884.9373 | 0.0564 | 149002.2428 | 0.0446 | 620327.2610 | 0.0973 | d170 | gps22 |
| 86 06 19 | vndn-ftdv | -1353879.7803 | 0.0006 | 806607.9909 | 0.0006 | 365384.0820 | 0.0006 | 1617749.1888 | 0.0006 | d170 | gps22 |
| 86 06 19 | vndn-rich | -3639390.0058 | 0.0006 | 1148606.5817 | 0.0006 | 856862.1455 | 0.0006 | 3911351.3560 | 0.0006 | d170 | gps22 |
| 86 12 29 | vndn-algo | -3596199.3110 | 0.0006 | -179389.8474 | 0.0006 | -964556.6846 | 0.0006 | 3727626.5639 | 0.0006 | d363 | gps22 |
| 86 12 29 | vndn-blan | 15869.6104 | 0.0316 | -91987.7991 | 0.0273 | -100575.7519 | 0.0223 | 137219.1006 | 0.0471 | d363 | gps22 |
| 86 12 29 | vndn-blhl | -9063.1592 | 0.0298 | -53779.9964 | 0.0260 | -73063.7374 | 0.0217 | 91174.2211 | 0.0446 | d363 | gps22 |
| 86 12 29 | vndn-cent | -50916.2543 | 0.0304 | 70573.0683 | 0.0273 | 51237.4180 | 0.0217 | 100986.6126 | 0.0459 | d363 | gps22 |
| 86 12 29 | vndn-cotr | -103066.3620 | 0.0310 | 90676.9443 | 0.0273 | 39955.3389 | 0.0217 | 142973.4671 | 0.0471 | d363 | gps22 |
| 86 12 29 | vndn-fibr | -123397.5248 | 0.0285 | 9472.0553 | 0.0254 | -76598.1364 | 0.0211 | 145547.0490 | 0.0434 | d363 | gps22 |
| 86 12 29 | vndn-ftor | 18955.0948 | 0.0006 | -171058.4915 | 0.0006 | -190650.1890 | 0.0006 | 256841.9703 | 0.0006 | d363 | gps22 |
| 86 12 29 | vndn-losp | -11450.2809 | 0.0285 | -17552.3681 | 0.0254 | -31041.7551 | 0.0205 | 37453.7731 | 0.0434 | d363 | gps22 |
| 86 12 29 | vndn-madc | -59573.2790 | 0.0285 | -2326.1158 | 0.0254 | -47858.9889 | 0.0205 | 76451.7443 | 0.0428 | d363 | gps22 |
| 86 12 29 | vndn-ovro | -267649.2059 | 0.0006 | -47649.1492 | 0.0006 | -241259.3565 | 0.0006 | 363472.9920 | 0.0006 | d363 | gps22 |
| 86 12 29 | vndn-plat | -1437363.5316 | 0.0006 | 195002.5429 | 0.0006 | -497054.2139 | 0.0006 | 1533330.6249 | 0.0006 | d363 | gps22 |
| 86 12 30 | vndn-algo | -3596199.3113 | 0.0006 | -179389.8470 | 0.0006 | -964556.6850 | 0.0006 | 3727626.5642 | 0.0006 | d364 | gps22 |
| 86 12 30 | vndn-blan | 15869.6201 | 0.0409 | -91987.7891 | 0.0347 | -100575.7575 | 0.0291 | 137219.0992 | 0.0614 | d364 | gps22 |
| 86 12 30 | vndn-blhl | -9063.1558 | 0.0384 | -53779.9927 | 0.0335 | -73063.7370 | 0.0273 | 91174.2183 | 0.0583 | d364 | gps22 |
| 86 12 30 | vndn-cent | -50916.2442 | 0.0391 | 70573.0810 | 0.0347 | 51237.4053 | 0.0273 | 100986.6099 | 0.0595 | d364 | gps22 |
| 86 12 30 | vndn-cotr | -103066.3904 | 0.0403 | 90676.9253 | 0.0360 | 39955.3600 | 0.0285 | 142973.4815 | 0.0608 | d364 | gps22 |
| 86 12 30 | vndn-fibr | -123397.5172 | 0.0372 | 9472.0470 | 0.0329 | -76598.1271 | 0.0267 | 145547.0371 | 0.0564 | d364 | gps22 |
| 86 12 30 | vndn-ftor | 18955.0947 | 0.0006 | -171058.4924 | 0.0006 | -190650.1890 | 0.0006 | 256841.9709 | 0.0006 | d364 | gps22 |
| 86 12 30 | vndn-lacu | -69188.5257 | 0.0378 | 45831.5444 | 0.0335 | 4986.9953 | 0.0267 | 83141.1611 | 0.0570 | d364 | gps22 |
| 86 12 30 | vndn-losp | -11450.2766 | 0.0366 | -17552.3528 | 0.0322 | -31041.7634 | 0.0260 | 37453.7715 | 0.0552 | d364 | gps22 |
| 86 12 30 | vndn-ovro | -267649.2056 | 0.0006 | -47649.1496 | 0.0006 | -241259.3563 | 0.0006 | 363472.9917 | 0.0006 | d364 | gps22 |
| 86 12 30 | vndn-plat | -1437363.5316 | 0.0006 | 195002.5429 | 0.0006 | -497054.2139 | 0.0006 | 1533330.6249 | 0.0006 | d364 | gps22 |
| 86 12 31 | vndn-algo | -3596199.3112 | 0.0006 | -179389.8469 | 0.0006 | -964556.6855 | 0.0006 | 3727626.5643 | 0.0006 | d365 | gps22 |
| 86 12 31 | vndn-blan | 15869.6638 | 0.0304 | -91987.7588 | 0.0260 | -100575.7976 | 0.0217 | 137219.1133 | 0.0453 | d365 | gps22 |
| 86 12 31 | vndn-blhl | -9063.1390 | 0.0285 | -53779.9858 | 0.0254 | -73063.7531 | 0.0205 | 91174.2254 | 0.0434 | d365 | gps22 |
| 86 12 31 | vndn-cent | -50916.2586 | 0.0291 | 70573.0894 | 0.0260 | 51237.4173 | 0.0205 | 100986.6292 | 0.0446 | d365 | gps22 |
| 86 12 31 | vndn-cotr | -103066.4236 | 0.0304 | 90676.9022 | 0.0267 | 39955.3946 | 0.0217 | 142973.5004 | 0.0459 | d365 | gps22 |
| 86 12 31 | vndn-fibr | -123397.5205 | 0.0279 | 9472.0465 | 0.0248 | -76598.1276 | 0.0198 | 145547.0401 | 0.0422 | d365 | gps22 |
| 86 12 31 | vndn-ftor | 18955.0950 | 0.0006 | -171058.4918 | 0.0006 | -190650.1900 | 0.0006 | 256841.9713 | 0.0006 | d365 | gps22 |
| 86 12 31 | vndn-lacu | -69188.5448 | 0.0279 | 45831.5342 | 0.0254 | 4987.0162 | 0.0198 | 83141.1726 | 0.0428 | d365 | gps22 |
| 86 12 31 | vndn-ovro | -267649.2056 | 0.0006 | -47649.1496 | 0.0006 | -241259.3567 | 0.0006 | 363472.9920 | 0.0006 | d365 | gps22 |
| 86 12 31 | vndn-plat | -1437363.5315 | 0.0006 | 195002.5429 | 0.0006 | -497054.2144 | 0.0006 | 1533330.6250 | 0.0006 | d365 | gps22 |
| 87 01 01 | vndn-algo | -3596199.3112 | 0.0006 | -179389.8464 | 0.0006 | -964556.6857 | 0.0006 | 3727626.5643 | 0.0006 | d001 | gps22 |

| | | | | | | | | | | | | |
|---|---|---|---|---|---|---|---|---|---|---|---|---|
| 87 | 01 | 01 | vndn-blan | 15869.6775 | 0.0304 | -91987.8218 | 0.0260 | -100575.7788 | 0.0217 | 137219.1433 | 0.0459 d001 | gps22 |
| 87 | 01 | 01 | vndn-blhl | -9063.1191 | 0.0285 | -53779.9498 | 0.0248 | -73063.7691 | 0.0205 | 91174.2150 | 0.0434 d001 | gps22 |
| 87 | 01 | 01 | vndn-cent | -50916.2434 | 0.0291 | 70573.1318 | 0.0260 | 51237.3755 | 0.0205 | 100986.6299 | 0.0440 d001 | gps22 |
| 87 | 01 | 01 | vndn-cotr | -103066.3715 | 0.0298 | 90676.9738 | 0.0267 | 39955.3272 | 0.0211 | 142973.4894 | 0.0453 d001 | gps22 |
| 87 | 01 | 01 | vndn-fibr | -123397.5011 | 0.0273 | 9472.0741 | 0.0248 | -76598.1458 | 0.0198 | 145547.0350 | 0.0422 d001 | gps22 |
| 87 | 01 | 01 | vndn-ftor | 18955.0948 | 0.0006 | -171058.4914 | 0.0006 | -190650.1901 | 0.0006 | 256841.9711 | 0.0006 d001 | gps22 |
| 87 | 01 | 01 | vndn-lacu | -69188.5320 | 0.0279 | 45831.5764 | 0.0248 | 4986.9851 | 0.0198 | 83141.1834 | 0.0422 d001 | gps22 |
| 87 | 01 | 01 | vndn-losp | -11450.2093 | 0.0273 | -17552.2054 | 0.0242 | -31041.8631 | 0.0198 | 37453.7645 | 0.0415 d001 | gps22 |
| 87 | 01 | 01 | vndn-madc | -59573.2699 | 0.0273 | -2326.0828 | 0.0242 | -47858.9993 | 0.0198 | 76451.7427 | 0.0415 d001 | gps22 |
| 87 | 01 | 01 | vndn-ovro | -267649.2056 | 0.0006 | -47649.1490 | 0.0006 | -241259.3569 | 0.0006 | 363472.9920 | 0.0006 d001 | gps22 |
| 87 | 01 | 01 | vndn-plat | -1437363.5315 | 0.0006 | 195002.5435 | 0.0006 | -497054.2146 | 0.0006 | 1533330.6251 | 0.0006 d001 | gps22 |
| 87 | 01 | 02 | vndn-algo | -3596199.3112 | 0.0006 | -179389.8464 | 0.0006 | -964556.6857 | 0.0006 | 3727626.5643 | 0.0006 c002 | gps22 |
| 87 | 01 | 02 | vndn-blan | 15869.6406 | 0.0378 | -91987.8436 | 0.0285 | -100575.7613 | 0.0242 | 137219.1409 | 0.0533 c002 | gps22 |
| 87 | 01 | 02 | vndn-blhl | -9063.1680 | 0.0353 | -53779.9735 | 0.0273 | -73063.7425 | 0.0229 | 91174.2125 | 0.0502 c002 | gps22 |
| 87 | 01 | 02 | vndn-cent | -50916.2285 | 0.0366 | 70573.1684 | 0.0279 | 51237.3642 | 0.0229 | 100986.6423 | 0.0515 c002 | gps22 |
| 87 | 01 | 02 | vndn-cotr | -103066.3459 | 0.0372 | 90677.0347 | 0.0285 | 39955.2946 | 0.0236 | 142973.5005 | 0.0527 c002 | gps22 |
| 87 | 01 | 02 | vndn-fibr | -123397.4927 | 0.0341 | 9472.1126 | 0.0267 | -76598.1711 | 0.0223 | 145547.0437 | 0.0484 c002 | gps22 |
| 87 | 01 | 02 | vndn-ftor | 18955.0955 | 0.0006 | -171058.4915 | 0.0006 | -190650.1897 | 0.0006 | 256841.9709 | 0.0006 c002 | gps22 |
| 87 | 01 | 02 | vndn-lacu | -69188.5097 | 0.0353 | 45831.6208 | 0.0267 | 4986.9612 | 0.0223 | 83141.1879 | 0.0496 c002 | gps22 |
| 87 | 01 | 02 | vndn-madc | -59573.2702 | 0.0341 | -2326.0797 | 0.0267 | -47859.0024 | 0.0223 | 76451.7447 | 0.0484 c002 | gps22 |
| 87 | 01 | 02 | vndn-ovro | -267649.2056 | 0.0006 | -47649.1490 | 0.0006 | -241259.3569 | 0.0006 | 363472.9920 | 0.0006 c002 | gps22 |
| 87 | 01 | 02 | vndn-plat | -1437363.5315 | 0.0006 | 195002.5435 | 0.0006 | -497054.2146 | 0.0006 | 1533330.6251 | 0.0006 c002 | gps22 |
| 87 | 01 | 03 | vndn-algo | -3596199.3109 | 0.0000 | -179389.8472 | 0.0000 | -964556.6854 | 0.0000 | 3727626.5640 | 0.0000 c003 | gps22 |
| 87 | 01 | 03 | vndn-brus | -142535.9552 | 0.0477 | 162974.2139 | 0.0415 | 105450.8962 | 0.0329 | 240825.6307 | 0.0713 c003 | gps22 |
| 87 | 01 | 03 | vndn-chaf | -94195.8814 | 0.0397 | 73137.6094 | 0.0360 | 23211.6142 | 0.0291 | 121493.8394 | 0.0614 c003 | gps22 |
| 87 | 01 | 03 | vndn-devl | -49317.4899 | 0.0415 | 67509.4675 | 0.0384 | 47909.5292 | 0.0304 | 96359.0473 | 0.0639 c003 | gps22 |
| 87 | 01 | 03 | vndn-fibr | -123397.4948 | 0.0384 | 9472.0264 | 0.0341 | -76598.1181 | 0.0279 | 145547.0120 | 0.0583 c003 | gps22 |
| 87 | 01 | 03 | vndn-ftor | 18955.0951 | 0.0000 | -171058.4922 | 0.0000 | -190650.1894 | 0.0000 | 256841.9711 | 0.0000 c003 | gps22 |
| 87 | 01 | 03 | vndn-gavi | -31016.2188 | 0.0378 | 22865.3265 | 0.0341 | 4565.9261 | 0.0273 | 38803.0497 | 0.0577 c003 | gps22 |
| 87 | 01 | 03 | vndn-lacu | -69188.4881 | 0.0384 | 45831.5869 | 0.0341 | 4986.9719 | 0.0273 | 83141.1519 | 0.0583 c003 | gps22 |
| 87 | 01 | 03 | vndn-ovro | -267649.2052 | 0.0000 | -47649.1499 | 0.0000 | -241259.3567 | 0.0000 | 363472.9917 | 0.0000 c003 | gps22 |
| 87 | 01 | 03 | vndn-plat | -1437363.5312 | 0.0000 | 195002.5426 | 0.0000 | -497054.2143 | 0.0000 | 1533330.6246 | 0.0000 c003 | gps22 |
| 87 | 01 | 03 | vndn-pver | -152618.7969 | 0.0000 | 144583.9248 | 0.0000 | 74540.6180 | 0.0000 | 223054.5050 | 0.0000 c003 | gps22 |
| 87 | 01 | 04 | vndn-algo | -3596199.3109 | 0.0000 | -179389.8472 | 0.0000 | -964556.6854 | 0.0000 | 3727626.5640 | 0.0000 c004 | gps22 |
| 87 | 01 | 04 | vndn-brus | -142536.0980 | 0.0663 | 162974.2023 | 0.0564 | 105451.0155 | 0.0446 | 240825.7597 | 0.0980 c004 | gps22 |
| 87 | 01 | 04 | vndn-devl | -49317.5943 | 0.0539 | 67509.4388 | 0.0477 | 47909.6038 | 0.0378 | 96359.1178 | 0.0812 c004 | gps22 |
| 87 | 01 | 04 | vndn-fibr | -123397.5403 | 0.0515 | 9472.0301 | 0.0459 | -76598.1219 | 0.0372 | 145547.0528 | 0.0781 c004 | gps22 |
| 87 | 01 | 04 | vndn-ftor | 18955.0958 | 0.0000 | -171058.4926 | 0.0000 | -190650.1900 | 0.0000 | 256841.9718 | 0.0000 c004 | gps22 |
| 87 | 01 | 04 | vndn-gavi | -31016.2196 | 0.0502 | 22865.3417 | 0.0446 | 4565.9136 | 0.0360 | 38803.0578 | 0.0763 c004 | gps22 |
| 87 | 01 | 04 | vndn-lacu | -69188.5707 | 0.0515 | 45831.5604 | 0.0459 | 4987.0236 | 0.0366 | 83141.2091 | 0.0781 c004 | gps22 |
| 87 | 01 | 04 | vndn-ovro | -267649.2051 | 0.0000 | -47649.1495 | 0.0000 | -241259.3573 | 0.0000 | 363472.9920 | 0.0000 c004 | gps22 |
| 87 | 01 | 04 | vndn-plat | -1437363.5312 | 0.0000 | 195002.5426 | 0.0000 | -497054.2143 | 0.0000 | 1533330.6246 | 0.0000 c004 | gps22 |

| | | | | | | | | | | | |
|---|---|---|---|---|---|---|---|---|---|---|---|
| 87 01 04 | vndn-pver | -152618.7971 | 0.0000 | 144583.9239 | 0.0000 | 74540.6180 | 0.0000 | 223054.5046 | 0.0000 | c004 | gps22 |
| 87 01 04 | vndn-sole | -21279.9368 | 0.0533 | 56708.8390 | 0.0477 | 55253.5541 | 0.0378 | 81985.8730 | 0.0806 | c004 | gps22 |
| 87 01 04 | vndn-soli | -93313.6733 | 0.0533 | 72503.1279 | 0.0471 | 23600.1639 | 0.0378 | 120503.5805 | 0.0806 | c004 | gps22 |
| 87 01 05 | vndn-algo | -3596199.3110 | 0.0000 | -179389.8468 | 0.0000 | -964556.6856 | 0.0000 | 3727626.5641 | 0.0000 | d005 | gps22 |
| 87 01 05 | vndn-brus | -142535.9513 | 0.0546 | 162974.1479 | 0.0484 | 105450.9568 | 0.0378 | 240825.6103 | 0.0825 | d005 | gps22 |
| 87 01 05 | vndn-devl | -49317.4740 | 0.0515 | 67509.4470 | 0.0459 | 47909.5433 | 0.0378 | 96359.0319 | 0.0781 | d005 | gps22 |
| 87 01 05 | vndn-fibr | -123397.5556 | 0.0453 | 9472.0443 | 0.0403 | -76598.1185 | 0.0329 | 145547.0649 | 0.0688 | d005 | gps22 |
| 87 01 05 | vndn-ftor | 18955.0956 | 0.0000 | -171058.4917 | 0.0000 | -190650.1898 | 0.0000 | 256841.9711 | 0.0000 | d005 | gps22 |
| 87 01 05 | vndn-gavi | -31016.1724 | 0.0508 | 22865.3432 | 0.0434 | 4565.8994 | 0.0353 | 38803.0193 | 0.0756 | d005 | gps22 |
| 87 01 05 | vndn-lacu | -69188.5415 | 0.0453 | 45831.5522 | 0.0409 | 4987.0159 | 0.0329 | 83141.1798 | 0.0694 | d005 | gps22 |
| 87 01 05 | vndn-ovro | -267649.2052 | 0.0000 | -47649.1490 | 0.0000 | -241259.3575 | 0.0000 | 363472.9921 | 0.0000 | d005 | gps22 |
| 87 01 05 | vndn-plat | -1437363.5313 | 0.0000 | 195002.5431 | 0.0000 | -497054.2145 | 0.0000 | 1533330.6248 | 0.0000 | d005 | gps22 |
| 87 01 05 | vndn-pver | -152618.7975 | 0.0000 | 144583.9251 | 0.0000 | 74540.6174 | 0.0000 | 223054.5055 | 0.0000 | d005 | gps22 |
| 87 01 05 | vndn-sole | -21279.8192 | 0.0471 | 56708.8635 | 0.0422 | 55253.4940 | 0.0335 | 81985.8189 | 0.0713 | d005 | gps22 |
| 87 01 05 | vndn-soli | -93313.6150 | 0.0465 | 72503.1379 | 0.0415 | 23600.1258 | 0.0335 | 120503.5339 | 0.0713 | d005 | gps22 |
| 87 01 06 | pver-algo | -3443580.5139 | 0.0000 | -323973.7716 | 0.0000 | -1039097.3028 | 0.0000 | 3611499.5452 | 0.0000 | d006 | gps22 |
| 87 01 06 | pver-brus | 10082.8443 | 0.0372 | 18390.3289 | 0.0341 | 30910.2801 | 0.0267 | 37353.8935 | 0.0570 | d006 | gps22 |
| 87 01 06 | pver-devl | 103301.2815 | 0.0384 | -77074.4288 | 0.0341 | -26631.0637 | 0.0273 | 131608.6467 | 0.0583 | d006 | gps22 |
| 87 01 06 | pver-fibr | 29221.2850 | 0.0397 | -135111.8269 | 0.0353 | -151138.7625 | 0.0291 | 204821.9099 | 0.0608 | d006 | gps22 |
| 87 01 06 | pver-ftor | 171573.8928 | 0.0000 | -315642.4171 | 0.0000 | -265190.8067 | 0.0000 | 446535.4410 | 0.0000 | d006 | gps22 |
| 87 01 06 | pver-lacu | 83430.2982 | 0.0384 | -98752.3108 | 0.0341 | -69553.6353 | 0.0279 | 146800.3465 | 0.0583 | d006 | gps22 |
| 87 01 06 | pver-ovro | -115030.4081 | 0.0000 | -192233.0739 | 0.0000 | -315799.9747 | 0.0000 | 387188.8086 | 0.0000 | d006 | gps22 |
| 87 01 06 | pver-plat | -1284744.7342 | 0.0000 | 50418.6182 | 0.0000 | -571594.8317 | 0.0000 | 1407064.9312 | 0.0000 | d006 | gps22 |
| 87 01 06 | pver-sole | 131338.9542 | 0.0397 | -87875.0060 | 0.0353 | -19287.1265 | 0.0285 | 159197.7727 | 0.0601 | d006 | gps22 |
| 87 01 06 | pver-soli | 59305.2260 | 0.0378 | -72080.6950 | 0.0341 | -50940.5477 | 0.0273 | 106337.5560 | 0.0577 | d006 | gps22 |
| 87 01 06 | pver-vndn | 152618.7971 | 0.0000 | -144583.9249 | 0.0000 | -74540.6172 | 0.0000 | 223054.5049 | 0.0000 | d006 | gps22 |
| 87 01 06 | pver-vlsr | 152647.1798 | 0.0000 | -144578.8969 | 0.0000 | -74512.0703 | 0.0000 | 223061.1297 | 0.0000 | d006 | gps22 |
| 87 01 07 | vndn-algo | -3596199.3110 | 0.0000 | -179389.8468 | 0.0000 | -964556.6856 | 0.0000 | 3727626.5641 | 0.0000 | d007 | gps22 |
| 87 01 07 | vndn-brus | -142535.9663 | 0.1215 | 162974.1716 | 0.0707 | 105450.9028 | 0.0515 | 240825.6116 | 0.1494 | d007 | gps22 |
| 87 01 07 | vndn-devl | -49317.5015 | 0.0391 | 67509.4619 | 0.0347 | 47909.5356 | 0.0279 | 96359.0525 | 0.0595 | d007 | gps22 |
| 87 01 07 | vndn-fibr | -123397.5249 | 0.0378 | 9472.0400 | 0.0335 | -76598.1262 | 0.0273 | 145547.0427 | 0.0570 | d007 | gps22 |
| 87 01 07 | vndn-ftor | 18955.0951 | 0.0000 | -171058.4918 | 0.0000 | -190650.1902 | 0.0000 | 256841.9714 | 0.0000 | d007 | gps22 |
| 87 01 07 | vndn-lacu | -69188.4748 | 0.0378 | 45831.5844 | 0.0335 | 4986.9668 | 0.0273 | 83141.1391 | 0.0577 | d007 | gps22 |
| 87 01 07 | vndn-mill | -29088.5947 | 0.0378 | 20540.3707 | 0.0341 | 4163.0454 | 0.0273 | 35852.2540 | 0.0577 | d007 | gps22 |
| 87 01 07 | vndn-ovro | -267649.2052 | 0.0000 | -47649.1490 | 0.0000 | -241259.3575 | 0.0000 | 363472.9921 | 0.0000 | d007 | gps22 |
| 87 01 07 | vndn-plat | -1437363.5313 | 0.0000 | 195002.5431 | 0.0000 | -497054.2145 | 0.0000 | 1533330.6248 | 0.0000 | d007 | gps22 |
| 87 01 07 | vndn-pver | -152618.7972 | 0.0000 | 144583.9244 | 0.0000 | 74540.6177 | 0.0000 | 223054.5048 | 0.0000 | d007 | gps22 |
| 87 01 07 | vndn-sole | -21279.8167 | 0.0391 | 56708.8867 | 0.0347 | 55253.4701 | 0.0279 | 81985.8182 | 0.0595 | d007 | gps22 |
| 87 01 07 | vndn-soli | -93313.6211 | 0.0391 | 72503.1237 | 0.0347 | 23600.1219 | 0.0279 | 120503.5294 | 0.0589 | d007 | gps22 |
| 87 09 23 | vndn-blhl | -9063.1961 | 0.0391 | -53780.0511 | 0.0366 | -73063.6951 | 0.0291 | 91174.2231 | 0.0608 | c266 | gps22 |
| 87 09 23 | vndn-cent | -50916.2472 | 0.0775 | 70573.0347 | 0.0632 | 51237.4486 | 0.0378 | 100986.6010 | 0.1066 | c266 | gps22 |
| 87 09 23 | vndn-ftor | 18955.0949 | 0.0006 | -171058.4923 | 0.0006 | -190650.1895 | 0.0006 | 256841.9712 | 0.0006 | c266 | gps22 |

| | | | | | | | | | | | |
|---|---|---|---|---|---|---|---|---|---|---|---|
| 87 09 23 | vndn-moja | -321856.9819 | 0.0006 | 121282.2216 | 0.0006 | -71033.0026 | 0.0006 | 351207.8894 | 0.0006 | c266 | gps22 |
| 87 09 23 | vndn-ovro | -267649.2066 | 0.0006 | -47649.1488 | 0.0006 | -241259.3576 | 0.0006 | 363472.9932 | 0.0006 | c266 | gps22 |
| 87 09 23 | vndn-pver | -152618.7978 | 0.0006 | 144583.9246 | 0.0006 | 74540.6170 | 0.0006 | 223054.5052 | 0.0006 | c266 | gps22 |
| 87 09 23 | vndn-scrw | -40197.6532 | 0.0570 | 58619.3951 | 0.0477 | 44151.9179 | 0.0335 | 83674.8269 | 0.0818 | c266 | gps22 |
| 87 09 23 | vndn-wsfd | -4170304.6809 | 0.0006 | -67360.1484 | 0.0006 | -698618.3306 | 0.0006 | 4228953.3094 | 0.0006 | c266 | gps22 |
| 87 09 24 | vndn-blhl | -9063.1766 | 0.0360 | -53780.0399 | 0.0335 | -73063.7096 | 0.0267 | 91174.2262 | 0.0564 | a267 | gps22 |
| 87 09 24 | vndn-cent | -50916.2376 | 0.0378 | 70573.0622 | 0.0335 | 51237.4335 | 0.0267 | 100986.6078 | 0.0570 | a267 | gps22 |
| 87 09 24 | vndn-ftor | 18955.0945 | 0.0006 | -171058.4922 | 0.0006 | -190650.1893 | 0.0006 | 256841.9710 | 0.0006 | a267 | gps22 |
| 87 09 24 | vndn-moja | -321856.9816 | 0.0006 | 121282.2217 | 0.0006 | -71033.0019 | 0.0006 | 351207.8890 | 0.0006 | a267 | gps22 |
| 87 09 24 | vndn-ovro | -267649.2063 | 0.0006 | -47649.1487 | 0.0006 | -241259.3569 | 0.0006 | 363472.9925 | 0.0006 | a267 | gps22 |
| 87 09 24 | vndn-plat | -1437363.5314 | 0.0006 | 195002.5431 | 0.0006 | -497054.2133 | 0.0006 | 1533330.6245 | 0.0006 | a267 | gps22 |
| 87 09 24 | vndn-pver | -152618.7976 | 0.0006 | 144583.9250 | 0.0006 | 74540.6184 | 0.0006 | 223054.5058 | 0.0006 | a267 | gps22 |
| 87 09 24 | vndn-scrw | -40197.6029 | 0.0558 | 58619.3888 | 0.0403 | 44151.9374 | 0.0285 | 83674.8086 | 0.0744 | a267 | gps22 |
| 87 09 24 | vndn-wsfd | -4170304.6806 | 0.0006 | -67360.1483 | 0.0006 | -698618.3299 | 0.0006 | 4228953.3090 | 0.0006 | a267 | gps22 |
| 87 09 26 | vndn-blhl | -9063.2172 | 0.0428 | -53780.1286 | 0.0322 | -73063.6390 | 0.0298 | 91174.2260 | 0.0614 | a269 | gps22 |
| 87 09 26 | vndn-ftor | 18955.0958 | 0.0006 | -171058.4921 | 0.0006 | -190650.1897 | 0.0006 | 256841.9713 | 0.0006 | a269 | gps22 |
| 87 09 26 | vndn-moja | -321856.9810 | 0.0006 | 121282.2215 | 0.0006 | -71033.0026 | 0.0006 | 351207.8885 | 0.0006 | a269 | gps22 |
| 87 09 26 | vndn-plat | -1437363.5308 | 0.0006 | 195002.5428 | 0.0006 | -497054.2140 | 0.0006 | 1533330.6242 | 0.0006 | a269 | gps22 |
| 87 09 26 | vndn-pver | -152618.7969 | 0.0006 | 144583.9245 | 0.0006 | 74540.6176 | 0.0006 | 223054.5047 | 0.0006 | a269 | gps22 |
| 87 09 26 | vndn-scre | -67996.1599 | 0.1079 | 75705.9510 | 0.0539 | 45914.5172 | 0.0589 | 111637.8595 | 0.1339 | a269 | gps22 |
| 87 09 26 | vndn-wsfd | -4170304.6800 | 0.0006 | -67360.1485 | 0.0006 | -698618.3306 | 0.0006 | 4228953.3085 | 0.0006 | a269 | gps22 |
| 87 09 27 | cent-moja | -270940.7384 | 0.0006 | 50709.1174 | 0.0006 | -122270.4021 | 0.0006 | 301546.5960 | 0.0006 | a270 | gps22 |
| 87 09 27 | cent-scre | -17080.0040 | 0.0477 | 5132.9415 | 0.0384 | -5322.8756 | 0.0279 | 18612.0023 | 0.0676 | a270 | gps22 |
| 87 09 27 | cent-wsfd | -4119388.4374 | 0.0006 | -137933.2526 | 0.0006 | -749855.7301 | 0.0006 | 4189352.0139 | 0.0006 | a270 | gps22 |
| 87 09 27 | cent-yknf | -1403091.0194 | 0.0006 | -1906191.7906 | 0.0006 | -2087242.4571 | 0.0006 | 3155758.6450 | 0.0006 | a270 | gps22 |
| 87 09 29 | lacu-vndn | 69188.5682 | 0.0555 | -45831.5266 | 0.0735 | -4987.0268 | 0.0555 | 83141.1886 | 0.1076 | | gipsy |
| 87 09 29 | sba2-lacu | -2586.2320 | 0.0589 | -4005.0647 | 0.0852 | -8826.6759 | 0.0642 | 10031.9164 | 0.1218 | | gipsy |
| 87 09 29 | sba2-vndn | 66602.3362 | 0.0629 | -49836.5913 | 0.0893 | -13813.7027 | 0.0676 | 84323.0419 | 0.1283 | | gipsy |
| 87 09 29 | sba2-cstl | 597.4081 | 0.0877 | -112488.9352 | 0.1101 | -139852.8626 | 0.0747 | 179479.6384 | 0.1593 | | gipsy |
| 87 09 29 | lacu-cstl | 3183.6401 | 0.0738 | -108483.8705 | 0.0936 | -131026.1867 | 0.0617 | 170137.4365 | 0.1342 | | gipsy |
| 87 10 01 | soli-chaf | -882.2422 | 0.0273 | 634.5629 | 0.0236 | -388.5513 | 0.0186 | 1154.1202 | 0.0409 | b274 | gps22 |
| 87 10 01 | soli-gras | 71909.8824 | 0.0391 | -72320.0069 | 0.0310 | -39703.1420 | 0.0248 | 109442.0124 | 0.0558 | b274 | gps22 |
| 87 10 01 | soli-moja | -228543.3634 | 0.0000 | 48779.0797 | 0.0000 | -94633.1219 | 0.0000 | 252124.7614 | 0.0000 | b274 | gps22 |
| 87 10 01 | soli-vndn | 93313.6185 | 0.0000 | -72503.1424 | 0.0000 | -23600.1196 | 0.0000 | 120503.5381 | 0.0000 | b274 | gps22 |
| 87 10 01 | soli-wsfd | -4076991.0624 | 0.0000 | -139863.2903 | 0.0000 | -722218.4499 | 0.0000 | 4142827.2173 | 0.0000 | b274 | gps22 |
| 87 10 05 | pver-cato | 21204.5317 | 0.0657 | -34955.8570 | 0.0502 | -31909.3823 | 0.0459 | 51862.8266 | 0.0949 | a278 | gps22 |
| 87 10 05 | pver-love | -622.7175 | 0.0552 | -52344.1757 | 0.0490 | -69480.3463 | 0.0397 | 86993.2126 | 0.0843 | a278 | gps22 |
| 87 10 05 | pver-safe | -921.7872 | 0.0738 | -39976.9796 | 0.0533 | -54509.7850 | 0.0484 | 67604.1807 | 0.1035 | a278 | gps22 |
| 87 10 06 | pver-cato | 21204.6174 | 0.0341 | -34955.4599 | 0.0316 | -31909.6921 | 0.0248 | 51862.7846 | 0.0533 | a279 | gps22 |
| 87 10 06 | pver-love | -622.7769 | 0.0477 | -52344.1889 | 0.0384 | -69480.3523 | 0.0316 | 86993.2257 | 0.0688 | a279 | gps22 |
| 87 10 06 | pver-ptdu | 25096.9977 | 0.0465 | -31883.3120 | 0.0329 | -23719.6640 | 0.0248 | 47000.2908 | 0.0620 | a279 | gps22 |
| 87 10 06 | pver-safe | -921.7911 | 0.0335 | -39976.9356 | 0.0304 | -54509.8035 | 0.0242 | 67604.1696 | 0.0515 | a279 | gps22 |

| | | | | | | | | | | | |
|---|---|---|---|---|---|---|---|---|---|---|---|
| 87 10 07 | pver-hapy | 18155.3011 | 0.0657 | -52806.2266 | 0.0552 | -56787.3759 | 0.0353 | 79642.4422 | 0.0930 | a280 | gps22 |
| 87 10 07 | pver-hopp | 16040.0676 | 0.0589 | -59578.3723 | 0.1097 | -68129.7427 | 0.0477 | 91915.8748 | 0.1333 | a280 | gps22 |
| 87 10 07 | pver-scla | 34352.0724 | 0.0267 | -59467.4193 | 0.0229 | -53821.5769 | 0.0186 | 87253.6588 | 0.0397 | a280 | gps22 |
| 87 10 08 | pver-hapy | 18155.3051 | 0.0229 | -52806.2980 | 0.0205 | -56787.3289 | 0.0167 | 79642.4568 | 0.0353 | a281 | gps22 |
| 87 10 08 | pver-hopp | 16040.0663 | 0.0229 | -59578.5440 | 0.0205 | -68129.6385 | 0.0167 | 91915.9087 | 0.0347 | a281 | gps22 |
| 87 10 08 | pver-scla | 34352.0973 | 0.0229 | -59467.4554 | 0.0205 | -53821.5615 | 0.0167 | 87253.6837 | 0.0347 | a281 | gps22 |
| 87 10 11 | nigu-nigb | 12.6253 | 0.0310 | 21.7057 | 0.0291 | 38.3629 | 0.0223 | 45.8503 | 0.0477 | b284 | gps22 |
| 88 03 08 | vndn-bluf | -119385.8744 | 0.0000 | 183426.8217 | 0.0000 | 150120.4812 | 0.0000 | 265395.0730 | 0.0000 | a068 | gps22 |
| 88 03 08 | vndn-brus | -142535.9798 | 0.0000 | 162974.1991 | 0.0000 | 105450.9273 | 0.0000 | 240825.6489 | 0.0000 | a068 | gps22 |
| 88 03 08 | vndn-cent | -50916.2445 | 0.0000 | 70573.0983 | 0.0000 | 51237.4030 | 0.0000 | 100986.6211 | 0.0000 | a068 | gps22 |
| 88 03 08 | vndn-nigu | -201050.9746 | 0.1042 | 186522.9339 | 0.0670 | 95618.6810 | 0.0744 | 290439.7208 | 0.1445 | a068 | gps22 |
| 88 03 08 | vndn-sbis | -92664.4748 | 0.0552 | 130832.6875 | 0.0391 | 99590.4354 | 0.0409 | 188738.3158 | 0.0787 | a068 | gps22 |
| 88 03 08 | vndn-smig | -1726.1234 | 0.0750 | 38711.4901 | 0.0496 | 47218.6030 | 0.0533 | 61083.1846 | 0.1048 | a068 | gps22 |
| 88 03 08 | vndn-sdad | -221687.4854 | 0.0000 | 243402.6618 | 0.0000 | 158259.5483 | 0.0000 | 365289.3121 | 0.0000 | a068 | gps22 |
| 88 03 09 | vndn-bluf | -119385.8744 | 0.0000 | 183426.8217 | 0.0000 | 150120.4808 | 0.0000 | 265395.0728 | 0.0000 | a069 | gps22 |
| 88 03 09 | vndn-brus | -142535.9803 | 0.0000 | 162974.1998 | 0.0000 | 105450.9272 | 0.0000 | 240825.6496 | 0.0000 | a069 | gps22 |
| 88 03 09 | vndn-cent | -50916.2445 | 0.0000 | 70573.0986 | 0.0000 | 51237.4033 | 0.0000 | 100986.6214 | 0.0000 | a069 | gps22 |
| 88 03 09 | vndn-nigu | -201050.9524 | 0.0440 | 186522.9329 | 0.0397 | 95618.6593 | 0.0329 | 290439.6977 | 0.0676 | a069 | gps22 |
| 88 03 09 | vndn-sbis | -92664.4373 | 0.0310 | 130832.6495 | 0.0310 | 99590.4299 | 0.0260 | 188738.2681 | 0.0508 | a069 | gps22 |
| 88 03 09 | vndn-smig | -1726.0681 | 0.0316 | 38711.4965 | 0.0291 | 47218.5875 | 0.0242 | 61083.1750 | 0.0490 | a069 | gps22 |
| 88 03 09 | vndn-sdad | -221687.4846 | 0.0000 | 243402.6620 | 0.0000 | 158259.5478 | 0.0000 | 365289.3116 | 0.0000 | a069 | gps22 |
| 88 03 10 | vndn-bluf | -119385.8663 | 0.0000 | 183426.8142 | 0.0000 | 150120.4769 | 0.0000 | 265395.0618 | 0.0000 | a070 | gps22 |
| 88 03 10 | vndn-brus | -142535.9667 | 0.0000 | 162974.2011 | 0.0000 | 105450.9294 | 0.0000 | 240825.6435 | 0.0000 | a070 | gps22 |
| 88 03 10 | vndn-cent | -50916.2446 | 0.0000 | 70573.1070 | 0.0000 | 51237.3972 | 0.0000 | 100986.6242 | 0.0000 | a070 | gps22 |
| 88 03 10 | vndn-nigu | -201050.8891 | 0.0676 | 186522.9055 | 0.0639 | 95618.7057 | 0.0496 | 290439.6515 | 0.1054 | a070 | gps22 |
| 88 03 10 | vndn-sbis | -92664.4239 | 0.0428 | 130832.6946 | 0.0403 | 99590.3743 | 0.0335 | 188738.2634 | 0.0676 | a070 | gps22 |
| 88 03 10 | vndn-smig | -1726.1197 | 0.0471 | 38711.5761 | 0.0446 | 47218.5311 | 0.0366 | 61083.1834 | 0.0744 | a070 | gps22 |
| 88 03 10 | vndn-sdad | -221687.4707 | 0.0000 | 243402.6547 | 0.0000 | 158259.5404 | 0.0000 | 365289.2951 | 0.0000 | a070 | gps22 |
| 88 03 17 | vndn-blhl | -9063.1291 | 0.0310 | -53779.9719 | 0.0285 | -73063.7721 | 0.0248 | 91174.2314 | 0.0490 | b077 | gps22 |
| 88 03 17 | vndn-cent | -50916.2153 | 0.0316 | 70573.0752 | 0.0291 | 51237.3959 | 0.0248 | 100986.5866 | 0.0496 | b077 | gps22 |
| 88 03 17 | vndn-fibr | -123397.5415 | 0.0465 | 9471.8415 | 0.0335 | -76598.0150 | 0.0366 | 145546.9853 | 0.0676 | b077 | gps22 |
| 88 03 17 | vndn-ftor | 18955.0950 | 0.0000 | -171058.4925 | 0.0000 | -190650.1889 | 0.0000 | 256841.9709 | 0.0000 | b077 | gps22 |
| 88 03 17 | vndn-lacu | -69188.5459 | 0.0409 | 45831.3835 | 0.0310 | 4987.0802 | 0.0316 | 83141.0943 | 0.0601 | b077 | gps22 |
| 88 03 17 | vndn-made | -59573.2963 | 0.0409 | -2326.2710 | 0.0353 | -47858.9083 | 0.0322 | 76451.7120 | 0.0632 | b077 | gps22 |
| 88 03 17 | vndn-ovro | -267649.2062 | 0.0000 | -47649.1498 | 0.0000 | -241259.3570 | 0.0000 | 363472.9927 | 0.0000 | b077 | gps22 |
| 88 03 17 | vndn-pibl | 15869.4941 | 0.0403 | -91987.9350 | 0.0316 | -100575.6204 | 0.0322 | 137219.0819 | 0.0601 | b077 | gps22 |
| 88 03 17 | vndn-pver | -152618.7979 | 0.0000 | 144583.9248 | 0.0000 | 74540.6178 | 0.0000 | 223054.5056 | 0.0000 | b077 | gps22 |
| 88 03 17 | vndn-twin | -49941.4381 | 0.0378 | 123735.4373 | 0.0366 | 121831.5681 | 0.0285 | 180686.2935 | 0.0595 | b077 | gps22 |
| 88 03 18 | vndn-blhl | -9063.1455 | 0.0248 | -53780.0208 | 0.0229 | -73063.7363 | 0.0205 | 91174.2332 | 0.0397 | a078 | gps22 |
| 88 03 18 | vndn-cent | -50916.2403 | 0.0254 | 70573.0903 | 0.0236 | 51237.4110 | 0.0198 | 100986.6173 | 0.0397 | a078 | gps22 |
| 88 03 18 | vndn-fibr | -123397.6031 | 0.0372 | 9471.8194 | 0.0285 | -76597.9516 | 0.0304 | 145547.0028 | 0.0564 | a078 | gps22 |
| 88 03 18 | vndn-ftor | 18955.0948 | 0.0000 | -171058.4916 | 0.0000 | -190650.1889 | 0.0000 | 256841.9702 | 0.0000 | a078 | gps22 |

| | | | | | | | | | | | | |
|---|---|---|---|---|---|---|---|---|---|---|---|---|
| 88 | 03 | 18 | vndn-lacu | -69188.5653 | 0.0335 | 45831.3953 | 0.0254 | 4987.0953 | 0.0260 | 83141.1179 | 0.0496 a078 | gps22 |
| 88 | 03 | 18 | vndn-losp | -11450.2811 | 0.0236 | -17552.3875 | 0.0223 | -31041.7482 | 0.0192 | 37453.7765 | 0.0378 a078 | gps22 |
| 88 | 03 | 18 | vndn-made | -59573.3143 | 0.0322 | -2326.3085 | 0.0254 | -47858.8615 | 0.0260 | 76451.6979 | 0.0484 a078 | gps22 |
| 88 | 03 | 18 | vndn-ovro | -267649.2061 | 0.0000 | -47649.1492 | 0.0000 | -241259.3569 | 0.0000 | 363472.9925 | 0.0000 a078 | gps22 |
| 88 | 03 | 18 | vndn-pibl | 15869.4962 | 0.0322 | -91987.9525 | 0.0254 | -100575.6165 | 0.0260 | 137219.0911 | 0.0484 a078 | gps22 |
| 88 | 03 | 18 | vndn-pver | -152618.7971 | 0.0000 | 144583.9247 | 0.0000 | 74540.6185 | 0.0000 | 223054.5052 | 0.0000 a078 | gps22 |
| 88 | 03 | 18 | vndn-twin | -49941.4717 | 0.0298 | 123735.4252 | 0.0273 | 121831.5872 | 0.0229 | 180686.3074 | 0.0465 a078 | gps22 |
| 88 | 05 | 10 | twin-jack | 1915.3937 | 0.0369 | -1610.9159 | 0.0722 | -771.9734 | 0.0450 | 2619.1079 | 0.0927 | gipsy |
| 88 | 05 | 10 | road-twin | -2185.3732 | 0.0419 | 2713.1103 | 0.0893 | 1974.6762 | 0.0533 | 4004.5187 | 0.1122 | gipsy |
| 88 | 05 | 10 | road-jack | -269.9795 | 0.0363 | 1102.1944 | 0.0691 | 1202.7028 | 0.0505 | 1653.5463 | 0.0930 | gipsy |
| 88 | 05 | 11 | twin-jack | 1915.3864 | 0.0366 | -1610.9089 | 0.0725 | -771.9741 | 0.0446 | 2619.0984 | 0.0927 | gipsy |
| 88 | 05 | 11 | road-twin | -2185.3677 | 0.0419 | 2713.0978 | 0.0905 | 1974.6797 | 0.0530 | 4004.5089 | 0.1132 | gipsy |
| 88 | 05 | 11 | road-jack | -269.9814 | 0.0350 | 1102.1888 | 0.0673 | 1202.7056 | 0.0490 | 1653.5449 | 0.0902 | gipsy |
| 88 | 05 | 13 | boul-harb | 4591.8624 | 0.0493 | -9888.5184 | 0.0967 | -9345.2137 | 0.0753 | 14359.7011 | 0.1321 | gipsy |
| 88 | 05 | 13 | boul-bluf | 3152.2602 | 0.0412 | -4055.3424 | 0.0775 | -2756.4015 | 0.0552 | 5829.2620 | 0.1035 | gipsy |
| 88 | 05 | 13 | harb-bluf | -1439.6023 | 0.0406 | 5833.1759 | 0.0821 | 6588.8122 | 0.0639 | 8916.8852 | 0.1116 | gipsy |
| 88 | 05 | 14 | boul-harb | 4591.8635 | 0.0434 | -9888.4914 | 0.0902 | -9345.2182 | 0.0673 | 14359.6858 | 0.1206 | gipsy |
| 88 | 05 | 14 | boul-bluf | 3152.2598 | 0.0387 | -4055.3287 | 0.0760 | -2756.4066 | 0.0530 | 5829.2547 | 0.1001 | gipsy |
| 88 | 05 | 14 | harb-bluf | -1439.6036 | 0.0369 | 5833.1626 | 0.0738 | 6588.8116 | 0.0573 | 8916.8764 | 0.1004 | gipsy |
| 88 | 05 | 15 | harb-bluf | -1439.6167 | 0.0372 | 5833.1546 | 0.0766 | 6588.8410 | 0.0629 | 8916.8949 | 0.1060 | gipsy |
| 88 | 05 | 17 | himt-lacu | -3784.4884 | 0.0635 | -30795.2304 | 0.0868 | -43316.5159 | 0.1159 | 53282.1651 | 0.1581 | gipsy |
| 88 | 05 | 18 | high-himt | 379.4756 | 0.0456 | -837.5497 | 0.0812 | -675.6496 | 0.0617 | 1141.0494 | 0.1119 | gipsy |
| 88 | 05 | 18 | high-lacu | -3404.8990 | 0.0567 | -31632.8881 | 0.0992 | -43992.1439 | 0.0893 | 54291.2670 | 0.1451 | gipsy |
| 88 | 05 | 18 | himt-lacu | -3784.3746 | 0.0511 | -30795.3384 | 0.0890 | -43316.4942 | 0.0818 | 53282.2018 | 0.1311 | gipsy |
| 88 | 05 | 19 | high-himt | 379.4181 | 0.2055 | -837.6867 | 0.4907 | -675.6054 | 0.1252 | 1141.1046 | 0.5465 | gipsy |
| 88 | 05 | 19 | high-lacu | -3405.0396 | 0.0536 | -31632.8360 | 0.0831 | -43991.9169 | 0.1004 | 54291.0615 | 0.1410 | gipsy |
| 88 | 05 | 19 | himt-lacu | -3784.4577 | 0.2058 | -30795.1493 | 0.4923 | -43316.3116 | 0.1386 | 53281.9499 | 0.5512 | gipsy |

Table B-5
SV3 Fiducial Station Coordinates (meters)

| ID | X | Y | Z |
|---|---|---|---|
| algo | 918127.7167 | -4346061.8756 | 4561984.2549 |
| aust | -743774.1273 | -5460643.7270 | 3200347.4262 |
| chur | -236416.9523 | -5430055.7677 | 3307612.1244 |
| ftdv | -1324191.8149 | -5332059.7133 | 3232043.4878 |
| ftor | -2697026.6896 | -4354393.2306 | 3788077.7592 |
| hayo | 1492410.0956 | -4457290.2044 | 4296819.1641 |
| moj1 | -2356424.4176 | -4646613.5373 | 3668462.4083 |
| moja | -2356214.6131 | -4646733.9445 | 3668460.5720 |
| ovro | -2410422.3887 | -4477802.5734 | 3838686.9267 |
| plat | -1240708.0633 | -4720454.2657 | 4094481.7835 |
| pver | -2525452.7972 | -4670035.6471 | 3522886.9520 |
| rich | 961318.4115 | -5674058.3042 | 2740565.4244 |
| vlsr | -2678099.9767 | -4525456.7503 | 3597399.0227 |
| vndn | -2678071.5945 | -4525451.7224 | 3597427.5698 |
| wsfd | 1492233.0859 | -4458091.5739 | 4296045.8999 |
| yknf | -1224064.3320 | -2689833.0360 | 5633432.6270 |